

---

# Drivers of Pleistocene to Holocene sea-level changes in the Southwestern Atlantic

---

Dissertation

for the award of the doctoral degree of

*Doctor rerum naturalium*

(Dr.rer.nat.)

submitted to the Department of Geosciences

University of Bremen



**Karla Zurisadai Rubio Sandoval**

Bremen, March 2024

*Science does not advance by the accumulation of truths but by eliminating errors.*

Sir Karl Popper, 1963

**Reviewers:**

Prof. Dr. Alessio Rovere  
Prof. Dr. Giovanni Scicchitano

**Examination Board:**

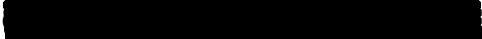
Prof. Dr. Alessio Rovere  
Prof. Dr. Giovanni Scicchitano  
Prof. Dr. Elda Miramontes García  
Dr. Jessica Hargreaves  
Dr. Patrick Boyden  
BSc. Nwachukwu Emeka Kelvin

**Day of Defense:**

8<sup>th</sup> May 2024

*Affirmation in lieu of an oath*

according to § 5 (5) of the Doctoral Degree Rules and Regulations of 28 April, 2021

I, Karla Zurisadai Rubio Sandoval, 

With my signature I affirm in lieu of an oath that I prepared the submitted dissertation independently and without illicit assistance from third parties, that I appropriately referenced any text or content from other sources, that I used only literature and resources listed in the dissertation, and that the electronic (PDF) and printed versions of the dissertation are identical.

I affirm in lieu of an oath that the information provided herein to the best of my knowledge is true and complete.

I am aware that a false affidavit is a criminal offence which is punishable by law in accordance with § 156 of the German Criminal Code (StGB) with up to three years imprisonment or a fine in case of intention, or in accordance with § 161 (1) of the German Criminal Code with up to one year imprisonment or a fine in case of negligence.

---

Place, Date

---

Signature

## Contents

<b>I. Acknowledgments</b> .....	i
<b>II. Author's Note</b> .....	ii
<b>III. Abstract</b> .....	iv
<b>IV. Zusammenfassung</b> .....	vi
<b>V. Resumen</b> .....	viii
<b>VI. Outline of manuscripts</b> .....	x
<b>1. Introduction</b> .....	1
1.1. From paleo-sea levels to future sea level rise: Unraveling trends of a warmer world.....	1
1.2. The southwestern Atlantic: An emerging hub for sea level research.....	2
1.3. Identifying research gaps.....	3
1.4. Motivation, research questions, and hypothesis.....	5
<b>2. Methodology</b> .....	6
<b>3. A review of last interglacial sea-level proxies in the western Atlantic and southwestern Caribbean, from Brazil to Honduras</b> .....	12
3.1. Abstract .....	12
3.2. Introduction.....	13
3.3. Types of sea-level indicators.....	14
3.4. Positioning and sea-level datums.....	17
3.5. Dating techniques.....	19
3.6. Relative sea-level data.....	20
3.7. Data availability.....	44
3.8. Further remarks and conclusions.....	44
3.9. Acknowledgements.....	50
<b>4. Holocene relative sea-level changes from the Atlantic coasts of South America</b> .....	51
4.1. Abstract .....	51
4.2. Introduction.....	51
4.3. Regional setting.....	52
4.4. Methods .....	55
4.5. Results.....	66
4.6. Discussion.....	77
4.7. Conclusions.....	83
4.8. Data availability.....	84
4.9. Acknowledgments.....	84
4.10. Supplementary material.....	85
<b>5. Quaternary and Pliocene sea-level changes at Camarones, central Patagonia, Argentina</b> .....	87
5.1. Abstract.....	87
5.2. Introduction.....	87
5.3. Study area .....	89
5.4. Methods .....	90
5.5. Results.....	95

5.6. Discussion .....	103
5.7. Conclusions .....	107
5.8. Data availability.....	108
5.9. Acknowledgments.....	109
5.10. Supplementary material.....	109
<b>6. Paleoenvironmental implications of Late Quaternary bioerosion traces in central Patagonia (southern Atlantic, Argentina).....</b>	<b>116</b>
6.1. Abstract.....	116
6.2. Introduction .....	116
6.3. Geological setting .....	119
6.4. Paleontological setting .....	120
6.5. Material and methods.....	120
6.6. Results .....	124
6.7. Discussion.....	132
6.8. Conclusion .....	137
6.9. Data availability.....	138
6.10. Acknowledgements .....	138
6.11. Supplementary material.....	139
<b>7. Extended discussion and final remarks.....</b>	<b>141</b>
<b>8. Outcome and research horizons .....</b>	<b>145</b>
<b>9. References .....</b>	<b>147</b>
<b>10. Appendix.....</b>	<b>196</b>
<b>11. Epilogue.....</b>	<b>202</b>

## I. Acknowledgments

Over my Ph.D. journey, I've had the valuable opportunity to deepen into paleo sea level research. This wouldn't have been possible without the immeasurable support of numerous individuals I've encountered along the way. Foremost, I extend my heartfelt gratitude to my supervisor, Alessio Rovere, whose guidance and assistance have been fundamental in every aspect of my project. Although most of the time we had to work remotely, I always felt his professional and personal support, I know that without him, the development and conclusion of this research would have been absolutely impossible. Molto grazie per tutto!

I express my gratitude to my GLOMAR thesis committee: Deirdre D. Ryan, Matteo Vacchi, and Sebastian Richiano for the insightful discussions and support throughout this journey. Thanks, D for all your interest in my personal and professional development.

I thank the University of Bremen, the Center for Environmental Marine Science (MARUM), the WARMCOAST project, and the Monika Segl program for their combined efforts in generously funding my Ph.D. position. I'm also grateful to the Bremen International Graduate School for Marine Science (GLOMAR) for providing enriching courses, and for building a strong student community, where I found friends and family. I feel honored for allowing me to be a doctoral representative, that opportunity pushed me to grow in many different ways.

Furthermore, I appreciate the camaraderie I shared with Kathrine Maxwell, Sofia Barragán Montilla, Patrick Boyden, Débora Raposo, and Hana Camelia. Even though we didn't get to share and interact for long, I always felt supported, understood, and motivated to pursue my goal.

Many thanks to Dierk Hebbeln's working group for hosting me in the last years of my Ph.D. journey. Thank you for being the working group that I could not have at the beginning of my doctorate due to different factors.

I'm immensely grateful to my colleagues and friends Rodrigo M., Eldo, Luis, Juán, Deno, and Mauricio, as well as my friends back home Rodrigo R., Paozz, Ricardo, Ilse y Jesús thank you for always being there for me and keeping me grounded even during the challenging times.

Toda mi gratitud a mi familia y a Baruch por su inquebrantable amor y confianza, por todo el apoyo desmesurado. Sin ustedes perseguir este sueño habría sido imposible. Los amo.

## II. Author's Note

In the following lines, I will not make any scientific statement, I simply take the liberty to express my opinions as a human being and in perspective of what I experienced in this Ph.D. journey.

Life is unexpected...

In these years of my Ph.D., plans, and circumstances changed drastically not only for me and my project but also for the world.

Since I started this adventure in December 2019, the world has faced not only climatic but also socio-political challenges. In four years, I saw the world destabilize, insolation records reached, hurricanes, a pandemic, and wars unleashed.

I see how many people suffer the consequences of a changing climate, changing governments, and changing political decisions. I saw economies collapse, and products become more expensive, and with pain in my heart, I saw how my Argentine colleagues, with whom I had the opportunity to work, were forced to fight for their rights facing a bad government.

I know that there are no perfect equations and that a balanced and fair world seems more of a utopia than a reality. But I also know that I have hope. I have hope in the good people in the world, I have hope in science and in individual actions to transform our context and our reality.

I believe in individuals who make a lasting impact and make a positive effect on the lives of others, I believe that there is still kindness and solidarity.

I believe in my friends and colleagues who every day work hard to follow their dreams and passions. I believe in their actions that have an impact on the world.

I believe in education and I know that it is one of the main tools for change. I believe in social activism.

I know that science, specifically climate science, will face enormous challenges in the coming years, but I believe that there are people who are extremely well-prepared to find solutions to mitigate the effects of our inordinate impact on the earth. And although I do not believe that the big governments will take the relevant decisions and actions, I know that we will keep fighting, every day, from our respective trenches.

I have hope for a better future, and because of that hope, I will work every day to be an agent of change.

## Author's Note Spanish version

En las siguientes líneas no haré ningún manifiesto científico, simplemente me tomo la libertad de expresar mis opiniones como persona y en perspectiva de lo que viví en esta jornada doctoral.

La vida es sorpresiva...

En estos años de mi doctorado los planes y circunstancias cambiaron drásticamente no sólo para mí y mi proyecto si no para el mundo.

Desde que inicie esta aventura en diciembre de 2019 el mundo se ha enfrentado a desafíos no sólo climáticos si no también socio-políticos. En cuatro años vi al mundo desestabilizarse, récords de insolación alcanzados, huracanes, una pandemia y guerras desatadas.

Veo como muchas personas sufren las consecuencias de un clima cambiante, de gobiernos y decisiones políticas cambiantes. Vi economías desplomarse, productos encarecerse y con dolor en mi corazón veo cómo mis colegas argentinos, con quienes tuve la oportunidad de trabajar, se ven obligados a luchar por sus derechos ante un mal gobierno.

Sé que no hay fórmulas perfectas, que un mundo equilibrado y justo parece más una utopía que una realidad. Pero también sé que tengo esperanza. Tengo esperanza en las buenas personas que hay en el mundo, tengo esperanza en la ciencia y en las acciones individuales para transformar nuestro entorno y nuestra realidad.

Creo en las personas que dejan huella y marcan de manera positiva la vida de los otros, creo que aún hay bondad y solidaridad.

Creo en mis amigos y colegas que todos los días trabajan duro por seguir sus sueños y pasiones. Creo que sus acciones tienen un impacto en el mundo que los rodea.

Creo en la educación y sé que es una de las herramientas principales para el cambio. Creo en las luchas sociales.

Sé que la ciencia, específicamente la ciencia climática se enfrentará a desafíos enormes en los próximos años, pero creo que hay personas muy preparadas para encontrar soluciones que mitiguen los efectos de nuestro impacto desmesurado en la tierra. Y aunque lamentablemente no creo que los grandes gobiernos tomen las decisiones y acciones pertinentes, sé que nos mantendremos luchando, todos los días, cada uno desde su trinchera.

Tengo esperanzas de un futuro mejor y por esa esperanza trabajaré todos los días para ser un agente de cambio.

### III. Abstract

Global mean sea levels have been rising since the last century; this trend is expected to continue as the planet faces a warmer future. However, the rate and magnitude of this rise remain subject to debate, making decisions about land use and coastal management difficult. Sea level changes are not linear. In fact, they are driven by an intricate relationship between eustatic (i.e., global), isostatic, and local factors. Therefore, there is a clear need for precise and accurate data covering various spatiotemporal scales. Quaternary sea-level records offer valuable data to improve our understanding of these complex sea-level dynamics and enhance the predictions of future sea-level scenarios. In particular, interglacial records provide sea-level variability data under warm climate conditions. Marine Isotope Stages (MIS) 11 (424 to 395 ka) and 5 (~125 to 80 ka) represent the most recent interglacial periods when the Earth's climate was warmer than the pre-industrial, and sea level was higher than today, leaving geological and biological traces of rising sea levels around the world.

Given its extension, the southwestern Atlantic region is susceptible to various eustatic and glacial-isostatic sea-level patterns, turning its coastlines into a hot spot for investigations into past sea-level dynamics. This dissertation aims to provide an overview of state-of-the-art sea-level research in this broad region. Through four chapters, we will provide context on the accuracy of published data from the Pleistocene to the Holocene interglacials, discuss the uncertainties surrounding them, and propose new methodological approaches to improve the interpretations.

The first chapter provides a literature review of the Last Interglacial (MIS 5) sea level research in a coastal profile from Brazil to Honduras, including the Caribbean islands of Aruba, Bonaire, and Curaçao. This review evaluates and standardizes the data using the World Atlas of Last Interglacial Shorelines template. In this endeavor, we fill the geographical gap between the existing sea-level compilations of Mexico and the northwestern Caribbean Sea and the Atlantic coasts from Argentina to Uruguay, resulting in a standardized transect that could be useful for assessing the glacial isostatic signals from near-intermediate- and far-field locations. Nevertheless, our review highlights that future research should improve the chronological control at several sites, and the coast of Brazil would benefit from a new measurement of paleo-sea levels, using more accurate measurement techniques to reduce uncertainties in the calculated sea level values.

Considering the uncertainties of the Last Interglacial sea-level reconstructions, in our second chapter, we explore whether Holocene sea-level indicators would allow better estimations of sea level and whether these data could be useful to better frame the data of its past climatic analog. To this end, we conducted a new review that compiles information from more than 150 years of research on the coastlines of Brazil, Uruguay, and Argentina. This new database produced 1024 standardized data points and helps to investigate the influence of tectonic setting and glacial isostatic adjustment on the sea level trends. We also provide new inferences of the magnitude and timing of the mid-Holocene highstand. However, we note that there is no significant improvement in the quality of the data, and many aspects of

Holocene reconstructions still need to be fixed, for example, the rigorous definition of modern analogs to quantify the relationship between geological indicators and the present sea level.

Under this context, in the last two chapters of the thesis, we propose new methodological approaches to improve our understanding of past sea level dynamics. To this end, we selected a region within the southwestern Atlantic to evaluate the possible most accurate ages and elevations obtained in sea level reconstructions during interglacial periods. We detected that the appropriate region would be the coastlines of Patagonia, Argentina since the literature highlights the presence of several geological sea-level indicators (i.e., beach ridges) from the Pliocene to the Holocene. Our research uses precise topographic techniques to measure the elevation of the geological deposits. Additionally, we utilize chronological methods such as amino acid racemization to evaluate the consistency in the chronological attribution of the deposits made by previous authors. We also propose a new methodology to estimate the indicative meaning of beach ridges using wave models with satellite data. Finally, through a bioerosion trace analysis, we identify similar environmental conditions between the Pleistocene interglacials and the Holocene. Our high-resolution data provide an important reference point for future studies aimed at unraveling the paleo-sea level trends in this locality.

By integrating information from the four investigations that are the core of this dissertation, we succeeded in completing previous global sea level compilations, unifying a pole-to-pole transect that provides valuable insights for assessing the future of global coastlines in a warmer world.

## IV. Zusammenfassung

Seit dem letzten Jahrhundert ist der mittlere globale Meeresspiegel angestiegen; dieser Trend wird sich voraussichtlich fortsetzen, da die Erde einer wärmeren Zukunft entgegensteht. Die Geschwindigkeit und das Ausmaß dieses Anstiegs sind jedoch nach wie vor umstritten, was Entscheidungen über Landnutzung und Küstenmanagement erschwert. Die Veränderungen des Meeresspiegels verlaufen nicht linear. Vielmehr werden sie von einer komplexen Beziehung zwischen eustatischen (d. h. globalen), isostatischen und lokalen Faktoren bestimmt. Daher besteht ein eindeutiger Bedarf an präzisen und punktgenauen Daten, die verschiedene räumliche und zeitliche Skalen abdecken. Quartäre Meeresspiegelaufzeichnungen bieten wertvolle Daten, um unser Verständnis dieser komplexen Meeresspiegeldynamik sowie die Vorhersage künftiger Meeresspiegelszenarien zu verbessern. Insbesondere interglaziale Aufzeichnungen liefern Daten zur Variabilität des Meeresspiegels unter warmen Klimabedingungen. Die marinen Isotopenstadien (MIS) 11 (424 bis 395 ka) und 5 (~125 bis 80 ka) repräsentieren die jüngsten interglazialen Perioden, in denen das Erdklima wärmer war als in der vorindustriellen Zeit und der Meeresspiegel höher lag als heute, was weltweit geologische und biologische Spuren des Meeresspiegelanstiegs hinterließ.

Aufgrund seiner Ausdehnung ist der Südwestatlantik anfällig für verschiedene eustatische und glazial-isostatische Meeresspiegelmuster, was seine Küsten zu einem Hotspot für die Erforschung der vergangenen Meeresspiegeldynamik macht. Ziel dieser Dissertation ist es, einen Überblick über den aktuellen Stand der Meeresspiegelforschung in dieser ausgedehnten Region zu geben. In vier Kapiteln werden wir die Genauigkeit der veröffentlichten Daten vom Pleistozän bis zu den Zwischeneiszeiten des Holozäns erläutern, die damit verbundenen Unsicherheiten diskutieren und neue methodische Ansätze zur Verbesserung der Interpretationen vorschlagen.

Das erste Kapitel bietet einen Literaturüberblick über die Forschung zum Meeresspiegel des letzten Interglazials (MIS 5) in einem Küstenprofil von Brasilien bis Honduras, einschließlich der karibischen Inseln Aruba, Bonaire und Curaçao. In diesem Bericht werden die Daten anhand der Vorlage des World Atlas of Last Interglacial Shorelines bewertet und standardisiert. Mit diesem Vorhaben schließen wir die geografische Lücke zwischen den bestehenden Meeresspiegelsammlungen für Mexiko und die nordwestliche Karibik sowie die Atlantikküsten von Argentinien bis Uruguay, wodurch ein standardisierter Transekt entsteht, der für die Bewertung der glazialen isostatischen Signale aus dem Nah- und Fernbereich nützlich sein könnte. Unsere Überprüfung zeigt jedoch, dass künftige Forschung die chronologische Kontrolle an mehreren Standorten verbessern sollte, und die brasilianische Küste würde von einer neuen Messung des Paläo-Meeresspiegels profitieren, bei der genauere Messverfahren eingesetzt werden, um die Unsicherheiten bei den berechneten Meeresspiegelwerten zu verringern.

In Anbetracht der Unsicherheiten bei der Rekonstruktion des Meeresspiegels des letzten Interglazials untersuchen wir in unserem zweiten Kapitel, ob holozäne Meeresspiegelindikatoren eine bessere Schätzung des Meeresspiegels ermöglichen würden

und ob diese Daten nützlich sein könnten, um die Daten des vergangenen Klimas besser zu erfassen. Zu diesem Zweck haben wir eine neue Untersuchung durchgeführt, die Informationen aus mehr als 150 Jahren Forschung an den Küsten Brasiliens, Uruguays und Argentiniens zusammenfasst. Diese neue Datenbank enthält 1024 standardisierte Datenpunkte und hilft bei der Untersuchung des Einflusses der tektonischen Gegebenheiten und der glazialen isostatischen Anpassung auf die Entwicklung des Meeresspiegels. Außerdem liefern wir neue Erkenntnisse über das Ausmaß und den Zeitpunkt des mittelholozänen Hochstands. Wir stellen jedoch fest, dass sich die Qualität der Daten nicht wesentlich verbessert hat und dass viele Aspekte der holozänen Rekonstruktionen noch festgelegt werden müssen, z. B. die strenge Definition moderner Analogie zur Quantifizierung der Beziehung zwischen geologischen Indikatoren und dem heutigen Meeresspiegel.

In diesem Zusammenhang schlagen wir in den letzten beiden Kapiteln der Arbeit neue methodische Ansätze vor, um unser Verständnis der vergangenen Meeresspiegeldynamik zu verbessern. Zu diesem Zweck haben wir eine Region im südwestlichen Atlantik ausgewählt, um die möglichen genauesten Alters- und Höhenangaben zu ermitteln, die bei der Rekonstruktion des Meeresspiegels während der Zwischeneiszeiten gewonnen wurden. Wir haben festgestellt, dass die Küstenlinie von Patagonien, Argentinien, die geeignete Region ist, da in der Literatur mehrere geologische Meeresspiegelindikatoren (z. B. Strandkämme) vom Pliozän bis zum Holozän zu finden sind. Bei unseren Untersuchungen setzen wir präzise topografische Techniken ein, um die Höhe der geologischen Ablagerungen zu messen. Außerdem verwenden wir chronologische Methoden wie die Aminosäure-Razemisierung, um die Konsistenz der chronologischen Zuordnung der Ablagerungen durch frühere Autoren zu bewerten. Wir schlagen auch eine neue Methode vor, um die indikative Bedeutung von Strandkämmen mit Hilfe von Wellenmodellen und Satellitendaten abzuschätzen. Schließlich identifizieren wir durch eine Analyse von Bioerosionsspuren ähnliche Umweltbedingungen zwischen den pleistozänen Interglazialen und dem Holozän. Unsere hochauflösenden Daten stellen einen wichtigen Bezugspunkt für künftige Studien dar, die darauf abzielen, die Paläo-Meeresspiegel-Trends an diesem Ort zu entschlüsseln.

Durch die Integration von Informationen aus den vier Untersuchungen, die den Kern dieser Dissertation bilden, ist es uns gelungen, frühere Zusammenstellungen des globalen Meeresspiegels zu vervollständigen und einen Pol-zu-Pol-Transekt zu vereinheitlichen, der wertvolle Erkenntnisse für die Bewertung der Zukunft der globalen Küsten in einer wärmeren Welt liefert.

## V. Resumen

El nivel del mar global ha incrementado desde el siglo pasado; se prevé que esta tendencia continúe a medida que el planeta se enfrente a un futuro más cálido. Sin embargo, la tasa de cambio y su magnitud siguen siendo objeto de debate, lo que dificulta la toma de decisiones sobre el uso del suelo y la gestión de las zonas costeras. Los cambios del nivel del mar no son lineales. De hecho, varían a través de una intrincada relación entre factores eustáticos (globales), isostáticos y locales. Por lo tanto, para modelar estos cambios se requieren datos precisos y exactos que abarquen varias escalas espaciotemporales. Los registros geológicos del Cuaternario ofrecen datos valiosos para mejorar nuestra comprensión de esta compleja dinámica y así mejorar las predicciones de escenarios futuros. En particular, los registros interglaciares proporcionan datos sobre la variabilidad del nivel del mar en condiciones climáticas cálidas. Los estadios isotópicos marinos (MIS, por sus siglas en inglés) 11 (424 a 395 mil años) y 5 (~125 a 80 mil años) representan los periodos interglaciares más recientes, cuando el clima de la Tierra era más cálido que durante el periodo preindustrial y el nivel del mar era más alto que el actual, dejando huellas geológicas y biológicas de este incremento en todo el mundo.

Dada su extensión, la región del Atlántico suroccidental es susceptible a diversos patrones del nivel del mar eustáticos y glaciar-isostáticos, lo que convierte a sus costas en un foco de interés para las investigaciones sobre la dinámica del nivel del mar en el pasado. El objetivo de esta tesis doctoral es ofrecer una visión general del estado actual de la investigación sobre el nivel del mar en esta región. A lo largo de cuatro capítulos, ofreceremos un contexto sobre la precisión de los datos publicados desde los periodos interglaciares del Pleistoceno hasta el Holoceno, discutiremos las incertidumbres que los rodean y propondremos nuevos enfoques metodológicos para mejorar las interpretaciones.

El primer capítulo ofrece una revisión bibliográfica de las investigaciones sobre el nivel del mar del Último Interglaciario (MIS 5) en un perfil costero desde Brasil hasta Honduras, incluyendo las islas caribeñas de Aruba, Bonaire y Curaçao. Esta revisión evalúa y estandariza los datos utilizando la plantilla del Atlas Mundial de las Líneas Costeras del Último Interglaciario (WALIS, por sus siglas en inglés). En este esfuerzo, llenamos el vacío geográfico existente entre las compilaciones del nivel del mar de México y el noroeste del Mar Caribe y las costas atlánticas desde Argentina hasta Uruguay, resultando en un transecto de datos que podría ser útil para evaluar las señales isostáticas glaciares de localidades de campo cercano-intermedio y lejano. No obstante, nuestra revisión resalta la necesidad de futuras investigaciones para mejorar el control cronológico en varios lugares, y que la costa de Brasil se beneficiaría de un nuevo análisis de los depósitos paleo-marinos, utilizando técnicas de medición más precisas para reducir las incertidumbres en los valores calculados del nivel del mar.

Considerando las incertidumbres de las reconstrucciones del nivel del mar del Último Interglaciario, en nuestro segundo capítulo, exploramos si los indicadores del nivel del mar del Holoceno permitirían mejores estimaciones y si estos datos podrían ser útiles para contextualizar mejor los datos de su análogo climático pasado. Para ello, realizamos una nueva revisión que recopila información de más de 150 años de investigación en las costas de

Brasil, Uruguay y Argentina. Esta nueva base de datos produjo 1024 datos estandarizados y ayudó a investigar la influencia de la configuración tectónica y el ajuste isostático glacial en las tendencias del nivel del mar. También aportamos nuevas inferencias sobre la magnitud y temporalidad del período de máxima elevación del nivel del mar del Holoceno. Sin embargo, observamos que dentro de estos datos no existe una mejora significativa en su calidad, y que aún deben optimizarse muchos aspectos en las reconstrucciones del Holoceno, por ejemplo, la definición rigurosa de análogos modernos para cuantificar la relación entre los indicadores geológicos y el nivel del mar actual.

En este contexto, en los dos últimos capítulos de la tesis proponemos nuevos enfoques metodológicos para mejorar nuestra comprensión de la dinámica del nivel del mar en el pasado. Para ello, seleccionamos una región dentro del Atlántico suroccidental con la finalidad de evaluar las posibles edades y elevaciones más precisas que pueden obtenerse en las reconstrucciones del nivel del mar durante los periodos interglaciares. Detectamos que la región adecuada para este estudio serían las costas de la Patagonia, Argentina, ya que la bibliografía destaca la presencia de varios indicadores geológicos del nivel del mar (cordones litorales) desde el Plioceno hasta el Holoceno. Nuestra investigación utiliza técnicas topográficas precisas para medir la elevación de estos depósitos geológicos. Además, utilizamos métodos cronológicos como la racemización de aminoácidos para evaluar la coherencia en la atribución cronológica de los cordones litorales realizada por previos autores. También proponemos una nueva metodología para estimar su significado indicativo utilizando modelos de oleaje con datos satelitales. Por último, mediante un análisis de trazas de bioerosión, identificamos condiciones ambientales similares entre los interglaciares del Pleistoceno y el Holoceno. Nuestros datos de alta resolución constituyen un importante punto de referencia para futuros estudios destinados a desentrañar las tendencias de los niveles marinos pasados en esta localidad.

Al integrar la información de las cuatro investigaciones que constituyen el corazón de esta disertación, conseguimos completar las bases de datos sobre el nivel del mar global previamente publicadas, unificando un transecto polo a polo que proporciona valiosas perspectivas para evaluar el futuro de las costas en un mundo más cálido.

## VI. Outline of manuscripts

This doctoral thesis is a cumulative dissertation that consists of four manuscripts in various stages of publication (Chapters 3, 4, 5, 6). These manuscripts are framed by an accompanying text (Chapters 1, 2, 7, 8). Hereafter, a brief summary with a list of authors, publication status, and overview of the main research highlights of each paper is presented, in addition to the details of the authors' and my own contributions.

### CHAPTER 3- A review of last interglacial sea-level proxies in the western Atlantic and southwestern Caribbean, from Brazil to Honduras

Karla Rubio-Sandoval, Alessio Rovere, Ciro Cerrone, Paolo Stocchi, Thomas Lorscheid, Thomas Felis, Ann-Kathrin Petersen, and Deirdre D. Ryan

*Published in Earth System Science Data (2021), 13(10), 4819-4845.*

#### Research highlights:

- Description of the most common sea-level indicators in the area and their indicative meanings (relationship between the indicator and the sea level).
- Standardization of 50 sea-level index points and 5 limiting data, providing information on the paleo-relative sea-level values reached during the last interglacial.
- Discussion of the possible process that could affect the eustatic signal of the relative sea levels.
- Outline the data quality and the research gaps in the area, highlighting the most promising sites to unravel past sea-level changes.

#### Author contributions:

KRS compiled the database and wrote the manuscript with help from AR and DDR. AR, TL, TF, CC, AKP, and PS contributed original field data from Bonaire and Curaçao. All authors gave input on the manuscript, revised the final text, and agreed with its contents.

#### Detailed own contributions:

For this paper, I extensively searched online catalogs for any prior research related to the last interglacial sea levels in the western Atlantic and southwestern Caribbean. I compiled 36 papers, reviewed them, and gathered all available data and metadata. I integrated all collected data into the standardized "World Atlas of Last Interglacial Shorelines" database. Finally, I drafted the manuscript and compiled replies to the reviewers during the review process.

## CHAPTER 4- Holocene relative sea-level changes from the Atlantic coasts of South America

Karla Rubio-Sandoval, Timothy Shaw, Matteo Vacchi, Nicole Khan, Benjamin Horton, Rodolfo Angulo, Marta Pappalardo, Augusto Ferreira-Júnior, Sebastian Richiano, Cristina Souza, Paulo Giannini, Deirdre D. Ryan, Evan J. Gowan, and Alessio Rovere

*In preparation for submission to The Holocene*

### Research highlights:

- Description of the most common Holocene sea-level indicators in the area and their indicative meanings.
- Standardization of 726 sea-level index points and 298 limiting data providing valuable information to unravel the magnitude and timing of widely described mid-Holocene highstand and the subsequent relative sea-level trends.
- Discussion of the influence of glacial isostatic adjustment (GIA) and local tectonics on the relative sea level signals.
- Address the existing gap in standardized sea-level data for the Atlantic coasts, contributing to a pole-to-pole data transect that could improve current glacial isostatic adjustment models and provide valuable insights for optimizing global sea-level estimates.

### Author contributions:

KRS compiled the database and wrote the manuscript with help from AR, TAS, NK, NH, JRA, ALFJ, JRR, GCL, and MCS provide preliminary data and references. MV support during the radiocarbon calibrations, NK to develop and interpret the spatiotemporal empirical hierarchical models, and EJJ to develop GIA models and interpretations. AJR provides valuable comments to improve the correction of Brazil's data. All authors gave input on the manuscript, revised the final text, and agreed with its contents.

### Detailed own contributions:

I conducted a thorough search of literature related to the Holocene sea level changes in the southwestern Atlantic. I reviewed 128 studies published between 1964 and 2023. Subsequently, I integrated the data and metadata of each reference into the standardized "Holocene Sea Level" database. I critically evaluated the quality of the data, contacted researchers to disentangle uncertainties, and developed the data analysis. I drafted the manuscript and created most of the figures.

## CHAPTER 5- Quaternary and Pliocene sea-level changes at Camarones, central Patagonia, Argentina

Karla Rubio-Sandoval, Deirdre D. Ryan, Sebastian Richiano, Luciana M. Giachetti, Andrew Hollyday, Jordon Bright, Evan J. Gowan, Marta Pappalardo, Jacqueline Austermann, Darrell S. Kaufman, and Alessio Rovere

*Submitted to Quaternary Science Reviews (2024)*

### Research highlights:

- Analysis of the sea-level imprints from four interglacial periods (from the Holocene to the Early Pliocene) in a locality of the southwestern Atlantic with a high-precision GNSS survey.
- Determination of the indicative range of the interglacial beach ridges by using a novel and accurate approach based on satellite-derived wave measurements and wave runup models.
- Present the paleo-relative sea level estimations for each interglacial and compare the results with published GIA and mantle dynamic topography (DT) predictions.
- Provided new amino acid racemization (AAR) and Radiocarbon data by analyzing *Ameghinomya antiqua* shells of the beach ridges. These results complement Electron Spin Resonance and U-series ages obtained by previous studies and allow a chronological attribution of the deposits.

### Author contributions:

KR, DDR, SR, LMG, and AR planned the field campaign, conducted field measurements, and collected samples. AR analyzed the GNSS datasets and ran the wave runup models. DDR, JB, and DSK processed and analyzed AAR data. AH, JA and EJG developed the DT and GIA models. KR wrote the initial manuscript; all authors reviewed and edited it.

### Detailed own contributions:

This manuscript was created by incorporating data gathered during a month-long field expedition in Argentina with data already collected within A. Rovere's research group. In the planning phase, I participated in online discussions with the working team to identify potential outcrops to be analyzed. I read literature and analyzed previous AAR data results from a previous field campaign to become familiar with the type of samples I would need to collect. Prior to the fieldwork, I received training to conduct GNSS surveys and keep in touch with Argentinean colleagues to ensure the acquisition of sample permits. Upon arrival in Argentina, I tested the GNSS equipment and led the preparation of materials to be used in the field. Throughout the fieldwork, I conducted all GNSS surveys for each outcrop with support from LMG when an extra set of hands was required. Additionally, I sampled shells for the AAR

dating. After returning from the field, I processed all GNSS data and shell samples (species identification and creation of a photographic catalog); I prepared the shell samples to be shipped to the Amino Acid Geochronology Laboratory at Northern Arizona University. Finally, I wrote the initial manuscript.

## CHAPTER 6- Paleoenvironmental implications of Late Quaternary bioerosion traces in central Patagonia (southern Atlantic, Argentina)

Luciana M. Giachetti, Sebastian Richiano, Karla Rubio-Sandoval, Clara B. Giachetti, Deirdre D. Ryan, Darrell S. Kaufman, Jordon Bright, Alessio Rovere, Diana Elizabeth Fernández

*Submitted to the Journal of Quaternary Sciences (2024)*

### Research highlights:

- Use bioerosion traces to unravel paleoenvironmental and paleoclimatic changes in the southern Atlantic.
- Addresses discrepancies in age assessments of Quaternary marine deposits in the study area by employing AAR analyses on mollusk shells, providing chronological insights into the geological history of the region.
- Discussion of the distinct bioerosion patterns across different geological periods, suggesting environmental changes during the Quaternary and reinforcing the hypothesis of a link between bioerosion, productivity, and circulation in the southern Atlantic Ocean.

### Author contributions:

LMG, SR, KR, CBG, and DEF planned the field campaign, conducted field sample collection, and identified shells selected for the AAR analysis. DDR, JB, and DSK processed and analyzed the shell samples, and KR processed and analyzed the AAR results. LMG wrote the initial manuscript, and KR led the AAR writing section. All authors reviewed and edited the manuscript.

### Detailed own contributions:

In this collaborative paper, I was involved in the field expedition where I collected mollusk shells for the AAR dating. After returning from the field, I developed the species identification, created a photographic catalog, and prepared the shell samples to be shipped to the Amino Acid Geochronology Laboratory. After receiving the results, I processed and analyzed them with the assistance of the expert DDR. Finally, I wrote the sections on AAR methodology, results, and discussion, and I also prepared the figures and tables of those sections.

# 1. Introduction

## 1.1. From paleo-sea levels to future sea level rise: Unraveling trends of a warmer world

Future sea level rise poses a potential hazard for populations residing in coastal regions, economies, and ecosystems (Horton et al., 2018). According to the last report of the Intergovernmental Panel on Climate Change (IPCC; 2022), global mean sea level has been increasing at an accelerated rate since the 20th century (from  $1.4 \text{ mm/yr}^{-1}$  to  $3.6 \text{ mm/yr}^{-1}$  between 1901 and 2015). As sea-level projections rely on establishing a strong correlation between sea level and climate forcing, this relationship underscores the need for robust and accurate data spanning different time scales. However, the majority of available instrumental records mainly cover the last 100 years (Holgate et al., 2012; Rovere et al., 2016a; Cipollini et al., 2017). This limited instrumental timeframe captures only one distinctive climate pattern, characterized by rising temperatures and sea levels, a scenario that is climatically mild according to the geological standards. Therefore, geological records offer valuable supplementary data on past sea-level responses to Earth's climate variations (Rovere et al., 2016b; Horton et al., 2018; Khan et al., 2019; Rovere et al., 2020).

Geological proxies from several coastal areas around the globe provide evidence of higher sea levels during the Earth's warm climate intervals, also known as interglacials (Siddall et al., 2007; Raymo et al., 2011; Rovere et al., 2023). Interglacials, including the current Holocene epoch, are the end-members of the glacial cycles and are characterized by elevated temperatures and low land ice extension. Focusing on a sea-level perspective, eleven interglacials in the last 800,000 years provide robust insights into the global past sea-level variability (Berger et al., 2016). Of these, Marine Isotope Stages (MIS) 11 (424 to 395 ka) and 5 (the Last Interglacial; ~125 to 80 ka) are often cited as process analogs of future sea level responses under warmer conditions (Hearty et al., 1999; Roberts et al., 2012; Rovere et al., 2016b; Dumitru et al., 2023). The high  $\text{CO}_2$  concentrations that characterize the MIS 11 led to a warmer atmosphere, driving global mean sea level higher by an estimated ranging from 6 to 13 m above the present (Raymo and Mitrovica, 2012; Chen et al., 2014; Berger et al., 2016), whereas during the Last Interglacial (ca.  $2^\circ\text{C}$  higher than today) sea level were higher by around 5 to 10 m (Wilcox et al., 2020; Fox-Kemper et al., 2023). Although other estimations suggest lower values ( $< 5 \text{ m}$ ), but still higher than present levels (Clark et al., 2020; Dyer et al., 2021; Dumitru et al., 2023).

Nevertheless, sea-level changes are not globally uniform, as relative sea level (RSL) can be influenced by different factors, including eustatic contributors like changes in land ice volume and thermal expansion, as well as isostatic factors related to glacial and hydrological processes (Khan et al., 2015). Other influencing factors can be tectonics, dynamic topography, and local conditions, such as changes in tidal patterns (Horton et al., 2013). These post-depositional displacements need to be considered to achieve reliable spatiotemporal paleo-sea level estimations (Rovere et al., 2016a).

As emphasized by Khan et al. (2019), estimating RSL rates, mechanisms, and spatial variations require a comprehensive and standardized compilation of geological sea-level reconstructions. These standardized datasets must follow a rigorous protocol to discriminate

data and assess the reliability of the RSL reconstructions accounting for all sources of uncertainties (Hijma et al., 2015). Following the approach described by van de Plassche (1986) and Shennan (2015), any geological proxy (landforms, deposits, or biological structures) must have four attributes to serve as sea level indicator: I) a precise geographic location, II) their elevation above/below the present sea level need to be measured, III) their indicative meaning (the relationship between the indicator and the sea level at the time of formation) must be quantified, and IV) its age must be known. Based on this protocol, nowadays, two main databases compile global information on interglacial RSLs: The World Atlas of Last Interglacial Shorelines (WALIS) (Rovere et al., 2023) and HOLSEA (Khan et al., 2019). These databases aim to unify and standardize data reported for the Last Interglacial and Holocene RSLs, respectively. The advantage of such databases lies in the possibility of allowing comparisons across different regions, collecting information on the timing and mechanisms of ice sheet melting scenarios, and ultimately contributing to the improvement of future sea-level rise projections. In this dissertation, we follow the WALIS and HOLSEA templates to fill information gaps concerning sea level dynamics in the southwestern Atlantic (see chapters 3 and 4).

## 1.2. The southwestern Atlantic: An emerging hub for sea level research

The southwestern Atlantic is a large area comprising the coastlines of the countries from Argentina to Venezuela. The exceptional climatic conditions in this vast coastal region, where chemical weathering is reduced, allow the preservation of diverse geological proxies from beach landforms to fixed biological indicators (Danielo, 1976; Angulo and de Souza, 2014; Pappalardo et al., 2015). It is, therefore, not a surprise to find descriptions of these indicators back to the 19<sup>th</sup> century with the descriptions of the marine terraces in Argentina by Charles Darwin during his exploration aboard the Beagle vessel in 1851, and later the first attempts at a sea-level reconstruction in Brazil by Hartt (1870). Even though it wasn't until van Andel and Laborel's research in 1964 that the first radiocarbon dates on the paleo-sea level indicators were presented, allowing a more reliable sea-level estimation. After this geochronological breakthrough, sea level research in the southwestern Atlantic has evolved with several studies investigating more areas and progressively better age control (Tomazelli et al., 2006; Wong et al., 2009; Schellmann and Radtke, 2010; Björck et al., 2021). To the present date, geological proxies dating from the Pliocene to the Holocene have been described by different authors, but no single standardized database exists (Angulo et al., 2006; Schellmann and Radtke, 2010; Pappalardo et al., 2015; Rovere et al., 2020).

From a geodynamic perspective, this coastal sector lies on the South American Plate and is, for the most part, a passive margin, so the tectonic activity is restricted to Venezuela, Pernambuco and Paraíba states in northern Brazil, and Tierra del Fuego, Argentina (Bezerra and Vita-Finzi, 2000; Barreto et al., 2002; Van Daele et al., 2011; Isla and Angulo, 2016). This characteristic simplifies the paleo-sea level reconstructions because these areas experience fewer local changes in land elevation over time, reducing the post-depositional displacements, but despite this, little is known about the state-of-the-art of sea level research in this broad region. The only study that unifies RSL information from Suriname to Argentina is the work of

Milne et al. (2005); this research underscores the low quality of the Holocene RSL data and its numerous uncertainties. In this way, the southwestern Atlantic coastline emerges as a promising domain for future research to enhance our understanding of its paleo-sea level dynamics.

### 1.3. Identifying research gaps

Based on the information in the previous sections, we can conclude that databases play a crucial role in identifying RSL patterns across different spatiotemporal scales. Consequently, they hold the potential for refining projections of sea-level dynamics in a warmer future. Additionally, while the southwest Atlantic is a promising site for sea level research, there are still several aspects in the study of these shorelines that need to be addressed:

1. Numerous researchers have documented paleo shorelines dated to different interglacials, especially from the Pleistocene and Holocene (Tomazelli et al., 2006; Angulo et al., 2016; Wong et al., 2009; Schellmann and Radtke, 2010; Pappalardo et al., 2015). However, this information is typically not presented in a systematic or standardized format that follows the rigorous methodological protocols outlined in the handbook of sea-level research (Shennan, 2015). Therefore, there is the need to evaluate and report the published paleo-sea level data in a structured way; this will allow us to define the state-of-the-art and, moreover, the further improvement of the global sea level estimations during these warm climatic intervals.
2. Determining the elevation of a paleo-sea level indicator is a critical aspect to be measured in the field. Methodological inaccuracies or the incorrect selection of a reference system to establish the altitudes in relation to the sea level, also known as datums (Woodroffe and Barlow, 2015), can significantly impact the calculated paleo-sea level. Generally, it is advisable to survey paleo-sea level indicators using high-precision GPS or leveling techniques (Adebisi et al., 2021). Until very recently, measurements of the indicator elevations in the southwestern Atlantic were conducted with metered rods or less precise leveling tools, or worse; the elevation techniques were not even described in the published papers. This lack of precision meant the necessary accuracy to estimate the paleo RSL could not be achieved. While recent studies employ high-precision survey methods (e.g., Tomazelli et al., 2006; Suguio et al., 2011; Castro et al., 2014; Bini et al., 2018; Angulo et al., 2022; Richiano et al., 2022), these are still largely an exception within this area.
3. The recorded elevation of a sea level indicator doesn't directly correspond to the paleo-sea level. This discrepancy arises because most indicators don't form precisely at mean sea level; instead, they have a quantifiable relationship correlated with that level. As previously described, this quantifiable relationship is known as the indicative meaning (van De Plassche, 1986; Shennan, 2015). Therefore, determining the indicative meaning for each sea level indicator is crucial to associate its elevation with the paleo RSL. However, in

the southwestern Atlantic, the standardized quantifications of the indicative meaning were only recently considered (Schellmann and Radtke, 2010; Martinez and Rojas, 2013; Pappalardo et al., 2015; Rovere et al., 2020), and they need to be applied to both newly collected and reanalyzed data. Without an incorporation of the indicative meaning, the elevation of the paleo-sea level cannot be accurately calculated.

4. The age attribution of many different sea-level indicators poses considerable challenges. However, unraveling the timing and modes of the paleo-sea level without accurate age determination becomes impossible. In the southwestern Atlantic, a longstanding debate revolves around the age of Quaternary shorelines in Argentina (Codignotto et al., 1988; Rutter et al., 1990; Schellmann and Radtke, 2010). The deposits in this region lack commonly used materials for age constraints, such as sediments for luminescence analysis or coral fossils for the U/Th technique. The most frequent paleo-sea level indicators in Argentina are beach ridges rich in marine fossil shells. While some researchers test some methodological modifications to date these fossil remains with electron spin resonance or U/Th series (Schellmann et al., 2008; Pappalardo et al., 2015), some uncertainties remain as mollusk shells are open systems (Schellmann and Radtke, 2010). Moreover, there is also a lack of data to correct the marine reservoir effect in this area, which precludes the recalibration of the Holocene ages (Reimer and Reimer, 2001). On the other hand, in the coastal sector from French Guyana to Venezuela, the geomorphological analysis of the coastal deposits suggests evidence of Last Interglacial transgressive sequences, but the precise age attribution remains unresolved (Audemard, 1996; Wong et al. 2009).
5. Finally, even with precise knowledge of the elevation and age of the paleo-sea level indicators, calculating global mean sea levels (GMSL) requires the estimation and modeling of the post-depositional displacements. Influences such as glacial isostatic adjustment (GIA) (Milne and Mitrovica, 2008; Peltier et al., 2015) or Dynamic Topography (DT) (Austermann et al., 2017) can contribute to several meters of variation in the paleo-sea level estimations. However, these effects are occasionally examined and considered in the Pleistocene and Holocene sea-level quantifications of the southwestern Atlantic (Rostami et al., 2000; Milne et al., 2005; Austermann et al., 2017; Hollyday et al., 2023).

#### 1.4. Motivation, research questions, and hypothesis

Undertaking the effort to summarize the long history of scientific endeavors around the paleo-sea level research in the southwestern Atlantic, coupled with new research efforts to minimize the uncertainties surrounding the previous sea-level reconstructions, could yield a valuable dataset that holds the potential to create a comprehensive pole-to-pole transect of the western Atlantic, once the previously standardized data from the northern hemisphere is integrated (the Caribbean by Khan et al. 2017, and Simms 2021; USA by Englehart and Horton, 2012, and Baril et al., 2023; Canada by Vacci et al., 2018; Greenland by Gowan, 2013; Southern Maine by Kahn et al. 2015). This broad transect would offer the opportunity to refine existing glacial isostatic adjustment models, contribute to unraveling the intricate evolution of ice sheets in a future warmer world, and provide valuable insights to improve global sea level rise estimations.

Here, I outline three research questions aimed at addressing the knowledge gaps identified in section 1.3. These questions are the backbone of the four manuscripts comprising this dissertation:

1. How accurate are Pleistocene and Holocene sea-level data available in the literature for the coasts of the southwestern Atlantic?
2. What are the Holocene patterns and rates of RSL changes? Does this data help better constrain the departures from eustasy caused by glacial isostatic adjustment in MIS 5e?
3. What are the highest possible age and elevation accuracies that can be obtained for MIS 11 and MIS 5e sea-level reconstructions in a coastal site of the southwestern Atlantic?

Based on these research questions and the previous context, the following hypothesis is postulated: We can develop a robust dataset by systematically evaluating and standardizing Pleistocene and Holocene sea-level data along the southwestern Atlantic coast. This dataset, coupled with new research data with precise elevation measurements and age accuracy, has the potential to improve our understanding of the past sea-level variations in this area and to test the former GIA and DT models.

## 2. Methodology

This chapter summarizes the different methodologies used throughout the dissertation. The reader will be referred to the following chapters in each section for an extended explanation.

### 2.1. Sea level database criteria

#### Chapters 3 and 4

Consistent screening criteria for data and metadata were defined and followed during the assessment and standardization of all documented paleo-sea-level indicators to be included in the WALIS and HOLSEA databases. These criteria involved identifying the indicator type, evaluating the surveying methodology employed in the original publication, and standardizing chronological metadata, including recalibration of radiocarbon ages. Subsequently, indicative meanings were recalculated using the established framework outlined in Shennan et al. (2015).

### 2.2. GNSS survey

#### Chapter 5

Global Navigation Satellite Systems (GNSS) were employed to acquire precise horizontal and vertical positions for survey points within the paleo-shorelines (beach ridges) in Camarones, Argentina. This involved utilizing a pair of Emlid REACH RS+ single-band GNSS receivers in a Base-Rover configuration, complemented by handheld Bad Elf GNSS Receivers as a backup (Figure 2.1.A). Due to the remote location of Camarones, real-time kinetic (RTK) corrections were precluded; therefore, the GNSS data needed to be post-processed. Initially, Base Station data underwent online processing using the Canadian Spatial Reference System Precise Point Positioning (CSRS-PPP) tool provided by Natural Resources Canada (NRCan). Following this, Rover data was corrected using the Post Processed Kinematic (PPK) workflow in the software EMLID Studio. To evaluate consistency, a benchmark point called "GPS N°35" located in the proximity of the town of Camarones, was measured (Figure 2.1. B). Ultimately, each surveyed point was converted from ellipsoid to mean sea level.

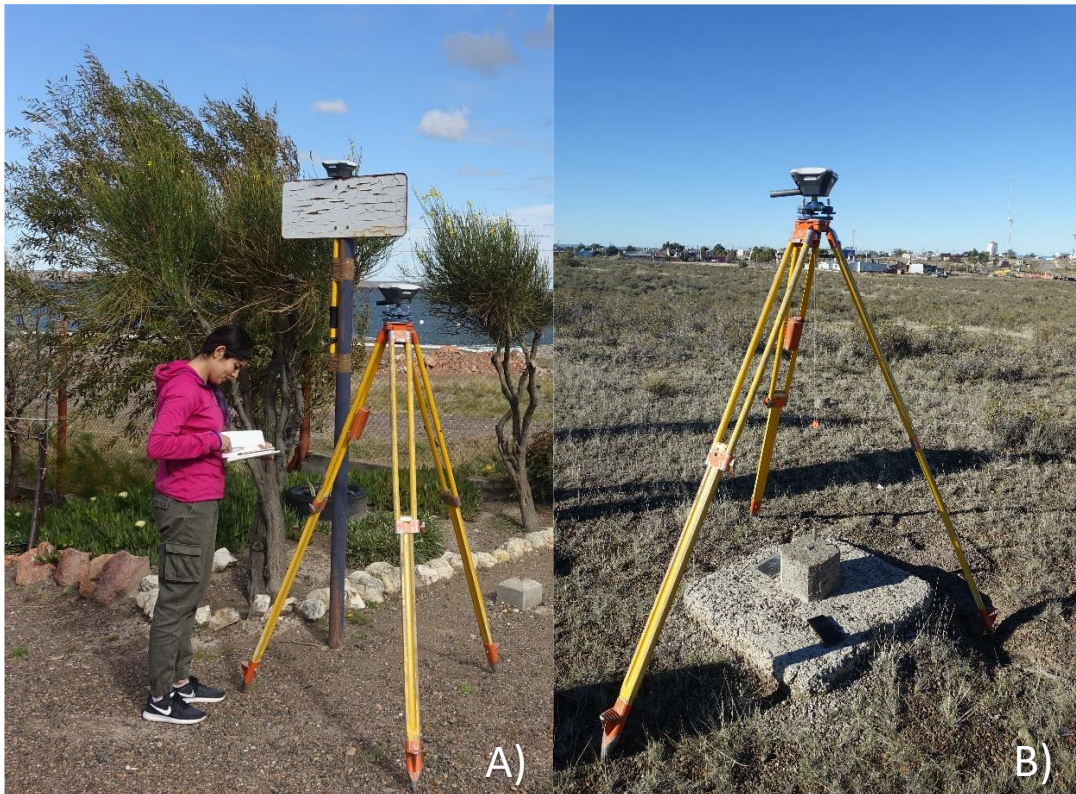


**Figure 2.1.** GNSS receivers. A) Base-Rover GNSS: The base station was located on top of a pole with a full view of the sky and was left static, collecting data for a variable amount of time, including between 5 and 14 hours over five separate deployments (Photo by Sebastian Richiano). B) Survey the "GPS N°35" benchmark point (note the town of Camarones in the background; Photo by Karla Rubio Sandoval).

## 2.3. Models

Different models were used to elucidate the intricate paleo-sea level patterns. Here is a brief description of them:

### 2.3.1. Glacial Isostatic Adjustment Models

Chapters 3, 4, and 5

Three approaches were followed to model the GIA signals in the southwestern Atlantic over different time frames: one model for the Pleistocene patterns and two for the Holocene.

We modeled the GIA-influenced RSL variations for the Pleistocene record through the solution of the gravitationally self-consistent sea-level equation, as Spada and Stocchi (2007) outlined. We employed a solid Earth model that is spherically symmetric and characterized by self-gravitation and rotation. We divided it into shells with a linear Maxwell viscoelastic rheology. The mantle, divided into three layers, undergoes vertical stratification of viscosity in accordance with the VM2 mantle viscosity profile proposed by Peltier (2004). We force our model with the ANICE–SELEN ice sheet chronology, which consists of four ice sheets (North America, Eurasia, Greenland, and Antarctica) and covers the last 410 ka of climate fluctuations

(i.e., four glacial-to-interglacial cycles; de Boer et al., 2014). Specifically, we imposed a global mean sea-level scenario for the Last Interglacial period where the Greenland and Antarctic ice sheets released 2.5 and 1.0 meters of equivalent eustatic sea level, respectively, at 127 ka.

The Holocene sea level data was compared with the ICE6G and PaleoMIST models, computed at 500-year time steps using the SELEN program (Spada and Stocchi, 2007). The model ICE6G includes rotational effects and a sea level equivalent ice volume of 0.9 m for the Patagonian Ice Sheet during the Last Glacial Maximum (LGM) (Peltier et al., 2015). The modification of PaleoMIST has a sea level equivalent ice volume of 0.8 m at the LGM, which decreases to present-day values at 12.5 ka (Gowan et al., 2021).

### 2.3.2. Spatio-Temporal Empirical Hierarchical Model (STEHM)

#### Chapter 4

To derive local RSL curves for each identified area within the HOLSEA database, we utilized the STEHM introduced by Ashe et al. (2019). STEHM operates across three hierarchical levels: 1) a data level, where the model accounts for the variability between the different sea-level index points (SLIPs; the discrete position of past RSL in space and time) with both vertical and temporal noise; 2) a process level, distinguishing RSL changes common across the particular regions; and 3) a hyperparameter level, establishing prior expectations regarding the dominant spatial and temporal scales of RSL variability (Khan et al., 2022).

### 2.3.3. Wave runup models and wave data

#### Chapters 4 and 5

To assess the indicative meaning of beach ridges, we computed wave runup models integrated into the py-wave-runup tool developed by Leaman et al. (2020). The models need input parameters such as beach slope ( $\beta$ ), significant wave height ( $H_s$ ), and period ( $T_p$ ). The beach slope was determined at different transects along the Argentinean coastline utilizing the CoastSat.Slope toolbox introduced by Vos et al. (2019, 2020). Through this toolbox, we conducted an analysis of Landsat and Sentinel satellite data spanning from 2000 to 2023, in conjunction with tides extracted from the FES2014 global tidal model by Lyard et al. (2021) and Carrere et al. (2016). For the computation of  $H_s$  and  $T_p$ , we utilized the RADWave tool developed by Smith et al. (2020), enabling the extraction of satellite altimetry data.

### 2.3.4. Dynamic Topography

#### Chapter 5

We follow the methodology outlined in Hollyday et al. (2023) to model the effects of DT. Therefore, we created a set of mantle convection simulations that mirror the dynamic patterns of the Patagonian slab window and short-wavelength DT behaviors. We utilized various shoreline elevations and residual topography data from nearby oceanic basins to compare data and models, thereby refining solutions for otherwise highly uncertain changes in DT.

## 2.4. Geochronology

### 2.4.1. Radiocarbon

#### Chapters 4, 5, and 6

Radiocarbon dating employs the decay of a carbon isotope, specifically the radioactive isotope  $^{14}\text{C}$ , to assess the age of objects containing carbon-based material. With a half-life of  $5.7 \pm 30$  ka, the detection of  $^{14}\text{C}$  serves as a valuable method for estimating the age of specimens formed within the last 55 ka (Hajdas et al. 2021). As the production of atmospheric radiocarbon has varied through geological time, we recalibrated all radiocarbon ages (new and published) into sidereal years with a  $2\sigma$  range using CALIB software (version 8.2). Marine and estuarine samples were calibrated using the Marine20 curve, while terrestrial samples were calibrated using the Intcal20 and SHcal20 curves (Stuiver and Polach, 1977; Heaton et al., 2020; Reimer et al., 2020; Hogg et al., 2020). Marine reservoir corrections were applied based on the most relevant available data for each study area according to the Marine Reservoir Correction Database (Reimer and Reimer, 2001). To address potential sample contamination of bulk peat samples, a  $\pm 100$  yr error was applied, following the analysis by Hu (2010).

### 2.4.2. Amino Acid Racemization (AAR)

#### Chapters 5 and 6

Amino acids play a crucial role in living organisms, serving as essential protein components and as enzymes that facilitate biochemical reactions (Kvenvolden, 1975). Twenty amino acids commonly occur in the proteins of organisms, but only two forms of these amino acids are possible: L- and D-, which are mirror images of each other (Figure 2.2). An L-amino acid rotates plane-polarized light to the left (levorotary), while a D-amino acid rotates it to the right (dextrorotary) (Kvenvolden, 1975). The proteins found in living animals and plants are predominantly composed of L-amino acids due to enzymes that selectively use the L-form. After the cessation of metabolic processes responsible for maintaining L- and D-

disequilibrium, L-amino acids undergo reversible transformation into D- until an equilibrium mixture of both is achieved; this phenomenon is known as racemization. Therefore, racemization has been directly linked to the time that has elapsed since the organism's death (Kaufman and Manley, 1998).

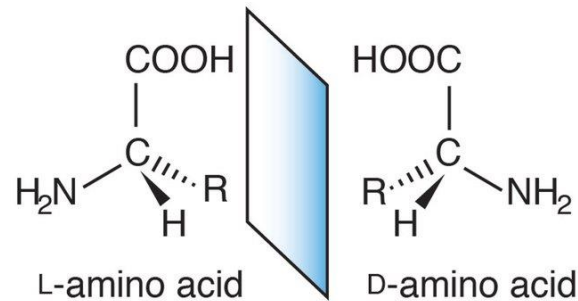


**Figure 2.2.** Generalized L- and D-amino acid enantiomers (Sasabe et al. 2018).

In this dissertation, we use amino acid racemization to evaluate and establish the chronology of coastal deposits from Patagonia, Argentina. Articulated and disarticulated valves of *A. antiqua* (formerly *Prothotaca antiqua*) were gathered from beach ridge deposits. We selected between four and eight shells from each Pleistocene site, considering their robust features, such as the completeness of the valve and minimal signs of wearing, abrasion, or dissolution. Subsampling, sample preparation, and analysis took place at the Amino Acid Geochronology Laboratory at Northern Arizona University. Shells were subsampled at the hinge-umbo region, and the sample preparation and hydrolysis procedures followed the methodology established by Kaufman and Manley (1998). All AAR results underwent data screening to identify and discard D/L values that could compromise the chronology assignment. Aspartic and glutamic acids' D/L values were utilized to evaluate amino acid abundance and variance and establish the relative age.

### 2.4.3. Other geochronological approaches

#### Chapters 3 and 4

U/Th, optically stimulated luminescence (OSL), thermoluminescence (TL), and electron spin resonance (ESR) have been used to determine the chronology of several deposits in the southwestern Atlantic and are mentioned in the literature. Therefore, a brief description of them seems pertinent.

U/Th dating relies on the identification of  $^{234}\text{U}$  and  $^{230}\text{Th}$  through mass spectrometry. The decay process involves  $^{234}\text{U}$  transforming into  $^{230}\text{Th}$ . In U/Th dating, it is crucial to know or calculate the initial ratio of  $^{230}\text{Th}/^{234}\text{U}$  at the time of sample formation, as the determination of the sample's age is based on the difference between the initial ratio and the ratio present in the sample being dated. The methodology assumes the sample remains a closed system, meaning it does not exchange  $^{230}\text{Th}$  or  $^{234}\text{U}$  with the surrounding environment (Hellstrom and Pickering, 2015).

OSL refers to a procedure where a previously irradiated material (exposed to ionizing radiation) emits a light signal in proportion to the absorbed dose when subjected to suitable optical stimulation. This method determines the time elapsed since sediment grains were deposited and protected from subsequent exposure to light or heat, a condition that frequently resets the luminescence signal (Pradhan et al., 2008).

TL dating relies on the capacity of natural minerals to absorb and retain energy from ionizing radiation. When these minerals are heated to a specific high temperature, some stored energy is emitted as light. In the TL dating process, a sample is heated to induce the release of this light, and its measurement helps determine the last time the sample was heated (Pradhan et al., 2008).

ESR dating measures the quantity of unpaired electrons in crystalline structures previously exposed to natural radiation. The age of a material can be determined by assessing the radiation dosage it has received since its formation (Radtke et al., 1988).

### 3. A review of last interglacial sea-level proxies in the western Atlantic and southwestern Caribbean, from Brazil to Honduras

K. Rubio-Sandoval, A. Rovere, C. Cerrone, P. Stocchi, T. Lorscheid, T. Felis, A.K. Petersen, and D.D. Ryan

Originally published in Earth System Science Data (2021), 13(10), 4819-4845.

#### 3.1. Abstract

We use a standardized template for Pleistocene sea-level data to review last interglacial (Marine Isotope Stage 5 – MIS 5) sea-level indicators along the coasts of the western Atlantic and southwestern Caribbean, on a transect spanning from Brazil to Honduras and including the islands of Aruba, Bonaire, and Curaçao. We identified six main types of sea-level indicators (beach deposits, coral reef terraces, lagoonal deposits, marine terraces, *Ophiomorpha* burrows, and tidal notches) and produced 55 standardized data points, each constrained by one or more geochronological methods. Sea-level indicators are well preserved along the Brazilian coasts, providing an almost continuous north-to-south transect. However, this continuity disappears north of the Rio Grande do Norte Brazilian state. According to the sea-level index points (discrete past position of relative sea level in space and time) the paleo-sea level values range from ~ 5.6 to 20 m above sea level (a.s.l.) in the continental sector and from ~ 2 to 10 m a.s.l. in the Caribbean islands. In this paper, we address the uncertainties surrounding these values. From our review, we identify that the coasts of northern Brazil, French Guiana, Suriname, Guyana, and Venezuela would benefit from a renewed study of Pleistocene sea-level indicators, as it was not possible to identify sea-level index points for the last interglacial coastal outcrops of these countries. Future research must also be directed at improving the chronological control at several locations, and several sites would benefit from the re-measurement of sea-level index points using more accurate elevation measurement techniques. The database compiled in this study is available in spreadsheet format at the following link: <https://doi.org/10.5281/zenodo.5516444> (Version 1.02; Rubio-Sandoval et al., 2021).

### 3.2. Introduction

In this paper, we present the results of a literature survey on the last interglacial shorelines (here broadly defined as having formed during Marine Isotope Stage (MIS) 5, 132–80 ka) along the Atlantic coasts of the following countries and territories: Brazil, French Guiana, Suriname, Guyana, Venezuela, Bonaire, Curaçao, Aruba, Colombia, Panama, Costa Rica, Nicaragua, and Honduras. The area covered by this review spans a large latitudinal gradient, including a passive margin (the central southern coasts of Brazil) and areas located within the Caribbean Plate (Figure 3.1). The large geographic span of this review was selected to fill the geographic gap between the existing sea-level compilation of Simms (2021, Mexico and the northwestern Caribbean Sea) and Gowan et al. (2021, Atlantic coasts of Argentina and Uruguay).

While we found reports on Pleistocene shorelines in most of the countries and territories listed above, we could only extract sea-level index points (or marine-/terrestrial-limiting points) for Brazil, Bonaire, Curaçao, and the islands of Providencia and San Andrés in Colombia (Figure 3.1). This was broadly caused by a lack of enough published metadata to allow a proper standardization of sea-level data for the remaining coastal areas.

We used published peer-reviewed scientific papers to compile a database of MIS 5 relative sea-level indicators using the standardized framework of WALIS, the World Atlas of Last Interglacial Shorelines (Rovere et al., 2020). Overall, we report data contained in 36 papers, from which we extracted 50 relative sea-level (RSL) index points, 4 marine-limiting data points, and 1 terrestrial-limiting data point. Age constraints are associated with each geological sea-level proxy using luminescence (n=21), U series (n=48), and electron spin resonance (ESR, n=24) dating techniques. Several outcrops were assigned minimum ages based on limiting radiocarbon ages or other non-radiometric age constraints (e.g., chronostratigraphic correlations). The database is available with open access at this link: <https://doi.org/10.5281/zenodo.5516444> (Version 1.02; Rubio-Sandoval et al., 2021).

In the following sections, we first discuss the elevation measurement methods, sea-level datums, and the main dating techniques used by the original authors. We then describe the sea-level indicators identified in this work by region. We then discuss data quality, processes causing departures from eustasy, and the presence in our area of interest of sea-level index points associated with older Pleistocene interglacials or the Holocene. Finally, we discuss potential future research directions that may be required to improve the quantity and quality of the data contained in our review.

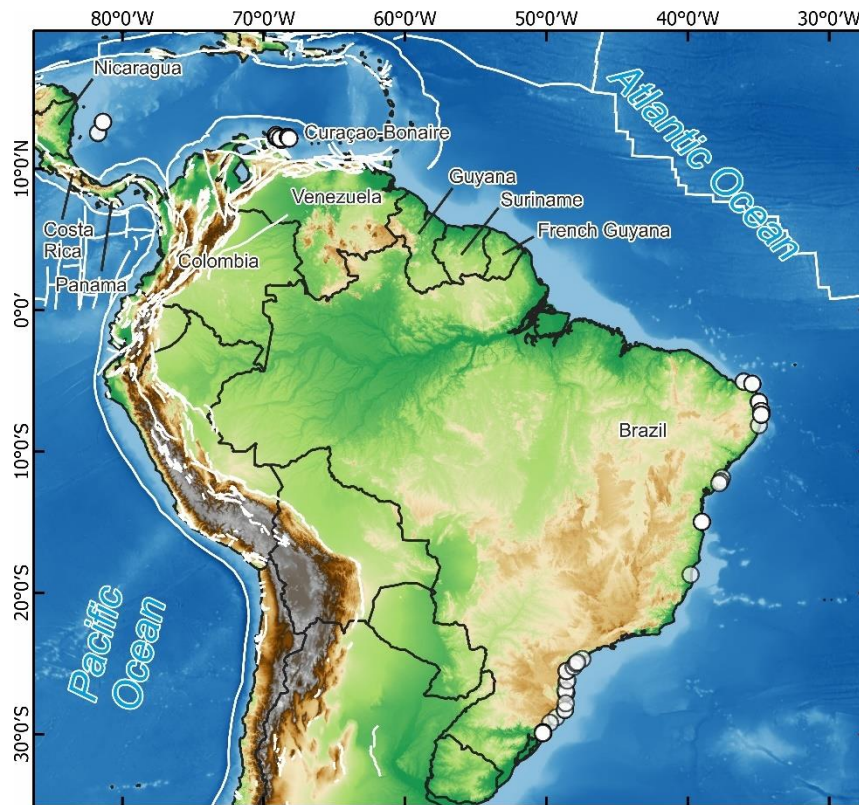


**Figure 3.1.** General overview of the areas surveyed in this study. Dots show the location of sea-level data points inserted in WALIS. White lines indicate the location of active faults and tectonic plate boundaries from the Global Active Faults Database (Styron and Pagani, 2020). Basemap compiled by terrestris (<https://www.terrestris.de>, last access: 18 October 2021), with data from GEBCO (<https://doi.org/10.5285/836f016a-33be-6ddc-e053-6c86abc0788e>), SRTM 30 m by NASA EOSDIS Land Processes Distributed Active Archive Center (LP DAAC, <https://lpdaac.usgs.gov/>, last access: 18 October 2021), and Natural Earth (<http://www.natureearthdata.com>, last access: 18 October 2021).

### 3.3. Types of sea-level indicators

Within the region of interest (Figure 3.1), we identified six main types of sea-level indicators (Table 3.1.). In addition to these, cheniers of a possible last interglacial (LIG) age were reported in French Guiana and Suriname, and beach ridges were described in Venezuela. However, these latter instances were not included in the database due to an overall lack of sufficient information to produce standardized index points at these locations. To correlate each point with a paleo-relative sea level, we applied the concept of indicative meaning that was introduced for Holocene sea-level studies (Shennan, 1982, 1986, 1989; Shennan et al., 1983) and recently also adopted for Pleistocene sea-level index points (Rovere et al., 2016). The indicative meaning “describes the central tendency (reference water level) and 2-sigma vertical range (indicative range) of the indicator’s distribution relative to tidal levels” (Khan et al., 2019). In the database, we calculated the reference water level (RWL) and indicative range (IR) for each sea-level index point either using modern analogs (when reported by the original

study) or applying ex situ quantifications derived from global wave and tide atlases, through the IMCalc tool (Lorscheid and Rovere, 2019).

In Brazil, marine terraces are the most widespread indicator type, although fossil beaches are also common. At several locations in Brazil, sandy sediments are characterized by the presence of the *Ophiomorpha* burrows ichnofacies (Barbosa et al., 1986; Bittencourt et al., 1979; Tomazelli and Dillenburg, 2007). The main observed ichnospecies is *Ophiomorpha nodosa*, which through comparison with burrows left by modern counterparts (*Callianassa major*; Frey et al., 1978) is considered an excellent sea-level indicator. Tomazelli and Dillenburg (2007) indicate that *Ophiomorpha* burrows allow the definition of the average low tide level during the deposition. However, we decided to adopt a more conservative indicative meaning (mean sea level (MSL) to  $-4$  m) as Frey et al. (1978) report that, depending on the geographic region and environmental conditions, the burrows can also be found in shallow subtidal environments.

Several authors described coral reef terraces for the islands of Bonaire, Curaçao, and Aruba, located offshore Venezuela (Alexander, 1961; Schubert and Szabo, 1978; Schellmann et al., 2004). Several sea-level indicators, derived from coral reef terraces, are well preserved on the islands of Bonaire and Curaçao (Muhs et al., 2012; Felis et al., 2015; Obert et al., 2016; Lorscheid et al., 2017). Coral reef terraces are also reported on the Colombian islands of Providencia and San Andrés (Geister, 1972, 1986), located in the Caribbean Sea, offshore Nicaragua. At both islands, the whole reef complex is subdivided into different units according to their topography and ecology (Geister, 1992).

**Table 3.1.** Sea-level indicators in the study area, with reference water level (RWL) and indicative range (IR) quantifications. db denotes breaking depth; ld denotes lagoonal depth; MHHW denotes mean higher high water; MLLW denotes mean lower low water; MSL denotes mean sea level; Ob denotes ordinary berm; SWSH denotes storm wave swash height.

Name of RSL indicator	Description of RSL indicator	RWL	Description of IR	Indicator reference(s)
Beach deposit or beachrock	Definition by Mauz et al. (2015): “Beachrocks are lithified coastal deposits that are organized in sequences of slabs with seaward inclination generally between 5° and 15°”.	(Ob + db)/2	Ob to db	Mauz et al. (2015), Rovere et al. (2016)
Coral reef terrace (general definition)	Coral-built flat surface, corresponding to the area between shallow-water reef terrace and reef crest. The definition of indicative meaning is derived from Rovere et al. (2016), and it represents the broadest possible indicative range that can be refined with information on coral living ranges.	(MLLW + db)/2	MLLW to db	Rovere et al. (2016), Lorscheid and Rovere (2019)
Lagoonal deposit	Lagoonal deposits consist of silty and/or clayey sediments, horizontally laminated (Zecchin et al., 2004) and associated with fossils of brackish or marine water fauna.	(MLLW + ld)/2	MLLW to ld	Rovere et al. (2016), Zecchin et al. (2004)
Marine terrace	Definition by Pirazzoli (2005): “Any relatively flat surface of marine origin.”	(SWSH + db)/2	SWSH to db	Pirazzoli (2005), Rovere et al. (2016)
<i>Ophiomorpha</i> burrow	<i>Ophiomorpha</i> is an ichnogenus that includes burrow structures built on sandy substrates extending from the MSL down to 2 to 4 m below the surface where they divide into horizontal and inclined galleries. The burrows present a broad spectrum of morphologies and environmental distributions, mostly developing in intertidal to very shallow waters.	MSL	MSL to -4 m	Frey et al. (1978), Martins et al. (2018)
Tidal notch	Definition by Antonioli et al. (2015): “Indentations or undercuttings cut into rocky coasts by processes acting in the tidal zone (such as tidal wetting and drying cycles, bioerosion, or mechanical action).”	(MHHW + MLLW)/2	MHHW to MLLW	Antonioli et al. (2015), Rovere et al. (2016)

### 3.4. Positioning and sea-level datums

In general, the majority of studies we reviewed do not report how elevations were measured (Figure 3.2a). Whenever this was the case, we assumed an elevation measurement error equal to 20 % of the elevation reported (Rovere et al., 2016). This was also applied when elevations were derived from cross-section drawings in the original publications. Other elevation measurement methods include differential GPS, metered tape or rod, topographic mapping, and total station (Figure 3.2a). Among these, the most accurate technique is differential GPS, used by Tomazelli and Dillenburg (2007) and Martins et al. (2018) in Brazil to report the elevations for the maximum height of *Ophiomorpha* burrows. Differential GPSs were also used by Muhs et al. (2012) and Lorscheid et al. (2017) in Curaçao and Bonaire, respectively. In this study, we also report new differential GPS elevation measurements taken by Alessio Rovere, Thomas Felis, and Thomas Lorscheid in 2016 on Bonaire at the same sites reported in Felis et al. (2015) and Obert et al. (2016). In northern Brazil, Suguio et al. (2011) used a total station to measure the elevation of different outcrops and referred the measurements to mean sea level using the tide-table predictions from two local stations. This technique also offers a good degree of absolute elevation accuracy ( $\pm 0.1$  m/ $\pm 0.2$  m), depending on the reference point and its distance from the base station. The rest of the elevation measurement methods reported have different degrees of precision depending on the reference object scale.

In Brazil, elevations were referred to different datums, such as mean low water springs (Tomazelli and Dillenburg, 2007), the local geoid (Martins et al., 2018), and local sea-level datums such as the Brazilian Córrego Alegre national datum (Suguio et al., 2011). Similarly, in Curaçao, a variety of datums are used: high tide level (Schellmann et al., 2004), CARIB97, and the locally resolved geoid for the Caribbean Sea (Muhs et al., 2012). The new GPS measurements from Bonaire reported for the first time in this paper are referred to the EGM2008 geoid (Figure 3.2b, Table 3.2).

To obtain the geographic coordinates of the sites, in several cases it was necessary to use Google Earth or to geocode location names to gather latitude and longitude values. Relatively few studies provided site coordinates (Figure 3.2c). Hence, we remark that, for some sites, the coordinates are to be interpreted as merely indicative of the general location of the site.

A review of last interglacial sea-level proxies in the western Atlantic and southwestern Caribbean, from Brazil to Honduras

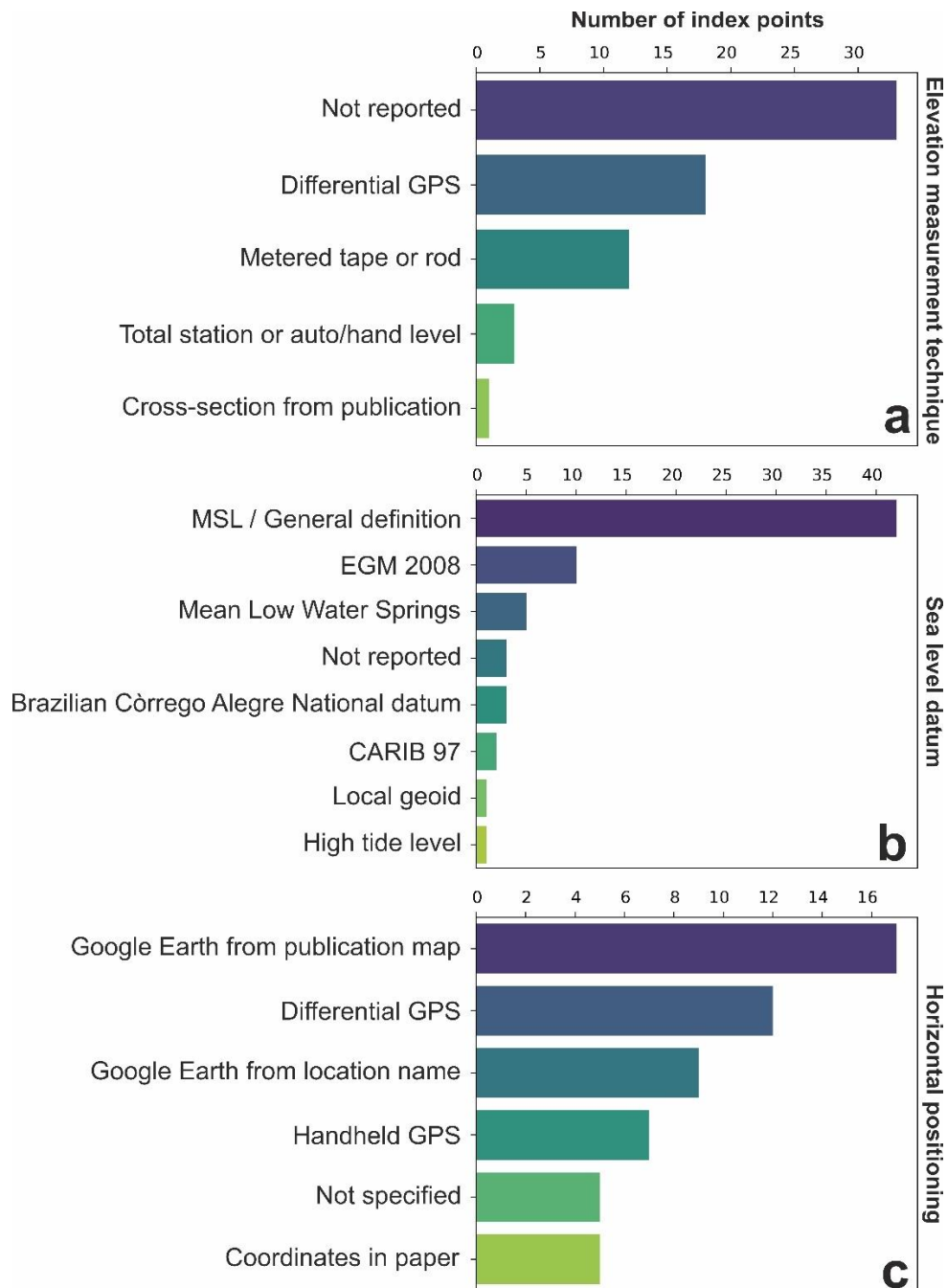


**Figure 3.2.** Frequency of elevation measurement techniques (a), datums (b), and horizontal positioning techniques (c) used in the database.

**Table 3.2.** Elevation datums.

Datum name	Datum description	Datum uncertainty	Reference(s)
Brazilian Córrego Alegre national datum	Local datum for Brazil	Not available	Suguio et al. (2011)
CARIB97	From Smith and Small (1999): “A 2 × 2 arc-minute resolution geoid model, CARIB97, has been computed covering the Caribbean Sea. The geoid undulations refer to the GRS-80 ellipsoid, centered at the ITRF94 (1996.0) origin.”	From the original source: “Comparison of CARIB97 geoid heights to 31 GPS/tidal (ITRF94/local) benchmarks shows an average offset (h–H–N) of 51 cm, with a root mean square (RMS) of 62 cm about the average.”	Smith and Small (1999)
EGM2008	From Pavlis et al. (2012): “EGM2008 is a spherical harmonic model of the Earth’s gravitational potential.”	From Pavlis et al. (2012): “Over areas covered with high-quality gravity data, the discrepancies between EGM2008 geoid undulations and independent GPS/Leveling values are in the order of ±5 cm to ±10 cm.”	Pavlis et al. (2012)
High tide level	Described by Kennedy et al. (2007) as the swash limit and the extent of fixed biological indicators, such as mollusks, having a restricted vertical range.	Per Rees-Jones et al. (2000), accurate to ±2 m up to 15 m a.s.l and ±5 to ±10 m above 15 m a.s.l. Uncertainty will be dependent upon measurement method.	Kennedy et al. (2007), Rees-Jones et al. (2000)
Local geoid	Geoid calculated ad hoc for the surveyed area.	Usually very accurate. A few centimeters.	
Mean low water springs	From Baker and Watkins (1991): “The average of the heights ... of each pair of successive low waters during that period of about 24 hours in each semi-lunation (approximately every 14 days), when the range of the tide is greatest.”	Declared ±0.1 m if datum is derived from 1 year and ±0.25 m if measured over 1 month.	Baker and Watkins (1991)
Mean sea level, general definition	General definition of MSL, with no indications on the datum to which it is referred.	A datum uncertainty may be established on a case-by-case basis.	
Not reported	The sea-level datum is not reported and impossible to derive from metadata.	n/a	

### 3.5. Dating techniques

The last interglacial deposits in the western Atlantic and southwestern Caribbean have been dated using a wide variety of techniques: U series, optically stimulated luminescence (OSL), thermoluminescence (TL), electron spin resonance (ESR), chronostratigraphy, and radiocarbon dates providing minimum ages. The abundance and preservation of corals on the islands Curaçao and Bonaire allow the application of U series to provide reliable age assignments (Muhs et al., 2012; Felis et al., 2015; Obert et al., 2016; Lorscheid et al., 2017). ESR has also been used by Schellmann et al. (2004) to date the coral reef terraces of Curaçao mainly to confirm the age of LIG deposits previously dated with U series by Schubert and Szabo (1978) and to present for the first time radiometric ages for older deposits.

Fossil corals have been preserved only at one site along the Brazilian coast. OSL and TL techniques have been used in different outcrops in northern and southern Brazil to assess the chronology of Pleistocene marine terraces (Poupeau et al., 1988; Barreto et al., 2002; Suguio et al., 2003, 2011; Buchmann and Tomazelli, 2003; Giannini et al., 2007).

## A review of last interglacial sea-level proxies in the western Atlantic and southwestern Caribbean, from Brazil to Honduras

Other age assignments rely on relative dating based on the cross-correlation of outcrops due to the stratigraphic similarities or radiocarbon dates (e.g., Bittencourt et al., 1979; Suguio et al., 1982; Angulo et al., 2002). When an outcrop had only minimum radiocarbon ages (radiocarbon ages above the detection limit), the deposit is considered older than Holocene. There are three chronostratigraphic constraints in Brazil (Barrier III in the Rio Grande do Sul state, the Cananéia Formation in the São Paulo state, and Sector I deposits in the Bahia state; see regional descriptions in Sect. 3.6 for details) and one in Bonaire (lower terrace). In Brazil, the chronostratigraphic constraints are common due to the preservation of Pleistocene deposits and their almost uninterrupted extension along the coastal plain. The Barrier III, Cananéia Formation, and Sector I deposits have been dated using OSL, TL, or U-series techniques and were attributed broader MIS 5 or more detailed MIS 5e ages (Tomazelli and Dillenburger, 2007; Suguio et al., 2003; Martin et al., 1982).

### 3.6. Relative sea-level data

In the following sections, we describe the sea-level indicators in our database divided by country and, where applicable, by lower administrative boundaries (e.g., states, regions, provinces). An overview of the sites, the correlated paleo RSL, and the chronological attribution associated with them are reported in Table 3.3. We refer to the sea-level indicators included in the database with their WALIS RSL ID number, shortened here to RSL ID. This number is included in the first column of the “RSL proxies” spreadsheet within the database and is a unique ID attributed automatically to each data point entered into WALIS.

**Table 3.3.** Proxies compiled in this study. Elevation and paleo RSL errors are reported as  $1\sigma$ ; age uncertainties (where an absolute age is indicated) are  $2\sigma$ . Type of data points: SLI denotes sea-level indicator; TLI denotes terrestrial limiting; MLI denotes marine limiting. Dating techniques are abbreviated as follows: LUM is luminescence; STRAT is chronostratigraphic constraints; Other is other age attribution; U–Th is U series; ESR is electron spin resonance. \* denotes ages recalculated by Chutcharavan and Dutton (2021). For the U-series ages on Bonaire, Brocas et al. (2016) report the following average ages: 1 BON-5-A is  $121\pm 1.1$  ka. 2 BON-26-A is  $124.9\pm 1.9$  ka. 3 BON-24-AII.2 is  $125.5\pm 2.4$  ka. 4 BON-12-A is  $123.9\pm 1.3$  ka.

WALIS RSL ID	Latitude, longitude (°)	Site	Nation (region)	Type of data point	Elevation (m)	Paleo RSL (m)	Dating technique (published sample ID)	Age (ka)
154	-29.928, -50.222	Osório Outcrop 04	Brazil (R.G. do Sul)	SLI	$5.37 \pm 0.6$	$5.62 \pm 0.65$	LUM (RMG-04B) STRAT	> 85.1 MIS 5
155	-29.923, -50.259	Osório Outcrop 05	Brazil (R.G. do Sul)	SLI	$7.72 \pm 0.5$	$7.97 \pm 0.55$	LUM (RMG-04B) STRAT	> 85.1 MIS 5
153	-29.903, -50.233	Osório Outcrop 03	Brazil (R.G. do Sul)	SLI	$7.27 \pm 1$	$7.52 \pm 1.03$	LUM (RMG-04B) STRAT	> 85.1 MIS 5
152	-29.88, -50.233	Osório Outcrop 02	Brazil (R.G. do Sul)	SLI	$5.73 \pm 0.7$	$5.98 \pm 0.74$	LUM (RMG-04B) STRAT	> 85.1 MIS 5
143	-29.862, -50.247	Osório Outcrop 01	Brazil (R.G. do Sul)	SLI	$5.13 \pm 0.7$	$5.38 \pm 0.74$	LUM (RMG-04B) STRAT	> 85.1 MIS 5
1288	-29.193802, -49.754044	Vila Conceição	Brazil (Santa Catarina)	SLI	$9 \pm 5$	$9.18 \pm 5.1$	STRAT	MIS 5
1286	-28.813156, -49.311895	Coqueiros	Brazil (Santa Catarina)	SLI	$12 \pm 2$	$13 \pm 2.23$	STRAT	MIS 5
1300	-28.285437, -48.698703	Guaiúba	Brazil (Santa Catarina)	TLI	$6.5 \pm 1$	–	LUM (G(E)6) LUM (G(E)7)	$129.1 \pm 15$ $103.5 \pm 11.7$
178	-27.8188, -48.6341	Pinheira	Brazil (Santa Catarina)	SLI	$4.5 \pm 0.2$	$6.5 \pm 2$	STRAT	MIS 5
1296	-27.096637, -48.617834	Itapema	Brazil (Santa Catarina)	SLI	$7.35 \pm 1$	$7.32 \pm 1.81$	STRAT	MIS 5
1297	-27.074291, -48.597176	Itapema Plaza Hotel	Brazil (Santa Catarina)	SLI	$7.55 \pm 1$	$7.52 \pm 1.81$	STRAT	MIS 5
1298	-26.922263, -48.643516	Itajaí south of cemetery	Brazil (Santa Catarina)	SLI	$8.68 \pm 1$	$8.64 \pm 1.8$	STRAT	MIS 5

A review of last interglacial sea-level proxies in the western Atlantic and southwestern Caribbean, from Brazil to Honduras

**Table 3.3.** Continued

WALIS RSL ID	Latitude, longitude (°)	Site	Nation (region)	Type of data point	Elevation (m)	Paleo RSL (m)	Dating technique (published sample ID)	Age (ka)
1287	-26.32769, -48.594331	Tapera	Brazil (Santa Catarina)	SLI	11.5 ± 4.6	11.62 ± 4.75	STRAT	MIS 5
179	-26.2133, -48.52361	São Francisco do Sul Island	Brazil (Santa Catarina)	SLI	13.5 ± 3.53	13.58 ± 3.69	STRAT	MIS 5
181	-25.537397, -48.578236	Areal das Ilhas III P 01.06.05	Brazil (Paraná)	SLI	5.5 ± 1	7.5 ± 2.23	Other (CENA-1070) Other (CENA-121)	> MIS 1 > MIS 1
186	-25.245, -48.0783	Canal do Varadouro	Brazil (Paraná)	MLI	4.8 ± 1	–	Other (CENA-121)	> MIS 1
202	-25.00388, -47.919722	Cananéia Island	Brazil (São Paulo)	SLI	7.5 ± 2.06	7.25 ± 2.33	STRAT	MIS 5
203	-24.92055, -47.8275	Comprida Island	Brazil (São Paulo)	SLI	5 ± 1	4.75 ± 1.48	STRAT	MIS 5
1299	-24.679948, -47.464543	Icapara	Brazil (São Paulo)	SLI	9.28 ± 1	9.06 ± 1.56	STRAT	MIS 5
204	-18.711944, -39.804166	São Mateus	Brazil (Esp. Santo)	SLI	8.5 ± 1	8.11 ± 1.7	STRAT	MIS 5e
168	-14.98, -39.003333	Fazenda Jariri	Brazil (Bahia)	SLI	1.27 ± 1	7.77 ± 3.64	U–Th (CP-2) U–Th (CP-1) U–Th (CP-8) U–Th (CP-6) U–Th (CP-7)	116 ± 6.9 122 ± 6.1 124 ± 8.7 132 ± 9 142 ± 9.7
171	-12.25, -37.779	Subaúma	Brazil (Bahia)	SLI	7.3 ± 1	7.27 ± 2.36	STRAT	MIS 5e
170	-12.115, -37.685	Palame	Brazil (Bahia)	SLI	7.3 ± 1	7.27 ± 2.36	STRAT	MIS 5e
169	-11.851, -37.577	Conde	Brazil (Bahia)	SLI	7.3 ± 1	7.27 ± 2.36	STRAT	MIS 5e
218	-8.14555, -34.9708	Lagoa Olhos d'Água Boa Viagem	Brazil (Pernambuco)	SLI	10.39 ± 2.23	10.38 ± 3.15	STRAT	MIS 5e
222	-7.396035, -34.805984	Pitimbu Beach PB17	Brazil (Paraíba)	SLI	5.6 ± 1.5	5.53 ± 2.41	LUM (PB17A) LUM (PB17A) LUM (PB17B) LUM (PB17B)	101 ± 9 100 ± 11 71 ± 7.7 46 ± 4

A review of last interglacial sea-level proxies in the western Atlantic and southwestern Caribbean, from Brazil to Honduras

**Table 3.3.** Continued

WALIS RSL ID	Latitude, longitude (°)	Site	Nation (region)	Type of data point	Elevation (m)	Paleo RSL (m)	Dating technique (published sample ID)	Age (ka)
221	-7.140833, -34.80861	Cabo Branco PB10	Brazil (Paraíba)	SLI	9.8 ± 1.5	11.8 ± 2.5	LUM (PB10A)	108 ± 8
							LUM (PB10A)	110 ± 20
							LUM (PB10B)	138 ± 5
							LUM (PB10B)	120 ± 2
220	-6.490277, -34.969722	Cordosas Beach PB7	Brazil (Paraíba)	SLI	9 ± 1.5	8.99 ± 2.64	LUM (PB07B)	88.9 ± 6
							LUM (PB07B)	70.3 ± 5
							LUM (PB07C)	110 ± 6.2
							LUM (PB07C)	86 ± 5
163	-5.213, -35.433	Touros outcrop	Brazil (R.G. do Norte)	SLI	20 ± 2	19.99 ± 3.03	LUM (32-98)	117 ± 10
							LUM (32-98)	117 ± 10
							LUM (39-98)	110 ± 10
144	-5.056, -36.043	São Bento outcrop	Brazil (R.G. do Norte)	SLI	20 ± 2	19.88 ± 2.99	LUM (32-98)	117 ± 10
							LUM (32-98)	117 ± 10
532	12.052154, -68.747586	Oostpunt	Curaçao	MLI	3.25 ± 0.99	–	ESR (K4010)	112 ± 9
							ESR (K4011)	111 ± 10
537	12.155712, -68.82698	Boca Grandi	Curaçao	SLI	5.5 ± 1.2	6.45 ± 1.46	ESR (K4040)	120 ± 13
							ESR (K4042)	117 ± 9
							ESR (K4043)	116 ± 12
3553	12.235586, -69.104427	Punta Halvedag	Curaçao	SLI	10 ± 0.95	10.98 ± 1.28	U–Th (Cur-Dat-16)	124.8 ± 0.7*
							U–Th (Cur-Dat-17)	129.7 ± 0.6*
							U–Th (Cur-Dat-17-A dup)	131.4 ± 1*
							U–Th (Cur-Dat-17-A)	133.8 ± 0.6*
536	12.157296, -68.829802	Boca Labadera	Curaçao	SLI	5.5 ± 1.2	6.45 ± 1.46	ESR (K4036)	112 ± 9
							ESR (K4037)	120 ± 13
535	12.262312, -69.042612	Boca San Pedro	Curaçao	SLI	6.5 ± 1.39	7.55 ± 1.67	ESR (K4029)	117 ± 12
							ESR (K4031)	118 ± 80
							ESR (K4032)	103 ± 11
							ESR (K4030)	124 ± 13
3563	12.277474, -69.051679	Boca Ascension	Curaçao	MLI	10 ± 2	–	ESR (K4003)	124 ± 8

A review of last interglacial sea-level proxies in the western Atlantic and southwestern Caribbean, from Brazil to Honduras

**Table 3.3.** Continued

WALIS RSL ID	Latitude, longitude (°)	Site	Nation (region)	Type of data point	Elevation (m)	Paleo RSL (m)	Dating technique (published sample ID)	Age (ka)
3554	12.339078, -69.153554	Knipbai	Curaçao	MLI	3 ± 1.37	–	U–Th (Cur-Dat-5)	124 ± 0.5*
							U–Th (Cur-Dat-5-P)	127 ± 0.6*
533	12.373829, -69.125355	Boca Cortalein	Curaçao	SLI	10 ± 2	11.05 ± 2.2	U–Th (Cur-Dat-1-A)	128 ± 1.1*
							U–Th (Cur-Dat-1)	128.1 ± 0.9*
							ESR (K4019)	123 ± 9
							ESR (K4020)	125 ± 11
						ESR (K4021)	118 ± 8	
3559	12.378402, -69.132382	Boca Mansaliña	Curaçao	SLI	7.5 ± 1.58	8.55 ± 1.83	U–Th (Cur-Dat-4)	126.4 ± 0.6*
							U–Th (Cur-Dat-4 dup)	126.7 ± 0.8*
							ESR (K4049)	118 ± 9
534	12.385825, -69.141518	Dos Bocas	Curaçao	SLI	10 ± 2	11.05 ± 2.2	ESR (K4024)	120 ± 11
							ESR (K4025)	116 ± 19
							ESR (K4026)	113 ± 10
531	12.387517, -69.144038	Un Boca	Curaçao	SLI	10 ± 2	11.05 ± 2.2	U–Th (Cur-33-d)	118.8 ± 0.8*
							U–Th (Cur-32)	128 ± 7
							U–Th (Cur-33)	127 ± 7
							U–Th (Cur-32-d)	133.1 ± 0.8*
							ESR (K4006)	116 ± 11
							ESR (K4007)	124 ± 11
							ESR (K4009a)	140 ± 9
							ESR (K4009b)	108 ± 8
ESR (K4009b1)	101 ± 7							
694	12.156163, -68.207258	South of Boca Washikemba	Bonaire	SLI	5.19 ± 0.28	6.22 ± 0.95	U–Th (BON-5-A, Bulk)1	120 ± 1.8
							U–Th (BON-5-A, Theca)1	118.9 ± 2
							U–Th (BON-5-A, Bulk)1	122.5 ± 1.7
							U–Th (BON-5-A, Theca)1	121.3 ± 1.8
							U–Th (BON-5-A, Theca)1	120.1 ± 2.4
							U–Th (BON-5-A, Theca)1	119.4 ± 2.7
							U–Th (BON-5-D)	117.7 ± 0.8
1369	12.20234, -68.310734	Notch 1	Bonaire	SLI	6.66 ± 0.18	6.66 ± 0.31	STRAT	MIS 5e
1370	12.204183, -68.312796	Notch 2	Bonaire	SLI	6.61 ± 0.11	6.61 ± 0.28	STRAT	MIS 5e
1371	12.206776, -68.316292	Notch 3	Bonaire	SLI	6.96 ± 0.15	6.96 ± 0.3	STRAT	MIS 5e

A review of last interglacial sea-level proxies in the western Atlantic and southwestern Caribbean, from Brazil to Honduras

**Table 3.3.** Continued

WALIS RSL ID	Latitude, longitude (°)	Site	Nation (region)	Type of data point	Elevation (m)	Paleo RSL (m)	Dating technique (published sample ID)	Age (ka)
1372	12.2104, -68.321163	Notch 4	Bonaire	SLI	6.83 ± 0.15	6.83 ± 0.3	STRAT	MIS 5e
1373	12.211271, -68.323699	Notch 5	Bonaire	SLI	7.21 ± 0.17	7.21 ± 0.31	STRAT	MIS 5e
1374	12.215117, -68.335901	Notch 6	Bonaire	SLI	7.26 ± 0.12	7.26 ± 0.28	STRAT	MIS 5e
693	12.237155, -68.285762	Boca Olivia	Bonaire	SLI	8.84 ± 0.27	9.87 ± 0.95	U-Th (BON-26-A, Theca)2	126.1 ± 2.3
							U-Th (BON-24-AII.2 Bulk)3	126.7 ± 0.97
							U-Th (BON-24-AII.2 Theca)3	122.6 ± 1.9
							U-Th (BON-26-A, Theca)2	124.2 ± 1.5
							U-Th (BON-24-AII.2 Theca)3	125.9 ± 1.8
							U-Th (BON-24-AII.2 Bulk)3	128.2 ± 2
							U-Th (BON-17-AI, Theca)	121.72 ± 0.91
692	12.247984, -68.296485	South of Boca Onima	Bonaire	SLI	5.72 ± 0.3	6.75 ± 0.96	U-Th (BON-17-AI, Theca)	122.4 ± 1.7
							U-Th (BON-17-AI, Theca)	124.2 ± 1.8
							U-Th (BON-17-AI, Theca)	124.9 ± 2.2
							U-Th (BON-12-A, Bulk)4	124.68 ± 0.98
							U-Th (BON-12-A, Theca)4	122 ± 1.6
							U-Th (BON-13-AI.1, Theca)	125.8 ± 1.6
							U-Th (BON-12-A, Bulk)4	124.8 ± 1.6
							U-Th (BON-12-A, Theca)4	123.6 ± 1.6
							U-Th (BON-33-BI.2, Theca)	129.7 ± 1.7
							3472	12.270639, -68.342514

**Table 3.3.** Continued

WALIS RSL ID	Latitude, longitude (°)	Site	Nation (region)	Type of data point	Elevation (m)	Paleo RSL (m)	Dating technique (published sample ID)	Age (ka)
3681	12.524347, -81.729865	San Andrés, Southwest Cove	Colombia (San Andrés and Providencia)	SLI	1.5 ± 0.5	4.5 ± 2.06	Other (Ge 72, 3769A)	> MIS 1
3682	12.556155, -81.731978	San Andrés, May Cliff	Colombia (San Andrés and Providencia)	SLI	6 ± 0.5	12 ± 4.03	Other (Ge 72, 4109)	> MIS 1
950	13.321004, -81.387253	Providencia, South Point	Colombia (San Andrés and Providencia)	SLI	3 ± 1.5	13 ± 10.11	U–Th Other (Ge 92)	118.8 ± 35.64 > MIS 1
3683	13.324392, -81.376752	Providencia, South Point	Colombia (San Andrés and Providencia)	SLI	1.8 ± 0.5	21.8 ± 20	U–Th  Other (Ge 72, 4110 a) Other (Ge 72, 4110 b)	118.8 ± 35.64  > MIS 1 > MIS 1

### 3.6.1. Brazil

Studies describing the marine deposits in Brazil date back to the late 1800s (Hartt and Agassiz, 1870). In the early 1970s, the study of Quaternary coastal deposits began with Suguio and Petri (1973) describing the Iguape–Cananéia lagoonal region at the border between the regions of São Paulo and Paraná (Figure 3.3). Later, the stratigraphic units of the state of Bahia were analyzed by Bittencourt et al. (1979) and further by Martin et al. (1982) and Bernat et al. (1983). These authors gathered new information on past sea-level changes and their meaning in the context of tectonic deformations. In the 1980s and 1990s, the exploration of Pleistocene deposits was extended to the states neighboring Bahia. In the south, Pleistocene outcrops were reported in Espírito Santo (Suguio et al., 1982), Rio de Janeiro (Martin et al., 1986, 1998), São Paulo (Suguio and Martin, 1995), and on the southern border of Brazil at Rio Grande do Sul (Villwock, 1984; Poupeau et al., 1988). To the north, studies focussed on the states of Sergipe (Bittencourt et al., 1983), Alagoas (Bittencourt et al., 1983; Barbosa et al., 1986), and Pernambuco (Martin et al., 1986; Dominguez et al., 1990). Most published papers presented data related to the Quaternary transgressive history of Brazil, describing the so-called “Penultimate Transgression” (called the “Cananéia Transgression” in the São Paulo state), attributed to MIS 5e (~120 ka). The main highstand of this transgression was reported at an elevation of ca. 8 m above sea level (a.s.l.). In general, the study of the Last Interglacial in Brazil is hindered by the small number of reliable chronological constraints. Therefore, the most recent studies were directed to use radiometric dating techniques (such as OSL or TL) to establish radiometric ages for Pleistocene deposits (Barreto et al., 2002; Buchmann and Tomazelli, 2003; Suguio et al., 2003; Tomazelli and Dillenburg, 2007; Rossetti et al., 2011; Suguio et al., 2011; Bezerra et al., 2015).

## A review of last interglacial sea-level proxies in the western Atlantic and southwestern Caribbean, from Brazil to Honduras

The collective effort from these researchers over the years has made possible the knowledge of the Brazilian coastal plain geomorphological history and the description of the Pleistocene sea-level changes, preserved mostly in the form of beach and coastal deposits. According to the literature, the last interglacial sequences are present almost continuously on a north–south gradient from Rio Grande do Sul to Rio Grande do Norte, leaving only eroded remains in the most northern states (Figure 3.3). Listed below are the published descriptions of the LIG deposits in this country, divided by administrative units (states).

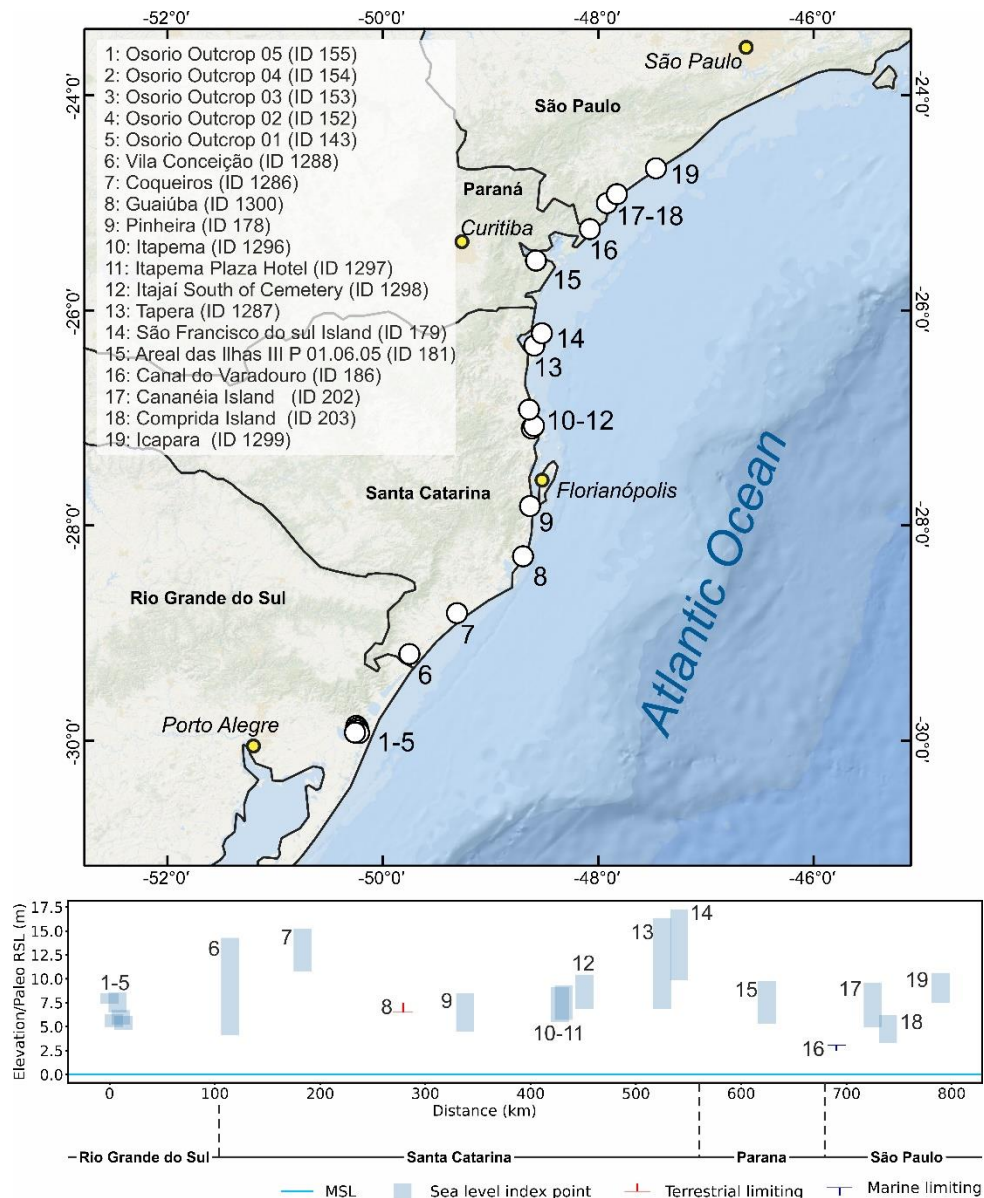


**Figure 3.3.** Last interglacial sea-level data in the Brazilian states of Rio Grande do Sul, Santa Catarina, Paraná, and São Paulo. Upper panel: map of sites. Basemap: Esri, Garmin, GEBCO, NOAA NGDC (now NCEI), and other contributors. Lower panel: distance–elevation plot.

### 3.6.1.1. Rio Grande do Sul

Villwock (1984) and Tomazelli et al. (2006) described a system of Pleistocene lagoon barriers sub-parallel to the modern coast throughout the Rio Grande do Sul coastal area. Among these barriers (named I, II, and III), Barrier III is the best preserved and has an almost continuous extension between the cities of Tramandaí (to the north) and Chuí (to the south). This barrier was associated with the LIG transgression because it occurs at the back of the Holocene lagoon-barrier system (Tomazelli et al., 2006). Tomazelli and Dillenburg (2007) re-assessed the age and elevations of Barrier III deposits at Osório, describing five outcrops of foreshore sands with abundant *Ophiomorpha* ichnofossils (RSL IDs 143 and 152 to 155) (Figure 3.3). The deposits are 4–5 m thick, and their reported elevations refer to the maximum elevation of *Ophiomorpha* burrows, ranging from  $5.13 \pm 0.7$  to  $7.72 \pm 0.5$  m above mean low water springs (elevations measured with differential GPS). The authors recognize that there are limited chronological data for these outcrops but highlight that a minimum age for the foreshore deposits is available for one of the sites, where coastal dunes covering the foreshore sands were dated with TL to 85 ka (Poupeau et al., 1988). Buchmann and Tomazelli (2003) used TL to date a similar foreshore deposit at Bujuru (Conceição Lighthouse) to  $109 \pm 7.5$  ka. One photo in Dillenburg et al. (2009) (their Figure 3.16) shows that this outcrop is possibly located a few meters above the modern sea level. In our literature survey, we were not able to find further details on the luminescence age reported by this study or on elevation measurements of this outcrop; therefore we do not include it in our database.

### 3.6.1.2. Santa Catarina

In the state of Santa Catarina, deposits correlated with Barrier III deposits of Rio Grande do Sul (lagoon and barrier facies) were reported in a series of 1 : 100 000 geomorphological maps (Horn Filho et al., 2014, and references therein). The deposits are mapped as widespread across the coastal plain. A geological field trip guide by Horn Filho et al. (2017) describes Upper Pleistocene lagoonal/beach deposits at three sites: Vila Conceição (RSL ID 1288), Coqueiros (RSL ID 1286), and Tapera (RSL ID 1287). These three outcrops are located at elevations of 9–12 m a.s.l., but their elevations are bounded by large uncertainties as it is unclear how they were measured (Figure 3.3).

More accurate elevation measurements are available in recent work by Martins et al. (2018). These authors investigated *Ophiomorpha* burrows within Barrier III deposits at Pinheira (RSL ID 178). They used differential GPS to measure the top of *Ophiomorpha* at 4.5 m a.s.l. (Figure 3.3).

Another site where beach/shallow marine (occasionally with *Ophiomorpha* burrows) deposits occur is São Francisco do Sul Island, located on the northern coast of the Santa Catarina state (Horn Filho and Simó, 2008). These deposits were reported at 10–17 m a.s.l. (RSL ID 179) but were assigned, in our database, as low quality due to uncertainties in their location and elevation. A detailed map (1 : 10 000) of the coastal deposits on São Francisco do Sul Island shows the distribution of Pleistocene lagoonal and beach deposits in this area (Horn

Filho and Vieira, 2017). Accurate elevation measurements of these units will help to shed light on the correlation of these deposits with other sea-level indicators in the Santa Catarina state.

Summarizing the sandy marine terraces on the Santa Catarina state coast, Martin et al. (1988) report three additional sites attributed broadly to MIS 5: two at Itapema and one at Itajaí (RSL IDs 1296 to 1298). These are located at 6–8 m a.s.l. (Figure 3.3).

Approximately 8 km south of Imbituba, Giannini et al. (2007) used OSL to date deposits associated with “alluvial-eolian deflation” and “eolian accumulation” facies. These deposits yielded ages of  $129.1 \pm 15$  ka and  $103.5 \pm 11.7$  ka, respectively. The deflation facies is located at a lower elevation (6.5 m a.s.l.) than the accumulation facies and was inserted into WALIS (RSL ID 1300) as a terrestrial-limiting point.

### 3.6.1.3. Paraná

In the state of Paraná, Branco et al. (2010) report a Pleistocene barrier at elevations between 5 and 10 m a.s.l. Among 19 stratigraphic sections, they report the presence of *Ophiomorpha* burrows at Section P 01.06.05 (RSL ID 181) at 5.5 m a.s.l. (Figure 3.3).

Angulo et al. (2002) describe a marine terrace deposited on an estuarine paleo-channel in Canal do Varadouro (RSL ID 186) (Figure 3.3). The sediments are approximately 1 m thick and have an undulated lamination, suggesting that they formed within an intertidal environment. The reported elevation is 4 m above the current high tide level (4.8 m a.s.l.). For both sites in the state of Paraná, only minimum ages are available.

### 3.6.1.4. São Paulo

In the southern part of the São Paulo state, the Pleistocene Cananéia Formation (a sandy coastal unit first described by Suguio and Petri, 1973) is reported in the Iguape–Cananéia lagoon region on Cananéia and Comprida islands (Figure 3.3). The formation is capped by a member characterized by sands with *Ophiomorpha* burrows (Martin and Suguio, 1976). This formation was initially considered MIS 5 based on minimum radiocarbon ages (Martin and Suguio, 1976), an age later confirmed by OSL and TL ages of 94 ka (average age from Watanabe et al., 1997), and  $81.55 \pm 4.5$  ka (average age from Suguio et al., 2003). We identified two (poorly constrained) sea-level index points on Cananéia and Comprida islands (RSL IDs 202, 203). Both data points are derived from Martin and Suguio (1976). From the description in the paper, we interpreted them as marine terraces. On Cananéia Island, the Cananéia Formation is located between 5–6 and 9–10 m a.s.l. On Comprida Island, the altitudes vary from 2.5 to 3 m a.s.l. in the south and from 5 to 6 m a.s.l. in the north. As this difference is related to differential erosion to which the area was subject during the Holocene transgressive phase, we used the highest occurrence of the terrace as the reported elevation.

A cross-section in Martin et al. (1988) reports another sea-level indicator associated with the Cananéia Formation close to Icapara (RSL ID 1299) at 8.5 m above high tide (Figure 3.3).

#### 3.6.1.5. Rio de Janeiro

Martin et al. (1998) describe Pleistocene beach barriers and sandy terraces in the Rio de Janeiro state. These are located at 6–8 m a.s.l. (Isla and Angulo, 2016) and have been assigned to the Last Interglacial based on infinite radiocarbon ages. As no details on sea-level indicators are available for these terraces, we did not insert them into WALIS.

#### 3.6.1.6. Espírito Santo

Suguio et al. (1982) studied the area near the Doce River mouth in the state of Espírito Santo. The authors describe the Pleistocene marine terraces which created an almost-continuous strip of 4 km along the north section of the coastal plain. In the São Mateus area, these marine terraces reach a height of 9 to 10 m a.s.l. datum (RSL ID 204) (Figure 3.4), while to the south (close to the river entrance) the elevation ranges from 6 to 10 m and the terrace loses its continuity as a result of the erosive effect of the Holocene transgression. The authors did not present specific ages for these deposits but assume a stratigraphic correlation with those of the neighboring state Bahia (see below), which indicates deposition during the LIG.

A review of last interglacial sea-level proxies in the western Atlantic and southwestern Caribbean, from Brazil to Honduras

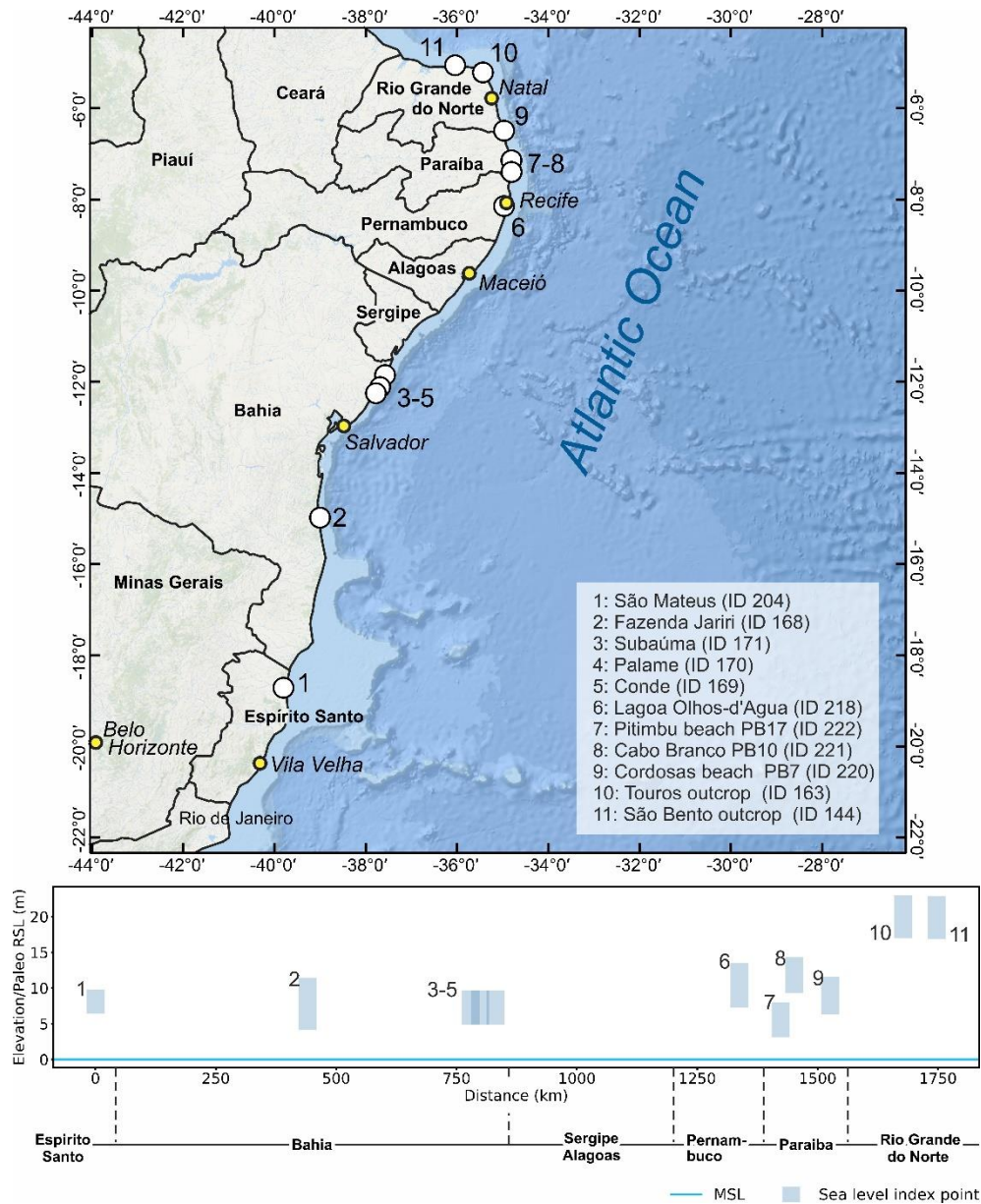


**Figure 3.4.** Last interglacial sea-level data in the Brazilian states of Espírito Santo, Bahia, Pernambuco, Paraíba, and Rio Grande do Norte. Upper panel: map of sites. Basemap: Esri, Garmin, GEBCO, NOAA NGDC (now NCEI), and other contributors. Lower panel: distance–elevation plot.

### 3.6.1.7. Bahia

In the state of Bahia, Martin et al. (1982) identified a fossil coral reef at “Fazenda Jariri” at an elevation corresponding to the modern high tide mark ( $1.27 \pm 1$  m a.s.l.; RSL ID 168) (Figure 3.4). They sampled 15 *Siderastrea* spp. corals, most likely, the species *Siderastrea stellata*, which is endemic to the coasts of Brazil and is reported as a primary bioconstructor in the shallow-water reefs in this area (Laborel, 1970). *S. stellata* is common in intertidal pools (de Oliveira Soares et al., 2017) with an average living range constrained between  $-3$  and  $-10$  m depth (Segal and Castro, 2000). We used these values as upper and lower limits,

respectively, of the indicative range to calculate paleo RSL for this site at  $7.8 \pm 3.6$  m. These corals yielded (alpha-counting) U-series ages between  $116 \pm 6.9$  and  $142 \pm 9.7$  ka.

Another three sites in the Bahia state are reported by Bittencourt et al. (1979): Conde, Palame, and Subaúma (RSL IDs 169, 170, 171) (Figure 3.4). At these sites, the authors report that “the remnants of the penultimate transgression are indicated by a sand terrace, the top of which is situated 6 m above high tide level”. These deposits are associated with the so-called “Bahia Sector I” stratigraphy, which is attributed to MIS 5e thanks to the ages of Martin et al. (1982).

#### 3.6.1.8. Sergipe and Alagoas

To complement the work carried out by Bittencourt et al. (1979), Bittencourt et al. (1983) analyzed the Pleistocene marine terraces deposited in the Sergipe state and south of the state of Alagoas. According to the authors, these sandy marine terraces present the same sedimentological and geomorphological characteristics as those observed in Bahia (Sect. 5.1.7). Therefore, the deposits can be inferred as spatially continuous from Bahia to Sergipe and Alagoas states (Barbosa et al., 1986). While the interglacial terraces are presented in maps within these publications, no precise location information is given; therefore these data were not inserted into WALIS.

#### 3.6.1.9. Pernambuco

The Pleistocene marine terraces in the state of Pernambuco were described by Dominguez et al. (1990). Their elevations range from 7 to 11 m above the present high tide level; some outcrops show traces of ancient beach ridges in the region between Lagoa Olhos d'Agua and Boa Viagem (RSL ID 218) (Figure 3.4). These terraces have similar sedimentological characteristics as those described in the states of Alagoas, Sergipe, and Bahia, suggesting a depositional continuity; however, in Pernambuco they are mostly present in small patches, arranged discontinuously along the coast. There are no absolute ages for the region, but these deposits are correlated with those in the state of Bahia (Dominguez et al., 1990).

There are indications of additional MIS 5 marine-associated deposits within the Pernambuco state. Suguio et al. (2005) and later Suguio et al. (2011) reported MIS 5 TL and OSL ages for sands that could be either marine or eolian in origin. Pending further clarifications on these deposits, we did not insert them into WALIS. On the island of Fernando de Noronha, eolianites within Unit I of the Pleistocene Caracas Formation (Almeida, 1955) returned minimum radiocarbon ages of 50 000 years BP (Angulo et al., 2013). The poor constraint on age and location has precluded entry of these deposits into WALIS.

#### 3.6.1.10. Paraíba

Suguio et al. (2005, 2011) described Late Pleistocene marine terraces in the Paraíba state and dated them using TL and OSL techniques. Information to derive index points is given for only three of the nine dated outcrops. Two samples collected above 4.1 ± 1.5 m a.s.l. at Pitimbu Beach (Figure 3.4) (RSL ID 220) yield TL ages of 101 ± 9 ka (PB17A) and 71 ± 7.7 ka (PB17B) and OSL ages of 100 ± 11 ka (PB17A) and 46 ± 4 ka (PB17B). These samples were collected from a massive sandstone unit, overlying a planar cross-stratification in sandstone. As no further details are given in the original papers, we interpret these sediments as part of a marine terrace and assign this data point a large indicative range. A unit composed of loose sands was dated at Cordosas Beach (RSL ID 222) and yielded TL ages of 88.96 ka (PB07B) and 110 ± 6.2 ka (PB07C) and OSL ages of 70.3 ± 5 ka (PB07B) and 86 ± 5 ka (PB07C). The best described among the outcrops of Suguio et al. (2011) is the one at Cabo Branco cliff (RSL ID 221) (Figure 3.4). Here, at 9.8 m a.s.l., a sandstone facies is characterized by planar cross-stratification and *Ophiomorpha* burrows. This deposit yielded a TL age of 138 ± 5 ka and an OSL age of 120 ± 2 ka (sample PB10B). A sandstone unit immediately above the location where these samples were taken (sample PB10A) was dated 108 ± 8 ka (TL) and 110 ± 20 ka (OSL).

#### 3.6.1.11. Rio Grande do Norte

Barreto et al. (2002) described two distinct marine terraces in the state of Rio Grande do Norte. The sediments of these terraces were grouped into two stratigraphic units, dated to 220–206 and 117–110 ka with luminescence techniques. The younger 117–110 ka marine terrace deposit is preserved for about 120 km along the E–W coast and was associated with the highstand of MIS 5e. Two outcrops of this terrace, between São Bento and Touros, were described (RSL IDs 144, 163). The elevations of the shallow-water facies reported by Barreto et al. (2002) range from 1–10 m a.s.l. and 2 km north of the town of Zumbi rise to a maximum of 20 m (Figure 3.4). Therefore, the authors suggested a regional tectonic uplift by 10–12 m (considering the mean reported MIS 5e highstand of Brazil: 8 ± 2 m a.s.l.; Barreto et al., 2002).

#### 3.6.1.12. Amapá

In the northernmost states of Brazil, information on Pleistocene marine deposits was generally lacking until the recent work of Bezerra et al. (2015) in the state of Amapá. These authors define the Pleistocene “Itaubal Formation” and subdivide it into two progradational units (upper and lower), separated by an unconformity. Using OSL ages, the Itaубal lower unit was constrained to MIS 5 (120 to 71 ka). Detailed facies analysis along several outcrops allowed Bezerra et al. (2015) to assert that the Itaубal lower unit is representative of “subtidal and tide-influenced meandering stream and floodplain deposits”. While this study presents accurate chronological data and detailed facies analysis of the lower unit, it is not possible to insert any index point into the database due to the lack of any absolute elevation measurements constrained to the modern sea level (only outcrop thickness is

reported). However, we remark that this area looks promising for future research, especially because of the limited number of LIG deposits preserved in northern Brazil.

### 3.6.2. French Guiana, Suriname, and Guyana

French Guiana, Suriname, and Guyana share a very similar geological setting. Along the coasts of these three countries, different authors report the presence of littoral deposits that were emplaced by previous sea-level highstands (Brinkman and Pons, 1968; Iriondo, 2013). These deposits were studied by Choubert (1956) and Boyé and Cruys (1961), who described a unit made of sands and clays parallel to the shoreline that was initially attributed to the Riss-Würm (MIS 5) transgressive event. In French Guiana and Suriname, similar sedimentological facies are named the “Coswine Series” and “Coropina Series”, respectively. Brinkman and Pons (1968) propose that the Coswine and Coropina series are divided into two members, the Para Member (attributed to the Middle Pleistocene) and the Lelydorp Member (attributed to the Eemian interglacial, MIS 5e). These authors suggest that the Lelydorp Member outcrops between the towns of Cayenne and Organabo in French Guiana and the district of Coronie in Suriname.

The attribution of the Lelydorp member to MIS 5e was due to a radiocarbon date above the detection limit considered a minimum age by Brinkman and Pons (1968) (48 000 years BP, sample ID GRN 4718). Wong (1992) continued with the study of this region publishing “the Quaternary stratigraphy of Suriname”, in which he addressed the problem related to the chronological assignment of these eroded and weathered records. Wong et al. (2009) used paleomagnetic data to estimate ages along the Suriname coastal plain. The results suggest that the Lelydorp Member is of Early Pleistocene age, hence much older than hitherto assumed. Due to the lack of precise chronologic constraints, and with the work of Wong et al. (2009) essentially pre-dating the units previously assumed to be of last interglacial age, no data have been inserted in WALIS for French Guiana, Guyana, and Suriname.

### 3.6.3. Venezuela

The Pleistocene marine deposits of Venezuela are well known and have been extensively described by Bermudez and Farias (1975). As early as the late 1700s, Humboldt remarked upon formations now recognized as Pleistocene age within the state of Sucre (Bermudez and Farias, 1975). A couple of centuries later, Bermudez (1969) presented a detailed account of the Quaternary and recent stratigraphy of Venezuela. In this study, the author mentions Pleistocene marine units on Cabo Blanco (state of Miranda); on the south coast of the island of Tortuga; and on the islands Cubagua, Coche, and Margarita. In Cabo Blanco, Bermudez (1969) describes Pleistocene “raised beaches”, located at 62 m a.s.l. Danielo (1976) worked on the northern coasts of Venezuela and reported the presence of several Pleistocene beach deposits on the Araya and Paraguaná peninsulas, as well as in Puerto Cumareboy and Margarita regions. Among the different sea-level proxies on the northern coasts of Venezuela identified by the author, it appears that two would correlate

with MIS 5, notably the so-called “Tyrrhénien I” (25–30 m) and the “Oujien” (6–8 m). Unfortunately, there is no dating associated with these deposits, therefore they could not be included in our database.

The Paraguaná Peninsula is one of the most studied sites in Venezuela that concerns Quaternary outcrops. Here, Rey (1996), described a 1.7 m thick conglomeratic sequence containing fragments of mollusks and foraminifera. The author interprets the depositional environment as that of a high-energy beach and reports that this unit cannot be older than the Pleistocene due to the presence of the marine foraminifera *Globorotalia truncatulinoides*. Audemard (1996a, b) reported several Pleistocene coastal outcrops along the Paraguaná Peninsula. On the southern coast of the peninsula, at Punta Cardón, Audemard (1996a, b) reports the presence of a fossil coral reef, with a height of 1.5 m, and species of the genera *Porites* preserved in living position within a “reddish sand matrix”. The author attributes this reef tentatively to MIS 5. To the west of the Paraguaná Peninsula, Audemard (1996a) reports a terrace with heights from 4 to 5 m a.s.l. This terrace presents sediments with different grain sizes and fragments of shells and corals. One radiocarbon analysis was performed on a coral fragment; its age was above the detection limit, and the author assigns an MIS 5 age. To the north of the Paraguaná Peninsula, the same author describes two eroded “isolated beach deposits” at Punta Macolla; despite not presenting an elevation for these, he correlates them with MIS 5.

After the work of Audemard (1996b), no further references could be found in this review. Up to now, none of the studies listed above presents radiometric dates, and the estimated ages were based on either geomorphological (Danielo, 1976; Audemard, 1996a, b; Rey, 1996) or biological (Bermudez, 1969; Bermudez and Farias, 1975) characteristics of the deposits described. Only the work of Audemard (1996a) refers to a single coral radiocarbon sample with an age beyond the dating limit. None of the studies listed was included in WALIS.

#### 3.6.4. Aruba, Curaçao, and Bonaire (ABC) islands

Aruba, Curaçao, and Bonaire islands lie in front of Venezuela, forming the so-called “ABC islands” group. These three islands are included in this review due to their proximity to the Venezuelan coast and the quantity of last interglacial sea-level indicators that have been reported along their shores. The Pleistocene sea-level record at these islands is mostly preserved in the form of staircases of coral reef terraces (Alexander, 1961; Herweijer and Focke, 1978). These are usually wider along the windward sides of the islands than their leeward sides. The terraces display shore-parallel changes in elevation, which would suggest they have been affected by tectonic processes. This seems likely as they are located between the south Caribbean and South American plates (Hippolyte and Mann, 2011). The reef terraces are often interrupted by *bocas*, i.e., incisions in the continuity of the Pleistocene reefs that expose the stratigraphy of the terrace, which can be also observed along sea cliffs. These outcrops facilitated the study of paleo-ecological properties of Pleistocene reefs (Pandolfi and Jackson, 2001; Meyer et al., 2003) and their dating (Schellmann et al., 2004; Obert et al., 2016; Felis et al., 2015; Schubert and Szabo, 1978; Hamelin et al., 1991) and helped unravel their

significance in the context of paleo-relative sea-level changes (Lorscheid et al., 2017; Muhs et al., 2012; Kim and Lee, 1999). The evidence of MIS 5e reef terrace development on each island is briefly described in the following.

#### 3.6.4.1. Aruba

In Aruba, the so-called “third terrace” (third terrace level counting from the modern sea level) was attributed to a “Sangamonian” (i.e., MIS 5e) age by Alexander (1961). The terrace is reported as well developed and is parallel to the shore along the northwestern coasts of the island. The terrace elevation is “25 feet” (7.6 m) a.s.l. While Pleistocene marine terraces appear prominent in the landscape of Aruba, we could not find any description or absolute ages to confirm the MIS 5e age designation; therefore, we did not insert any data point for Aruba into the database.

#### 3.6.4.2. Curaçao

Several last interglacial MIS 5e index points were reported from the island of Curaçao (Figure 3.5). The first U-series ages on corals from Curaçao were reported by Schubert and Szabo (1978) and later revisited by Muhs et al. (2012). We included in WALIS the sites reported by Schellmann et al. (2004), analyzed with ESR, and those reported by Muhs et al. (2012), measured with a differential GPS and analyzed with U series. In reporting U-series and ESR data for Curaçao, we included only those ages within MIS 5e. We did not insert into the database the U-series ages obtained by Hamelin et al. (1991), as they were rejected by the original authors due to (i) large difference in ages (multiple kiloyears) between different subsamples of the same coral or (ii) being outside the acceptable range for initial uranium isotopic composition.

A review of last interglacial sea-level proxies in the western Atlantic and southwestern Caribbean, from Brazil to Honduras

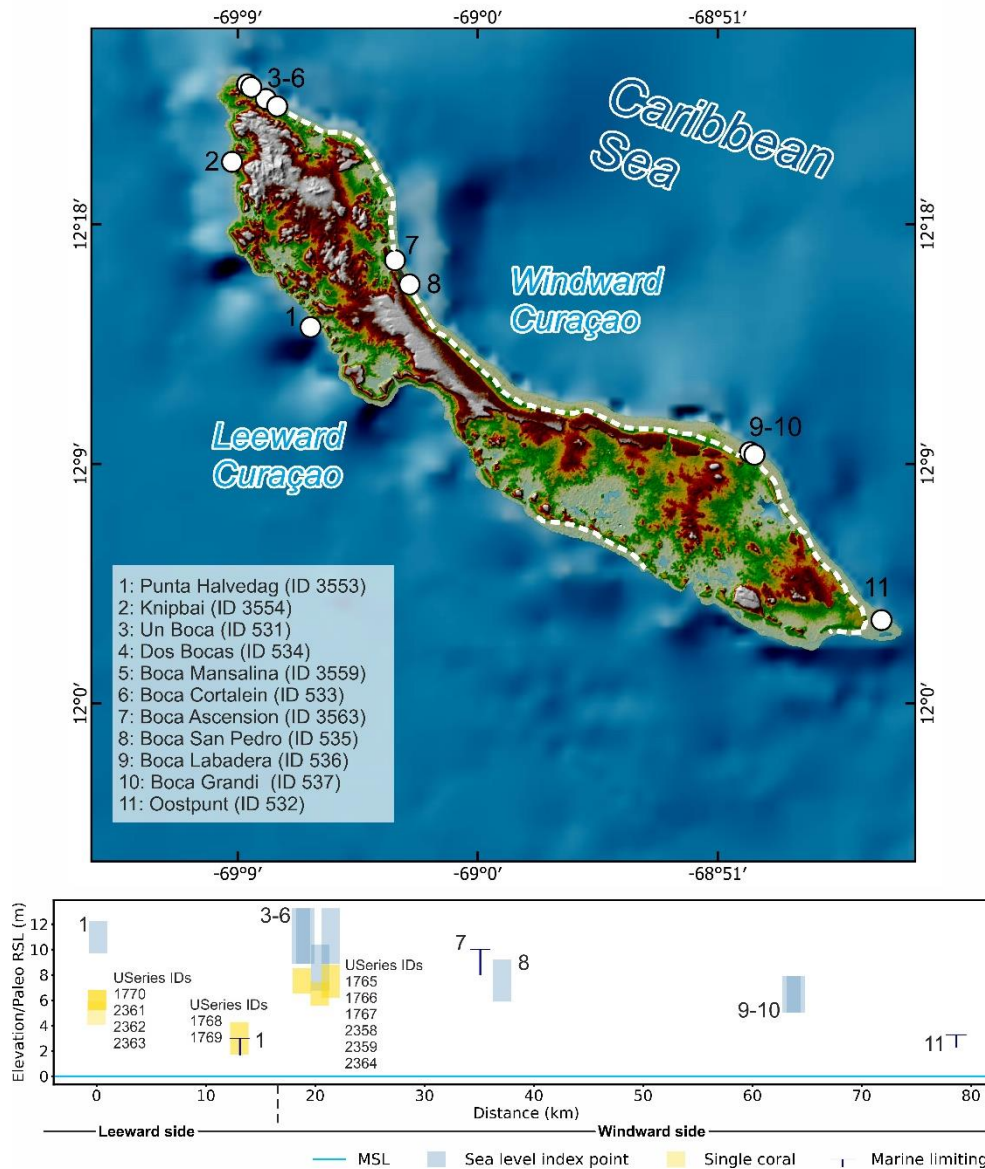


**Figure 3.5.** Last interglacial sea-level data in Curaçao. Upper panel: map of reported sites. The dashed line shows the location of the last interglacial terrace. The “single coral” data points represent coral elevations as reported in Chutcharavan and Dutton (2021). Background map compiled with data from GEBCO (<https://doi.org/10.5285/836f016a-33be-6ddc-e053-6c86abc0788e>) and SRTM 30 m by NASA EOSDIS Land Processes Distributed Active Archive Center (LP DAAC, <https://lpdaac.usgs.gov/>). Lower panel: distance–elevation plot.

In general, within the *bocas* dissecting the lower terrace of Curaçao, there are two distinct units where well-preserved corals (often in growth position) appear: the Cortalein (lower) and Hato (upper) units (Figure 3.6). Both ESR and U-series ages confirm that the Cortalein unit was forming during MIS 7 (ca. 200 ka), while the Hato unit is MIS 5e in age (Muhs et al., 2012; Schellmann et al., 2004). We report in the database only the dated samples collected from the Hato unit. In the following paragraphs, we report sample IDs as indicated in Table 2 of Schellmann et al. (2004) and Table 1 of Muhs et al. (2012) (for U series).

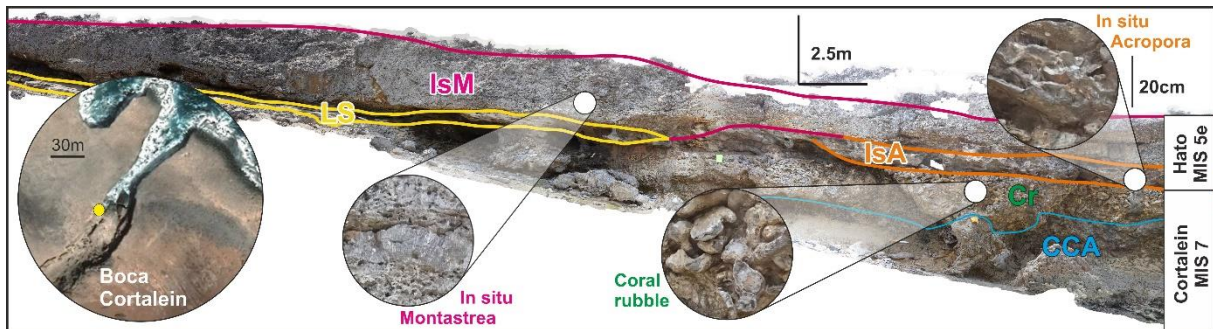


**Figure 3.6.** Last Photomosaic with the interpretation of the paleo reef units of MIS 7 and MIS 5e age at Boca Cortalein, Curaçao (originally by Ann-Kathrin Petersen, edited by Alessio Rovere). IsM: in situ *Montastraea* sp.; LS: layered sediments (beachrock); IsA: in situ *Acropora* sp.; Cr: coral rubble; CCA: solitary corals and calcareous algae.

The elevations reported by Muhs et al. (2012) are referenced to the CARIB97 geoid (Smith and Small, 1999). We assigned an elevation uncertainty of 0.95 m, calculated from the root mean square of the sum of squares of the maximum error reported by Muhs et al. (2012) (0.8 m) and the CARIB97 datum uncertainty (0.51 m). Elevations for the sites mentioned in Schellmann et al. (2004) were taken directly from their Table 2, were referred to a general “mean sea level” datum, and were assigned an arbitrary uncertainty of 20 % of the measured elevation. A similar approach was used in reporting sites investigated by Schubert and Szabo (1978).

On the leeward (southeastern) side of the island, a reef sequence at Punta Halvedag (RSL ID 3553) was reported up to 10 m above the present sea level. For this sequence, we included in WALIS four ages reported by Muhs et al. (2012) on two corals (Cur-Dat-16 and Cur-Dat-17). Muhs et al. (2012) were concerned about the U values for seawater and considered the ages to be overestimated by ~ 2.5–3.5 ka. Therefore, in WALIS we constrain the Punta Halvedag site as “younger than” these two corals, with the caveat that their age is most likely MIS 5e. North of Punta Halvedag, the same reef sequence is visible at Knipbai (RSL ID 3554). As little information on the stratigraphic context is given for this site, we inserted it into WALIS as a marine-limiting data point. From the Hato unit at this location, one *Acropora palmata* was dated (Cur-Dat-5; Muhs et al., 2012). Muhs et al. (2012) report that this coral “shows evidence of U gain, which would tend to bias the sample to a younger apparent age”. Therefore, in WALIS we constrain the Knipbai site as “older than” this coral.

On the windward (northwestern) side of the island, most of the locations reported in WALIS have been surveyed inside *bocas*, where corals have been dated with both ESR and U series. At Un Boca, three coral samples (99-6, 99-7, 99-9) yielded ESR ages between  $101 \pm 7$  and  $140 \pm 9$  ka (Schellmann et al., 2004). The top elevation of in situ corals at Un Boca is 10 m with significant uncertainties that stem from the unreported elevation measurement method. At Un Boca (RSL ID 531), Muhs et al. (2012) re-dated two corals, that had already been dated to MIS 5e by Schubert and Szabo (1978). The new analyses yielded ages of  $118.1 \pm 0.8$  ka (Cur-33-d, *Acropora palmata*) and  $132.3 \pm 0.8$  ka (Cur-33-d, *Diploria* sp.). The authors note that the sample Cur-32-d is probably biased old by 2.5–3.5 ka. One *Acropora palmata* coral (original ID 00-7) was analyzed by Schellmann et al. (2004) at a site located a few hundred meters south

of Un Boca, called Dos Bocas (RSL ID 534). Three subsamples of this coral yielded ESR ages between  $113 \pm 10$  and  $120 \pm 11$  ka. The reef terrace at Dos Bocas was assigned the same elevation as Un Boca, based on the data reported by Schellmann et al. (2004). Slightly more than 1 km south of Dos Bocas, another site (Boca Mansaliña, RSL ID 3559) yielded one *Acropora palmata* coral (sample 00-13) analyzed using ESR to provide an age of  $118 \pm 9$  ka (Schellmann et al., 2004) and one *Siderastrea siderea* coral (sample Cur-Dat-4), of which two subsamples gave U-series ages of  $125.7 \pm 0.7$  and  $126.0 \pm 0.8$  ka. The highest in situ coral at this location is reported at 7–8 m a.s.l., and it appears to have been sampled close to the top of the terrace (Figure 8 panel 3 of Schellmann et al., 2004, and Figure 8a of Muhs et al., 2012). *Acropora palmata* corals were also dated with ESR (00-5) and U series (Cur-Dat-1) at Boca Cortalein (RSL ID 533), yielding ages between 118–125 ka (with error bars between 8–11 ka) and a U-series average age of 127.3 ka (on two subsamples of the same coral). Also, at Boca Cortalein, we approximate the height of the reef terrace with the highest in situ coral, which is reported at 10 m a.s.l. (Schellmann et al., 2004). Approximately 15 to 18 km south of Boca Cortalein, three additional sites were reported by Schellmann et al. (2004) and Muhs et al. (2012). At Boca Ascension (RSL ID 3563), a *Montastraea* sp. coral yielded an ESR age of  $124 \pm 8$  ka (99-3; Schellmann et al., 2004), but not enough stratigraphic information was given to establish a sea-level index point; therefore we insert this site into WALIS as marine limiting. At Boca San Pedro (RSL ID 535), four *Acropora palmata* corals (00-9) were collected at 6–7 m a.s.l. and were dated with ESR to 103–124 ka (Schellmann et al., 2004). In this case, a cross-section (Figure 5-2 of Schellmann et al., 2004) shows that the highest of these corals was sampled close to the top of a reef terrace; therefore we consider this point a valid sea-level indicator.

Towards the southern part of the island, south of Curaçao International Airport, two nearby sites were dated with ESR by Schellmann et al. (2004): Boca Labadera (RSL ID 536) and Boca Grandi (RSL ID 537). These sites have ages ranging between  $120 \pm 13$  and  $112 \pm 9$  ka. At these two sites, all dated samples ( $n=5$ , WALIS ESR IDs 124 to 128) are close to the top of the terrace, were measured at 5–6 m a.s.l., and have been treated in WALIS as valid sea-level indicators. At the southern tip of Curaçao, one site was reported by Schellmann et al. (2004) as “Sheraton Hotel” and is here reported as Oostpunt (RSL ID 532). Here, two *Acropora palmata* corals (001-1) were sampled at 2.5–4 m. As no information is given on the stratigraphy of the reef terrace at this site, we insert this point into WALIS as a marine-limiting point.

### 3.6.4.3. Bonaire

The general coastal setting of Bonaire, similarly to that of Curaçao and Aruba, is characterized by broad (hundreds of meters wide) paleo reef terraces on the windward (northern and eastern) side of the island and narrow (tens of meters or less) paleo reef terraces on the leeward (southwestern) side (Figure 3.7).

A review of last interglacial sea-level proxies in the western Atlantic and southwestern Caribbean, from Brazil to Honduras

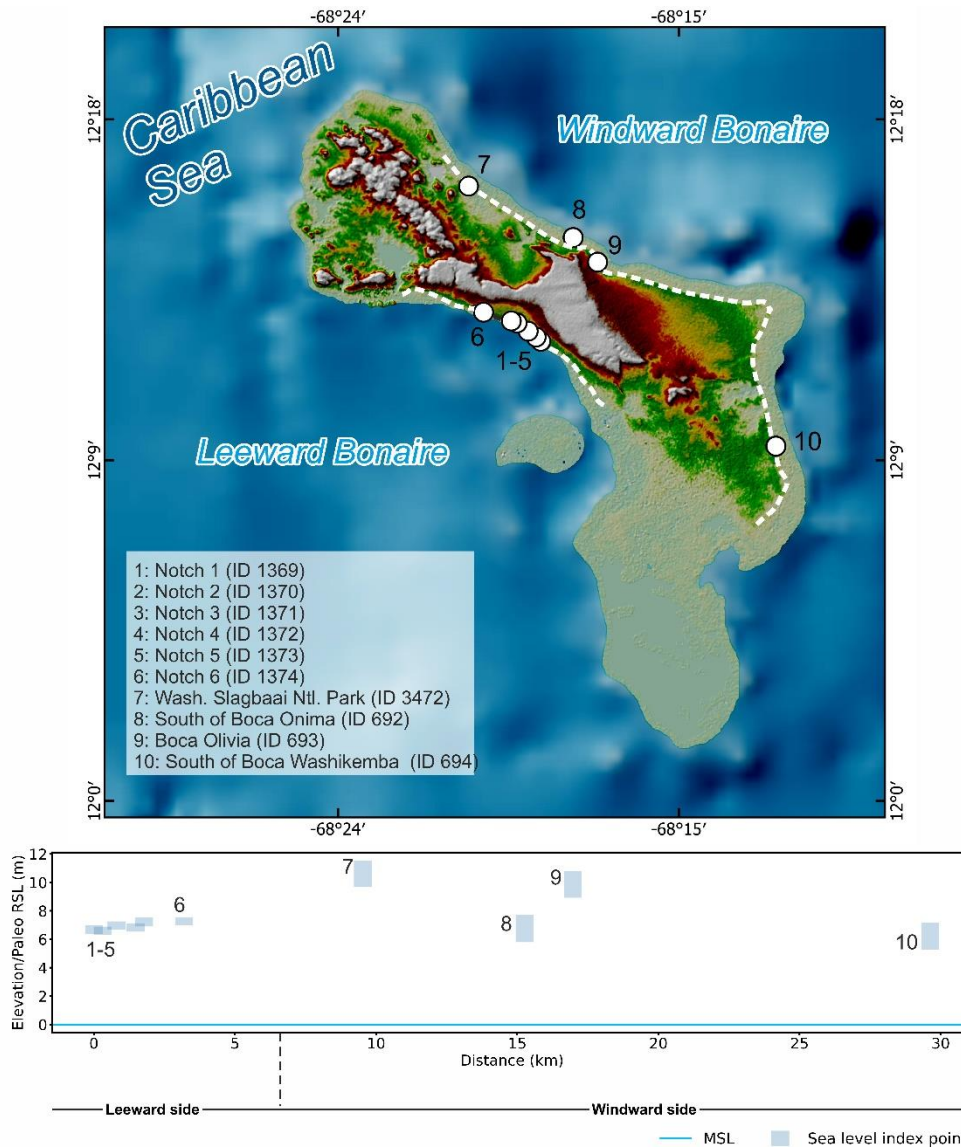


**Figure 3.7.** Last interglacial sea-level data in Bonaire. Upper panel: map of sites. The dashed line shows the location of the last interglacial terrace. Basemap compiled with data from GEBCO (<https://doi.org/10.5285/836f016a-33be-6ddc-e053-6c86abc0788e>) and SRTM 30 m by NASA EOSDIS Land Processes Distributed Active Archive Center (LP DAAC, <https://lpdaac.usgs.gov/>). Lower panel: distance–elevation plot.

On the leeward side, Lorscheid et al. (2017) measured six tidal notches carved into limestones older than MIS 5e (Figure 3.8a). The elevations of the notches were measured with a combination of differential GPS and laser rangefinders and are reported at between 6.61 and 7.26 m a.s.l. (RSL IDs 1369 to 1374). Samples of a fossil coral from the terrace immediately below the notches yielded initial activity ratios higher than expected from the modern seawater value and were therefore considered unreliable by Lorscheid et al. (2017). Nevertheless, the notches are considered coeval with the terrace immediately below (Figure 3.8b), which is correlated with the better-dated terrace level on the windward side of the island, described below.



**Figure 3.8.** (a) Tidal notch on the leeward side of Bonaire; (b) last interglacial reef 1–2 m below the location of the photo shown in (a); (c) exposed reef section on the windward side of Bonaire; (d) large massive coral eroded on top of the MIS 5e terrace on the windward side of Bonaire; (e) panorama view of the MIS 5e terrace on the windward side of Bonaire. Photos by Thomas Lorscheid (a), Alessio Rovere (b, c, e), and Thomas Felis (d).

Felis et al. (2015) and Obert et al. (2016) report several U-series ages from different skeletal parts (theca walls or bulk material) of nine corals located on top of the lower reef terrace characterizing the windward (northern and eastern) side of Bonaire (Figure 3.8c, d, e). As there are multiple subsamples for some individual corals, Brocas et al. (2016) calculate the weighted mean and weighted standard error of five of these nine corals giving a range from  $120.5 \pm 1.1$  to  $125.85 \pm 2.46$  ka. Of the 42 ages reported by Obert et al. (2016) and 1 age reported by Felis et al. (2015), we inserted into WALIS only those accepted within the original publication (based on progressively less strict criteria), restricting the number of available ages to 25 (8 corals). The elevation of these samples was initially measured using an altimeter “calibrated” to the sea level at the time of measurement. The sampling sites were then revisited by Thomas Lorscheid, Alessio Rovere, and Thomas Felis in 2016, and each sampled

coral on top of the reef terrace was re-measured with differential GPS and referred to the EGM2008 geoid. We report these new measurements in this paper for the first time. To provide additional constraint to each sample, an elevation was also recorded at the nearest accessible instance of the coral reef inner margin, which we consider here to approximate the paleo-sea level with an indicative range included between the mean lower low water and the breaking depth, which we derived from IMCalc (Lorscheid and Rovere, 2019).

South of Boca Washikemba, Obert et al. (2016) and Felis et al. (2015) dated two corals: BON-5-A ( $120.5 \pm 1.1$  ka average age according to Brocas et al., 2016) and BON-5-D ( $117.7 \pm 0.8$  ka). The inner margin of the reef terrace 3 km north was measured at  $5.19 \pm 0.28$  m, where in situ massive corals can be recognized (RSL ID 694). While this is the only site dated on the eastern coast of Bonaire, the wide coral reef terrace is almost continuous until a second site is reached on the northeastern coastline (identified within WALIS as Boca Olivia, RSL ID 693), where Obert et al. (2016) dated two other corals BON-26-A and BON-24-AII.2, giving average ages of  $124.9 \pm 19$  and  $125.5 \pm 2.4$  ka, respectively (Brocas et al., 2016). The inner margin of the coral reef terrace was measured 500 m inland of these two corals, at an elevation of  $8.84 \pm 0.27$  m. At 3 km north of this point, south of Boca Onima (RSL ID 692), three corals (BON-17-AI, BON-12-A, and BON-13-AI.1) yielded an average age of  $124.3 \pm 1.5$  ka (Obert et al., 2016; Brocas et al., 2016). The inner margin correlated to these corals was measured very close to the sample locations, at an elevation of  $5.72 \pm 0.3$  m. At 4 km north of Boca Onima close to the Washington Slagbaai National Park border (RSL ID 3472), Obert et al. (2016) dated one coral (BON-33-BI.2) to  $129.7 \pm 1.7$  ka. The inner margin of the terrace closest to this coral was measured at  $9.58 \pm 0.14$  m. The measured elevations show a trend of becoming higher towards the north. That the coral ages reveal a broad trend from younger at lower elevations in the south to older at higher elevations in the north, with intermediate ages at intermediate elevations in between, has been noted by Obert et al. (2016) and attributed to the slight tilting of the island with relative uplift in the north and submergence in the south (Hippolyte and Mann, 2011). Consequently, this trend is unlikely to reflect past sea-level variations (Obert et al., 2016).

### 3.6.5. Colombia to Honduras

The coastal deposits of Colombia associated with the LIG have been mainly studied and described on offshore islands (Porta and Solé de Porta, 1960; Bürgl, 1961; Geister, 1972, 1986, 1992). Porta et al. (2008) mentioned the existence of marine terraces and coral platforms of different elevations along the mainland Colombian coast, mainly between Cartagena and Barranquilla; however, no further details are given on their ages or elevations or specific locations.

Porta and Solé de Porta (1960) describe the Quaternary coastal deposits on Tierra Bomba Island. While the main focus of their paper is to describe the marine faunas of the islands, the authors mention Pleistocene marine terraces with heights of more than 20 m; however, none of these deposits are directly correlated with the Last Interglacial. One year later, Bürgl (1961) mentions three geological and geomorphological units on the island of San Andrés: (i) a marine platform of recent age, (ii) a terrestrial platform of Pleistocene age, and

(iii) inland limestones of Miocene age. Geister (1972) hypothesizes that the deposits on the “terrestrial” platform were formed during a marine transgression and correlates them with coral terraces observed on Providencia (Figure 3.9) according to its geomorphology. Geister (1986) suggests the Providencia terraces are of Sangamon Interglacial age (MIS 5) based on a minimum radiocarbon age. The same author (Geister, 1992) later described this and the rest of the coral deposits of Providencia. He highlights that this fossil reef terrace is the only emerged relict of the Pleistocene complex which now underlies the Holocene deposits.

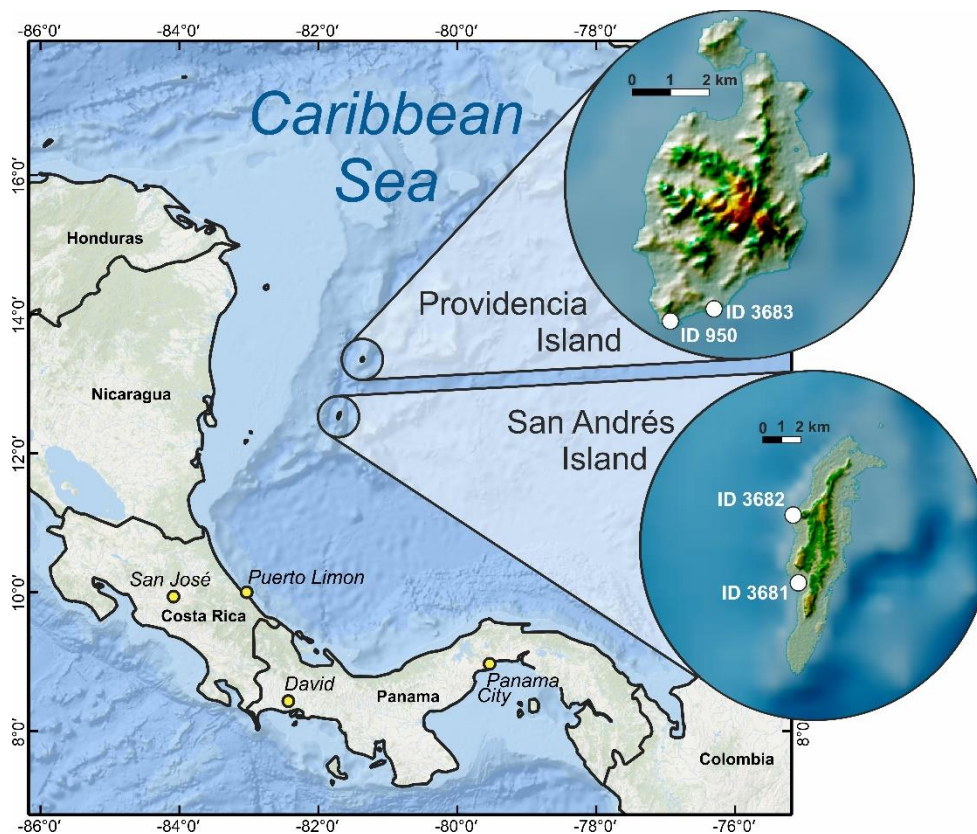


**Figure 3.9.** Location of Providencia and San Andrés islands within the Caribbean Sea. The insets show last interglacial sea-level data on the two islands. Basemap: Esri, Garmin, GEBCO, NOAA NGDC (now NCEI), SRTM 30 m by NASA EOSDIS Land Processes Distributed Active Archive Center (LP DAAC, <https://lpdaac.usgs.gov/>).

Literature describing MIS 5 relative sea-level indicators in Panama, Costa Rica, Nicaragua, and Honduras is scarce. Only one study in Costa Rica mentions the presence of a paleo-coral reef for which an Eemian age (MIS 5e) is postulated, in Puerto Viejo (Bergoening, 2006). We surmise that it is possible that MIS 5 outcrops have not yet been described or do not exist in Panama, Nicaragua, and Honduras. For Panama and Costa Rica, several studies focus on the Pacific zone (Bee, 1999; Davidson, 2010; Bauch et al., 2011), which is out of the area of interest for this paper. No studies have been found in Nicaragua and Honduras, but we do not discard the possible existence of descriptions of MIS 5 outcrops in journals that we could not access online.

### 3.6.5.1. San Andrés

From the work of Geister (1972), it is possible to derive two sea-level indicators (generally defined as reef terraces) on the island of San Andrés. One is located on the south of the island at a point called Southwest Cove (RSL ID 3681) and the second to the north, at May Cliff (RSL ID 3682) (Figure 3.9). The elevation of the Southwest Cove site was 1.5 m a.s.l., and the coral sampled belonged to the species *Acropora palmata*, which has an average living range between -1 and -5 m depth (Lighty et al., 1982). We use these values as the upper and lower limit, respectively, of the indicative range to calculate the paleo RSL for this site at  $4.5 \pm 2.06$  m (RSL ID 3681). This sample was radiocarbon dated, giving an age of  $26\,020 \pm 675$  years BP, which according to the authors should be considered a minimum age. The May Cliff sample comes from a *Dendrogyra cylindrus* coral (from -2 to -10 m living range in San Andrés, as reported by Cavada-Blanco et al., 2016) found at 6 m a.s.l. with a minimum radiocarbon age of  $33\,000 \pm 770$  years BP. Considering the average living range of *D. cylindrus* (Cavada-Blanco et al., 2016) on this island, the paleo RSL calculated is  $12 \pm 4.03$  m (RSL ID 3682).

### 3.6.5.2. Providencia

To the south of the island of Providencia, Geister (1972) reports the elevation and two radiocarbon dates ( $33\,310 \pm 2300$  years BP and  $29\,270 \pm 930$  years BP) of a specimen of the coral *Siderastrea radians*. The reported elevation of the sample is 1.8 m a.s.l., and both radiocarbon dates were considered minimum ages. Twenty years later, the same author describes a coral reef terrace at about +3 m at a site called South Point (RSL ID 950) (Figure 3.9). One U-series age confirms the association of these deposits with MIS 5e, albeit with a large error ( $118 \pm 11.0$  ka; U-Series ID 2026) (Geister, 1992).

## 3.7. Data availability

The western Atlantic and southwestern Caribbean database is available at <https://doi.org/10.5281/zenodo.5516444> (Version 1.02; Rubio-Sandoval et al., 2021). The description of the database fields can be found at <https://zenodo.org/record/3961544> (Rovere et al., 2020).

## 3.8. Further remarks and conclusions

### 3.8.1. Data quality

Each RSL data point in our compilation has been assigned two quality scores, one for age and one for RSL information. The quality ranking goes from 0 (rejected) to 5 (excellent) and follows the guidelines given in Rovere et al. (2020). Thanks to the standardized WALIS interface, similar scores are also available for RSL data points located to the south and to the north of our region, which were compiled into WALIS by Gowan et al. (2021) and Simms (2021). In Figure 3.10, we compare the quality scores assigned in our review to those assigned by these

## A review of last interglacial sea-level proxies in the western Atlantic and southwestern Caribbean, from Brazil to Honduras

studies. This comparison shows that the quality of both age and RSL information for our study area is, in general, higher than those in the nearby sites. However, the high scores on both properties are driven by the sites in the ABC islands, and no site in Brazil goes above the “average” age scores. Concerning the RSL information, in Brazil only the sites described by Tomazelli and Dillenburger (2007) and Martins et al. (2018) have been scored as “good” to “excellent”. This means that, potentially, these sites have final uncertainties in the paleo RSL below 2 m, but their attribution to MIS 5e should be supported by more reliable dating.

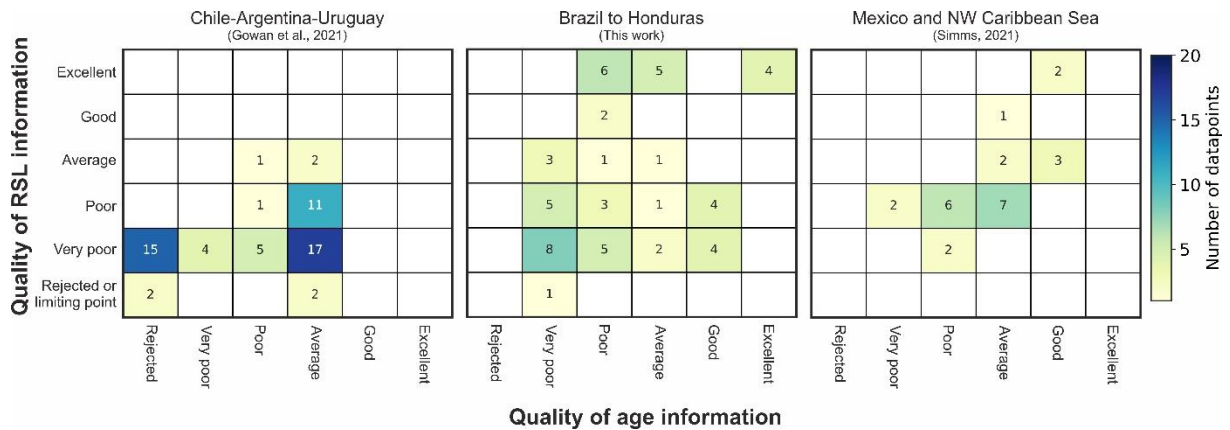


**Figure 3.10.** Quality of RSL and age information as estimated by (from left to right) Gowan et al. (2021) for Chile–Argentina–Uruguay, Brazil–Honduras (this study), and Mexico and the NW Caribbean Sea (Simms, 2021). All studies used the same rationale to give a score to age and RSL information (see Rovere et al., 2020).

### 3.8.2. Departures from the eustatic signal

While in the WALIS interface there is the option to compile data and metadata on tectonic rates that affect each reported RSL data point, we chose to leave these fields blank. The reason behind this choice is that late Quaternary tectonic rates along the coasts covered by our review are often back-calculated from the elevation of the last interglacial shoreline and assumptions about the MIS 5e eustatic sea level, and therefore inserting such rates into the database would be affected by circularity. However, we remark that the area is characterized by different tectonic settings. The southern portion of Brazil (Figure 3.3) is located roughly in the center of the South American Plate and hence sits on a passive margin. Towards the north (Figure 3.4), several authors noted an increase in seismicity and highlighted the presence of faults offsetting Neogene deposits (Bezerra et al., 2006).

As remarked in the regional descriptions above, in this area last interglacial deposits appear higher than 20 m and are hence considered uplifted (Barreto et al., 2002). The ABC islands are located on the Caribbean Plate, hence the elevation of MIS 5e sites on these islands is affected by tectonic displacement. Based on several levels of Quaternary reef terraces, Muhs et al. (2012) calculated that sites on the island of Curaçao are characterized by uplift rates on the order of 0.026–0.054 m/ka. Similarly, the island of Bonaire has also been affected by tectonic uplift, which appears to have caused a tilting of the island. Lorscheid et al. (2017)

report that this tilting is 192 mm/km to the southeast, with the direction of the tilting comparing well with the one reported by Hippolyte and Mann (2011).

Besides tectonics, other regional processes might influence the elevation of RSL indicators in the area of interest. Earth dynamic topography has been shown to cause significant departures from eustasy in last interglacial sea-level records also along passive margins. Along the coasts of Brazil, Earth dynamic topography might contribute to several meters of uplift (Austermann et al., 2017, their Figure 3A, C). However, these predictions are still bounded by significant uncertainties (Austermann et al., 2017, their Figure 3B) and cannot be employed to “correct” the RSL records shown here.

Another significant factor that may have caused the displacement of last interglacial RSL data points is sediment isostasy (Pico, 2020), which is defined as the isostatic response to sediments deposited by large rivers on the shelf. In particular, this process may affect areas close to the Amazon river (Pico, 2020, their Figure 3) causing net land subsidence on the order of tens of meters. This could explain why we did not find studies describing last interglacial RSL data points in this area, hinting that they might be located well below the modern sea level.

A further process that has surely affected the current elevations of last interglacial RSL sea-level proxies along the coasts of Brazil to Honduras is glacio- and hydro-isostatic adjustment (GIA), which is caused by the isostatic response of the Earth to mass fluctuations of continental ice sheets. GIA consists of both solid Earth and mean sea surface (i.e., geoid) vertical variations that show up as relative sea-level (RSL) variations. The deviation of the local GIA-modulated RSL changes from the global mean, i.e., “eustatic”, sea-level change, depends primarily on the distance from the ice sheets. During glacial periods such as MIS 6, the crust subsides underneath a growing ice sheet in response to the ice load. The upper mantle material is therefore pushed outwards to accommodate the bending lithosphere. At the same time, the increased mutual gravitational pull between the ice mass and the ocean water causes the latter to rise in the proximity of the ice margins. As a result, ice-proximal locations experience RSL rise, which is significantly larger than the eustatic fall. Further away from the ice margins, the crust undergoes uplift in response to the upper mantle flow that is directed radially outwards and upwards. This is the so-called uplifting peripheral forebulge area, where the local glacial RSL drop is significantly larger (and faster in time) with respect to the global eustatic drop. Moving away from the forebulge, the local RSL drop tends to approximate the global eustatic signal, with deviations that depend on the water-loading redistributions in response to solid Earth and gravitational as well as rotational perturbations.

During deglacial and interglacial periods such as MIS 5, the GIA process operates in the same way, but the overall trend switches. Accordingly, RSL drop is expected over the previously ice-covered region, while the collapse of the uplifted peripheral forebulge results in RSL rise larger than the eustatic one. Interestingly, during the termination of the deglacial phases, the far-field areas that are either along the continental margins or in the equatorial band comprised between the tropics do experience a noticeable RSL fluctuation that consists of an early highstand (above the eustatic value), which is then followed by a drop. Two processes are at work here: (i) the so-called continental levering, which consists of an upward tilt of the continental margins in response to the subsidence of the ocean basins which are

loaded with meltwater, and (ii) the ocean syphoning, where water migrates towards the collapsing peripheral forebulges in response to ocean mass conservation.

### 3.8.3. Last interglacial sea-level fluctuations

The current research status of the Last Interglacial in the western Atlantic and southwestern Caribbean does not allow for the discernment of sea-level oscillations within MIS 5e, since most studies in the region lack the refined chronology necessary to identify such detailed sea-level patterns. However, we remark that this area might help to solve several questions related to the presence and magnitude of sea-level oscillations during MIS 5e if high-quality data were to become available.

To illustrate this point, we model the GIA-modulated RSL changes by solving the gravitationally self-consistent sea-level equation (SLE; Spada and Stocchi, 2007). We use a solid Earth model that is spherically symmetric, self-gravitating, and rotating and is divided into shells that are characterized by a linear Maxwell viscoelastic rheology. We divide the mantle into three layers and impose a vertical stratification of viscosity following the VM2 mantle viscosity profile of Peltier (2004). We force our model with the ANICE–SELEN ice sheet chronology, which consists of four ice sheets (North America, Eurasia, Greenland, and Antarctica) and covers the last 410 kyr of climate fluctuations (i.e., four glacial-to-interglacial cycles; de Boer et al., 2014). For the MIS 5e interglacial, we impose a global mean-sea-level scenario where Greenland and Antarctic ice sheets release 2.5 and 1.0 m ESL equivalent, respectively, at 127 ka. The Greenland Ice Sheet remains stationary until 117 ka, while the Antarctic Ice Sheet releases another 4.5 m after 120 ka. This scenario is in line with the “two-stepped” last interglacial sea level proposed by Hearty et al. (2007) and O'Leary et al. (2013), which is still debated as little evidence supports the notion of a rapid collapse of the Antarctic Ice Sheet (AIS; Barlow et al., 2018; Polyak et al., 2018).

The GIA model shows a strong latitudinal dependence of the RSL change along the transect composed by our compilation and those of Gowan et al. (2021) to the south and that of Simms (2021) to the north (Figure 3.11b). Such a regionally varying RSL pattern depends on the interplay between the collapsing forebulge in the north and the continental levering and ocean syphoning in the south.

A review of last interglacial sea-level proxies in the western Atlantic and southwestern Caribbean, from Brazil to Honduras

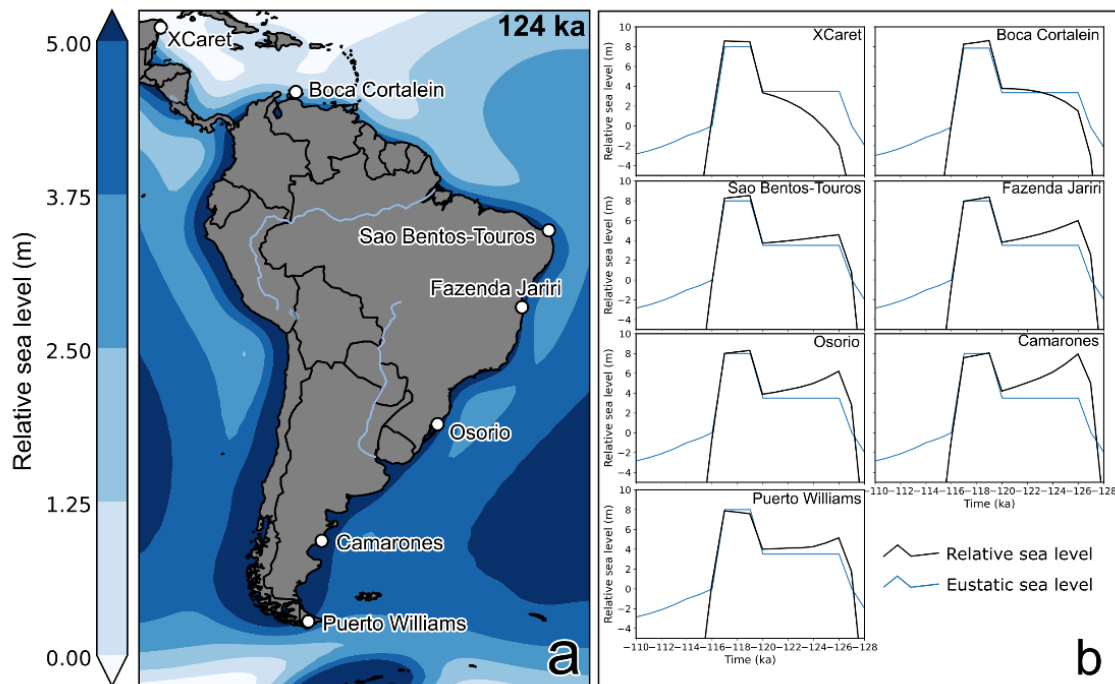


**Figure 3.11. (a)** Relative sea level as predicted by the ANICE–SELEN model at 124 ka along a transect including selected sites in our review and those of Gowan et al. (2021) and Simms (2021); **(b)** time vs. RSL at each location shown in **(a)**.

In particular, at the northernmost site of Xcaret, the predicted RSL elevation at 127 ka is still  $\sim 6$  m lower than the eustatic value (i.e., +3.5 m a.s.l.). This stems from the local contribution of the collapsing forebulge that was uplifted in response to the North American ice sheet glaciation at MIS 6. The viscous response of the upper mantle results in a delay of the local RSL change, which reaches, through a monotonic rise, the actual eustatic value only at 120 ka, i.e., immediately before the final jump that is caused by the AIS melting. A similar trend, albeit smaller in amplitude, is predicted at Boca Cortalein, thus implying that the forebulge-related processes cease to exist between Venezuela and northern Brazil, where a true eustatic “sea-level jump” is expected. The predicted RSL curve at São Bento–Touros is close to the eustatic, although the combination of levering and syphoning is visible in the form of a  $\sim 1.0$  m highstand at 127 ka, which is then followed by an RSL drop towards the eustatic value at 120 ka. The GIA-driven highstand at 127 ka increases towards the south and reaches its maximum at Camarones, i.e., at a significant distance from the North American ice sheet and Antarctica. Interestingly, the predicted highstand at 127 ka is of the same magnitude as the final peak between 119 and 117 ka. Under such a scenario, there should be evidence, along all the coasts of Argentina and central Brazil, of a high-to-low sea-level swing, caused by the interplay between GIA and eustatic changes. At Puerto Williams, instead, the proximity to the AIS results in a much lower highstand at 127 ka, most likely as a function of the reduced gravitational pull after MIS 6 and MIS 5e melting.

The effects of solid Earth and gravitational perturbations are also visible in the predicted elevations of the final jump that is caused by the AIS fast melting. The southernmost sites, being closer to the AIS, are affected by the geoid drop that is caused by the reduced

gravitational pull. As a result, the predicted highstand is slightly lower than the eustatic one. On the other hand, the northernmost sites experience a higher-than-eustatic peak, again as expected by the self-gravitation process.

#### 3.8.4. Other interglacials and Holocene sea-level indicators

Among the studies reviewed, there are some reported ages/inferences related to other Quaternary sea-level highstands. In Brazil, Barreto et al. (2002) and Suguio et al. (2011) describe shorelines with elevations ranging from  $-2$  to  $10$  m a.s.l. that were associated with MIS 7 (substage 7c). In Curaçao, Schellmann et al. (2004) and Muhs et al. (2012) associate the lower terrace with MIS 7, estimating a paleo-sea level between  $-3.3$  and  $+2.3$  m, and the middle terrace with MIS 11, estimating a paleo-sea level ranging between approximately  $+8.3$  and  $+10$  m.

For the Holocene, the work of Khan et al. (2017) presents standardized sea-level index points in Honduras, Panama, Venezuela, Curaçao, Guyana, and Suriname. A review of Holocene studies in Brazil was conducted by Angulo et al. (2006) and a database is available, although it is not yet standardized to state-of-the-art templates for Holocene sea-level studies (i.e., Khan et al., 2019).

#### 3.8.5. Future research directions

There are several lines of inquiry that merit attention which concern LIG sea-level studies in the area covered by this database.

Except for the islands of Bonaire and Curaçao, the age control on sea-level index points associated with MIS 5 is generally poor. Most locations have limited chronological control, relying upon minimum radiocarbon ages or chronostratigraphic correlations between sites. In Brazil, more accurate chronological techniques have been employed to date Pleistocene sediments (i.e., OSL and TL), but there is a general lack of reporting standards of geochemical values and metadata, which makes it difficult to assess the reliability of each sample.

With a few exceptions (Tomazelli and Dillenburg, 2007; Martins et al., 2018), the elevation of Brazilian sea-level proxies should be better measured with state-of-the-art techniques, such as differential global navigation satellite systems (GNSSs), to reduce the currently large uncertainties. Therefore, a research priority for the vast area between Rio Grande do Sul and Rio Grande do Norte (Figs. 3 and 4) is to perform new fieldwork aimed at re-measuring and re-dating the sites reported in our database, providing enough data and metadata on both elevation and age.

In Venezuela, the Paraguaná Peninsula appears as a potential target for investigations on LIG shorelines. Here, there is a general need for better site descriptions, location information, and measurement. Coupled with U-series and/or OSL ages at selected sites, this will enable the possibility of adding to our database several sea-level index points. Concerning French Guiana, Suriname, and Guyana, there is evidence that LIG transgressive sequences are

preserved, but the central need is to identify key sites and provide reliable geological descriptions, ages, and elevation measurements. Similarly, in the long stretch of coast from Colombia to Honduras, a research priority for future studies is to identify whether last interglacial sites are present. The fossil coral reef in Puerto Viejo (Costa Rica) reported in Bergoeing (2006) may represent the starting point for investigations on LIG sea-level changes in the region, which might also encompass a better description and dating of the reefs of the San Andrés and Providencia islands.

In Bonaire and Curaçao, the sea-level index points are generally well described, precisely measured, and dated. This stands in strong contrast with the neighboring area of Aruba, where reef terraces are only generally reported in the literature and for which age control and stratigraphic descriptions are not available. Completing the LIG history of the ABC islands by including details on the fossil reefs of Aruba appears to be a priority in this area.

Together with the data compiled in Simms (2021) and Gowan et al. (2021), the data in this paper provide a unique transect across the forebulge of the former Antarctic Ice Sheet. The location of this transect may be used to test different ice melting histories, including testing the possibility of a rapid Antarctic Ice Sheet collapse during the Last Interglacial. This will be possible only by largely improving, with new field data, the data quality both of RSL index points and of their associated age.

### 3.9. Acknowledgements

This work is part of the PhD thesis of Karla Rubio-Sandoval, funded by the ERC Starting Grant WARMCOASTS (ERC-StG-802414). We would like to thank Peter Augustinus, Edward Antony, Theo Wong, Franck Audemard, Alcina Barreto, and Afonso Nogueira for clarifying aspects of the RSL indicators across different areas of the region reviewed. Figures 4, 3 and 9 were created using ArcGIS® software by Esri. ArcGIS® and ArcMap™ are the intellectual property of Esri and are used herein under license © Esri. All rights reserved. For more information about Esri® software, please visit <https://www.esri.com> (last access: 18 October 2021). The data used in this study were compiled in WALIS, a sea-level database interface developed by the ERC Starting Grant WARMCOASTS (ERC-StG-802414), in collaboration with the PALSEA (PAGES and INQUA) working group. The database structure was designed by Alessio Rovere, Deirdre D. Ryan, Thomas Lorscheid, Andrea Dutton, Peter Chutcharavan, Dominik Brill, Nathan Jankowski, Daniela Mueller, Melanie Bartz, Evan Gowan, and Kim Cohen. The data points used in this study were contributed to WALIS by Karla Rubio-Sandoval and Alessio Rovere, with Peter Chutcharavan assisting with some U-series data entry.

## 4. Holocene relative sea-level changes from the Atlantic coasts of South America

K. Rubio-Sandoval, T.A. Shaw, M. Vacchi, N., Khan, B.P. Horton, J.R. Angulo, M. Pappalardo, A.L. Ferreira-Júnior, S. Richiano, M.C. de Souza, P. C. Giannini, D.D. Ryan, E.J. Gowan, A. Rovere

In preparation for submission to *The Holocene*

### 4.1. Abstract

The critical review of 1024 sea-level data points from Brazil, Uruguay, Argentina, and the Chilean part of Tierra del Fuego resulted in the first standardized Holocene sea-level database of a wide portion of the southwestern Atlantic Ocean. We use a spatiotemporal empirical hierarchical model to estimate the relative sea level position and its rates of change over 1000 years' time slices. Our data show that several regions experienced a mid-Holocene highstand with relative sea level rising 2 to ~4 m above present, followed by a subsequent fall to its modern position. This trend seems to be predominantly driven by glacio-isostatic processes. The predicted rates of relative sea-level change show higher values during the transition between the early to the mid-Holocene, with a maximum of 1.19 mm/yr in the region of Pernambuco and Algoas (Brazil) and a minimum of 0.22 mm/yr in the region of South São Paulo, Paraná, and Santa Catarina (Brazil). Following the end of Northern Hemisphere deglaciation, mid-to-late Holocene rates slowed through the present in the northern sector of the southwestern Atlantic. In contrast, the south (from Río de la Plata to Tierra del Fuego) shows a relative sea level rate increase in the last ~3000 years, suggesting an effect of different factors such as tectonics or Antarctic ice sheet dynamics, which may need further research. Our database fills the existing gap of standardized sea-level data for the Atlantic coasts, unifying a pole-to-pole transect initiated by other authors.

### 4.2. Introduction

The study of postglacial relative sea level (RSL) changes is fundamental to understanding the behavior of sea level to ice melting and the subsequent isostatic crustal response and other vertical movements caused by local factors, such as tectonics or sediment compaction (Khan et al., 2015). Most studies of postglacial RSL evolution patterns are local in nature, as they report the age and elevation of sea level index points (SLIPs) at specific locations. However, there is a long-lasting effort in the sea-level community to standardize such data into sea-level databases with wider coverage (Düsterhus et al., 2016; Khan et al., 2019; Rovere et al., 2023).

A coordinated effort to build a global sea-level database since the Last Glacial Maximum (LGM) was initiated by the HOLSEA project (Khan et al., 2019), which brought forward rigorous standards when reporting sea-level data (Shennan et al., 1993; van de Plassche, 1986). The advantage of such databases resides in the possibility to investigate

spatial and temporal patterns of RSL changes, ultimately gathering information on the timing and modes of ice sheet melting since the LGM and to help inform future sea-level rise scenarios (Horton et al., 2018).

A notable gap in the standardized HOLSEA database is present along the Atlantic coasts of South America, where previous studies compile published and unpublished data at eight sites from Jamaica to the Beagle Channel (Milne et al., 2005; Khan et al., 2019). Here, we expand upon the work of Milne et al. (2005) and Angulo et al. (2006) revising literature on Holocene data along the coasts of Brazil, Uruguay, Argentina, and the Chilean part of Tierra del Fuego. We produced a new suite of sea-level data following the HOLSEA standardized protocol, which has been included into the interface of the World Atlas of Last Interglacial Shorelines (Rovere et al., 2023). We applied a temporal and spatial model to the new standardized sea-level data to quantify changes in the RSL through time and compared these results with glacial isostatic adjustment (GIA) model predictions. This work, coupled with the reviews on the Last Interglacial (125,000 years) sea-level data from Argentina (Gowan et al., 2021a) and Brazil to Honduras (Rubio-Sandoval et al., 2021), completes an overview of sea-level changes since the late Pleistocene in this broad region.

### 4.3. Regional setting

The sea level database spans the Southwestern Atlantic and includes Holocene sea-level data points located along the coasts of Brazil, Uruguay, and Argentina (with some indicators also located on the Chilean part of Tierra del Fuego) (Figure 4.1). Most of the region is located on the South America Plate and is, for the most part, a passive margin. However, towards the northern part of Brazil (e.g., Pernambuco and Paraíba), several authors noted an increase in seismicity and highlighted the presence of faults offsetting Neogene deposits (Barreto et al., 2002; Bezerra and Vita-Finzi, 2000). In the far south, Tierra del Fuego is affected by the interaction between the Antarctic, Scotia, and South American plates (Isla and Angulo, 2016). Therefore, we remark that tectonics may play a role in the displacement of SLIPs in these two areas (Figure 4.1: regions 3 and 12).

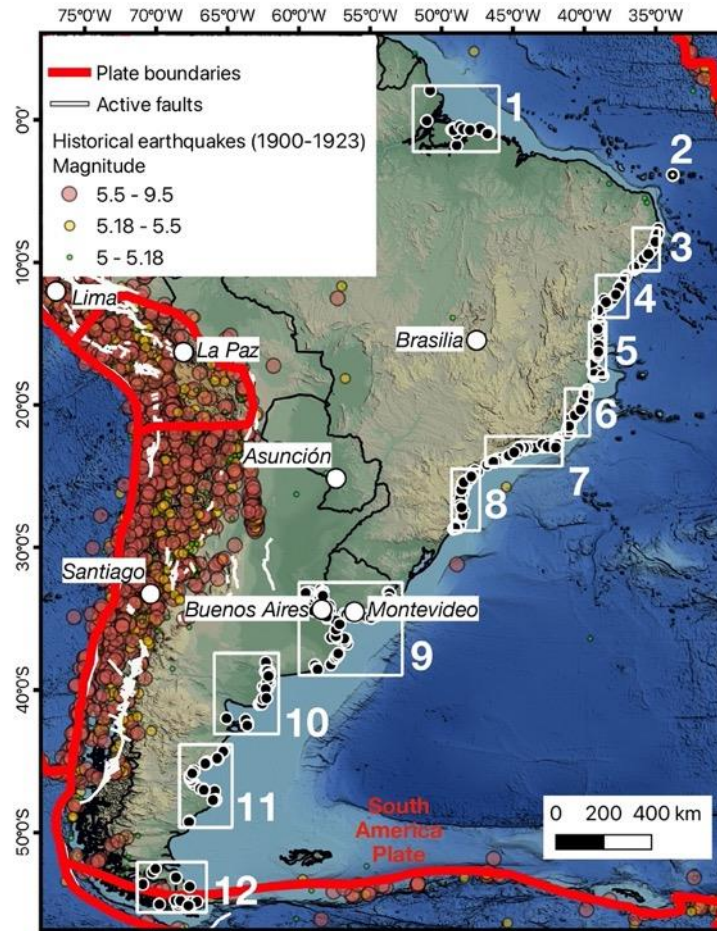


**Figure 4.1.** Geographic extent of the sea-level database, and subdivision in the regions described in the text. 1) Amazon river delta; 2) Atol das Rocas; 3) Pernambuco and Alagoas; 4) Sergipe and North Bahia; 5) Central and South Bahia; 6) Espírito Santo and North Rio de Janeiro; 7) South Rio de Janeiro and Central São Paulo; 8) South São Paulo, Paraná, and Santa Catarina; 9) Río de la Plata delta; 10) Bahia Blanca and Peninsula Valdés; 11) Bahía Vera to Puerto San Julián; 12) Tierra del Fuego. Credits: Base map from Ryan et al. (2009). Active faults from Styron (2019) and plate boundaries derived from Bird (2003), as modified by Hugo Ahlenius and Nordpil on GitHub (<https://github.com/fraxen/tectonicplates>). Historical earthquakes from US Geological Survey (2017).

The study of Holocene RSL changes in the southwestern Atlantic dates back to the 19<sup>th</sup> century, with several paleo-sea level indicators and initial trends of sea level change described along the Brazilian coastline (Angulo and de Souza, 2014). For example, between Rio de Janeiro and Cabo Frio, Hartt (1870) identified sea urchin beds above the high tide level (HTL) and interpreted them as indicators of higher sea levels. At the end of the 19<sup>th</sup> and beginning of the 20<sup>th</sup> centuries, works by Branner drew initial paleo sea-level inferences for the Fernando de Noronha archipelago, and in the northeast Brazilian coast (Branner, 1889, 1890, 1902, and 1904). Backeuser (1918) employed rock-boring mollusks to estimate sea-level changes along the coastline between Rio de Janeiro and Santa Catarina. However, it was not until the work of van Andel and Laborel (1964) that the earliest radiocarbon dates on SLIPs were presented, allowing more reliable spatiotemporal paleo-sea-level reconstructions. In the 1980s, Porter et al. (1984) quantified Holocene sea-level changes in Tierra del Fuego, Argentina, and Chile; and a decade later, the Holocene sea level variations in Uruguay began to be analyzed with the

work of Bracco (1991) and Bracco and Ures (1998). Since then, sea level research in the southwestern Atlantic has evolved with several studies investigating more areas and progressively better age control on SLIPs. More recent works started to investigate Holocene sea-level variations in combination with post-depositional displacement caused by GIA (e.g., Rostami et al., 2000; Milne et al., 2005).

Four seminal research papers summarizing Holocene RSL changes in the region present data with some degree of standardization and formed the starting point of our review. Angulo et al. (2006) compiled sea-level data along the Brazilian coastlines. They report and discuss the implications of more than 35 years of research by different groups and focus on sea-level variations in the mid to late Holocene. While highlighting discrepancies in the reported data, they describe a common trend of a mid-Holocene highstand with a subsequent fall to its present level (Figure 4.2A). In Uruguay, Bracco et al. (2011) describe the origin and geomorphological history of the Castillos Lagoon deposits, whose elevations decrease from ~4 m to ~2 m above sea level (a.s.l.) from the mid to late Holocene. However, they also describe SLIPs at elevations lower than 1 m a.s.l. around 4500 years cal BP (Figure 4.2B). Martínez and Rojas (2013) draw a sea-level curve based on data from beach ridge deposits, showing that the Uruguayan sea level was above the present level at approximately 6000 years cal BP and has been declining since then (Figure 4.2B). Finally, Schellmann and Radtke (2010) present a wide review of SLIPs surveyed along the middle and south Patagonian Atlantic coast. According to the authors, beach ridges and valley-mouth terraces data show varying elevations throughout the Holocene (Figure 4.2C). They estimate the Holocene sea-level transgression peaked at 6900 cal years BP, with RSL about 2-3 m a.s.l., and lasted until at least 6200 cal years BP, after which sea level declined to its present position. They also suggest that the mid and south Patagonian coast has likely been undergoing a slow glacio-isostatic uplift on the order of 0.3 - 0.4 mm/yr since the mid-Holocene. Some of this uplift resulted from the deglaciation of the Patagonian ice sheet, which covered the Andes Mountains in Chile and Argentina. Though the volume of the Patagonian ice sheet was relatively small (< 1.5 m sea level equivalent at the LGM, Davies et al 2020; Gowan et al 2021b), it may impact the RSL history in southern South America (Björck et al., 2021).

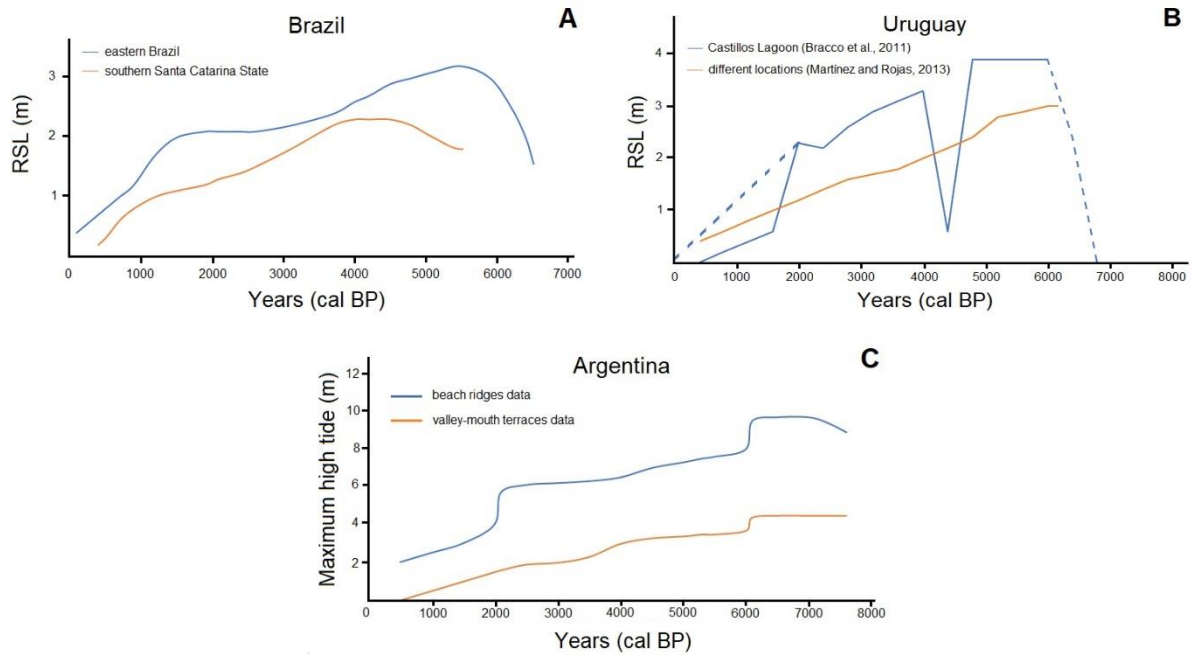


**Figure 4.2.** Sea level curves of data published by Angulo et al. (2006), Bracco et al. (2011), Martínez and Rojas (2013), and Schellmann and Radtke (2010). A) Curves derived from vermetid data of Brazil, B) Curves derived from lagoonal deposits from Castillos Lagoon, Uruguay (blue), and beach ridges data (orange) from different coastal sectors of Uruguay. C) Curves derived from beach ridges and valley-mouth terraces of the Patagonian coastline of Argentina. All curves were modified from the original papers' sources.

#### 4.4. Methods

The sea-level database presented in this work was compiled following the standardized protocol developed by the HOLSEA project (Khan et al., 2019), following the approach described by van de Plassche (1986) and Shennan (2015). To be considered as valid SLIP, any geological, sedimentary, or biological facies must have four main attributes:

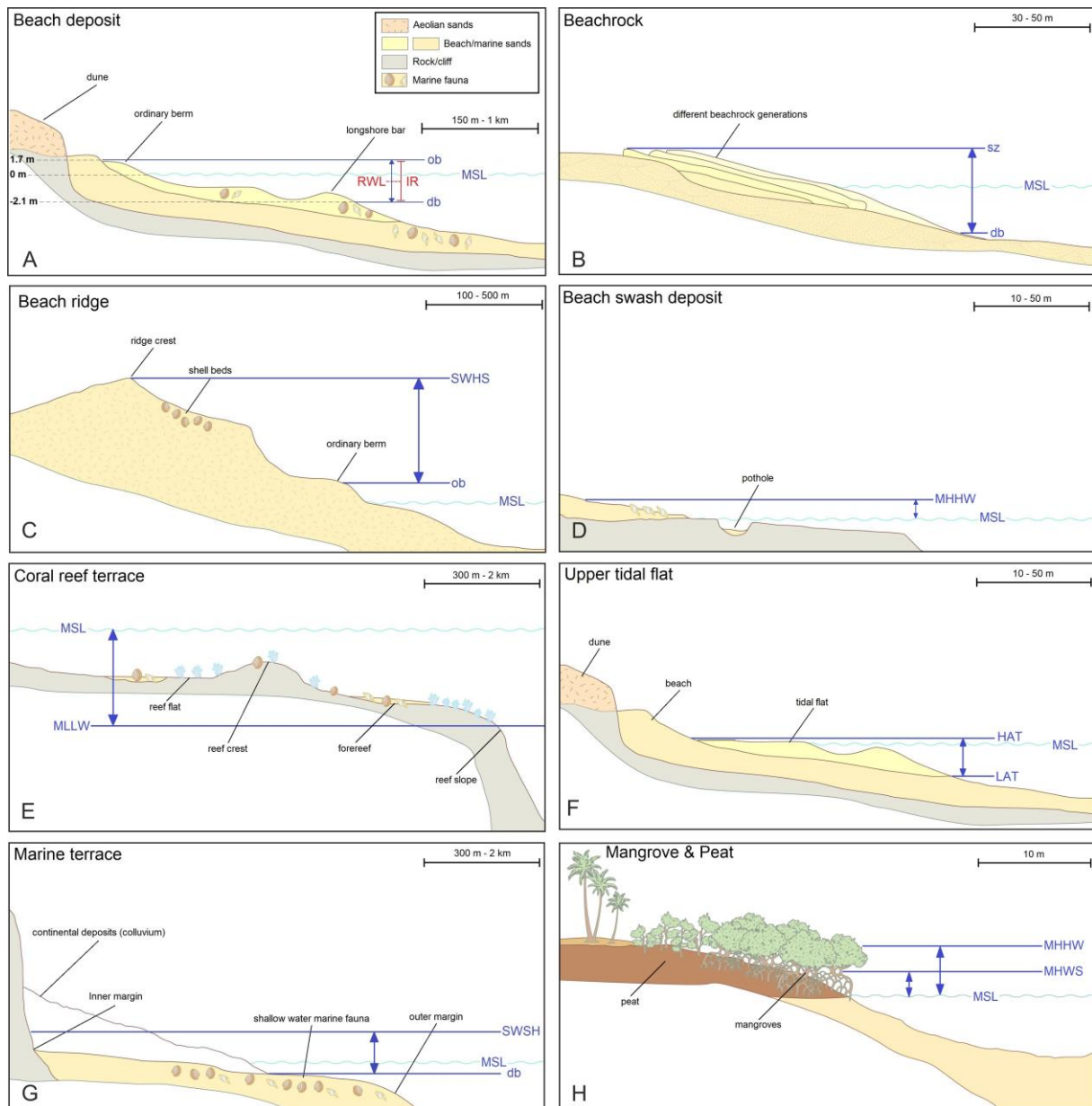
1. A precise geographic location.
2. High-precision elevation benchmarked to a tidal datum. However, when we found a sea-level indicator formed exactly at paleo mean sea level and its modern analog, benchmarking the elevation to a datum may not be necessary, although we do assume that the environmental conditions have not changed and that the relationship of the indicator growth to the inundation frequency is, therefore, the same.
3. A clear relationship between the indicator and the sea level. This relationship is known as the indicative meaning, comprising the Indicative Range (IR), and the Reference Water Level (RWL). The IR represents the vertical elevation range occupied by a sea-level indicator relative to contemporary tidal datums. The RWL is the midpoint of the IR.
4. The age of formation, traditionally obtained with radiometric dating techniques.

To populate the database, we used the WALIS web interface (Rovere et al., 2023), which was recently released in beta testing to include Holocene data. The database includes data and metadata extracted primarily from published scientific papers, conference proceedings, and (in a few cases) PhD theses. In the cases where the same sea-level indicator was reported in different publications, we tracked the original publication source but made a preference for the better-described and constrained SLIPs. The “notes” field of the database reports choices made when standardizing data to the required format, details on the interpretation of values reported in the original studies, or choices we made when different authors were reported on the same sample with different interpretations.

### 4.4.1. Indicative meaning and age component of sea-level indicators

The database includes several indicators defining the discrete position of past RSLs, such as beach deposits, beach ridges, coral reefs, fixed biological indicators, marine terraces, and sedimentary indicators (see Figure 4.3, 4.4, and Table 4.1 for details). The database also includes limiting data points, which provide an upper (terrestrial limiting) or lower (marine limiting) bound against the past RSL position. In our work, we have reviewed in detail all published RSL evidence and allocated each SLIP with an indicative meaning. If the information provided in the original literature was insufficient to quantify the indicative meaning through direct comparison with a modern analog, we calculated it using the IMCalc software (Lorscheid and Rovere, 2019). For the beach ridges, we calculate the indicative meaning using modern wave data and a set of wave runup models to estimate their upper (ordinary berm) and lower limits (higher storm berm). Through this process, we calculated the 2% exceedance wave runup level using the different models implemented into the py-wave-runup tool coded by Leaman et al. (2020).

## Holocene relative sea-level changes from the Atlantic coasts of South America



## Holocene relative sea-level changes from the Atlantic coasts of South America

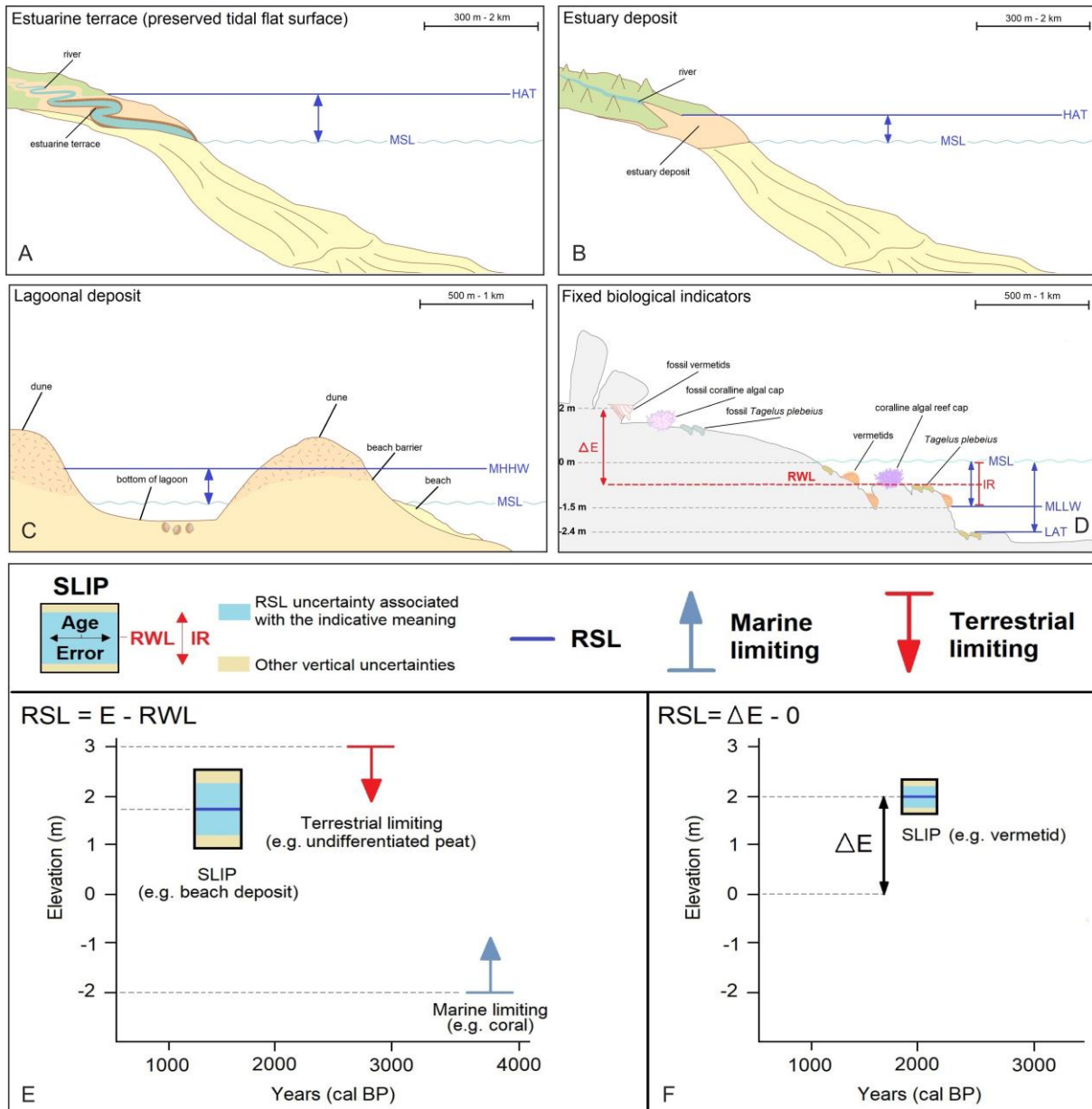


**Figure 4.4.** Schematic illustration of the paleo-sea level indicators with their upper and lower limits of the Indicative Range shown by the thin dark blue lines and blue arrows (see Table 4.1 for more details and definitions). A) to D) schemes of paleo-sea level indicators. E) and F) Schematic derivation of a SLIP using a published indicative meaning; E) Equation applied to paleo-sea level indicators not formed directly at paleo mean sea level (e.g. beach deposit), and schematic representation of a terrestrial limiting data point (downward-pointing red arrow) and marine limiting data point (upwards-pointing blue arrow); F) Equation applied to paleo-sea level indicators formed directly at the paleo mean sea level with modern analog (e.g. vermetid).  $\Delta E$  represents the elevation difference between the modern and fossil counterpart, as illustrated in panel D. RSL: relative sea level; RWL: reference water level; IR: indicative range; SLIP: sea-level index point; db: breaking depth; ob: ordinary berm; SWHS: storm wave swash height.

The models used to calculate the indicative meaning of beach ridges require as input the beach slope, significant wave height, and period. We gathered the beach slope at our four areas where beach ridges were reported in literature (i.e. Río de la Plata delta, Bahía Blanca to Peninsula Valdés, Bahía Vera to Puerto San Julián, and Tierra del Fuego) using the

CoastSat.Slope toolbox (Vos et al., 2019, 2020). This toolbox analyzed Landsat and Sentinel satellite data between 2000 and 2023, alongside tides extracted from the FES2014 global tidal model (Lyard et al., 2021; Carrere et al., 2016). To calculate wave height and period we used the RADWave tool (Smith et al., 2020), which allows querying satellite altimetry data. We extracted a time series of wave data between 66°W to 70°W and 38°S to 52°S, in a period included between Jan 1st, 2000, and Jan 1st, 2023. For the same time frame, we queried the FES2014 model and extracted water levels at a 15-minute interval. By coupling tidal and wave data via their UTC timestamps, we gathered a database with 231462 wave conditions. We selected a beach slope sampled from a normal distribution created with the mean and standard deviation of the beach slope for each condition. We used the "ensemble" function of py-wave-runup to run for each wave height and period eight different runup models (Supplementary Figure 4.1). We added (or subtracted) the corresponding water level at each calculated runup.

**Table 4.1.** Types of paleo-sea level indicators in the database, including their indicative range and number of occurrences. MLLW=Mean Lower Low Water; MHHW=Mean Higher High Water; MSL=Mean Sea Level; LAT=Lowest Astronomical Tide; HAT=highest astronomical tide; MHWS=Mean High Water Springs; GWL=Groundwater Level. \* denotes indicative ranges provided by the revised publications.

Primary indicator type	Secondary indicator type	Indicative range	Number of occurrences
Beach deposit	Beach deposit or beachrock	Breaking depth to ordinary berm	68
		MLLW-MHHW*	1
	Beach ridge	Back calculated from values reported by the original authors*	51
		Ordinary berm to storm wave swash height	287
Beach swash deposit	MHHW-MSL	1	
Coral reefs	Coral reef terrace	MSL-MLLW	16
Fixed biological indicators	Coralline algal reef cap	MSL - MLLW	1
	Tagelus plebeius	LAT to MSL	2
	Vermetids	MLLW to MSL	171
Marine terrace	Marine Terrace	Breaking depth to storm wave swash height	33

Table 4.1. Continued

Primary indicator type	Secondary indicator type	Indicative range	Number of occurrences
Sedimentary	Basal Peat (non-mangrove)	MHHW to MSL	2
	Estuarine Terrace (preserved tidal flat surface)	MSL to HAT	28
	Estuary deposit	HAT to MSL	2
	Lagoonal deposit	MHHW to MSL	2
	Mangrove	Measured on modern analog*	5
		MSL to MHWS	19
Upper Tidal Flat	LAT to HAT	3	
The data point is a marine or terrestrial limiting indicator		N/A	332

In our database, the age of the samples was determined using radiocarbon dating ( $^{14}\text{C}$ ). As the production of atmospheric radiocarbon has varied through geological time we recalibrated all radiocarbon ages reported in the literature into sidereal years with a  $2\sigma$  range. Age calibrations were done using the CALIB software (version 8.2). We use the Marine20 curve to calibrate marine and estuarine samples, and the Intcal20 and SHcal20 curves for terrestrial samples (Stuiver and Polach, 1977; Heaton et al., 2020; Reimer et al., 2020, Hogg et al., 2020). Marine reservoir corrections have been applied according to the closest available data for each study area (Macario et al., 2023). When a study site was located in an area with unknown Delta-R values, we used the Marine Reservoir Correction Database (Reimer and Reimer, 2001). Following the analysis by Hu (2010) of  $^{14}\text{C}$  ages from bulk peat samples, a  $\pm 100$   $^{14}\text{C}$  yr error was applied to account for sample contamination (Törnqvist et al., 2015). Codignotto et al. (1992), Björck et al. (2021), and Fasano et al. (1983) reported calibrated ages; therefore, we did not re-calibrate them.

All SLIPs in our database are presented as calibrated years before present (yr BP), where year 0 is AD 1950 (Stuiver and Polach, 1977). A concern with old radiocarbon ages is the correction for isotopic fractionation (Törnqvist et al., 2015). This correction became a standard procedure at most laboratories by the late 1970s (Stuiver and Polach, 1977), but some laboratories have only applied this correction since the mid-1980s (Hijma et al., 2015). When needed, we reported the values described by the authors or the marine carbonate standard  $\pm 3$  ‰ (Törnqvist et al., 2015). Further details and choices made while compiling the radiocarbon ages (e.g., lab code or whether a  $\delta^{13}\text{C}$  fractionation correction was added) are available in the database (see supplementary file).

#### 4.4.2. Elevation of sea-level datapoints

In our database, we gathered the elevation of each SLIP and vertical datum information from the original works, wherever available. Overall, we identified the elevation and vertical datum combinations shown in Table 4.2. We account for potential sources of error in the measurement of a sample elevation following the criteria described in the database protocol by Hijma et al. (2015) (Table 4.3). If either the measurement method or vertical datum was not reported, we set the elevation error to 20% of the measured elevation, with a lower error limit of 0.2 m (for elevations between -1 m and +1 m) and an upper error limit of 2 meters (for elevations higher than 10 m or deeper than -10 m). If neither the elevation measurement method nor the vertical datum was reported by the original publication, we set the elevation error to 40% of the measured elevation, with a lower error limit of 0.2 m (for elevations between -0.5 m and + 0.5 m) and an upper error limit of 2 meters (for elevations higher than 5 m or deeper than -5 m).

**Table 4.2.** Combinations of elevation measurement methods and vertical datums reported in the database.

Elevation measurement method	Vertical datum	Number of occurrences
Not reported	Not reported	360
	Mean Sea Level / General definition	222
	Mean sea level from tidal data	51
	Nazaré Pier	4
	Vermetid biological datum	153
Total station or Auto/hand level	High Tide Level	82
	Mean Sea Level / General definition	6
Differential GPS	Local geoid	24
	Mean sea level from tidal data	17
	EGM 2008	7
Handheld GPS	Mean Sea Level / General definition	8
Topographic map and digital elevation models	Mean Sea Level / General definition	7

**Table 4.2.** Continued

Elevation measurement method	Vertical datum	Number of occurrences
Barometric altimeter	Local geoid	12
	Mean sea level from tidal data	8
	High Tide Level	3
	Not reported	3
	Mean Sea Level / General definition	2
Multibeam bathymetry data + core depth	Mean Sea Level / General definition	48
Dumpy level	Vermetid biological datum	7

Some studies, in particular those along the coasts of Patagonia, report elevations relative to the high tide level or “high tide mark”. In these instances, the reported elevation was corrected to mean sea level by subtracting the difference between the local Mean Higher High Water (MHHW) and Mean Lower Low Water (MLLW) calculated using the IMCalc software (Lorscheid and Rovere, 2019). Several studies along the Brazilian coasts often report only a general “paleo sea level” value, not the sample elevation (e.g., Angulo et al., 2006; Toniolo et al., 2020). For our database, we considered these reported values as sample elevations and assigned a 40% uncertainty, as no other information was available on either the originally adopted indicative range or the originally measured elevation. A note was inserted in the record pointing to this choice for each of these SLIPs. A 40% uncertainty was also assigned for the Argentinian data reported by Codignotto et al. (1992), as little information on the samples is provided in the paper and previous studies.

**Table 4.3.** Sources of vertical uncertainties accounted for in the database. Each vertical uncertainty was applied as appropriate to different samples. SLIP: Sea-Level Index Point; RTK GPS: Real-Time Kinematic Global Positioning System; DEM: Digital Elevation Models. \*Source of uncertainty specifications.

<b>Core samples or sections</b>	
<b>Source of uncertainty</b>	<b>Description</b>
Sample thickness uncertainty	Half of the sample thickness
Sampling uncertainty	Depth range of the dated sample
	± 0.01 m if not specified
Core shortening/ stretching uncertainty	± 0.15 m for rotatory/vibracoring
	± 0.05 m for hand coring
	± 0.05 m for hand coring
	± 0.01 m for Russian sampler
	Assigned largest uncertainty (± 0.15 m) if type of corer was unclear
Non-vertical drilling uncertainty	2% (e.g., 0.02 m/m depth)
<b>Outcrops or other type of paleo-sea level indicators</b>	
Tidal uncertainty	Half of the tidal range
	Applies only to samples collected offshore with reference to the water's surface*
Water depth uncertainty	Uncertainty associated with the measurements of water depth, as reported
	± 0.05 m if not specified
Levelling uncertainty	± 0.01 m for high-precision levelling equipment (e.g., total station, dumpy level)
	± 0.03 m if levelling method is unknown, but the authors mentioned elevations measured/surveyed
	± 20% or 40% of reported elevations if further uncertainties regarding the SLIP levelling
GPS or RTK uncertainty	Uncertainty associated with RTK GPS measurements, as reported
	± 0.1 m if not specified
Benchmark uncertainty	± 0.1 m for reliable and stable benchmarks
	± Precision of benchmarks if further uncertainties
	Does not apply to samples that were not levelled to a benchmark*
Vegetation zone uncertainty	± 20% of the reported elevation range of vegetation
	Applies only to samples whose elevations were estimated from vegetation zones*
Map uncertainty	± 0,50 m for high-precision levelling (additional elevation methods are included)
	± 1 m if only a topographic map were used to determine sample elevation
DEM uncertainty	± 0,50 m (as recommended by Hijma et al., 2015 for areas with significant relief)

Data points were rejected when there was insufficient information within the original sources to gather essential data, such as the elevation of a sample. As an example, when the depth of a sample within the core was reported but not the core top elevation, we had to reject the data point. Marine samples with  $^{14}\text{C}$  age adjusted for Delta R < 603 were rejected because they were not valid for the calibration curve (Stuiver and Polach, 1977). Another reason for rejection, only if strictly necessary, was if a SLIP was at odds regarding the RSL estimate with coeval data points in the same area. However, rejected data points and associated radiocarbon ages were not eliminated from the database and are available for future re-assessment in case further information arises.

We highlight that the uncertainty and rejection of a data point does not reflect in any way the quality of the published papers where the data points are reported. The uncertainty assigned and the rejection of the data were exclusively designed to discern the suitability of each record to be used as a standardized SLIP or limiting point.

#### 4.4.3. Statistical model of Holocene RSL

To calculate local sea-level curves for each area identified within the database (see sections 4.5.1 and 4.5.2 for details), we applied the Spatio-Temporal Empirical Hierarchical Model (STEHM) by Ashe et al. (2019) to the SLIPs data. The STEHM has three levels: 1) a data level, which models the way different SLIPs record RSL with vertical and temporal noise; 2) a process level, which distinguishes between RSL changes that are common across the full database and those that are confined to the specific regions; and 3) a hyperparameter level, which characterizes prior expectations regarding dominant spatial and temporal scales of RSL variability (Khan et al., 2022). At the data level, we observe noisy RSL  $y_i$  and noisy age  $t_i$ :

$$y_i = f(x_i, t_i) + \epsilon^y_i + w(x_i, t_i) + y_0(x_i) \quad (1)$$

$$t_i = \hat{t}_i + \epsilon^t_i \quad (2)$$

where  $x_i$  and  $t_i$  are the geographic location and true age, respectively, of observations indexed by  $i$ ;  $f(x_i, t_i)$  is the true RSL value at  $x_i$  and  $t_i$ ;  $\epsilon^y_i$  is the vertical error of each RSL data point (assumed to be independent and normally distributed);  $w(x_i, t_i)$  is a supplemental white noise term that accounts for variations in the data that cannot be explained by the terms in the process-level model;  $y_0(x_i)$  is a site-specific datum offset to ensure that RSL data can be directly compared.  $\hat{t}_i$  is the mean estimated age of each RSL data point, and  $\epsilon^t_i$  is its error. The age uncertainties are incorporated using the noisy-input Gaussian Process (GP) method of McHutchon and Rasmussen (2011), which uses a first-order Taylor-series approximation to translate errors in the independent variable into equivalent errors in the dependent variable:

$$f(x_i, t_i) \approx f(x_i, \hat{t}_i) + \epsilon^t_i \frac{\partial f(x_i, \hat{t}_i)}{\partial t} \quad (3)$$

At the process level, we model the sea-level field,  $f(x_i, t_i)$ , as the sum of two component fields,  $f(x, t) = r(t) + l(x, t)$ , where  $x$  represents geographic location and  $t$  represents time. The two components are: a common regional term,  $r(t)$ , representing the time-varying signal shared by all sites included in the analysis, and a local term,  $l(x, t)$ , representing site-specific processes. The priors for each term in the model are mean-zero Gaussian processes (Rasmussen and Williams, 2006) with 3/2 Matérn covariance functions (see Ashe et al., 2019 for more details). Hyperparameters defining prior expectations of the amplitudes and spatio-temporal scales of variability were estimated through maximum-likelihood optimization (Supplementary Table 4.1).

### 4.4.4. Glacial isostatic adjustment models

In this paper, we compare the measured paleo-sea level indicators to calculated sea level from GIA models. We use the model SELEN to calculate the sea level (Spada and Stocchi, 2007; de Boer et al., 2014, 2017). SELEN assumes the Earth's rheology is spherically symmetric with an elastic lithosphere and a Maxwell viscoelastic mantle and calculates sea level using a constant time step. This version of SELEN also considers migrating shorelines and Earth's rotational effects. In this study, we compute the sea level at 500-year time steps.

The first model we use to compare with our data compilation is ICE-6G\_C (VM5a) (referred to as ICE6G in the rest of this paper) (Argus et al., 2014; Peltier et al., 2015). The version of the model we use includes a global ice sheet history going back to 122,000 years. The time step for this model is not constant and is larger than 500 years prior to 21,000 years cal BP, so we linearly interpolate the ice sheet thickness between the time steps. The ice volume of the ICE6G model was tuned to a paleo sea level record from Barbados and refined to fit present-day vertical land motion in areas covered by Late Pleistocene ice sheets. The VM5a Earth model that was used in conjunction with ICE6G\_C has a 60 km thick lithosphere, a 40 km thick layer below the lithosphere with a viscosity of  $1 \times 10^{22}$  Pa s, a  $5 \times 10^{20}$  Pa s upper mantle, a  $1.6 \times 10^{21}$  Pa s lower mantle between 660 and 1160 km depth, and the rest of the lower mantle with a viscosity of  $3.2 \times 10^{21}$  Pa s. Peltier et al. (2015) used the Holocene sea-level indicators from southeastern South America, as compiled in Rostami et al. (2000), to evaluate the ICE6G model. They attributed the Holocene highstand position to rotational effects. By including rotational effects, the calculated sea level from ICE6G was better able to match the highstand in many locations along the eastern South American coast. The Patagonian Ice Sheet in ICE6G has a sea level equivalent ice volume of 0.9 m at the LGM, which decreases to its present-day value at 15,500 years cal BP.

The second model is the PaleoMIST 1.0 reconstruction (Gowan et al., 2021b). This model was designed as a preliminary ice sheet and topography reconstruction for the past 80,000 years, at 2500-year time steps. The Earth model used with PaleoMIST has a 120 km thick lithosphere,  $4 \times 10^{20}$  Pa s upper mantle, and  $4 \times 10^{22}$  Pa s lower mantle. The ice thickness has been linearly interpolated to 500-year time steps for the calculations in this study. The model was tuned with sea level observations from the Laurentide and Eurasian ice sheets, and was not rigorously evaluated against far-field sea level records such as those in eastern South

America. Some initial calculations for southeastern South America presented by Gowan et al. (2021a) demonstrated that the sea level highstand may not have happened simultaneously along the coast. Subsequent analysis of PaleoMIST 1.0 demonstrated that the ice volume during the mid to late Holocene is too great to account for far-field sea level observations (Gowan, 2023). Almost all of this excess ice volume is located in Antarctica, so in this paper, we have modified PaleoMIST 1.0 to use the present-day Antarctica ice sheet configuration from 5000 years BP to mitigate this issue. The Patagonian Ice Sheet in PaleoMIST has a sea level equivalent ice volume of 0.8 m at the LGM, which decreases to present-day values at 12,500 years cal BP.

### 4.5. Results

The spatial extent covered by the database spans between 0° and 60° latitude South and between 40° and 70° longitude West (Figure 4.1). We reviewed data from 128 studies published between 1964 and 2023 (Figure 4.5C) to gather 1024 valid data points (726 SLIPs, 97 terrestrial and 201 marine limiting points), each associated with its temporal and vertical uncertainty. We rejected 286 data points because the necessary information required by the standard sea-level database protocols was not achieved. We divided our database into 12 regions (Figure 4.1) based on data availability, tectonic setting, and the distance from the Antarctic ice sheet. These areas are described in detail in the following sections. The database spans the last 12,500 years, with nearly 80% of the data younger than 6000 years cal BP (Figure 4.5A, D). In general, the majority of radiocarbon age errors are lower than 500 years (Figure 4.5E), and RSL elevation uncertainties (including elevation error and indicative meaning uncertainty) are between 0.5 m and 2 m (Figure 4.5F).

## Holocene relative sea-level changes from the Atlantic coasts of South America

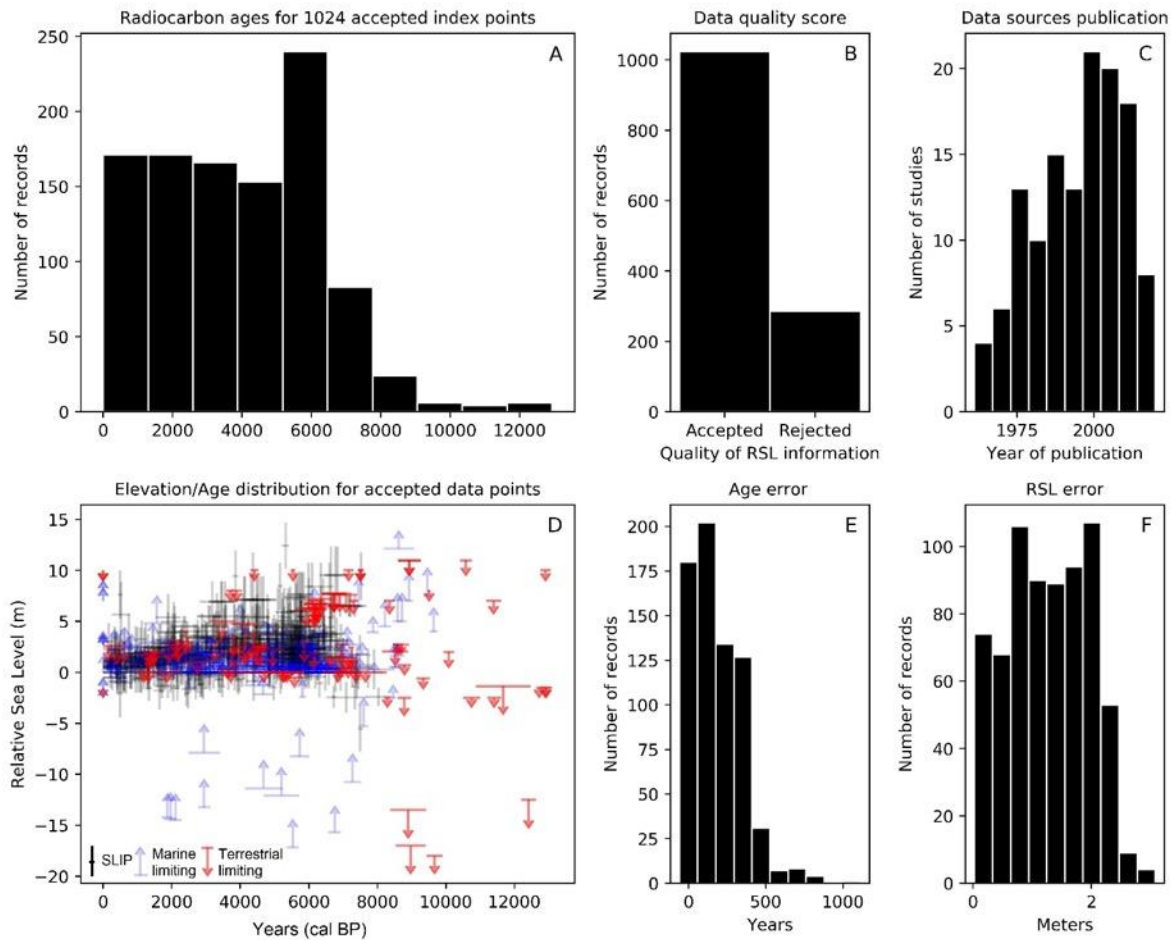


**Figure 4.5.** Details of the database including: A) Radiocarbon ages of the 1024 records. B) Quality of the data included in the database. C) Publication year of studies included in the database. D) Age vs. RSL elevation plot for the 1024 data points. Black crosses are SLIPs, upwards-pointing blue arrows are marine limiting points, and downward-pointing red arrows are terrestrial limiting points. E) and F), respectively, age and RSL errors for SLIPs included in the database.

### 4.5.1. Brazil

#### 4.5.1.1. Region 1: Amazon river delta

The region encompassing the Amazon river delta area is located in northern Brazil, between Amapá and Pará states. Within this region, we gathered 27 SLIPs and 15 limiting data. The prevalent types of SLIPs are mangroves (Cohen et al., 2005; Behling et al., 2001), estuarine deposits (Behling et al., 2004; Cohen et al., 2012), upper tidal flats (Cohen et al., 2012; Guimarães et al., 2012), and basal peat (non-mangrove) (Ribeiro et al., 2023).

The record in the Amazon river delta dates back to the early Holocene, with some limiting data placing the RSL below 0 m (Figure 4.6A). The oldest SLIP in this region places RSL at  $-6 \pm 1.9$  m below sea level (b.s.l.) at  $\sim 7500$  years cal BP (ID: 748). After, RSL rose to  $1.6 \pm 1.4$  m above sea level (a.s.l.) at  $\sim 5000$  years cal BP during the mid-Holocene. Since then, RSL oscillates between  $-0.6 \pm 1.2$  m b.s.l. (3900 years cal BP) and  $0.7 \pm 1.1$  m a.s.l. (400 years cal BP)

(Figure 4.6A). One SLIP (ID: 734) documents a high RSL value of  $ca. 2.9 \pm 1.4$  m a.s.l. at  $\sim 600$  years cal BP and should be revised as several SLIPs indicate that, at that time, RSL was close to its modern value. Application of the STEHM shows an increase in the RSL during the mid-Holocene (from  $\sim 8000$  to  $\sim 5000$  years cal BP) at an average rate of 0.30 mm/yr; after this increase, the rate of RSL change slowly decayed through the late Holocene at a mean rate of 0.16 mm/yr (Figure 4.6B, C). The GIA prediction from the model ICE6G fits the data, while PaleoMIST seems to underestimate the RSL at the beginning of the mid-Holocene (Figure 4.6B).

### 4.5.1.2. Region 2: Atol das Rocas

The Atol das Rocas is an atoll island located 250 km offshore the northeastern Brazilian coast. The RSL history in this area is based on 25 SLIPs and 6 limiting data. The predominant paleo-sea level indicators in this area are coral reef terraces (Gherardi and Bosence, 2005), beach deposits, and one lagoonal deposit (Angulo et al., 2022a; Kikuchi and Leao, 1997).

In Atol das Rocas there is an absence of early Holocene data. During the mid-Holocene, two limiting points indicate that the RSL was around -10 m b.s.l. at ca. 5000 years cal BP (Figure 4.6D). From 3000 years cal BP to the present, SLIPs are scattered but indicate that the local sea level in this region was consistently above present level (on average, +1.6 m). The great variability in the data is reflected in the STEHM, which shows a trend of a constant RSL with values from 5 m a.s.l to -5 m b.s.l since the mid-Holocene (Figure 4.6E). However, the rate of RSL change experienced a decay since ca. 2800 years cal BP with a mean value of 0.19 mm/yr (Figure 4.6F). GIA model predictions show that the sea level in this area was already close to its modern position around 5000 years cal BP, and GIA predictions are significantly lower than the observed RSL in the region (Figure 4.6E).

### 4.5.1.3. Region 3: Pernambuco and Alagoas

In this region, we reviewed 31 SLIPs, and 33 limiting data. Vermetid rims are the dominant paleo-sea level indicators in this area (Martin et al., 1996; Dominguez et al., 1990; Angulo et al., 2006), although beach deposits were also described (Dominguez et al., 1990) along with two data points from mangroves (Barbosa et al., 1986), and one from a coralline algal reef cap (Delibrias and Laborel, 1971; Laborel, 1969).

The records in Pernambuco and Alagoas date back to the mid-Holocene. The oldest SLIP (ID: 143) places the RSL at  $0.3 \pm 1.9$  m a.s.l. at  $\sim 7800$  years cal BP. After, sea level rose to  $ca. 5 \text{ m} \pm 1.8 \text{ m}$  at 3800 years cal BP. And has oscillated since, between  $-0.4 \pm 0.4$  m b.s.l. (3200 years cal BP) and  $2.3 \pm 0.8$  m a.s.l (200 years cal BP) (Figure 4.6G). According to the STEHM, after the mid-Holocene highstand (between  $\sim 8000$  and 7000 years cal BP) the RSL falls to its present position at a mean rate of 1.19 mm/yr (Figure 4.6I). Neither GIA model accurately reproduces the SLIP record. ICE6G GIA model predictions for sea level are greater than the RSL

history described by the STEHM. PaleoMIST predictions are lower than the data during the beginning of the mid-Holocene but higher since ~5000 years cal BP (Figure 4.6H).

### 4.5.1.4. Region 4: Sergipe and North Bahia

In the Sergipe and North Bahia region, we recognize 35 SLIPs, and 16 limiting data. In this region, there are three types of paleo-sea level indicators: vermetid rims (Bittencourt et al., 1978; Martin et al., 1979,1980; Delibrias and Laborel, 1971; Angulo et al., 2006), beach deposits (Bittencourt et al., 1978; Martin et al., 1979/1980), and mangroves (Martin et al., 1979/1980; Martin et al., 1982).

Here, SLIPs data begin in the mid-Holocene. The oldest SLIP (ID: 152) places the RSL at  $-2.4 \pm 0.8$  m b.s.l. at 8000 years cal BP (Figure 4.6J). From there, the RSL increases to  $\sim 1.7 \pm 1.9$  m a.s.l. ca. 5700 years cal BP. One point (ID: 211) documents the highest RSL value at 5400 years cal BP, positioning the sea level at  $5 \pm 1.9$  m a.s.l. After this sea level peak, RSL in this region plots between  $\sim 3$  to  $\sim 2$  m a.s.l. between 4000 to 2000 years cal BP, then it falls close to its modern position (Figure 4.6J). According to the STEHM, after the mid-Holocene highstand ( $\sim 8000$  years cal BP), the RSL falls to its present position; however, a secondary sea level rise occurred during the late Holocene from 4000 to 3000 years cal BP (Figure 4.6K). The highest rate of RSL change (1.13 mm/yr) is observed during the mid-Holocene (Figure 4.6L). The GIA model predictions are lower than the STEHM estimation (Figure 4.6K).

## Holocene relative sea-level changes from the Atlantic coasts of South America

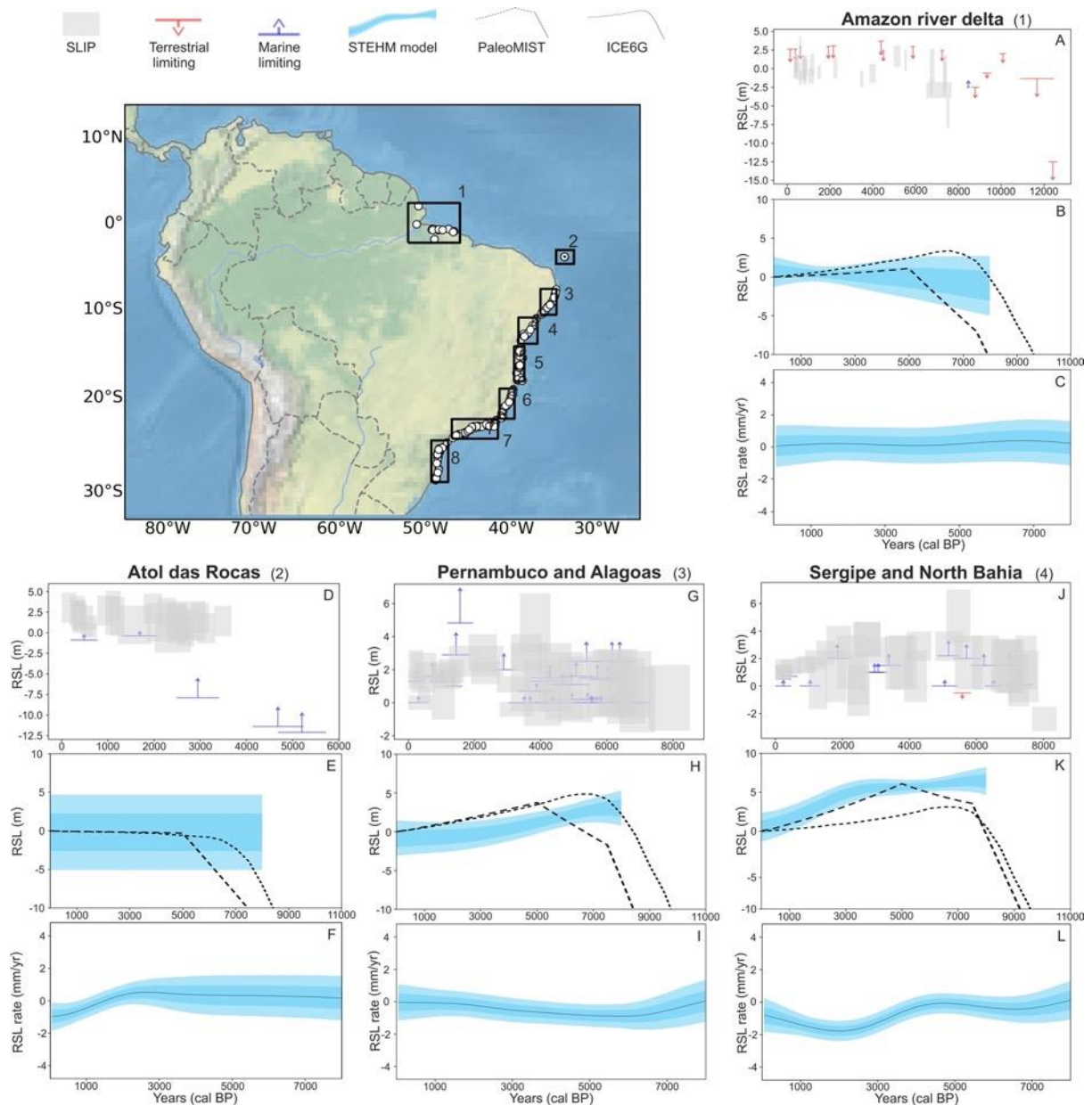


**Figure 4.6.** RSL reconstructions and rates from northern Brazil areas using the spatio-temporal model. For all plots, the model mean and  $1\sigma/2\sigma$  uncertainty are represented by a solid line and shaded envelopes, respectively. Index points (grey boxes) are plotted as calibrated age against changes in sea level relative to the present. Limiting points are plotted as a downward-pointing red arrow for terrestrial or an upwards-pointing blue arrow for marine. Dimensions of boxes and arrow symbols for each point are based on elevation and age ( $2\sigma$ ) errors. SLIP: sea-level index point; STEHM: spatio-temporal empirical hierarchical model; ICE6G (curved line) and PaleoMIST (straight line) represent the GIA models.

#### 4.5.1.5. Region 5: Central and South Bahia

The dataset includes Bahia state's central and southern sectors and is based on 37 SLIPs and 20 limiting data. This region shows a broad diversity of indicators, including beach deposits (Angulo et al., 2022b), vermetid rims (Bittencourt et al., 1978; Martin et al., 1979/1980; Martin et al., 1996; Angulo et al., 2022b; 2006), and mangroves (Fontes et al., 2017).

The record of this region dates back to the mid-Holocene. RSL changes in this area show slight oscillations over time, with values ranging from 4 m a.s.l. to -0.9 m b.s.l. Two data points (IDs: 249; 1214) show the highest RSL values ( $4.3 \pm 1.6$  m a.s.l. and  $4.5 \pm 1.7$  m a.s.l., respectively) at around 5000 years cal BP (Figure 4.7A). The STEHM shows a rising sea level between 8000 to ~5000 years cal BP with a rate of RSL change of 1.10 mm/yr. After this increase, the RSL falls at an average rate of 0.46 mm/yr (Figure 4.7B, C). The GIA model predictions of ICE6G show a good agreement with the RSL history reconstructed by the STEHM, while PaleoMIST underestimates the trend at the beginning of the mid-Holocene.

#### 4.5.1.6. Region 6: Espírito Santo and North Rio de Janeiro

Twelve SLIPs and 48 limiting data were reviewed in this region. The RSL history of this region is based primarily on limiting data (Delibrias and Laborel, 1971; Martin and Suguio, 1989; Martin et al., 1996; Martin et al., 1997). However, there are reports of a few SLIPs represented by vermetid rims (Martin and Suguio, 1989; Martin et al., 1996; Martin et al., 1996; Angulo et al., 2006; Angulo et al., 2016), and one SLIP associated with a beach deposit (Martin et al., 1996; Martin et al., 1997).

In this region, the data dates back to the mid-Holocene. The marine limiting data suggest that RSL remained above present since ca 7000 years cal. The oldest SLIP (ID: 347) places the sea level at  $1.7 \pm 0.6$  m a.s.l. at ~6000 years cal BP. A high RSL value slightly above 3 m a.s.l. remains constant during the mid-Holocene, with its highest value ( $3.6 \pm 1.3$  m a.s.l.) at 5000 years cal BP. During the late Holocene, RSL oscillates between  $3.5 \pm 1.3$  m a.s.l. to  $0.9 \pm 1.6$  m a.s.l., with the highest value ( $3.5 \pm 1.3$  m a.s.l.) at 3000 years cal BP and the lowest values towards the present (Figure 4.7D). As in the previous area, the STEHM shows a mid-Holocene highstand between ~8000 to ~5000 years cal BP; here, the rate of RSL change has an average value of 1.16 mm/yr. After this rise, there is an RSL fall trend with a mean rate of 0.26 mm/yr (Figure 4.7E, F). ICE6G GIA predictions fit the data, while PaleoMIST predictions are lower until ca. 5000 years cal BP (Figure 4.7E).

#### 4.5.1.7. Region 7: South Rio de Janeiro and Central São Paulo

The RSL history of this region is based on 56 SLIPs and 47 limiting data. Despite the large number of SLIPs in this area, only two types of indicators were described in this region:

vermetid rims (Delibrias and Laborel, 1971; Martin and Suguio, 1978; Suguio and Martin, 1978; Flexor and Martin, 1979; Martin et al., 1979; Martin et al., 1979/1980; Suguio et al., 1980; Martin et al., 1996; Angulo et al., 2006; Castro et al., 2014; Angulo et al., 2016; Castro et al., 2021), and beach deposits (Martin et al., 1979; Martin and Suguio, 1989; Angulo et al., 2006; Castro et al., 2014; Angulo et al., 2016; Castro et al., 2021).

The record in this area mainly corresponds to the mid-Holocene, and only two marine limiting data indicate a sea level of ca. -15 m b.s.l. during the early Holocene. Our data suggest that from ~7000 to 5000 years cal BP, the sea level was close to the mean sea level with an average value of ~1.1 m a.s.l. just one SLIP (ID: 464) shows a higher RSL value ( $2.3 \pm 1.5$  m a.s.l.) during ca.5800 years cal BP. The mid-Holocene highstand ( $3.8 \pm 1.4$  m a.s.l.) reached ca. 4900 years cal BP. Still, one SLIP (ID: 463) indicates a higher RSL ( $4.7 \pm 2.2$  m a.s.l.) at 3300 years cal BP. After this time, RSL falls gradually towards its modern position (Figure 4.7G). The STEHM shows a sea level rise around 8000 to 5000 years cal BP (RSL rate of 0.63 mm/yr) followed by a subsequent stable RSL through the present with changing rates of 0.09 mm/yr (Figure 4.7H, I). ICE6G GIA predictions fit the data, while PaleoMIST predictions are lower at the beginning of the mid-Holocene (Figure 4.7H).

### 4.5.1.8. South São Paulo, Paraná, and Santa Catarina

In South São Paulo, Paraná, and Santa Catarina states, the RSL history is described by 61 SLIPs and 32 limiting points. All the reported paleo-sea level indicators in this area are vermetid rims (Angulo, 1989;1992; Angulo et al., 1999; Souza et al., 2001; Angulo et al., 2002; Toniolo et al., 2020; Angulo et al., 2022c).

The record in South São Paulo, Paraná, and Santa Catarina date back to the mid-Holocene. The oldest SLIP (ID: 544) places the sea level at  $2.3 \pm 0.8$  m a.s.l. at 5600 years cal BP. The highest sea level value is observed around 5000 years cal BP, rising the sea level ca.  $3.8 \pm 1.4$  m a.s.l. Since then, the RSL gradually falls towards the present, ranging from  $\sim 3.3 \pm 1.0$  m a.s.l. to  $\sim 0.4 \pm 0.3$  m a.s.l. (Figure 4.7J). As in the previous area, the STEHM shows a sea level rise of around 8000 to 5000 years cal BP; after this highstand, the RSL slowly falls towards its modern position at an average rate of 0.37 mm/yr (Figure 4.7K, L). The GIA model predictions of ICE6G fit the data; PaleoMIST predictions are lower than the RSL trend described by the STEHM during the beginning of the mid-Holocene (Figure 4.7K).

## Holocene relative sea-level changes from the Atlantic coasts of South America

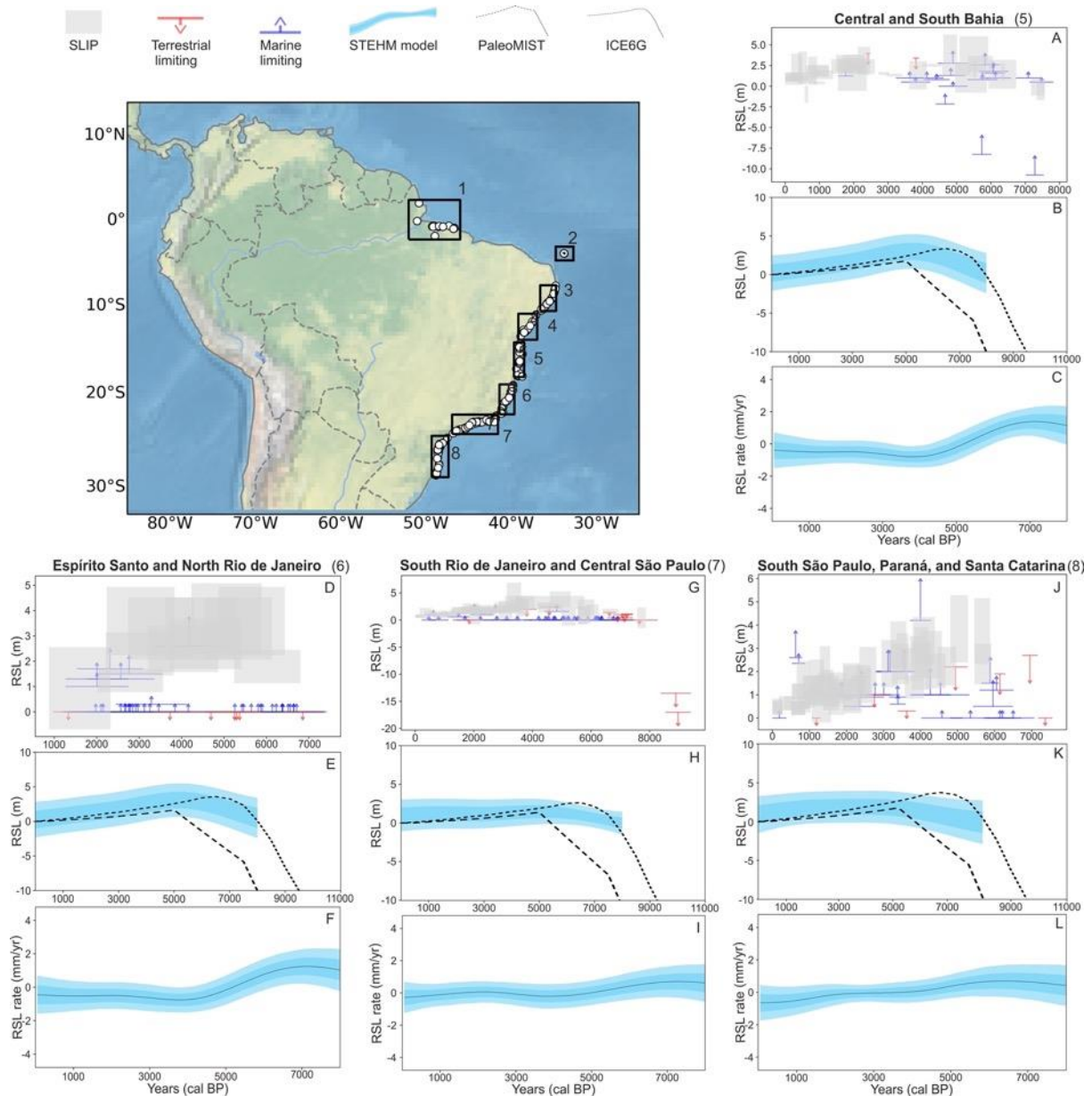


**Figure 4.7.** RSL reconstructions and rates from southern Brazil areas using the spatio-temporal model. For all plots, the model mean and  $1\sigma/2\sigma$  uncertainty are represented by a solid line and shaded envelopes, respectively. Index points (grey boxes) are plotted as calibrated age against changes in sea level relative to the present. Limiting points are plotted as a downward-pointing red arrow for terrestrial or an upwards-pointing blue arrow for marine. Dimensions of boxes and arrow symbols for each point are based on elevation and age ( $2\sigma$ ) errors. SLIP: sea-level index point; STEHM: spatio-temporal empirical hierarchical model; ICE6G (curved line) and PaleoMIST (straight line) represent the GIA models.

## 4.5.2. Uruguay – Argentina

### 4.5.2.1. Region 9: Río de la Plata delta

The RSL history of this region is described by 169 SLIPs and 26 limiting data. The main paleo-sea level indicators described in the region were beach ridges (Cortelezzi, 1977; Albero and Angiolini, 1983; Guida and González, 1984; Codignotto et al., 1992; Cortelezzi et al., 1992; Aguirre, 1993; Colado et al., 1995; Cavallotto, 1995; Cavallotto, 2002; Bracco and Ures, 1998; Bracco, 2000; Bracco et al., 2011; Martínez and Rojas, 2013; Prieto et al., 2017; Cavallotto et al., 2004; Cavallotto et al., 2005; Martínez et al., 2006), and estuary deposits (Albero and Angiolini, 1983; Fasano et al., 1983; González and Ravizza, 1987; Figini, 1992; Martínez et al., 2006; Amato and Busso, 2009; Prieto et al., 2017; Fucks and De Francesco, 2003). One upper tidal flat deposit, one beach swash deposit (Bracco and Ures, 1998; Prieto et al., 2017), and two biological indicators (deposits containing remnants of the mollusk *Tagelus plebeius*) were also described (Bracco et al., 2011).

The record in Rio de la Plata delta mainly corresponds to the mid-Holocene; only one terrestrial limiting data suggests that RSL was -18 m b.s.l. during the early Holocene. The oldest SLIP (ID: 296) places the sea level around  $3.1 \pm 0.6$  m a.s.l. at 6800 years cal BP. Two SLIPs (IDs: 47; 269) show the highest RSL value  $\sim 4.7$  m a.s.l. at 5300 years cal BP and 4900 years cal BP, respectively. Since then, the data shows an almost continuous RSL fall (Figure 4.8A). As shown by the STEHM, after the mid-Holocene highstand (from  $\sim 8500$  to  $\sim 5000$  years cal BP), the RSL falls at an average rate of 0.45 mm/yr (Figure 4.8B, C). The STEHM also shows a rate of RSL change increasing during the late Holocene (since 2900 years cal BP) with an average value of 0.42 mm/yr (Figure 4.8C). ICE6G GIA predictions fit the data, while PaleoMIST aligns with the data from 5000 to the present day.

### 4.5.2.2. Region 10: Bahía Blanca to Peninsula Valdés

The RSL history of Bahía Blanca and Peninsula Valdés states is based on 85 SLIPs and 10 limiting data points. Only two types of paleo-sea level indicators are reported along these coasts: beach ridges (Codignotto et al., 1992) and marine terraces (Rostami et al., 2000).

In this region, as in the previous one, data from the early Holocene is represented by limiting points. The oldest SLIP (ID: 1147) places the sea level at  $2.4 \pm 2.3$  m a.s.l. around 7000 years cal BP. Since then, RSL values oscillate indistinctly, ranging from  $8.4 \pm 2.3$  m a.s.l. to  $-1.57 \pm 1.2$  m a.s.l. However, a general trend of an RSL fall after the mid-Holocene highstand (6600 years cal BP) is observed. One SLIP (ID: 1164) shows the highest RSL value ( $12.4 \pm 2.3$  m a.s.l.) around 5300 years cal BP (Figure 4.8D). However, this value seems at odds with the sea level trend during that time. Therefore, this SLIP needs further examination. The STEHM shows a rising sea level from  $\sim 8500$  to 6500 years cal BP at a rate of 0.49 mm/yr; after this, an almost constant RSL fall is observed towards the present at an average value of 0.48 mm/yr (Figure 4.8E, F). Comparing GIA models' predictions with the data, ICE6G appears more consistent with the data at the beginning of the mid-Holocene. However, both GIA models underestimate the RSL trend since ca. 5000 years cal BP (Figure 4.8E).

#### 4.5.2.3. Region 11: Bahía Vera to Puerto San Julián

The area from Bahía Vera to Puerto San Julián includes an extensive coastline from the center of Chubut Province to the south of Santa Cruz Province in Argentina. The dataset here includes 130 SLIPs and 17 limiting data. The most common indicator in the region are beach ridges (Codignotto et al., 1992; Schellmann, 2007; Schellmann and Radtke, 2010; Ribolini et al., 2011; Zanchetta et al., 2012; Zanchetta et al., 2014), although marine terraces (Rostami et al., 2000; Schellmann and Radtke, 2000; 2003; 2010; Schellmann, 2007), and estuarine deposits (Bini et al., 2018) are also described.

The records in Bahía Vera and Puerto San Julián date back to the mid-Holocene, and in general, the data in this region appears to have a large variability. The oldest SLIP (ID: 1087) places the RSL at ca.  $9.4 \pm 2.3$  m a.s.l. at 7500 years cal BP. Since then, the dataset shows scattered SLIPs with values ranging from ca. 9 m a.s.l. to -1.0 m a.s.l. However, an RSL falling trend is observed (Figure 4.8G). Three SLIPs show the highest sea level value in the area ( $9.5 \pm 2.7$  m a.s.l.) at 6800, 6700, and 6600 years cal BP (IDs: 934, 933, 932; respectively). According to the STEHM, there is a fall in the RSL after the mid-Holocene highstand at an average rate of 0.33 mm/yr (Figure 4.8H,F). In this region, ICE6G GIA model predictions fit the data, while PaleoMIST predictions are lower from 8000 to 5000 years cal BP.

#### 4.5.2.4. Region 12: Tierra del Fuego

In the southernmost part of our area of interest, in Tierra del Fuego, the RSL history is based on 37 SLIPs, 49 limiting data. The indicators described are beach ridges (Rabassa et al., 2000; Codignotto et al., 1992; Gordillo et al., 1993; Bujalesky, 2007; Isla and Bujalesky, 2008), marine terraces (Gordillo et al., 1993; Bujalesky, 2007; Isla and Bujalesky, 2008), beach deposits (Porter et al., 1984), basal peat (non-mangrove) (Porter et al., 1984; Gordillo et al., 1993; Bujalesky, 2007; Isla and Bujalesky, 2008), and lagoon deposits (Björck et al., 2021).

In Tierra del Fuego, the data mainly corresponds to the mid-Holocene. However, some limiting data shows an early Holocene age (Figure 4.8J). The oldest SLIP (ID:983) places the RSL at  $1.9 \pm 2.1$  m b.s.l. ca. 6200 years cal BP. After that, a slight increase in sea level is observed with scattered values ranging from 1.6 m a.s.l. to  $\sim 4.5$  m a.s.l. up to 5700 years cal BP. The highest values of sea level,  $6.0 \pm 2.7$  m a.s.l. and  $4.6 \pm 1.7$  m a.s.l., are observed at 5600 and 4300 years cal BP, respectively. Despite the scattered values, a general trend of a falling sea level towards the present is observed (Figure 4.8J). As shown by the STEHM, there is a fall in the RSL since  $\sim 8500$  years cal BP at an average rate of 0.26 mm/yr (Figure 4.8K). The STEHM also suggests an increase in the rate of RSL change since 3000 years cal BP with an average value of 0.58 mm/yr (Figure 4.8I). In this area, only the ICE6G model shows a good agreement with the RSL history reconstructed by the STEHM after 5000 years cal BP.

## Holocene relative sea-level changes from the Atlantic coasts of South America

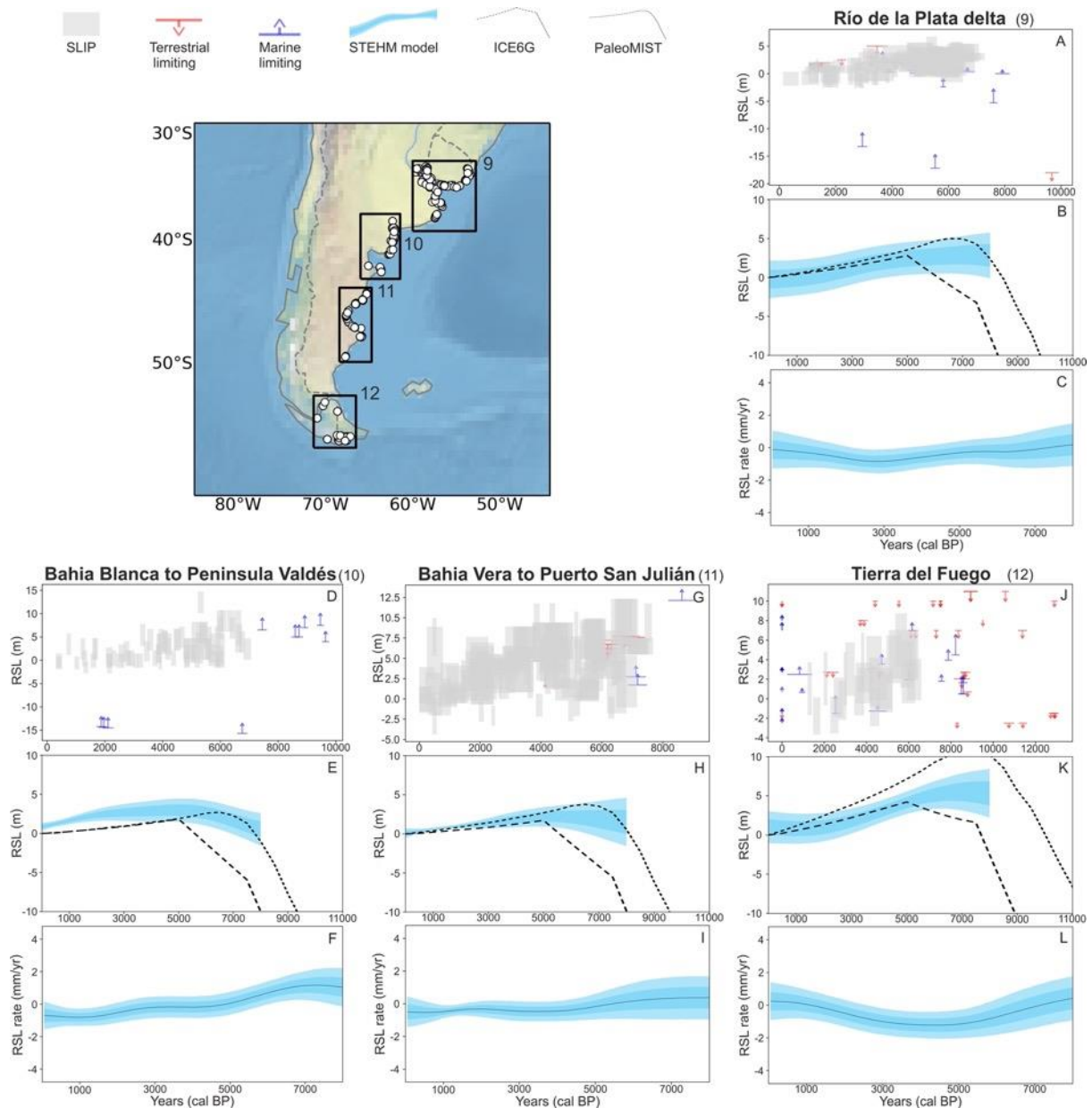


**Figure 4.8.** RSL reconstructions and rates from Uruguay and Argentina areas using the spatio-temporal model. For all plots, the model mean and  $1\sigma/2\sigma$  uncertainty are represented by a solid line and shaded envelopes, respectively. Index points (grey boxes) are plotted as calibrated age against changes in sea level relative to the present. Limiting points are plotted as a downward-pointing red arrow for terrestrial or an upwards-pointing blue arrow for marine. Dimensions of boxes and arrow symbols for each point are based on elevation and age ( $2\sigma$ ) errors. SLIP: sea-level index point; STEHM: spatio-temporal empirical hierarchical model; ICE6G (curved line) and PaleoMIST (straight line) represent the GIA models.

## 4.6. Discussion

### 4.6.1. The database, its applicability, and new inferences

In this work, we created a new standardized database of Holocene RSL in the southwestern Atlantic, building upon the effort of previous studies. The database includes 1024 data points, of which 726 are SLIPs, 97 are terrestrial limiting points, and 201 are marine limiting points. We rejected 286 data points due to a lack of required information specified by the standard protocols of the HOLSEA database (Khan et al., 2019).

Sea-level information is gathered from a diverse range of sea-level indicators, from beach deposits and sedimentary sequences to fixed biological indicators (see Table 4.1, Figures 4.3 and 4.4). Our results indicate that there is a generally good agreement in the RSL reconstructions derived from different indicators in most of the regions. However, in specific cases (areas 1 and 3), we observed that the RSL estimations derived from sedimentary sequences are close to 1 m lower than the RSL reconstructions derived from other indicators; this could be due to post-depositional lowering of samples resulting from compaction processes (Kahn et al., 2022). Despite this slight inconsistency, in general the RSL histories we reconstructed are consistent with previous compilations, for example, those of Angulo et al. (2006) and Milne et al. (2005). This is a further confirmation that the standardization of sea-level data allows gathering coherent results (Figure 4.9A, B), even with different methods used to quantify the indicative meaning of SLIPs.

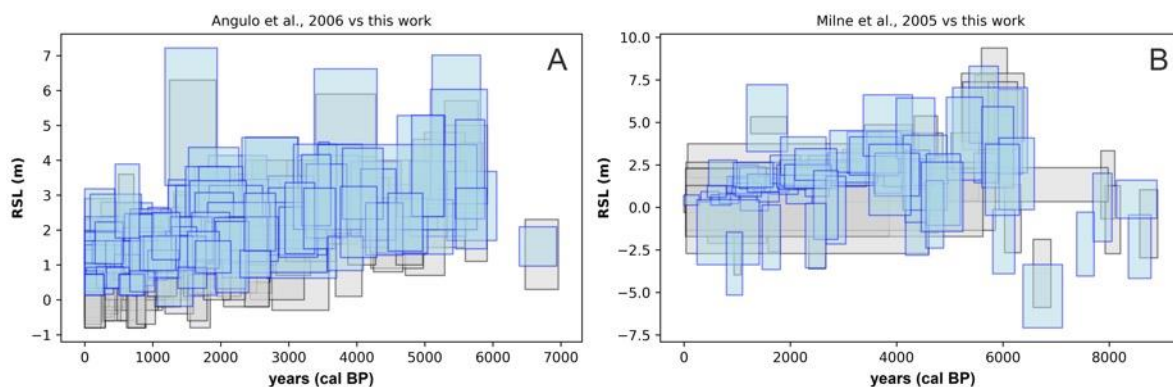


**Figure 4.9.** Comparison between our data (blue) and the standardized data of A) Angulo et al. (2006) and B) Milne et al. (2005) (grey).

In our database, vermetid rims and beach ridges represent the majority of data. We note that some sources of vertical errors and uncertainties associated with these indicators could modify the RSL interpretations reported in our work.

According to Laborel (1986), wave energy may affect the vertical distributions of vermetids by ca. 1 m. Angulo et al. (1999) highlight that there are three other sources of uncertainties in the evaluation of the paleo-sea level with vermetid fossils: I) remains may not correspond to the upper limit of the formation, II) changes in the hydrodynamic characteristics

of the coast through time, and III) the reference used to assess the vertical displacement of the vermetid reef. Rovere et al. (2015) underline that most vermetid species have a large living range. In fact, Spotorno et al. (2012) recorded *Petalonchus varians* in waters between 0 and 20 m deep along the Brazilian coast. To this end, in our database, we define an indicative range (MSL to MLLW) and a datum (vermetid biological datum) for these indicators that considers their vertical distribution and uncertainty.

On the other hand, paleo tidal range changes may affect the indicative meaning of those SLIPs whose upper or lower bounds are defined by tidal ranges (e.g., Hill et al., 2011; Hall et al., 2013; Horton et al., 2013; Khan et al., 2017; Sulzbach et al., 2023), this includes beach ridges. In this work, we adopted the interpretation by Lorscheid and Rovere (2019) and Rovere et al. (2016), who postulate that beach ridges form above sea level, between the ordinary berm and the storm wave swash height, following the definition of gravel beach ridges given by Tamura (2012). As per the definition, MHHW is used in calculating both the ordinary berm and the storm wave swash height of beach ridges (Lorscheid and Rovere, 2019). Therefore, paleo tidal range changes might assume particular relevance in areas with a wide continental shelf, such as the Amazon River and Rio de la Plata deltas, and in the Bahia Blanca area. To reduce the vertical source of error, in this work, we use satellite-derived wave measurements and wave runup models to calculate the indicative meaning of beach ridges following the methodology outlined in Rubio-Sandoval et al. (2024). This method appears to be more reliable (as it relies on local wave and beach topography data) than IMCalc software (Lorscheid and Rovere, 2019), which uses global wave atlases and global beach slope values.

Besides elevation and indicative range, age control also plays an important role in RSL reconstructions. The method selected to date a sea-level indicator and the availability of dateable material determine its age range and uncertainty (Bernal et al., 2010). In our database, radiocarbon dating is the primary method to date paleo-sea level indicators. Studies by Schellmann and Radtke (2000; 2007) and Schellmann et al. (2008) report that Electron Spin Resonance (ESR) and U-series dating were also used along the Patagonian coasts. However, these ages were not included in this new dataset, as Schellmann and Radtke (2010) remark that despite the methodological improvements, significant uncertainties persist when dating the Holocene mollusk shell deposits along the Patagonian Atlantic coast.

Our database mainly spans the mid-Holocene (beginning ca. 8200 years cal BP) to today, with few limiting data points dated to the early Holocene (Figure 4.6, 4.7, 4.8). Our decision to define the older sea level data points as limiting data is based on three main reasons: I) discrepancies in the RSL interpretations in the context of contemporaneous data points in the same area, II) a lack of detailed information to evaluate the elevation uncertainty, and III) the absence of the core's stratigraphic descriptions, raising concerns about their validity and relevance in this study's framework. Although the temporal scope of the new Holocene database limits the interpretations of the meltwater input in the area after the Last Glacial Maximum (LGM; Khan et al., 2019), it enables new inferences of the rates and timing of widely described mid-Holocene highstand (Angulo et al., 2006; Schellmann and Radtke, 2010; Bracco et al., 2011; Martínez and Rojas, 2013), the subsequent RSL trends, and GIA implications, as will be discussed in the following section.

#### 4.6.2. Holocene RSL variability along the southwestern Atlantic

We reconstructed Holocene RSL histories representing the local and regional sea-level variations over time along the southwestern Atlantic coastlines of Brazil, Uruguay, and Argentina (Figures 4.6, 4.7, and 4.8). Broadly, the observed and predicted RSL changes document a rapidly rising rate of sea level with a mean value of 0.80 mm/yr between ~8000 and ~5000 years cal BP, corresponding to the mid-Holocene transgression (Angulo and Lessa, 1997; Angulo et al., 2006; Schellmann and Radtke, 2010). This highstand reached about 2 to ~4 m above the present level, followed by a subsequent fall to its current position. It is worth noting that due to the broad spatial variability, this mid- to late-Holocene trend is variably affected by the ice and ocean mass redistribution and, in some cases, by local crustal tectonics across more than 50 degrees of latitude (Rostami et al., 2000; Milne et al., 2005).

In northeast Brazil, the estuarine deposits and mangroves from the Amazon River delta show a mid-Holocene highstand at ca. 2 m a.s.l. After this peak, the RSL slowly falls through the late Holocene at a mean rate of 0.16 mm/yr (Figure 4.6A). This trend seems to be different from the rest of the northeast sector (excluding Atol das rocas), where the areas from Pernambuco to north Bahía suggest a highstand (ca. 5 m a.s.l) between 8000 to 7000 years cal BP followed by a steep RSL fall towards the present (1.16 mm/yr). As already noted by Angulo et al. (2006) in the NE region of Brazil, SLIPs derived from mangrove swamp deposits indicate a lower sea level than expected, suggesting that neotectonics as well as wind-wave patterns may affect the RSL trend in this area. Moreover, we cannot neglect the effects of sedimentary compaction, which has been shown to affect this type of sea-level data by several meters (Hilma et al., 2015). Therefore, caution should be taken with the interpretation of the sea-level patterns observed in the estuarine area of the Amazon river delta, and further research may be directed to estimate the contribution of compaction to the reconstructed RSL.

The particular RSL trend in Atol das Rocas (Figure 4.6E) may have been determined by palaeoceanographic changes that add unquantified vertical uncertainties in the SLIPs (Shennan et al., 2018; Khan et al., 2019). As hydrodynamic conditions like waves, weather, and tidal regime affect the growth of coralline-algal reefs, these growth signals could overlap the RSL trends (Angulo et al., 2022a), resulting in a sea-level curve that does not agree with the expected regional patterns.

In the area including the Brazilian states of Sergipe and North Bahia, a secondary highstand is observed from 4000 to 3000 years cal BP (Figure 4.6K). The existence of late Holocene oscillations in Brazil is broadly discussed and debated (Angulo and Lessa, 1997; Martin et al., 1998; Martin et al., 2003; Angulo et al., 2006); however, based on the current data and uncertainties, we cannot suggest any further interpretations of their origin, reliability, and amplitude. Hence, more precise indicators are needed to test the hypothesis of this second highstand.

The southeast coastal sector of Brazil from central Bahia to Santa Catarina suggests a mid-Holocene rising sea level between ~8000 to ~5000 years cal BP at an average rate of 0.96 mm/yr. The RSL reaches its maximum value of ~3 m a.s.l. around 5000 years cal BP. After this highstand, the RSL follows a steady and slow fall (0.26 mm/yr) until its present position. The

difference between mid- to late-Holocene RSL rates creates a visible reduction in the amplitude of the sea-level fall (Figure 4.7B, E, H, K). This diminished trend was already noted by Martin et al. (1985), Suguio et al. (1985), and Angulo et al. (2006), who state that the lowering in the elevation and amplitude of the mid-Holocene highstand could be linked to a slight east-west geoidal shift between the states of Rio de Janeiro and Paraná.

Moving southwards, as shown by the STEHM in the areas from Río de la Plata delta to Tierra del Fuego, the mid-Holocene highstand occurred early in time (from ~8500 to ~6500 years cal BP) and, as expected, is followed by an RSL fall towards the late Holocene. However, the elevation of the highstand and the amplitude of the subsequent sea-level fall differ between these coastlines (Figure 4.8B, E, H, K). Milne et al. (2005) suggested that the combined effect of the West Antarctic ice sheet melting on the geoid during the early Holocene and the further dominant role of the crustal subsidence in some areas of this coastal sector produced the time difference of the predicted highstand. They also highlight that in this complex area, different processes can lead to vertical motion of both the land and ocean surfaces, producing a significant non-eustatic component of RSL change, which could be the reason for the variability in the observed RSL patterns. In fact, Rostami et al. (2000) estimate a constant tectonic rate of uplift of 0.09 m/1000 yr since the mid-Pleistocene in Patagonia, Argentina.

In Río de la Plata delta, Uruguay, our data suggest that after the mid-Holocene highstand, the RSL falls at an average rate of 0.45 mm/yr; However, this rate was not constant as indicated by the STEHM, which shows an increase in the rate of RSL during the late Holocene (since 2900 years cal BP). Cavallotto et al. (2004) also recognized a variable rate of sea-level fall. Later, Bracco et al. (2011; 2014) suggested that a rapid sea level fall would have taken place by 4300 years cal BP, whereas Martínez and Rojas (2013; 2014) debated it. Recently, Richiano et al. (2022) analyzed the evolution of all the beach ridges in the area and concluded that the Holocene ridge develops between 5200 and 3900 years cal BP, suggesting that during this period, there was a high tide level that allowed the development of these landforms. However, as already highlighted by Bracco et al. (2011), there is still no accurate data available to support either a gradual or abrupt late Holocene sea-level fall after ~3000 years cal BP.

The sea-level curve in the Bahía Blanca to Peninsula Valdés area shows a sea level transgressing between ~8500 to 6500 cal years BP at a rate of 0.49 mm/yr to reach a peak ~3 to 4 m a.s.l. Following this highstand, sea level has fallen to present levels at a consistent rate of approximately 0.48 mm/yr (Figure 4.8E, F). This trend agrees with the previous observations of Ribolini et al. (2011) and also with the model of Milne and Mitrovica (2008) for the Argentinean coastal sector, outlining an RSL estimate of about 5 m after the LGM. However, at present, there is insufficient information to understand the reasons for the particular amplitude of the sea-level curve in this area, and we cannot rule out the effect of the scattering data in this RSL signal. Therefore, the SLIPs in this area may need further examination.

Another interesting sea-level curve is observed in the area of Bahía Vera to Puerto San Julián, where the STEHM suggests a steep fall in the RSL after the mid-Holocene highstand at an average rate of 0.33 mm/yr (Figure 4.8H, I). Schellmann and Radtke (2010) describe this

RSL trend in the middle and south Patagonian and point out that the sea level differences could be partially associated with the variations on the  $^{14}\text{C}$  reservoir effect resulting in age uncertainties. Despite that we performed a local Delta-R correction when necessary to reduce these uncertainties, we must highlight the lack of Delta-R correction data in the Argentinean Patagonia; therefore, caution is needed in overinterpreting these data since this source of uncertainty can potentially lead to disparate SLIPs (Törnqvist et al., 2015).

Finally, in Tierra del Fuego, our model shows the highest elevations of the sea level peak of all the southwestern Atlantic region, close to 8 m a.s.l at ~8500 years cal BP. After this highstand, sea level fell at an average rate of 0.26 mm/yr (Figure 4.8K). The STEHM also suggests an increase in the rate of fall since 3000 years cal BP to an average of 0.58 mm/yr. However, based on the geographical and geological characteristics of this area, the shape of the sea-level curve may be influenced by many different factors, for instance, GIA (Björck et al., 2021), localized tectonics (Isla and Angulo, 2016; Rostami et al. 2000), or a chronological source error. As already stated, Schellmann and Radtke (2010) acknowledge that the discrepancies in the RSL changes in the Patagonian Atlantic coast may be due to hiatuses in the geomorphological and chronostratigraphic datasets. Whereas Björck et al. (2021) argue that since the Patagonian ice sheet covered Tierra del Fuego, GIA must be the main factor responsible for the elevated shorelines, as well as for the spatial and temporal variability of the RSL. Here, we must highlight that previously, Rostami et al. (2000) discussed the effect of the estimated Patagonian ice sheet thickness (~400 m), suggesting that it may not have a significant effect on the RSL predictions since this ice sheet may not lead to a significant sea-level rise driven by the proglacial forebulge collapse. Therefore, we emphasize that before generating a unique solution for the RSL history in this area, it is necessary to solve the limitations in the spatial and temporal coverage of the RSL data, together with an improvement in the knowledge of its glacial history.

Notwithstanding the caveats on the quality of reconstructed RSL histories for each area highlighted above, we note that the effect of GIA across the large latitudinal gradient covered by the database is evident, either from the data or the STEHM model (Figures 4.6, 4.7, 4.8). In general, the Holocene highstand occurs later and decreases in magnitude, moving towards the North, in accordance with the trend described by GIA models. As already demonstrated in Peltier et al. (2015), the highstand position in many locations can be obtained from the ICE6G, which was a result of including rotational effects in the sea level calculation. The modified PaleoMIST model used in this study generally does not fit the data constraints older than 5000 years cal BP, indicating that the global ice volume at the 7500-year cal BP time step is probably too large by at least 4 to 5 m sea level equivalent. The general success of the model after 5000 years cal BP supports the modification that Antarctic ice volume reached near present levels by that time.

It is not the aim of this paper to extrapolate the revised Holocene sea-level curves from a broader regional scale. But, some brief comparisons seem appropriate. Despite the uncertainties that surround the data, the RSL reconstructions here agree surprisingly well with the expected trend of the near- and far-field locations (with just some special exceptions discussed above). Our data in Tierra del Fuego is characterized as a near field location due to

its proximity to Antarctica; these areas reveal an intricately RSL fall after a maximum marine transgression due to the net effect of eustatic sea-level rise and glacio-isostatic uplift (Milne and Mitrovica, 2007). On the other hand, areas from Río de la Plata delta (Uruguay) to the Amazon river delta (Brazil) develop an RSL trend characteristic of a far-field location; this trend normally implies a mid-Holocene highstand (between 8000 to 4000 years cal BP) at a magnitude ranging from ca.1 to 6 m (Kahn et al., 2015). Therefore, the improvement of the data quality in this promising area, together with the integration of previously standardized data from the intermediate field (the Caribbean, Khan et al. 2017) and further north near-field locations (Atlantic USA, Englehart and Horton, 2012; Southern Maine; Kahn et al. 2015; Gulf of Maine, Baril et al., 2023; Canada, Vacchi et al., 2018; Greenland, Gowan et al., 2023) would allow a comprehensive pole-to-pole sea level dataset that could not only refine existing GIA models but also provide valuable insights for the optimization of global sea level estimates since the LGM.

### 4.6.3. Future research directions

As already noted by Milne et al. (2005) and later by Angulo et al. (2006), along the South Atlantic coasts, there is a general lack of accurately measured data. While more recent studies (Castro et al., 2014; Bini et al., 2018; Angulo et al., 2022a; Angulo et al., 2022b; Richiano et al., 2022) employ high-accuracy elevation measurements referred to rigorously defined vertical datums (e.g., using differential GPS and datums calculated via tide gauge data), these are still largely an exception within this area.

Also, there is a need for a rigorous definition of modern analogs to quantify the indicative meaning of SLIPs. Along the Brazilian coastlines, it appears that new studies applying the methodology proposed by Mauz et al. (2015) to the numerous beachrock deposits will help to improve the quality of a significant amount of SLIPs. Moreover, a re-analysis of vermetid rims, coupling the analysis of modern analogs with precise elevation measurements of their fossil counterparts, might help improve sea-level information at several sites, providing accurate SLIPs within a few decimeters.

While the methodology proposed by Rubio-Sandoval et al. (2024) to calculate the beach ridges' indicative meaning is self-consistent and reliable, there are some other issues to consider to improve it. For example, the increase or decrease correction of water levels associated with the storm surge under different climate conditions.

As already highlighted by Gowan et al. (2021a), further research must be directed at improving the chronological control in Argentina, as there is a long-lasting debate centered on the age of its Quaternary shorelines (Codignotto et al., 1988; Rutter et al., 1990; Schellmann and Radtke, 2010). Here, it is important to emphasize the need for data to correct the  $^{14}\text{C}$  reservoir effect in Patagonia, Argentina, which could have a great impact on the sea-level curve refinement.

As the data improves, future reviews could develop an objective characterization of the data quality based on the sample susceptibility to age and/or elevation errors, such as the one proposed by Than et al. (2023) for the Mid-Pacific.

### 4.7. Conclusions

We compiled a standardized database of published Holocene RSL data from Brazil, Uruguay, Argentina, and the Chilean part of Tierra del Fuego in the southwestern Atlantic. We reviewed data from 128 studies to gather 726 sea-level index points (SLIPs) and 298 limiting points, each associated with its temporal and vertical uncertainty. We rejected around 22 % of the data because the necessary information required by the standard sea-level database protocols was not achieved. We divided our database into 12 regions based on data availability, tectonic setting, and the distance from the Antarctic ice sheet.

After a critical examination, our database mainly spans since the mid-Holocene (ca. 8000 years cal BP) with few limiting data points correlated with the early Holocene. The temporal scope of this new Holocene database limits the interpretations of the meltwater input in the area after the Last Glacial Maximum, but it enables new inferences of the rates and timing of widely described mid-Holocene highstand, the subsequent late Holocene RSL fall, and GIA implications.

Generally, the observed and predicted RSL changes document a rapidly rising rate of sea level with a mean value of 0.80 mm/yr between ~8000 and ~5000 years cal BP, corresponding to the mid-Holocene transgression. During this transgression, RSL rose to about 2 to ~4 m above the present level, followed by a subsequent fall to its current position. In this complex area, different processes lead to vertical motion of both the land and ocean surfaces, modifying the mid to late Holocene RSL trend across the latitudinal gradient.

Excluding the atypical areas possibly affected by neotectonics or coastal dynamics, the northeast coastal sector of Brazil has a highstand (ca. 5 m a.s.l.) between 8000 to 7000 years cal BP followed by a steep fall towards the present (1.16 mm/yr). The southeast coastal sector of Brazil suggests a mid-Holocene transgression between ~8000 to ~5000 years cal BP. Sea level reaches its maximum peak at ~3 m a.s.l. around 5000 years cal BP. After this highstand, the sea level falls at a steady and slow rate (0.26 mm/yr) until its present position. From Río de la Plata delta to Tierra del Fuego, the mid-Holocene highstand occurred early in time (from ~8500 to ~6500 years cal BP) and, as expected, is followed by an RSL fall towards the late Holocene. However, the elevation of the highstand and the amplitude of the subsequent sea-level fall differ between all the coastlines, implying a significant non-eustatic component of the RSL (i.e. GIA, localized tectonics, and hiatuses in the geomorphological and chronostratigraphic datasets). We emphasize that before generating a unique RSL solution through the Holocene, it is necessary to solve the data limitations.

Despite the data quality issues raised above, we note that the effect of GIA across the large latitudinal gradient covered by the database is evident, either from the data or the reconstructed RSL. In general, the Holocene highstand occurs later and decreases in

magnitude, moving towards the North, in accordance with the trend outlined by the ICE6G GIA model. The modified PaleoMIST model used in this study generally does not fit the data constraints older than 5000 years cal BP, supporting the statement that Antarctic ice volume reached near present levels by that time.

Finally, we can surmise that the southwestern Atlantic coastline emerges as a promising area for RSL studies. Despite the uncertainties surrounding the available data, this region offers a valuable spot for unraveling past sea-level dynamics. Therefore, a need for additional fieldwork that follows the methodological sea-level standard protocols is evident.

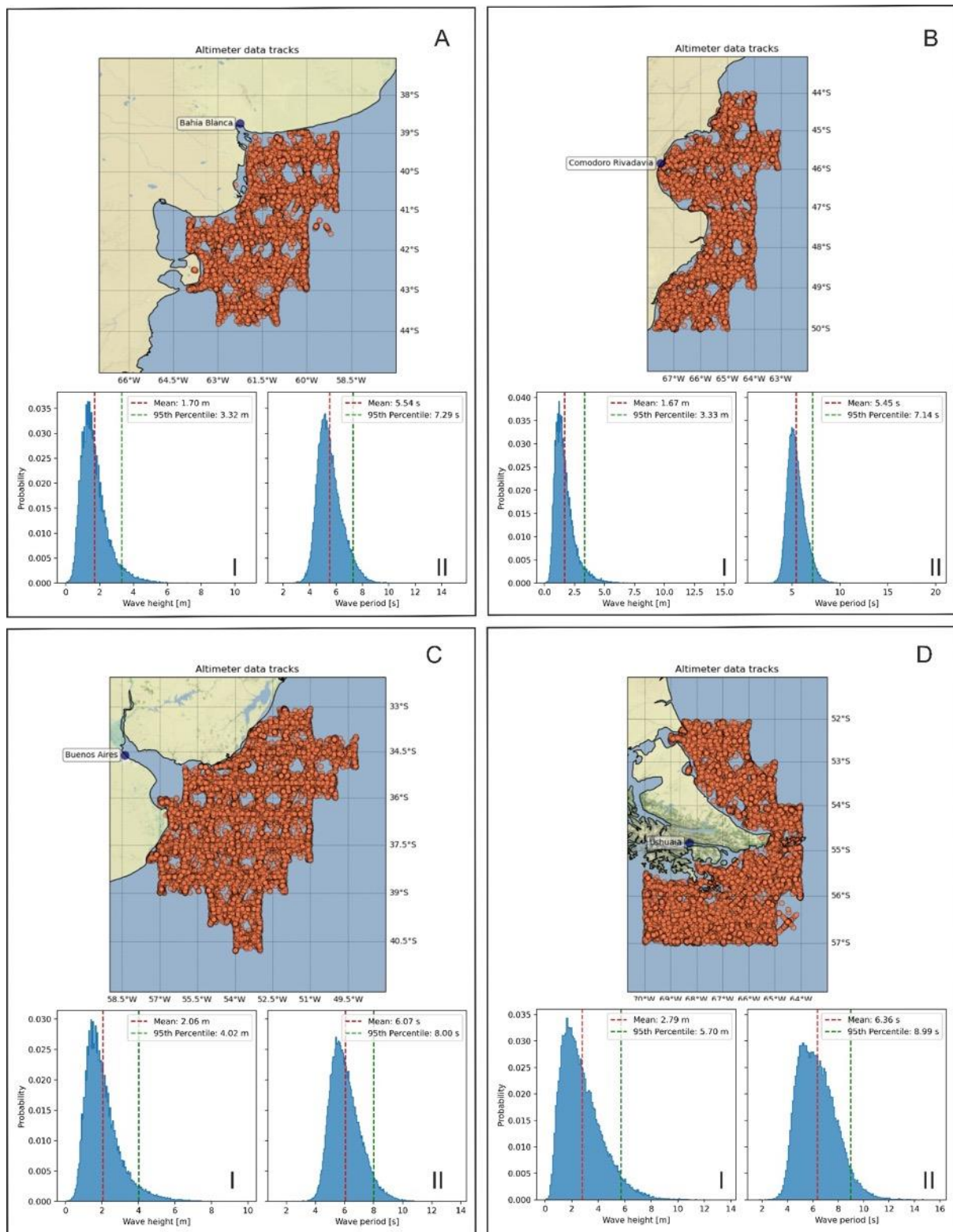
### 4.8. Data availability

The database is available at <https://doi.org/10.5281/zenodo.10819555> (Version 1.0; Rubio-Sandoval et al., 2024). Any modification to the database can be requested through the platform WALIS ([https://warmcoasts.eu/walis/Data\\_mod\\_request\\_open/](https://warmcoasts.eu/walis/Data_mod_request_open/)).

### 4.9. Acknowledgments

This work is part of the PhD thesis of Karla Rubio-Sandoval, funded by the European Research Council (ERC) under the European Union's Horizon 2020 research and innovation program (grant agreement no. 802414). Karla Rubio-Sandoval also acknowledges the Monika Segl program of MARUM, Bremen University, for additional support. Timothy Adam Shaw and Ben Horton were supported by the Singapore Ministry of Education Academic Research Fund MOE2019-T3-1 004, the National Research Foundation Singapore, the Singapore Ministry of Education under the Research Centers of Excellence initiative, and by the Nanyang Technological University. This work is an Earth Observatory of Singapore contribution. We would like to thank Abdulla S. Khan for technical support during the development of the database. We thank to the PALSEA working group for the useful discussions during the 2022 meeting in Singapore. PALSEA is a working group of the International Union for Quaternary Sciences (INQUA) and Past Global Changes (PAGES), which in turn received support from the Swiss Academy of Sciences and the Chinese Academy of Sciences. Figure 4.1 was created using ArcGIS® software by Esri. ArcGIS® and ArcMap™ are the intellectual property of Esri and are used herein under license © Esri. All rights reserved. For more information about Esri® software, please visit <https://www.esri.com> (last access: 20.06.2023). The data used in this study were compiled in WALIS, a sea-level database interface developed by the ERC Starting Grant WARMCOASTS (ERC-StG-802414) in collaboration with the PALSEA working group. The database structure was designed by Alessio Rovere, Deirdre D. Ryan, Thomas Lorscheid, Andrea Dutton, Peter Chutcharavan, Dominik Brill, Nathan Jankowski, Daniela Mueller, Melanie Bartz, Evan Gowan, and Kim Cohen. The beta-version of the WALIS data insertion interface for Holocene sea-level data was coded thanks to partial support by a PAGES Data Stewardship Scholarship.

4.10. Supplementary material



**Supplementary Figure 4.1.** Maps of satellite altimetry tracks extracted from offshore wave conditions (IMOS, 2023). A) Bahia Blanca, B) Comodoro Rivadavia, C) Buenos Aires, D) Ushuaia; I) and II) respectively, histograms of wave height and period per area.

**Supplementary Table 4.1.** Hyperparameters for the spatio-temporal empirical hierarchical model.

<b>Hyperparameters</b>	<b>Lower Bound</b>	<b>Upper Bound</b>	<b>Tuned value</b>
Matern global amplitude (mm)	1	25000	628,060442
Temporal parameter (years)	1	25000	535,822951
Linear amplitude	0,01	10000	1,45755676
Linear geographic length scale (angular deg)	1	12	7,00495584
Matern regional amplitude (mm)	0,01	25000	962,189422
Regional temporal parameter (years)	1	25000	1663,64684
Regional geographic length scale (angular deg)	0,05	12	0,238258
Matern local amplitude (mm)	0,01	25000	685,155044
Local temporal parameters (year)	1	25000	7369,11739
Local geographic length scale (angular deg)	0,001	5	0,002485
White noise (mm)	0,1	1.00E+06	0,1

## 5. Quaternary and Pliocene sea-level changes at Camarones, central Patagonia, Argentina

K. Rubio-Sandoval, D. D. Ryan, S. Richiano, L. M. Giachetti, A. Hollyday, J. Bright, E. J. Gowan, M. Pappalardo, J. Austermann, D. S. Kaufman, and A. Rovere

Submitted to Quaternary Science Reviews (2024)

### 5.1. Abstract

Geological indicators of past relative sea level changes are fundamental to reconstruct the extent of former ice sheet during past interglacials, which are considered analogs for future climate conditions. Four interglacials, dating from Holocene to Pliocene, have left sea-level imprints in the proximity of the coastal town of Camarones in Central Patagonia, Argentina. Sea-level index points were preserved as beach ridges deposited by storm waves above modern sea level. We used highly accurate survey techniques to measure the elevation of these deposits. Satellite-derived wave measurements and wave runup models were then employed to calculate their indicative meaning (i.e., their elevation with respect to sea level at the time of deposition). The paleo-relative sea levels (i.e., uncorrected for post-depositional vertical land motions) associated with the four interglacials (with  $1\sigma$  uncertainties) are  $6\pm 1.5$  m (Holocene);  $8.7\pm 2.1$  m (MIS 5e);  $14.5\pm 1.5$  m (MIS 9 or 11); and  $36.2\pm 2.7$  m (Early Pliocene). Ages have been obtained using both published (U-series, Electron Spin Resonance, and Radiocarbon) and new (Amino Acid Racemization and Radiocarbon) dating constraints. We compare our results with published glacial isostatic adjustment and mantle dynamic topography predictions, and we highlight that refining these models before calculating the global mean sea level for the interglacials mentioned above is necessary. Our high-resolution data provide a significant benchmark for paleo-relative sea level studies in the Southwestern Atlantic.

### 5.2. Introduction

Several past interglacials were characterized by global average temperatures warmer than pre-industrial, which resulted in smaller ice sheets and higher ocean volumes (Dutton et al., 2015). Geological records from several sites around the globe provide hard evidence that local sea levels during such periods were higher than today (Siddall et al., 2007; Raymo et al., 2011; Rovere et al., 2023b). Reconstructing global mean sea levels (GMSL) that characterize earlier interglacials helps to constrain models of polar ice melting in the near future (Gilford et al., 2020; DeConto et al., 2021) and ultimately lead to a better understanding of the physics that drive high-end melting scenarios (van de Wal et al., 2022). The Quaternary sea-level highstands have been studied at several locations on the world's coasts and continental shelves via both direct and indirect proxies. In general, the availability of direct proxies decreases with the age of the highstand (Khan et al., 2019a), which makes GMSL during early Quaternary and Pliocene interglacials more difficult to quantify. Further, direct proxies only

measure relative sea level (RSL), still uncorrected for uplift or subsidence that may be caused by different processes such as Glacial Isostatic Adjustment (GIA), mantle Dynamic Topography (DT) and tectonics (Rovere et al., 2016).

Interglacial peak sea level differs during the last 5 Myr in both magnitude and duration. During the Pliocene (~5.3 to 2.5 Ma), global temperatures were up to 4 °C higher than pre-industrial (Fedorov et al., 2013), and GMSL oscillated by tens of meters (Grant et al., 2019), with proxies suggesting that sea-level highstands were around 17 m higher than present in the mid-Pliocene (~3Ma) and around 25 m higher in the Early Pliocene Climatic Optimum (~5Ma, Dumitru et al., 2019). Pliocene ice models suggest that, during the warmest interglacials of this geological epoch, Greenland was ice-free, and the West Antarctic ice sheet was likely subject to periodic collapses (Naish et al., 2009; Solgaard et al., 2011). Regarding Quaternary highstands, several sites carry information on sea level during MIS 11c (424–395 ka, Hearty et al., 1999; Murray-Wallace, 2002; Olson and Hearty, 2009; Bowen, 2010; Roberts et al., 2012) an unusually long interglacial with high carbon dioxide levels (Tzedakis et al., 2022). Direct proxies, corrected for GIA and vertical land motions, suggest that MIS 11c GMSL was 8 to 11.5 m (Chen et al., 2014) or 6 to 13 m (Raymo and Mitrovica, 2012) above present. GMSL during MIS 9 (~331-310 ka) was reported close to the present-day sea level (Murray-Wallace, 2002; Siddall et al., 2007).

Evidence of Late Quaternary interglacials is more ubiquitous, with thousands of sites dated to MIS 5 (in particular MIS 5e, ~125 ka, Rovere et al., 2023b). In the AR6 IPCC REPORT, Fox-Kemper et al. (2021) remark that "it is virtually certain that [MIS 5e] GMSL was higher than today, likely by 5–10 m (medium confidence)". Recent works suggest that MIS 5e GMSL was instead generally lower than 5m, but still higher than present (Polyak et al., 2018; Clark et al., 2020; Dyer et al., 2021; Dumitru et al., 2023). Sea level during other stages of MIS 5, namely MIS 5c (~100 ka) and MIS 5a (~80 ka), is generally reported to have peaked from few tens of meters below up to close to present-day sea level (Muhs et al., 2012; Simms et al., 2016; Creveling et al., 2017; Thompson and Creveling, 2021; Tawil-Morsink et al., 2022; Marra et al., 2023).

During the current interglacial (~6 ka to present), recent work based on a global database of sea-level index points (Khan et al., 2019b) shows that it is likely that GMSL was higher (up to 1.5 m) than today during the mid-Holocene with a significant contribution of excess melt coming from the Antarctic ice sheet (Creel et al., 2023).

To reduce uncertainties on estimates of GMSL during past interglacials, it is essential to provide field constraints that have reliable chronological attribution, are precisely measured and have a quantifiable relationship to past sea level (i.e, indicative meaning, Shennan, 2015). Moreover, locations at passive margins that have preserved multiple highstands give an opportunity to better quantify post-depositional vertical land motions, as they are less subject to these effects (e.g., subduction or uplift during successive earthquake cycles, Yousefi et al., 2020).

Much of the Southern part of the Atlantic Ocean is a passive margin, and coastal deposits associated with past interglacials shape the morphology of the coastal landscape and record the history of relative sea-level change after deglaciation (see review works by Gowan et al., 2021a and Rubio-Sandoval et al., 2021). In this study, we present new data detailing Quaternary sea-level changes at Camarones, Central Patagonia, Argentina. We provide new

survey data and a new way of estimating the indicative meaning of beach ridges. We couple the results with dating on mollusk shells via Amino Acid Racemization. Building upon previously published stratigraphic data and radiometric ages, as well as GIA and DT models, we discuss possible GMSL inferences during past warm periods.

### 5.3. Study area

The Patagonia coastline of Argentina has been a target area for sea-level research for at least four decades (Bayarsky and Codignotto, 1982; Codignotto, 1983; Rutter et al., 1989) due to the exceptional preservation of geological records associated with former sea levels and for its location that makes it sensitive to isostatic rebound following the waxing and waning of the West Antarctic ice sheet (Rostami et al., 2000; Milne et al., 2005; Gowan et al., 2021a). Numerous works describe in detail the geomorphology and stratigraphic subdivision of the elevated littoral deposits along the coastlines of Patagonia (see an extensive review by Pedoja et al., 2011). One of the most complete descriptions of these deposits derives from the work of Feruglio (1949), who described six marine terrace systems based on their elevation and mollusk fauna. The elevation of these marine deposits ranges from 8 to 186 m above mean sea level. Along the shore, the presence of beach ridges at varying heights is also conspicuous, enough so that it was noted by Charles Darwin during his voyage on the Beagle vessel (Darwin, 1851).

Patagonian beach ridge deposits are typically composed of a sandy gravel matrix, rich in pebbles and mollusk shells (Schellmann and Radtke, 2000) and are - from a geomorphological standpoint - raised storm berms created by the deposition of sediments by wave runup. Different dating techniques have been employed to determine the age of these deposits: radiocarbon, U-series, Electron Spin Resonance and Strontium Isotope Stratigraphy (Schellmann and Radtke, 2000; Pappalardo et al., 2015; Rovere et al., 2020).

The small town of Camarones (Chubut Province, Argentina) lies at the northern end of the San Jorge Gulf, ~1300 km south of Buenos Aires (Figure 5.1). It is located on a passive margin and is embedded within the South America Plate, over 1000 km north of the boundary with the Scotia Plate. In proximity of Camarones, several authors reported relic beach ridges, emplaced by sea level during the Quaternary (Codignotto et al., 1992; Schellmann and Radtke, 2000, 2003, 2007, 2010; Ribolini et al., 2011; Zanchetta et al., 2012; Pappalardo et al., 2015; Bini et al., 2018) and the Pliocene (Feruglio, 1949; Del Río et al., 2013; Rovere et al., 2020). While located on a passive margin, these paleo shorelines were subject to substantial vertical land motions due to both glacial isostatic adjustment (Mitrovica et al., 2001; Peltier, 2002) in response to polar ice melting and, on longer time scales (hundred of thousands to millions of years), mantle dynamic topography (Braun, 2010; Austermann et al., 2017), which led to significant uplift over the past ~5 million years (Hollyday et al., 2023).

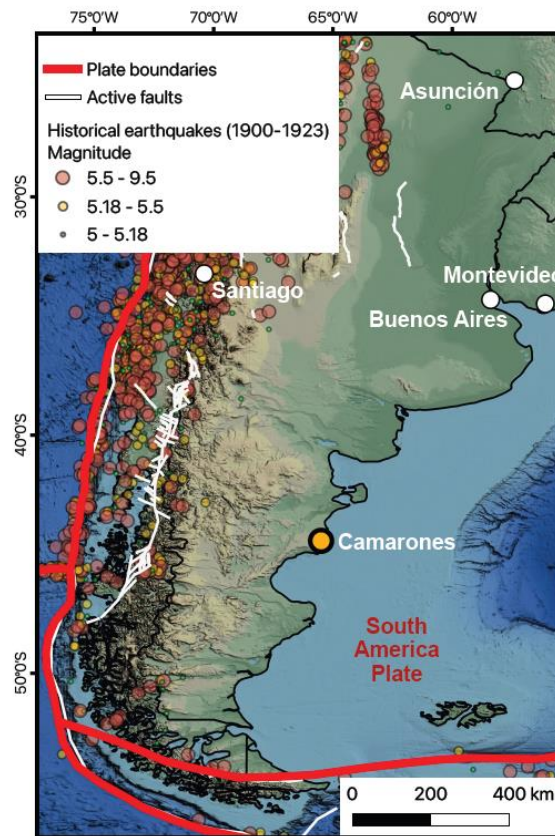


**Figure 5.1.** Study area. Location of Camarones within the Southern part of South America. Credits: Base map from Ryan et al. (2009). Active faults from Styron (2019) and plate boundaries derived from Bird (2003), as modified by Hugo Ahlenius and Nordpil on GitHub (<https://github.com/fraxen/tectonicplates>). Historical earthquakes from US Geological Survey (2017).

## 5.4. Methods

### 5.4.1. Elevation measurement

The elevations of sea-level index points described in this study were measured using differential Global Navigation Satellite systems (GNSS). The elevation of the Pliocene sea-level index points was surveyed in 2014 with a Trimble ProXRT receiver with Tornado antenna, receiving OmniSTAR HP real-time corrections, as described in Rovere et al. (2020). During that campaign, preliminary surveys on both modern and middle/late Pleistocene shorelines in the area were carried out. Those data are reported in this work following the same GNSS processing methods described in Rovere et al. (2020).

Two further field campaigns, focussed on MIS 5 beach ridges and modern data, were carried out in November 2019 and April 2022. In these campaigns, GNSS surveys were performed using a single-band EMLID RS+ GNSS composed of a base and a rover unit. In both campaigns, the base station was located on top of a pole with full view of the sky (Supplementary Figure 5.1A, B) and was left static collecting data for a variable amount of time including between 5 and 14 hours over five separate deployments (Supplementary Table 5.1). The data collected from the base station were processed using the Precise Point

Positioning service of the Natural Resources of Canada (NRCAN-PPP), and then averaged using the "GPS Utilities" scripts (Rovere, 2021). The results of the GNSS base processing are reported in Supplementary Table 5.1 and illustrated in Supplementary Figure 5.1C, D.

Once the base position and the associated positional errors were calculated, the rover data was processed using the Post Processed Kinematic (PPK) workflow in the software EMLID Studio. The collection of GNSS rover data was done in static mode for up to 10 minutes, depending on satellite visibility conditions. The workflow was validated by measuring twice (once in 2019 and once in 2022) a benchmark point called "GPS N°35" located in the proximity of the town of Camarones (Supplementary Figure 5.2A, B). The precise coordinates of this point are reported by the Argentinian "Instituto Geografico Nacional" (National Geographical Institute), which measured it in 1995. There is a very good agreement between our vertical measurements and the benchmark ellipsoid elevation (Supplementary Figure 5.2C). The Northing and Easting coordinates of our GNSS survey appear internally consistent but shifted by about half meter (Supplementary Figure 5.2D).

Data were originally recorded in WGS84 coordinates, with height above the ITRF2008 ellipsoid (these are the same datums to which the "GPS N°35" benchmark is referred). Orthometric heights (above mean sea level) were then calculated subtracting the GEOIDEAR16 geoid height from the measured ellipsoid height. It was estimated that the GEOIDEAR16 has an overall vertical accuracy of 0.1 m (Pinon et al., 2018). Pappalardo et al. (2019) has shown that, in some areas of Patagonia, referring GNSS data to the GEOIDEAR16 geoid might be affected by large discrepancies if compared with the sea level observed by tide gauge data. Therefore, we use two GNSS observations: one of instantaneous sea level and one of the high tide mark, to benchmark the GEOIDEAR16 geoid at this location. The results show that there is little to no discrepancy between observed elevations and tidal predicted values (Supplementary Figure 5.3). In any case, we remark that all the GNSS data collected in this work are also originally referred to the ITRF2008 ellipsoid, and ellipsoid elevations are given in the supplementary material in case new datums become available in the future (see Supplementary Information for details).

The elevation error ( $\sigma E$ ) of each GNSS point surveyed in the field was calculated using the following formula:

$$\sigma E = \sqrt{GNSS_e^2 + Base_e^2 + Geoid_e^2 + Bench_e^2} \quad (1)$$

Where  $GNSS_e$  is the error given as output by the GNSS system,  $Base_e$  (only for data collected in 2019 and 2022) is the elevation error of the base station (0.187 m),  $Geoid_e$  is the error associated with the GEOIDEAR16 (0.1 m), and  $Bench_e$  is the average of the absolute differences between the GNSS points and the benchmark "GPS N°35" (0.06 m).

In some instances, the same point or the same stratigraphic context within close points was measured during different campaigns. In these cases, elevations were averaged using the same processing scripts adopted for the base station described above (Rovere, 2021).

#### 5.4.2. Calculating the indicative meaning

For each point measured in the field representative of a past sea-level position, it is necessary to quantify its relationship to the former sea level calculating the indicative meaning (Van de Plassche, 2013; Shennan, 2015). The indicative meaning is composed of the reference water level (RWL) and the indicative range (IR), which are calculated as follows:

$$RWL = \frac{U_l + L_l}{2} \quad (2)$$

$$IR = U_l - L_l \quad (3)$$

Where  $U_l$  and  $L_l$  are, respectively, the upper and lower limits of occurrence of the same facies observed in the fossil record along the modern coast. Once RWL and IR are calculated, they are used to calculate paleo RSL and its associated uncertainty as follows:

$$RSL = E - RWL \quad (4)$$

$$\sigma_{RSL} = \sqrt{\sigma_E^2 + \left(\frac{IR}{2}\right)^2} \quad (5)$$

Where  $E$  is the measured elevation, and  $\sigma_{RSL}$  and  $\sigma_E$  are the uncertainties of relative sea level and measured elevation, respectively. For the Pliocene sea-level index points we maintained the indicative meaning quantified by Rovere et al. (2020). For Pleistocene deposits, we measured as a sea-level index point the top layer where articulated (not in living position, transported by low-energy processes) *Ameghinomya antiqua* shells are present within the beach ridge. On the modern beach, we observed that articulated mollusk shells (not living) formed distinct zones that are always included between the ordinary berm (created by fairweather waves) and a higher storm berm (created by sea storms in the area). To quantify the indicative meaning corresponding to these two morphological elements, we calculated the 2% exceedance wave runup level using different models implemented into the py-wave-runup tool coded by Leaman et al. (2020).

The models require as input the beach slope ( $\beta$ ), significant wave height ( $H_s$ ) and period ( $T_p$ ). We gathered the beach slope at six transects along the Camarones beach using the CoastSat.Slope toolbox (Vos et al., 2019, 2020). With this toolbox, we analysed Landsat and Sentinel satellite data between 2000 and 2023, alongside with tides extracted from the FES2014 global tidal model (Lyard et al., 2021; Carrere et al., 2016). We calculated that  $\beta$  is  $0.18 \pm 0.02$  ( $1\sigma$ ). To calculate  $H_s$  and  $T_p$  we used the RADWave tool (Smith et al., 2020), which allows querying satellite altimetry data. We extracted a time series of wave data between  $65^\circ\text{W}$  to  $61^\circ\text{W}$  and  $47^\circ\text{S}$  to  $43.5^\circ\text{S}$ , in a period included between Jan 1, 2000 and Jan 1, 2023 (Figure 5.2). For the same time frame, we queried the FES2014 model and extracted water levels at a 15-minute interval. Coupling tidal and wave data via their UTC timestamps we gathered a database with 43102 wave conditions. For each condition, we selected a beach

slope sampled from a normal distribution created with the mean and standard deviation of  $\beta$ . We used the "ensemble" function of pywave-runup to run, for each wave height and period, eight runup models. At each calculated runup, we added (or subtracted) the corresponding water level derived from the FES2014 tidal model. The Jupyter notebooks used for this workflow are shared as part of the Supplementary Information.

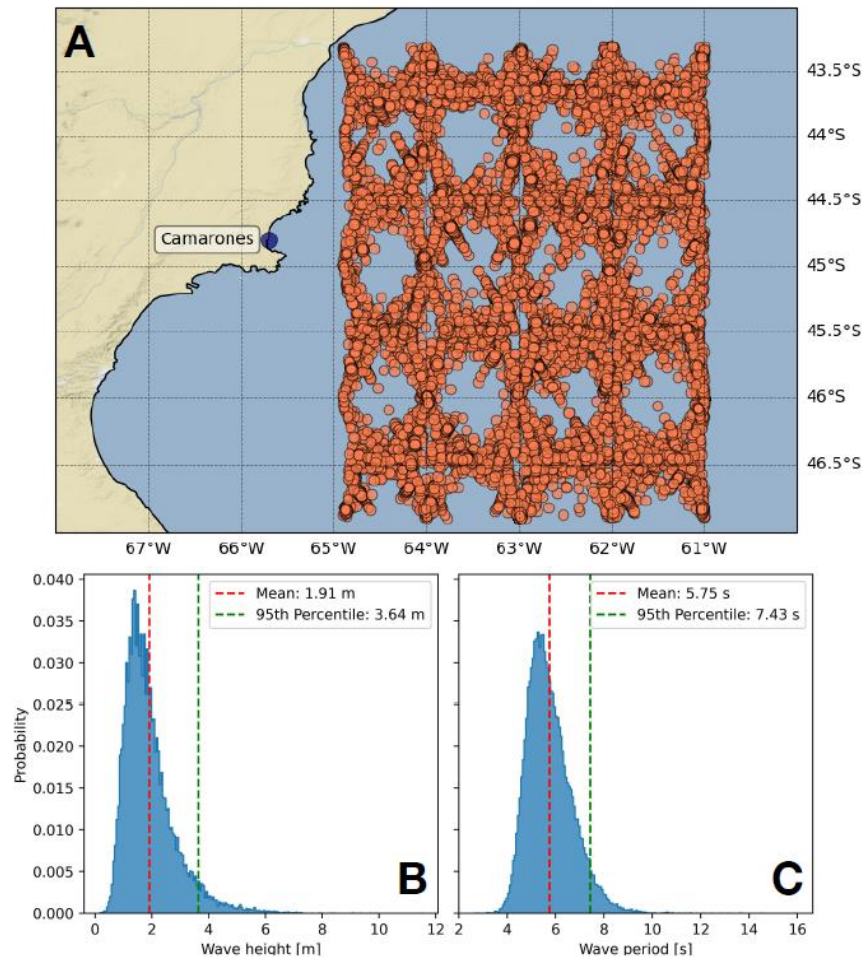


**Figure 5.2.** A) Map of satellite altimetry tracks from which wave conditions offshore of Camarones were extracted (IMOS, 2023). B) and C) respectively, histograms of wave height and period.

### 5.4.3. Geochronological methods

Earlier authors applied the methods of Electron spin Resonance (ESR) and U-series to *A. antiqua* shell to obtain ages for the beach deposits in the Camarones region and were successful in differentiating beach ridges of different ages within the broader Patagonian region (e.g., Schellmann and Radtke, 2000; Pappalardo et al., 2015). However, both methods are recognized as having drawbacks and issues when applied to marine mollusk shell, with a primary concern being whether the shell behaves as an open or closed system (e.g., see discussions in Schwarcz, 1994; Hillaire-Marcel et al., 1996; Schellmann and Radtke, 2000; Schellmann et al., 2008), although recent method advancements in ESR appear to address this concern (Duval et al., 2020). Another common geochronological method used for the analysis of beach ridges is luminescence dating (see review by Lamothe, 2016); however, the composition of the beach ridges in Camarones and, in general, along the Patagonian coasts of

Argentina (predominantly pebbles and cobbles with little to no sand) limits the application of that method with only one study showing reliable age estimates (Ribolini et al., 2011), albeit limited to the Early Holocene.

In our work we apply Amino Acid Racemization (AAR) and radiocarbon geochronological methods. AAR does not provide numerical ages (unless calibrated) but instead relative ages as indicated by the clustering of D/L values of amino acids and is useful in correlating deposits (see reviews of the method by Wehmiller, 1982; Wehmiller and Miller, 2000; Wehmiller, 2013b). AAR, like ESR and U-series, has been used successfully within Argentina to distinguish shells of MIS 5 age from earlier interglacials (see Gowan et al., 2021a, for review). Due to the uncertainties of each method, none are able to distinguish between MIS 5 substages (i.e., 5e, 5c, or 5a) with high certainty.

#### 5.4.3.1. Amino acid geochronology

Articulated and disarticulated valves of *A. antiqua* (formerly *Prothotaca antiqua*) were collected from beach ridge exposures at all sites except PE5E where only fragments of shell, tentatively identified as *A. antiqua*, were found on the surface. Between four and eight shells were selected from each Pleistocene site with consideration for their robust appearance, i.e., completeness of valve, a minimal indication of wearing, abrasion, or dissolution (the dated shells are shown in Supplementary Figure 5.4, 5.5).

Subsampling, sample preparation, and analysis were completed at the Amino Acid Geochronology Laboratory at Northern Arizona University. Shells were subsampled at the hinge-umbo region. Sample preparation and hydrolysis followed the methods established by Kaufman and Manley (1998). Samples were analyzed using an Agilent 1100 series RP-HPLC (reverse-phase – high-performance liquid chromatography) instrument. Inter-laboratory comparisons (ILCs), homogenous powders of Pleistocene mollusk samples, were used as comparative standards (Wehmiller, 2013a).

The results of AAR analyses were subject to data screening to identify and reject D/L values that would compromise the integrity of the sample group. We used aspartic and glutamic acids D/L values to assess amino acid abundance and variance, and relative age. The preference for these amino acids is due to their high chromatographic resolution and individual characteristics (Goodfriend, 1991). Aspartic acid is present in very high concentrations in younger fossils, whereas glutamic acid has a stable kinetic behavior and is a reliable amino acid for discriminating age based on the extent of racemization. Serine was also used in data screening. Serine decomposes rapidly, and excessive amounts of serine in Pleistocene samples indicate contamination by modern amino acids (Kosnik and Kaufman, 2008).

Using these criteria, all results were accepted except for those from PE5E. The D/L values from this site were extremely inconsistent. Two samples were immediately rejected for serine abundance. The remaining D/L values exhibited high variation within their sample group and in comparison with the other field sites. Due to the inconsistency of the results, the unknown environmental history, and as we were initially uncertain of the genus of the shell

fragments from which the samples were selected, we decided to reject all results from PE5E.

An additional valve of *A. antiqua* was collected from the modern beach berm of Camarones beach with paired analysis by radio- carbon (see below) to provide a comparison for the Pleistocene D/L values.

### 5.4.3.2. Radiocarbon

Two shells of the limpet *Nacella* sp., collected from a Holocene beach ridge, were selected for radiocarbon dating at the Beta Analytic laboratory using an in-house NEC accelerator mass spectrometer (AMS). Radiocarbon ages are reported as calibrated years (cal yr BP,  $2\sigma$ ) using CALIB software (version 8.2) and the MARINE20 curve (Heaton et al., 2020). A marine reservoir correction ( $\Delta R = -174 \pm 132$ ) has been applied according to the closest available data for the study area using the Marine Reservoir Correction Database (Reimer and Reimer, 2001).

One disarticulated valve of *A. antiqua* was collected from the modern beach berm of Camarones beach and dated using radiocarbon paired with AAR (see above). This analysis was done to provide a numerical age constraint for the Holocene D/L values.

## 5.5. Results

In the area of Camarones, we identified, sampled, and surveyed seven sites (plus the two already reported in Rovere et al., 2020), that are described below and shown in Figure 5.3.

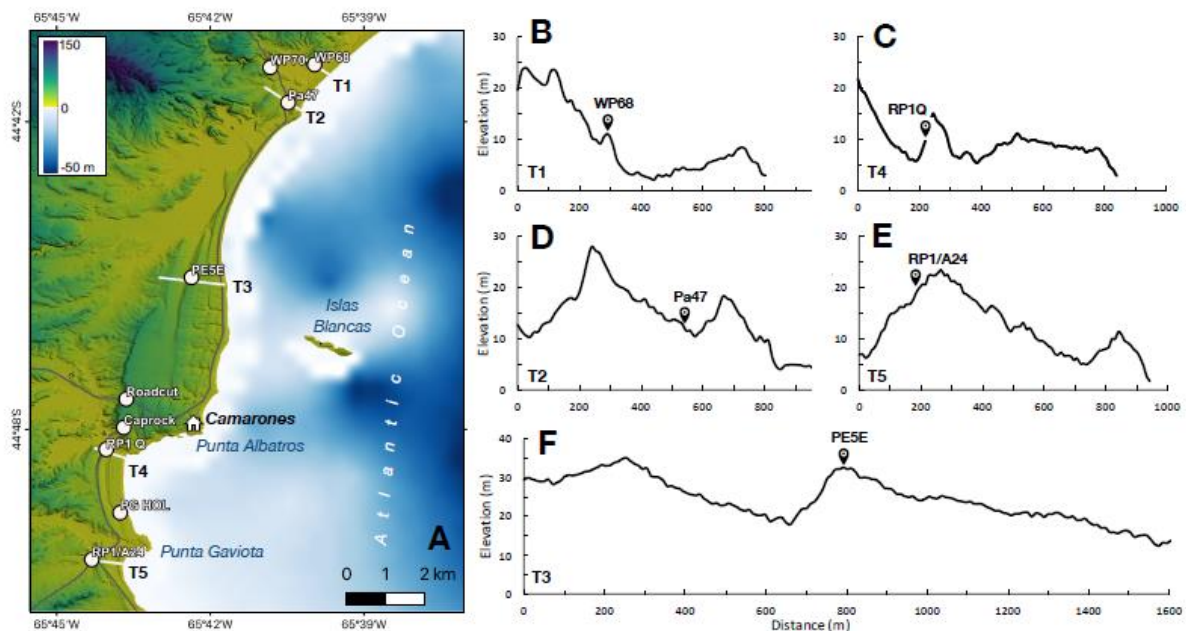


**Figure 5.3.** Pliocene, Pleistocene and Holocene sites. A) Map of the study area, showing the location of the town of Camarones and the sites reported in this study. Topography from TanDEM-X Digital Elevation Model and bathymetry from GEBCO Bathymetric Compilation Group 2023 (2023), B-F) Topographic transects and associated field sites described in the text.

### 5.5.1. Indicative meaning of beach ridges

Including the results of all runup models (Figure 5.4 and Supplementary Figure 5.6), we obtain that the 23-year average runup on the Camarones coast is 1.58 m, while the 95% extreme runup is 4.24 m. We use these two values as representative of the ordinary berm and the storm berm, respectively, which define respectively the lower and upper limits of the indicative range of beach ridges in the area. Using Equation 2 and Equation 3, we calculate that the RWL associated with the top of articulated shells in Camarones is 2.91 m and the associated IR is 2.66 m.

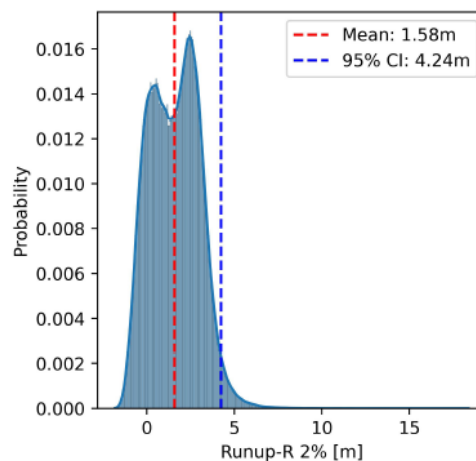


**Figure 5.4.** Calculation of the indicative range for beach ridges at Camarones. Plot showing the probability distribution of 2% exceedance wave runup level plus water level from the FES2014 model calculated at Camarones for different runup models (Holman, 1986; Ruggiero et al., 2001; Stockdon et al., 2006; Nielsen, 2009; Senechal et al., 2011; Vousdoukas et al., 2012; Passarella et al., 2018; Beuzen et al., 2019)

We note that the RWL calculated with our approach is comparable to that obtained via the IMCalc tool (RWL=2.3 m, IR=0.6 m, Lorscheid and Rovere, 2019), which employs the Stockdon et al. (2006) model, with less accurate wave and tidal data, and a general beach slope. However, this model underestimates the IR and the final uncertainty on paleo RSL would be lower, but less accurate if we had applied the IMCalc method.

### 5.5.2. Holocene

The Holocene sea-level record surrounding Camarones is represented by 76 sea-level index points located between Cabo Raso (60 km North of Camarones) and Bahia Bustamante (80 km South of Camarones, Figure 5.5A), that were reported by several authors (Codignotto et al., 1992; Schellmann and Radtke, 2003, 2007, 2010; Ribolini et al., 2011; Zanchetta et al., 2012; Bini et al., 2018). These datapoints are here reviewed (see Supplementary Information for details) following the HOLSEA standards (Khan et al., 2019b). In general, the Holocene data in this area extend back to 8 ka BP, with a highstand reaching up to 6-8 m above present sea level between 4 and 6 ka (Figure 5.5B). In 2019, we collected two shells of the limpet *Nacella* sp. from a Holocene beach ridge close to *Punta Gaviota* (site PG Hol). The shells were collected from the upper part of the ridge (elevation:  $8.7 \pm 0.22$  m,  $1\sigma$ ), and represent the highest occurrence of shells (in terms of elevation above sea level), located few decimeters from the top surface of

the ridge. Using the same indicative meaning adopted for Pleistocene ridges in the area, we calculate that the paleo RSL when this ridge was formed was  $6 \pm 1.5$  m ( $1\sigma$ ). Radiocarbon ages (see Supplementary Information for details) indicate an age of this beach ridge ranging from 2663 to 3369 cal yr BP ( $2\sigma$  range).

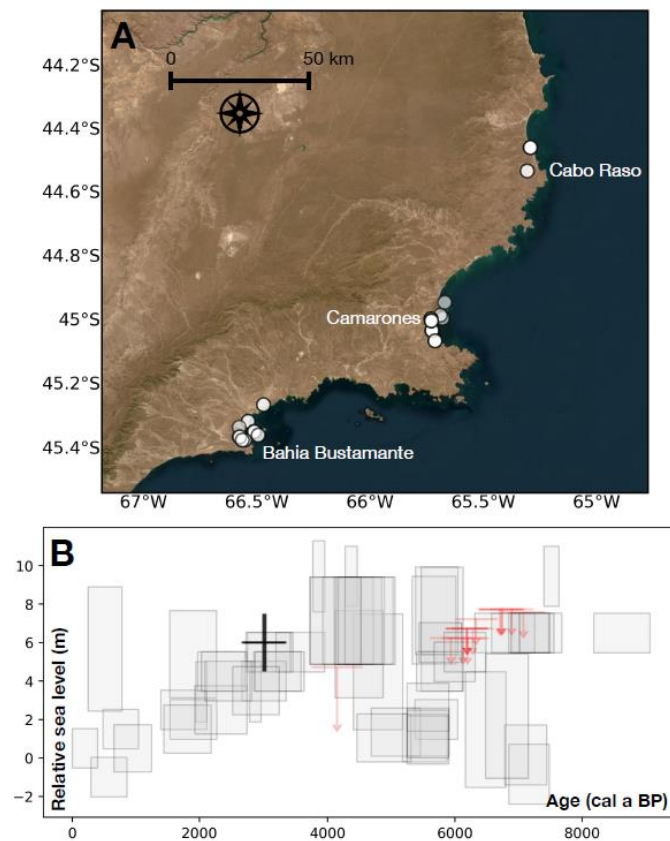


**Figure 5.5.** Holocene sea-level index points. A) map of Holocene sea-level index points in the broader area around Camarones (white dots). B) Relative sea level vs Age plot of the RSL index points shown in A). Red arrows show terrestrial limiting points, which indicate that sea level was below the horizontal red bar. The black cross indicates data gathered in this work, while the gray boxes indicate data from literature. Elevation error bars are  $1\sigma$ , while age error bars are  $2\sigma$ .

### 5.5.3. Pleistocene highstands

Within the study area, five Pleistocene beach ridges were resurveyed and sampled during our fieldwork. These deposits have been previously described and dated by several authors (Schellmann, 1998; Schellmann and Radtke, 2000; Pappalardo et al., 2015). In our work, we have retained the site names used in the studies cited above, unless specified in the text below. From north to south, the sites related to the Pleistocene highstands in the area are: WP68, WP70, Pa47, RP1 Quarry, and RP1/A24 (Figure 5.3A).

#### 5.5.3.1. WP68

The first beach ridge we surveyed is located about 40 km North of Camarones (Figure 5.3A). We maintained the site name of Pappalardo et al. (2015), who describe this site as composed by a ridge "*displaying poor morphological evidence but good lateral continuity towards NE*". Such morphology is evident from digital elevation models (Figure 5.3B). Pappalardo et al. (2015) dated an articulated specimen of *Ameghinomya antiqua* (formerly *Protothaca antiqua*) with U-series and obtained an age of  $131 \pm 1.1$  ka ( $2\sigma$  range). In our survey, we collected four shells of the same species (none articulated) from the surface of the ridge for AAR analysis (Supplementary Figure 5.5), which reaches a maximum elevation of  $12.2 \pm 0.23$  m ( $1\sigma$ ). This altitude is roughly the midpoint between ridge-top elevations recorded at sites Pa47 ( $11.3 \pm 0.2$  m) and RP1 Quarry ( $14 \pm 0.2$  m), described below.

#### 5.5.3.2. WP70

About 1.2 km West of WP68 (Figure 5.3A), we surveyed a marine deposit overlying a shore platform carved on the bedrock, previously described by Pappalardo et al. (2015). These authors dated an articulated *A. antiqua* shell collected from the marine deposit, which they described as sandy with sorted gravels and abundant marine shells. U-series analysis gave an age of  $127 \pm 1.2$  ka ( $2\sigma$ , sample WP70B). In 2022, we surveyed the contact between the bedrock platform and the overlying deposit to an elevation of  $13 \pm 0.22$  m ( $1\sigma$ ). We did not find any shell to sample within this deposit. However, ~173 m SW of the bedrock platform, we found a small quarry with a good lateral continuity where we sampled a layer containing *A. antiqua* shells (4 samples, no articulated shells, Supplementary Figure 5.4) at an elevation of  $10.3 \pm 0.22$  m ( $1\sigma$ ). We do not use this site in our paleo RSL calculations, as it is located within a former embayment, which could have been affected by stream erosion and redeposition after the emplacement of the marine deposits. However, we note that both the bedrock platform and the ridge are found at elevations consistent with those of RP1 Quarry and the Pa47 ridge, described below.

#### 5.5.3.3. Pa47

About 1.4 km South of WP70, (and ~11 km North of Camarones town, Figure 5.3A) we identified a beach ridge that abuts directly onto higher terrains (Figure 5.3D). Quarrying activities in this area have exposed a small outcrop of about 1.15 m in height. This outcrop is divided into two sedimentary units composed mainly of pebbles with a fining upward sequence. The upper part of the second unit shows soil development, and in its lower part includes shells of *A. antiqua*, with few articulated specimens. Within this unit, we also identify specimens of the mollusk *Tegula atra*, which is used as a Pleistocene biostratigraphical tool in the marine Quaternary of Argentina (Aguirre et al., 2013). The site name is derived from Schellmann and Radtke (2000), who collected shells from two layers at this site, one from the upper unit (Pa47c) and one from a lower unit (Pa47a). Several ESR and U-Series dates yielded average ages  $102 \pm 10$  ka and  $129 \pm 16$  ka for the upper and lower unit, respectively. During the 2022 campaign, we collected four disarticulated valves of *A. antiqua* from the upper unit (Supplementary Figure 5.4). The top of the beach ridge is  $11.3 \pm 0.2$  m ( $1\sigma$ ), and the articulated shells are located 28 cm below this point. This corresponds to a paleo RSL of  $8.4 \pm 1.5$  m ( $1\sigma$ ).

#### 5.5.3.4. RP1 Quarry

About 14 km South of Pa47 (and ~2 km south of the town of Camarones, Figure 5.3A), we re-surveyed a beach ridge along the *Ruta Provincial 1*. This site has the morphology of a single, isolated ridge (Figure 5.3C). The landward side of the beach ridge has been quarried (likely by roadworks), exposing the complete ridge stratigraphy in a clean vertical section on average ~4.5 m high (Figure 5.6A, B). Within this section, Pappalardo et al. (2015) identify two units of sorted coarse sands and gravels with abundant marine fauna separated by a centimeters thick layer of silty clay with gravel throughout. This section was revisited in the 2019 field campaign. The presence of two units (U1 and U2 in Figure 5.6D) was confirmed. The boundary between them is represented by discontinuous, lense-shaped, fine materials, with traces of oxidation pervading the lower unit. The lower unit (U1) is sandy, with scattered gravels and fragmented shells. Coarseness and the abundance of shells increase upwards, where the deposit becomes clast-supported. At this transition, articulated shells of *A. antiqua*, not in living position, cluster. A small barnacle colony (12 individuals, Figure 5.6E) was found in an upright position anchored to an *A. antiqua* shell at an elevation of  $10.3 \pm 0.22$  m ( $1\sigma$ ). The overlying unit (U2) is similar to the lower one but with whole and articulated valves of *A. antiqua* clustering at the bottom (Figure 5.6C). On the whole, the sequence can be interpreted as two beach ridge deposition phases separated by an ephemeral water body in an interridge swale deposit, as previously described by Pappalardo et al. (2015). These authors sampled a specimen of *A. antiqua* from the uppermost layer and employed U-series to date it to  $92 \pm 0.6$  ka ( $2\sigma$ , sample WP92A (3)). Within the layer dated by Pappalardo et al. (2015), we surveyed the highest occurrence of articulated shells at different positions along the exposed section (~30 m across) without recording significant height changes. Overall, averaging the elevation of 5 points, we calculate that the elevation of this layer is  $11.6 \pm 0.3$  m ( $1\sigma$ ), corresponding to a paleo RSL of  $8.9 \pm 1.5$  m ( $1\sigma$ ). At this site, we collected 7 specimens of *A. antiqua* for AAR analysis, two of them articulated (Supplementary Figure 5.4).

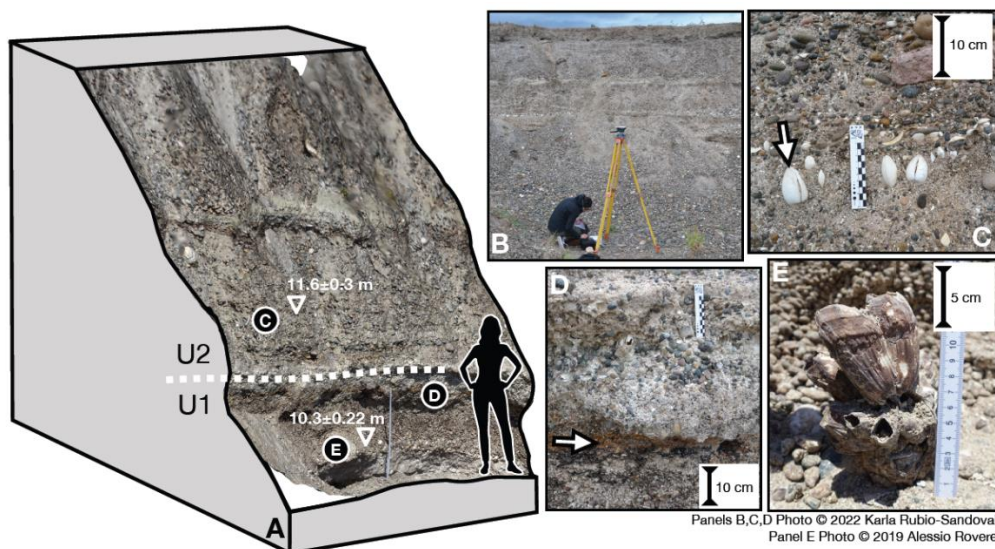


**Figure 5.6.** RP1 Quarry site. A) 3D view of the RP1 Quarry outcrop, reconstructed via overlapping field photos processed with Structure-From-Motion Multi View Stereo techniques. Downward pointing triangles with values show GNSS data collected at this site, while circled text refers to other panels in the figure. U1 and U2 refer to the two units identified in this outcrop, described in the main text. B) View of the main face of the RP1 Quarry outcrop. C) Uppermost articulated shells (arrow) within the beach ridge (U2), see location and elevation in panel A. D) Oxydised silty clay layer (arrow) with gravels already identified by Pappalardo et al. (2015), see location in panel A. E) Colony of barnacles (*Balanus* sp.) in living position, see location and elevation in panel A.

### 5.5.3.5. RP1/A24

South of the town of Camarones, about 1.5 km onshore *Punta Gaviota* (Figure 5.3A) and close to the intersection between *Ruta Provincial 1* and *Ruta Provincial A24*, we surveyed both in 2014 and in 2019 a site that we hereby call "RP1/A24" (Figure 5.7A-C). A road cut on the backshore slope of a beach ridge exposes part of the stratigraphy of this feature, formed by rounded pebbles embedded in a sandy matrix. Within the deposit, a layer containing a cluster of articulated *A. antiqua* mollusk shells is present. (Figure 5.3E). The coastal deposit was sampled and dated at the same site with both U-series and ESR by Schellmann (1998), as further described in Schellmann and Radtke (2000) (Sample Pa 35). These authors initially attributed this deposit to MIS 9, as it yielded ESR ages scattered between  $342 \pm 29$  ka and  $383 \pm 28$  ka. A U-series age on the same shells yielded an age of  $228 \pm 15$  ka, but Schellmann and Radtke (2000) state that it "*seem[s] to be too young by a factor of up to 2*", hence opening up the possibility that this shell dates to MIS 11. It is worth noting that Schellmann and Radtke (2000), discussing this site, surmise that ESR ages older than 300 ka are at the upper limit of the ESR dating technique, therefore they might be less reliable. One sample, labeled WP97(1), from the same deposit, was dated with U-series by Pappalardo et al. (2015), yielding an age of  $414 \pm 16$  ka ( $2\sigma$ ). We collected eight articulated *A. antiqua* shells at this site for AAR analysis (Supplementary Figure 5.5). We surveyed the elevation of the top of this deposit four times, three in 2014 and one in 2019, obtaining an average elevation of  $17.2 \pm 0.2$  m ( $1\sigma$ ), corresponding to a paleo RSL of  $14.5 \pm 1.5$  m ( $1\sigma$ ).



**Figure 5.7.** RP1/A24 site. A) overview of the beach ridge, with co-author E. J. Gowan measuring the highest occurrence of articulated *Ameghinomya antiqua* mollusk shells. B) and C) details of the beach ridge where articulated *Ameghinomya antiqua* mollusk shells occur.

#### 5.5.4. Pliocene highstand

Rovere et al. (2020) report two outcrops, that were named "Road-cut" and "Caprock" south of the town of Camarones (Figure 5.3A). Both are transgressive sequences on top of an uplifted shore platform. In both outcrops, there is a unit described as a conglomerate with bivalve shells that were reported as mostly intact and sometimes with articulated valves (Rovere et al., 2020). Strontium isotope stratigraphy dating on oyster shells assessed that this unit is Early Pliocene in age (4.69-5.23 Ma,  $2\sigma$ ). The elevation of this unit was measured at  $36.2 \pm 0.9$  m ( $1\sigma$ ) above mean sea level, and paleo RSL was reconstructed at  $36.2 \pm 2.7$  m ( $1\sigma$ ) above present sea level, as the unit was interpreted as indicative of a foreshore (intertidal) environment. About 4 km North of the Roadcut outcrop, we surveyed a beach ridge prominent within the landscape (PE5E, Figure 5.3A and F) that sits at elevations similar to those of the "Roadcut" and "Caprock". As the beach ridge did not have an exposed outcrop, we measured its top giving an elevation of  $31.7 \pm 0.2$  m ( $1\sigma$ ). From the ridge surface, we collected broken, rounded fragments tentatively identified as remains of *A. antiqua* shells, which appear highly reworked (Supplementary Figure 5.5).

#### 5.5.5. AAR results

In this work, we compare the results of previous dating (reported in the site descriptions above) with AAR on the same shell species with the aim of evaluating the consistency of the chronological attribution done by previous authors in this area. All our analytical results are reported in the Supplementary Information annexed to this paper. All dated shells are shown on Supplementary Figure 5.4 and 5.5. One *A. antiqua* shell collected from the modern beach ridge south of Camarones and seaward of the field site RP1 yielded a radiocarbon age of  $698 \pm 137$  cal a BP ( $2\sigma$ ).

Shells sampled from Pleistocene deposits have much higher D/L glutamic - aspartic acids ratios than the one sampled within the Holocene beach ridge (Figure 5.8). The aspartic and glutamic acids D/L values from the Pleistocene beach ridges form two distinct clusters indicating at least two different depositional periods (Figure 5.8, Supplementary Figure 5.7). Due to the close proximity of the sites and a regional mean annual temperature of  $13$  °C, the effective diagenetic temperature is expected to be consistent across all sites and we can discount temperature differences as a driver for the different groupings. Most sites are grouped within the younger cluster, whereas the older cluster is formed predominantly by shells collected from RP1/A24. These groupings are broadly consistent with the ESR and U-series ages reported by earlier authors (Schellmann and Radtke, 2000; Pappalardo et al., 2015).

AAR ratios from the four shells sampled at Pa47 are split between the two groups described above. The geomorphological evidence, elevation of articulated shells, and former ESR and U-series dating at site Pa47 align with those reported at RP1 Quarry, WP68, and WP70. Therefore, we suspect that Pa47 includes older reworked shells, possibly washed down from higher terrains (Figure 5.3D). Schellmann and Radtke (2000) and Pappalardo et al. (2015) identified an unconformity at this site, with the latter authors attributing the deposit above the unconformity to storm activity and reworking of earlier deposits. It is reasonable then to interpret the higher D/L values as reflecting the redeposition of shells from an earlier interglacial of similar, if not the same age, as RP1/A24.

The two AAR age clusters identified in the study area correspond well with the results of U-series and ESR ages, reported by previous authors (Figure 5.8), clustering within MIS 5 (possibly MIS 5e and MIS 9 or MIS 11, Supplementary Figure 5.7).

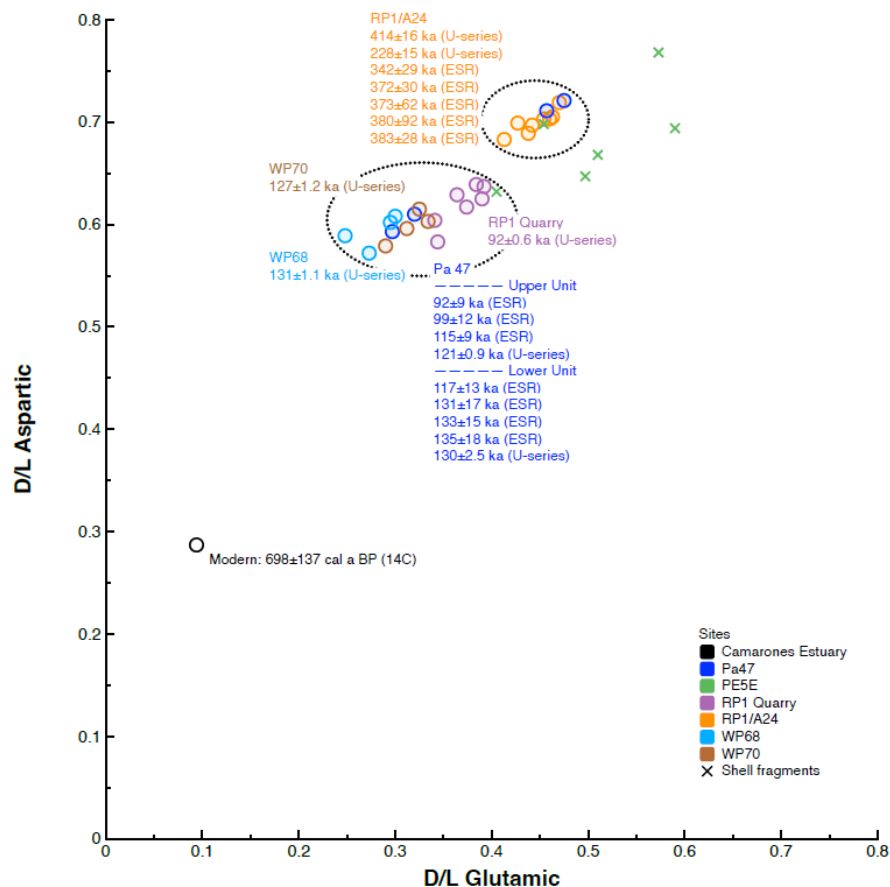


**Figure 5.8.** AAR, U-series, and ESR ages available in the Camarones area. Results of amino acid racemization (aspartic acid and glutamic acid D/L values) on specimens of *Ameghinomya antiqua* (formerly *Protothaca antiqua*) collected from beach ridges in the Camarones area. Colors identify different sites described in the text, and the colored text reports the results of radiometric dating on shells from the same beach ridges (age uncertainty assumed as  $2\sigma$ , data from Schellmann and Radtke, 2000; Pappalardo et al., 2015). The different symbols identify if the specimen was an integer valve (circle) or a shell fragment (cross, rejected). The dotted ellipses identify the two age groups discussed in the main text.

## 5.6. Discussion

In this work, we use both previously published and original data to investigate past sea-level highstands in the Camarones area. As highlighted by previous authors, within a short geographic distance around the town of Camarones, the imprint left by sea level during several past highstands has been left on the coastal landscape (Supplementary Figure 5.8). As such, this area has preserved an exceptional record of sea-level changes through time.

### 5.6.1. Relative sea level, GIA and post-depositional uplift

Data on the Holocene beach ridges show an RSL peak between ~4 and 7 ka, when sea level reached up to 4-8 m above present-day (Figure 5.5). These observations are in broad agreement with Glacial Isostatic Adjustment (GIA) models (Supplementary Figure 5.9), which predict a GIA-induced RSL peak of comparable magnitude and timing (Figure 5.9A). The Holocene provides important insight into how strandplains of beach ridges at this location (and arguably over the Patagonian coast) develop over an interglacial and are preserved during successive interglacial periods.

The highest ridges within a given interglacial are those deposited during the RSL highstand, which at this location is dictated by GIA processes including ocean siphoning, continental levering, and rotational feedbacks (Mitrovica and Milne, 2002; Peltier, 2002; Peltier et al., 2015). The influence of siphoning, and the rotational term means that the sea level highstand in Camarones and elsewhere in Patagonia is sensitive to the history of Northern Hemisphere ice sheets. So far, there is no strong evidence of the Patagonian ice sheet control on Holocene sea level in this area. Rostami et al. (2000) suggest that due to the small ice sheet thickness (ca. 400 m), there is no significant effect on the RSL along the coast of Argentina. However, Björck et al. (2021) state that the Patagonia ice cap may contribute to the GIA signal in the southern part of Patagonia.

As the GIA-driven sea-level regression evolves, it may leave behind a set of regressive ridges, that may be eroded away if RSL reaches a similar elevation during a successive highstand. It follows from this reasoning that the ridges we surveyed represent the peak relative sea level associated with each period. In fact, Rostami et al. (2000) highlight the absence of paleo shorelines deposited during MIS 7 in the Patagonian coastline of Argentina, suggesting a reoccupation of these deposits during the subsequent MIS 5 transgressive event, when the sea level rose to a higher elevation.

Our survey results at RP1 Quarry (RSL =  $8.9 \pm 1.5$  m,  $1\sigma$ ) and Pa47 (RSL =  $8.4 \pm 1.5$  m,  $1\sigma$ ) represent, on average, a paleo RSL of  $8.7 \pm 2.1$  m ( $1\sigma$ ). AAR clusters these sites as of similar age to WP68 and WP70 (Figure 5.8), which, albeit less indicative in terms of paleo RSL, are consistent in elevation. The radiometric ages of these sites are predominantly skewed towards the early part of MIS 5e, in agreement with both the evolution model proposed above and models predicting a GIA driven sea-level highstand of similar magnitude to the Holocene one at ~128 ka (Figure 5.9B, C). GIA models predict that a shoreline deposited 128 ka ago would have formed  $5.8 \pm 3.9$  m ( $1\sigma$ ) higher due to GIA alone, yielding a GIA-corrected relative sea level of  $2.9 \pm 4.4$  m ( $1\sigma$ ) above present.

From the work on early Pliocene shorelines in the region (Hollyday et al., 2023), it appears that Dynamic Topography (DT) has played a major role in uplifting shorelines through time at this location. The mean DT change since 1 Ma from the four best-fitting DT models of Hollyday et al. (2023) predicts an uplift of  $40.1 \pm 4.5$  m/Myr ( $1\sigma$ , equivalent to  $0.0401 \pm 0.0045$  mm/yr). This value may seem at odds with the elevation of the early Pliocene shoreline at  $36.2 \pm 2.7$  m, which has been used to calibrate the geodynamic model since it would imply that this shoreline was uplifted by approx. 200 m.

There are two reasons for this discrepancy. First, while the models of Hollyday et al. (2023) predict approximately linear DT change over 1 Myrs in this region, deformation is not linear over longer timespans. Second, Hollyday et al. (2023) explore uplift rates around the data location according to the spatial resolution of the seismic tomography model that determines the pattern of convection. Therefore, their estimate does not exactly align with the location of the shoreline.

Applying the above-mentioned rate to an age of 128 kyr yields  $5.1 \pm 0.6$  m of uplift. Austermann et al. (2017) use similar but uncalibrated geodynamic models and predict a similar but much more uncertain uplift of  $3.6 \pm 5.9$  m. Assuming the rate of Hollyday et al. (2023) yields an uplift corrected sea level estimate of  $-2.2 \pm 4.4$  m for MIS 5e for Camarones. To infer GMSL, this value further needs to account for the fingerprint signal of excess melt during MIS 5e (Hay et al., 2014). Melting from the West Antarctic ice sheet would cause sea level to rise less in Patagonia compared to other sites, which may explain this relatively low value. However, additional GIA modeling is required to investigate whether this value is reconcilable with sea level observations from other locations or whether the uplift rate requires revision.

The age attribution of this site is not straightforward. U-series places the ridge firmly within MIS 11 but the uncertainty of the ESR ages is suggestive of either an MIS 9 or 11 age. However, the ages suggest this site to be at the upper limit of the dating technique (Schellmann and Radtke, 2000). The AAR results are more indicative of MIS 9 (see below discussion).

There are no models available to correct a MIS 9 (~330 ka) shoreline for GIA at this location. However, if the same uplift rate as discussed above is applied here assuming an MIS 9 age it would result in an uplift-corrected sea level of  $1.3 \pm 2.1$  m ( $1\sigma$ ). If the GIA signal is small, this sea level inference would be in line with studies surmising that sea level during MIS 9 was close to present-day (Murray-Wallace, 2002).

For MIS 11, GIA models published by Raymo and Mitrovica (2012), predict that RSL was  $0.6 \pm 0.2$  m ( $1\sigma$ ) below GMSL at ~410 ka (Figure 5.9D). Additional melt during this time period might have changed the timing of peak sea level, which affects the GIA correction. We remark that the smaller uncertainty of this prediction compared to that reported for MIS 5e is due to the fact that the MIS 11 predictions employ fewer mantle viscosity profiles and ice sheet configurations than those employed for MIS 5e (Dyer et al., 2021). Using the rates from DT models to correct this shoreline for vertical land motion leads to a GIA and uplift corrected sea level of  $-1.3 \pm 2.4$  m ( $1\sigma$ ). While this still requires a correction for the fingerprint signal of excess melt it does appear low compared to existing estimates of GMSL during MIS 11 (Chen et al., 2014; Raymo and Mitrovica, 2012), which might indicate an overestimation of uplift driven by DT, an incorrect GIA correction, or an incorrect attribution to MIS 11, as discussed.

## Quaternary and Pliocene sea-level changes at Camarones, central Patagonia, Argentina

The highest ( $36.2 \pm 0.9$  m,  $1\sigma$ ) and oldest (4.69-5.23 Ma,  $2\sigma$ ) shoreline in the area was reported by Rovere et al. (2020). Here, we tentatively attribute the large ridge we surveyed to the North of Camarones (where sample PE5E has been collected) to the same Pliocene highstand. Analyzing this line of evidence in conjunction with other two sites of similar age along the Patagonian coast (Del Río et al., 2013). Hollyday et al. (2023) surmised that, once corrected for GIA and DT, these sites would indicate a GMSL of  $17.5 \pm 6.4$  m ( $1\sigma$ ).

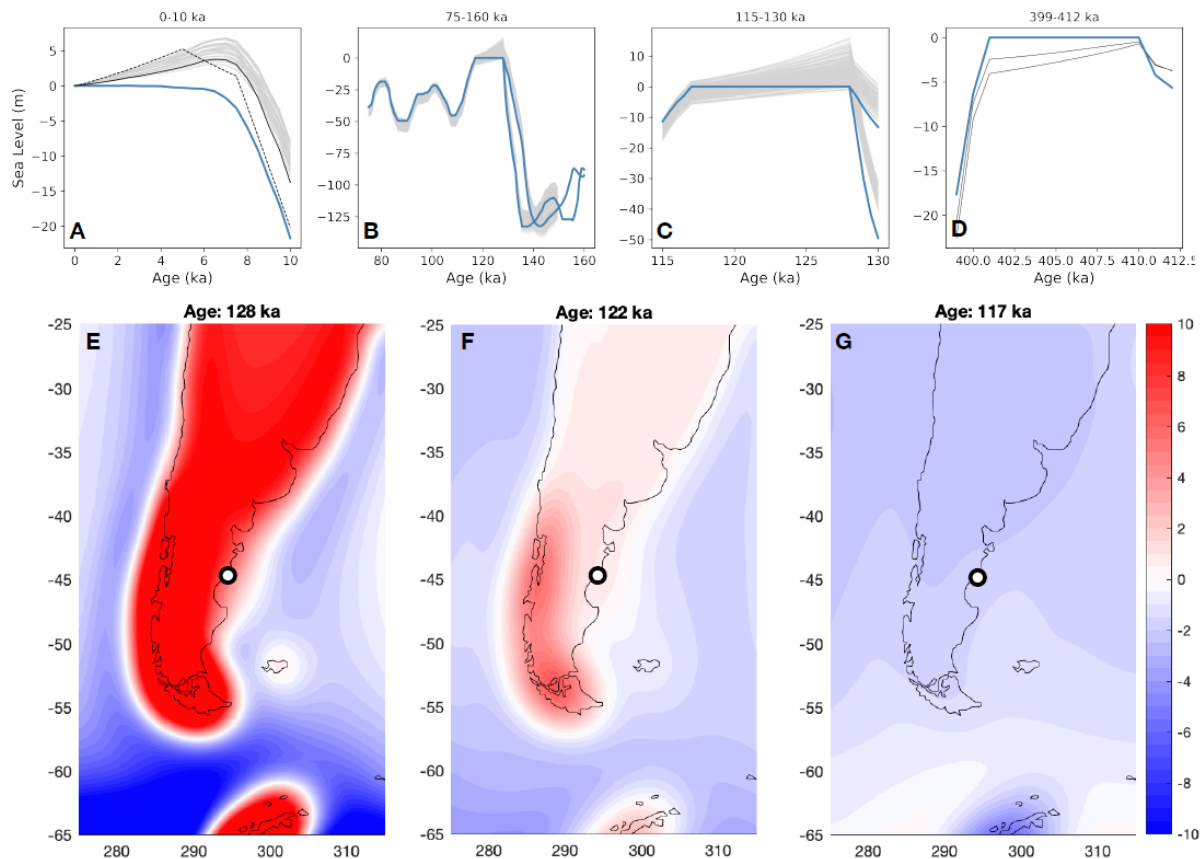


**Figure 5.9.** Published GIA models in the area of Camarones. A) Holocene (gray lines, GIA from Dyer et al., 2021, dashed line from Gowan et al., 2021b, solid black line from Peltier et al., 2015), B) MIS 5 (from Dyer et al., 2021), C) MIS 5e (from Dyer et al., 2021), D) MIS 11c (from Raymo and Mitrovica, 2012). The blue line in A-D represents GMSL. In B-C-D, the sea-level caps at 0m as per model input, to show only the background GIA response. E, F, and G, spatial pattern of mean GIA changes throughout MIS 5e across the broader South American region. The white dot shows the location of Camarones.

### 5.6.2. Geochronology

Some of the radiometric ages for the beach ridges we assign to MIS 5e suggest the presence of shells dating to MIS 5a and 5c within these ridges. If we accept the upper boundary possibility for preferred peak GMSL values during MIS 5a and 5c of +1 m and +2 m, respectively, as suggested by Creveling et al. (2017), it is possible that these substages peaked close to the MIS 5e shoreline and that shells were transported during the most extreme storms to the height of the earlier shoreline. Our results (Supplementary Figure 5.6I) show that this might be possible, as the 95% upper CI of wave runup in the area is 4.2 m. North of Camarones, in the Río de la Plata estuary, Rojas and Martínez (2016) reported higher-than-present littoral deposits of MIS 5a age. These deposits support the possibility that elevated MIS 5a aged deposits also exist in Camarones. However, the uncertainties within the geochronological methods must also be considered.

All three geochronological methods (ESR, U-series, and AAR) used to determine the age of the beach ridges at Camarones suffer from uncertainties associated with the nature of the shell structure and whether it behaves as an open or closed system. A closed system increases the likelihood that whatever variable the method measures, whether it is a trapped charge, uranium-thorium, or amino acids, is endogenous to the shell and has not been altered by external environmental factors after death and during diagenesis. For this reason, all these methods employ sample collection and preparation steps to minimize the inclusion of exogenous materials/isotopes in the sample, to minimize any physical or chemical alteration or diagenesis that may influence the result, and to account for any intra-shell variability. However, the integrity of the organic matrix of any shell and its rate of decay varies between mollusc species (Labonne and Hillaire-Marcel, 2000; Jedoui et al., 2003). The only way to accurately assess these variables in any species is through experimental studies designed for that purpose. This work has yet to be done for *A. antiqua*.

*A. antiqua* shells are relatively large, thick, and robust (Supplementary Figure 5.4, 5.5) and for these reasons, the inner portion of the shell structure is more likely to maintain its integrity through time, which has made it a preferred choice for geochronological methods in this and earlier studies. However, because of the uncertainties regarding the shell structure, it is important to apply multiple geochronological methods to *A. antiqua* in the absence of other complementary methods (i.e., luminescence dating of sediments). The coherence of results within the same unit, between, and within methods, reduces overall uncertainty that may result from the use of a single method.

There are some inconsistencies between the AAR D/L values and the radiometric ages. Sites WP68 and WP70, which have the highest U-series ages (within MIS 5, ~131 ka and ~127 ka, respectively), returned consistently lower (relatively) D/L values than site RP1, which provided the youngest U-series age (~92 ka, Figure 5.8). Although the mean D/L values of the seven shells collected from RP1 are consistent within two standard deviations the other MIS 5 ridges (WP68, WP70), glutamic D/L values from RP1 tend to plot higher in comparison with other sites and indicate a potentially older age. The U-series age was derived from a shell collected above the salitral lens identified by Pappalardo et al. (2015). The AAR result (ID 22680) of the shell we collected from the same unit is consistent within one standard deviation to the D/L values from WP68 and WP70. The remainder of the shells collected at RP1 for AAR analysis are from the lower unit and are stratigraphically consistent with earlier deposition. If

we are to consider RP1 to have been developed completely within MIS 5, the AAR results would imply that the lower unit exposed at RP1 formed early within MIS 5e and that the unit above the salitral lens and the other MIS 5e exposures around Camarones are from a later point within that interglacial. However, this would also indicate that U-series ages from these sites are overestimates (although still within MIS 5) and that the accompanying ESR ages, while also high, are more realistic with their larger uncertainties.

There is similar disagreement in the geochronology in the ridge surveyed at the RP1/A24 site, where RSL is estimated at  $14.5 \pm 1.5$  m ( $1 \sigma$ ). The U-series age of  $414 \pm 16$  ka is consistent with an MIS 11 age (Figure 5.8), whereas the ESR ages can be interpreted as indicative of either MIS 9 or MIS 11 and are at the limit of the dating technique (Schellmann and Radtke, 2000). The consistency of amino acid kinetic pathways indicates a preference for an MIS 9 age, i.e., the D/L values from the RP1/A24 fossils are lower than what would be expected for an MIS 11 fossil given the regional temperature (CMAT  $13^\circ\text{C}$ ) and D/L values of the apparent MIS 5-aged fossils.

### 5.7. Conclusions

In this work, we presented new data on a set of beach ridges of different ages in the area of Camarones along the coasts of Patagonia, Argentina. Although beach ridges are one of the most common landforms across the entire Patagonia coast, their use as reliable sea-level indicators poses a challenge due to their genesis, that is more related to wave intensity than directly to sea level. In this work, we outline a new self-consistent, repeatable, and reliable methodology to calculate their indicative meaning, i.e., to quantify the modern elevation of a fossil beach ridge with respect to paleo sea level. We build upon modern wave data and a suite of wave runup models to estimate their upper and lower limits. We surmise that this approach, using 23 years of wave data, is more robust than measuring the modern analogue (i.e., the ordinary and storm berms along the modern coast) at a single time, as in the case of beach ridges these might be ephemeral and dependent on recent storm activity rather than on long-term wave regimes. We highlight that there might be other issues to take into account, which we do not consider here. For example, the indicative meaning obtained with this method should be corrected for the increased or decreased water levels related to storm surge under different climate conditions (Scussolini et al., 2023).

In any case, the method to estimate the indicative meaning adopted here appears more reliable (as it is based on local wave and beach topography data) than the one proposed by Lorscheid and Rovere (2019), who use global wave atlases and global beach slope values. For this reason, we surmise that an update of the recent work of Gowan et al. (2021a), that was carried out revising the indicative ranges of Pleistocene beach ridges along the Patagonian coast done using the methodology proposed by Lorscheid and Rovere (2019) may be granted.

Additionally, we provided new AAR data by analyzing *A. antiqua* shells, our results complement ESR and U-series ages obtained by previous works. This chronostratigraphic approach helped identify four interglacial beach ridge systems from the present-day coastline up to 2 km inland. The first (lowermost and seaward) ridge formed under a paleo RSL of  $6 \pm 1.5$  m and is correlated with the late Holocene. The second (paleo RSL  $8.7 \pm 2.1$  m) is correlated to MIS 5e. The third Pleistocene ridge system could be associated with either MIS 9 or MIS 11 (paleo RSL  $14.5 \pm 1.5$  m), and the fourth (which was already reported by Rovere et al., 2020) is associated with the Early Pliocene (paleo RSL  $36.2 \pm 2.7$  m).

There are still some discrepancies between ages of shells within the same beach ridge. For example, some radiometric ages also seem to suggest that we cannot rule out that the MIS 5e ridge in this area was reoccupied during MIS 5a and 5c, or at least that extreme storms during these highstands transported shells into the MIS 5e beach ridge. Due to the limitation of the dating techniques, it also is difficult to disentangle MIS 11 from MIS 9. However, AAR results suggest that it is likely that there is an imprint of MIS 9 sea level at Camarones. This would represent one of the few direct observations of sea level during this highstand globally.

Our research highlights that there is a need of refined GIA predictions to back-calculate GMSL from the observed proxy data in this area. For MIS 5e, a refinement of the broad span of GIA predictions, accounting for the spatially varying sea level signature of excess melt, and further corrections for vertical land motions are needed before obtaining a reliable global mean sea level estimate.

Finally, we hypothesize that further melt during the LIG may have affected when peak sea level is attained at this location and therefore the GIA correction for this site. One strategy to reduce uncertainties in this regard may be to select the mantle viscosity profiles providing a better match with Holocene sea-level index points, and then investigating the corresponding predictions for MIS 5e and MIS 11. However, observations during different interglacials may be sensitive to different parts of the mantle depending on the melt history and melt source. Also, DT rates may need refinement. Those derived from published models (which were calibrated over the coasts of Patagonia by Hollyday et al., 2023) may overestimate the amount of uplift.

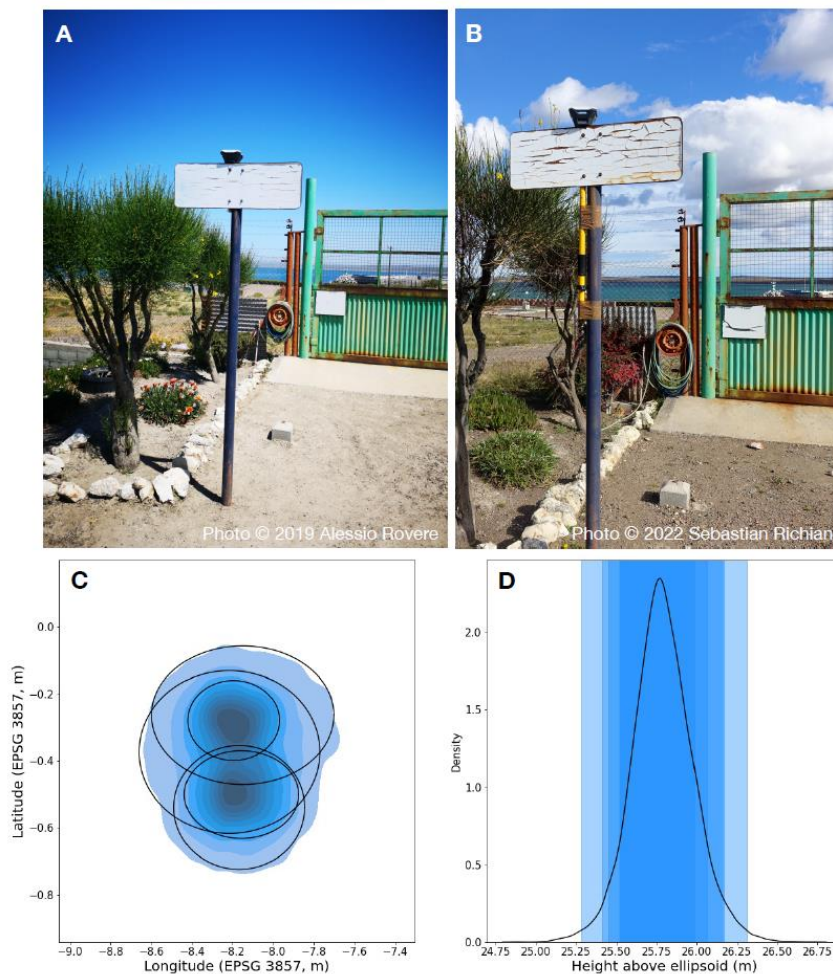
### 5.8. Data availability

All the raw data described in this paper (license CC-BY4.0) is available on Zenodo as Rovere et al. (2023a).

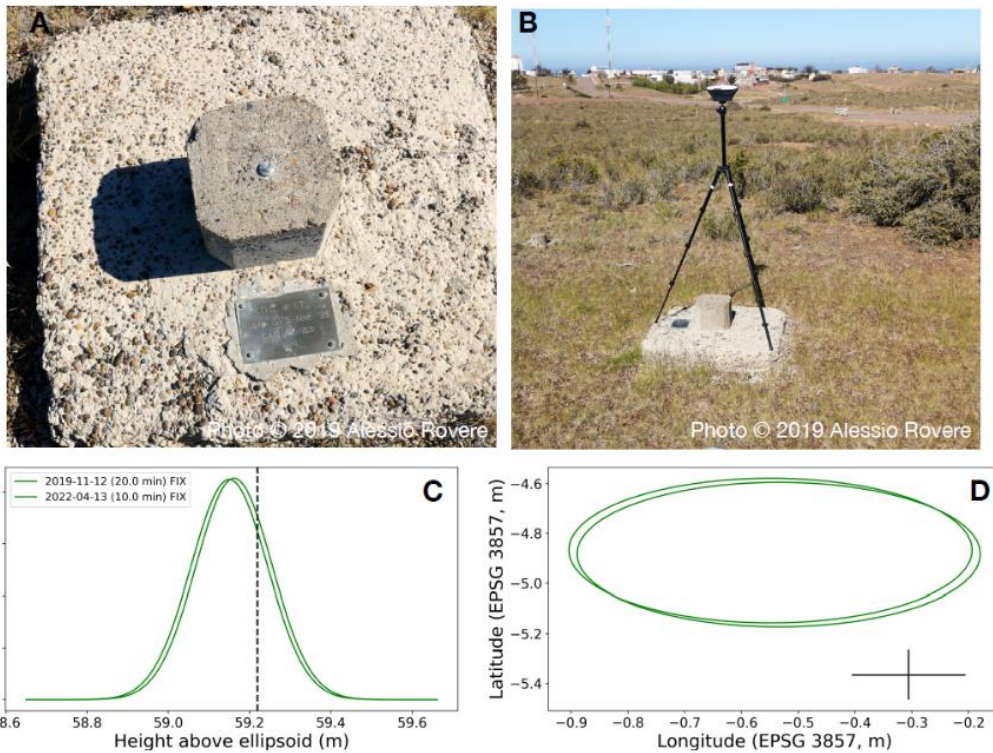
## 5.9. Acknowledgments

TanDEM-X digital elevation data used in Figure 5.3 are under copyright by the German Aerospace Center. All rights reserved; used here with permission within the Project DEM\_GEOL1210. Wave data used in this work were derived from IMOS. Australia's Integrated Marine Observing System (IMOS) is enabled by the National Collaborative Research Infrastructure Strategy (NCRIS). It is operated by a consortium of institutions as an unincorporated joint venture, with the University of Tasmania as Lead Agent.", "Australian Research Council (ARC) Grants: DP130100215 and DP160100738", "CSIRO Oceans and Atmosphere", "The University of Melbourne. Tidal data are extracted from FES2014, a product by NOVELTIS, LEGOS, CLS Space Oceanography Division, and CNES. It is distributed by AVISO, with support from CNES (<http://www.aviso.altimetry.fr/>). The authors acknowledge PALSEA for useful discussions during annual meetings. PALSEA is a working group of the International Union for Quaternary Sciences (INQUA) and Past Global Changes (PAGES), which in turn received support from the Swiss Academy of Sciences and the Chinese Academy of Sciences.

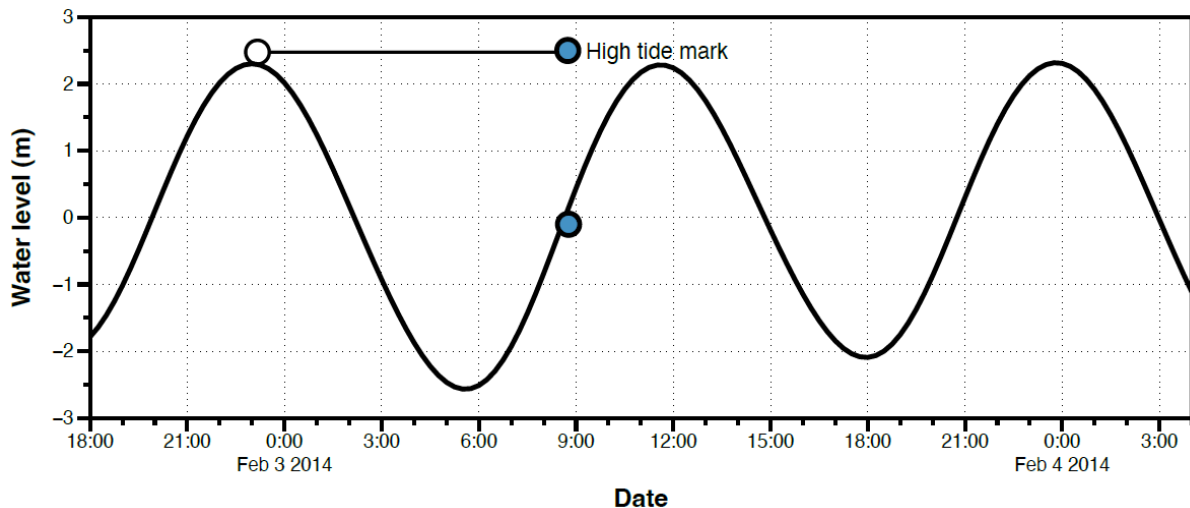
## 5.10. Supplementary material



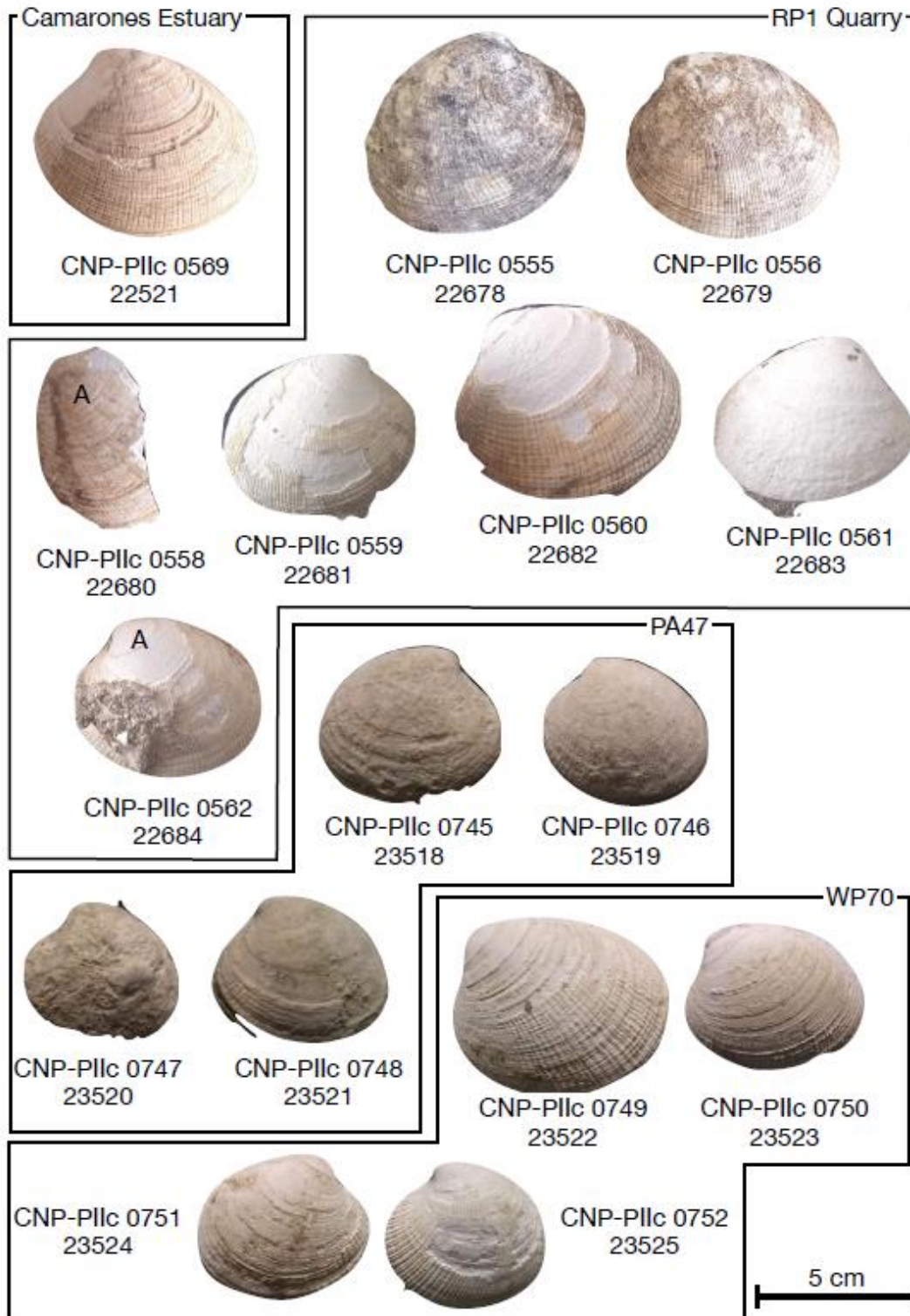
**Supplementary Figure 5.1.** Base station as deployed in A) 2019 and B) 2022. C) Average Northing and Easting of the base position. D) Average height above ellipsoid. The Blue shades in C) and D) represent the probability distribution of the location of each point.



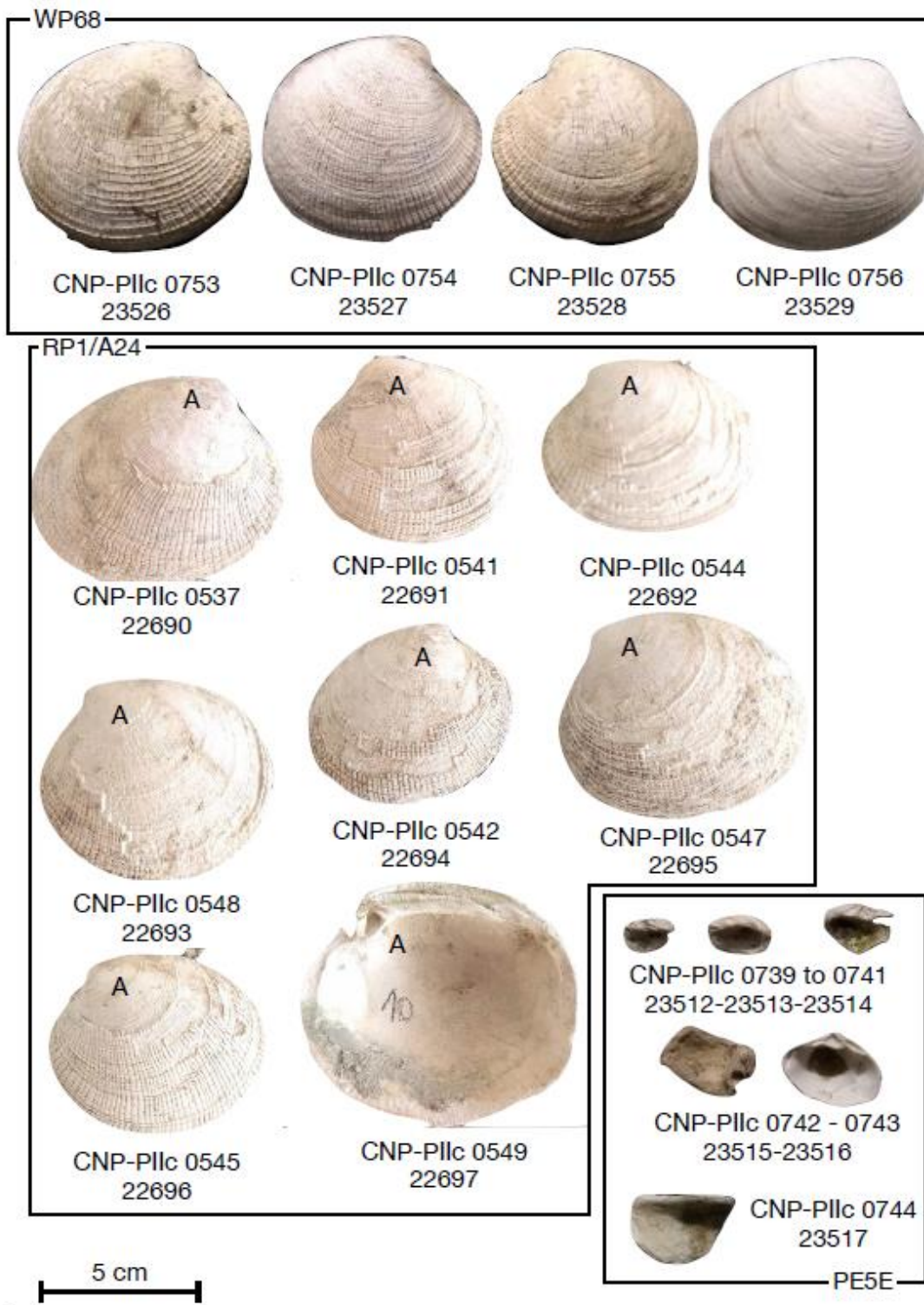
**Supplementary Figure 5.2.** A) detail and B) location of the "GPS N°35" benchmark point (note the town of Camarones on the background of B). C) and D) Comparison between GNSS points and coordinates of the benchmark point "GPS N°35". C) Height above ellipsoid. Dashed black line shows the benchmark elevation; D) Northing and Easting. The black cross represents the benchmark position with 10 cm error bars.



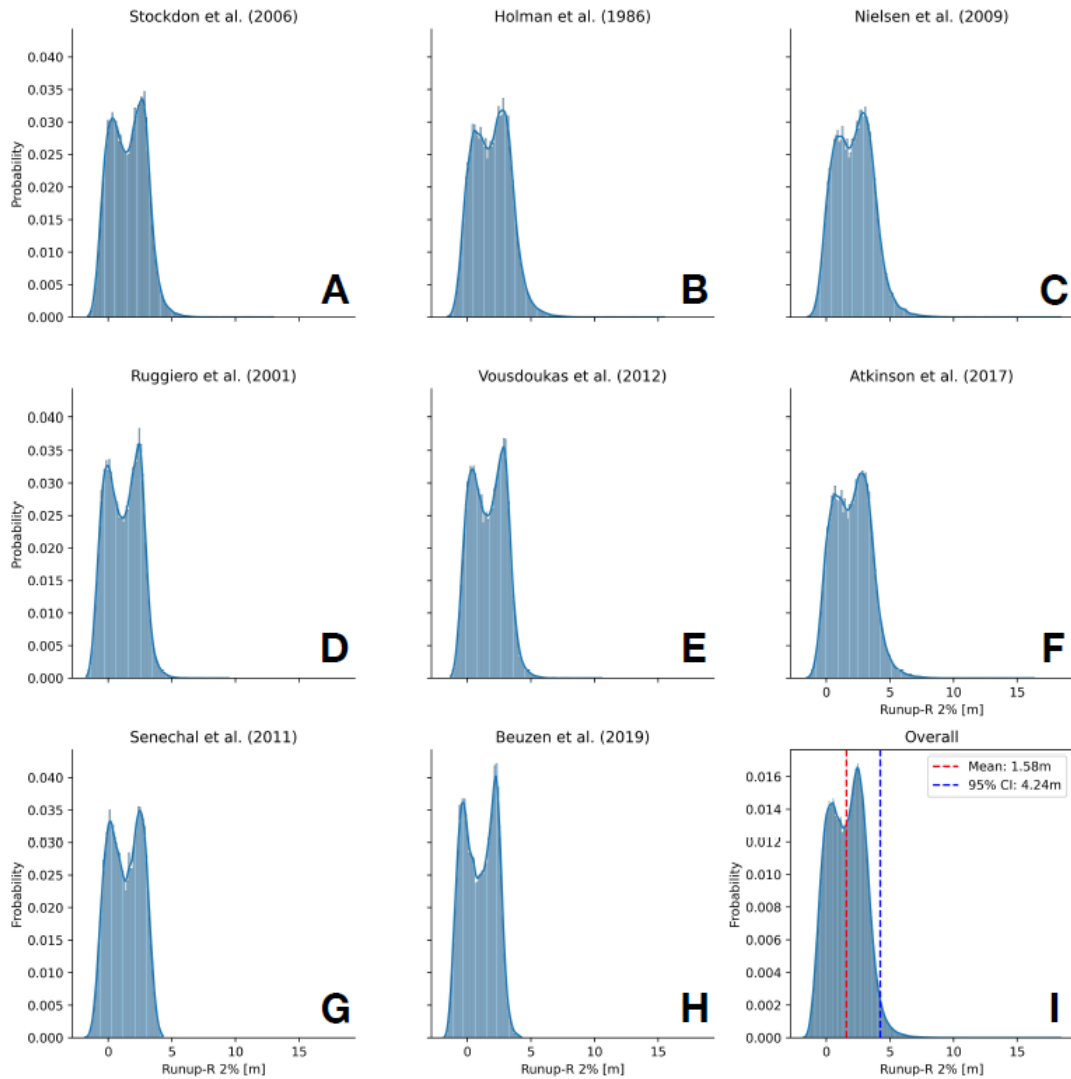
**Supplementary Figure 5.3.** Sea level and high tide mark measured on February 3rd, 2014, referred to the GEOIDEAR 16 and compared with the tidal model output. The high tide mark measured on February 3rd corresponds to the previous high tide, which happened during the night of February 2nd. These data show that the GEOIDEAR 16, in the area of Camarones, relates well to sea level.



**Supplementary Figure 5.4.** Shells selected for AAR analysis from the Camarones Estuary (modern shell), RP1 Quarry, Pa47, and WP70. The labels below each shell describe the unique ID given by the Invertebrate Paleontology and Invertebrate Ichnology Collection (CNP-Pllc; acronyms in Spanish) of the Patagonian Institute of Geology and Palaeontology (upper label) and NAU laboratory number (lower label). The label "A" on some shells indicates that they were part of an articulated pair of valves.

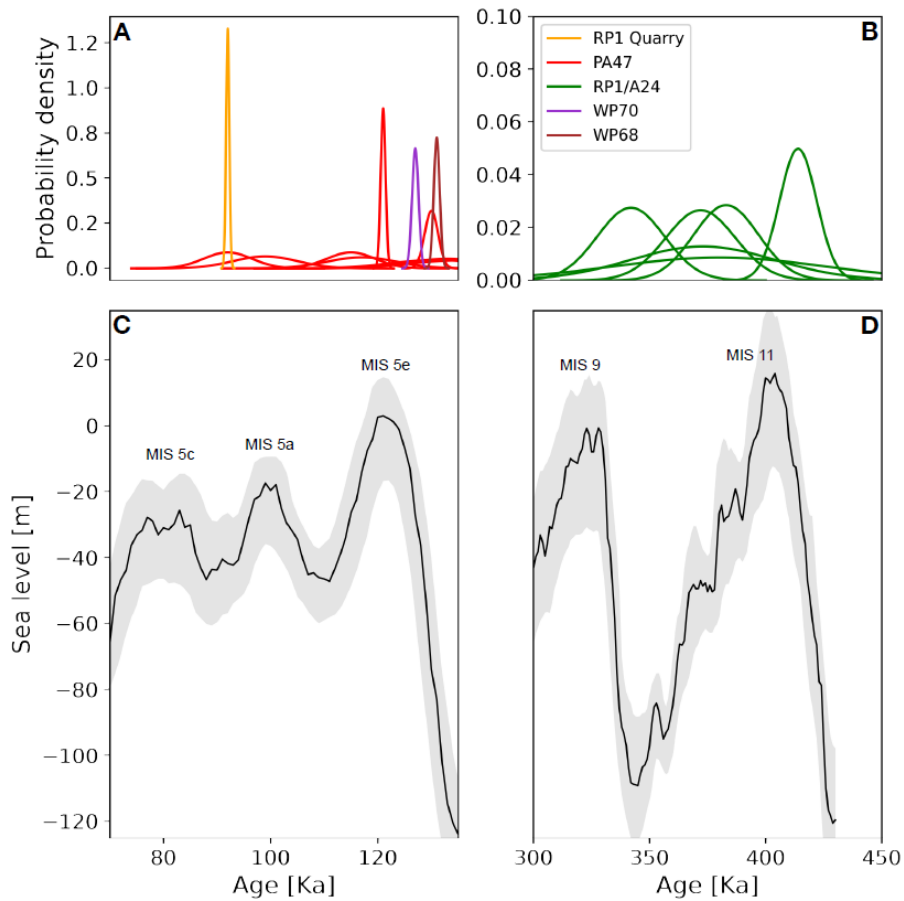


**Supplementary Figure 5.5.** Shells selected for AAR analysis from sites WP68, RP1/A24, and PE5E. The labels below each shell describe the unique ID given by the Invertebrate Paleontology and Invertebrate Ichnology Collection (CNP-Pllc; acronyms in Spanish) of the Patagonian Institute of Geology and Palaeontology (upper label) and NAU laboratory number (lower label). The label "A" on some shells indicates that they were part of an articulated pair of valves.

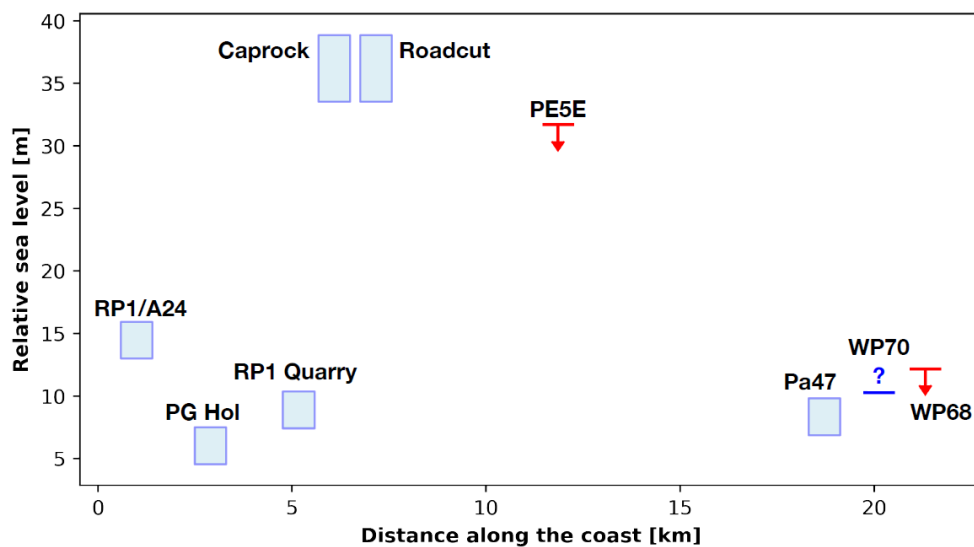


**Supplementary Figure 5.6.** Calculation of the indicative range of beach ridges at Camarones. Each plot shows the probability distribution of 2% exceedance wave runup level plus water level from the FES2014 model calculated at Camarones for different runup models, respectively: A) Stockdon et al. (2006); B) Holman (1986); C) Nielsen (2009); D) Ruggiero et al. (2001); E) Vousdoukas et al. (2012); F) Senechal et al. (2011); G) Beuzen et al. (2019); H) Passarella et al. (2018); I) Overall, including the results shown in A-H).

Quaternary and Pliocene sea-level changes at Camarones, central Patagonia, Argentina

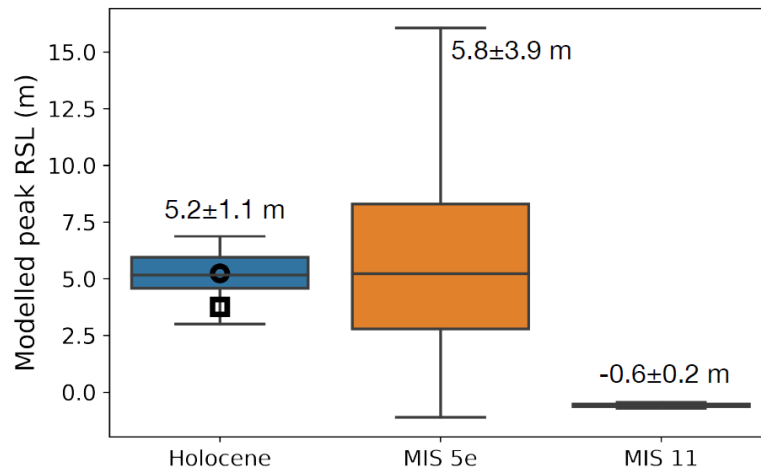


**Supplementary Figure 5.7.** A) and B) Kernel density estimate plots of literature ESR and U-series (Schellmann and Radtke, 2000; Pappalardo et al., 2015) ages at the different Camarones sites, shown in Figure 5.8. C) and D) Late Pleistocene sea level from ocean sediment cores by Spratt and Lisiecki (2016). The gray band represents the upper and lower 95% confidence intervals.



**Supplementary Figure 5.8.** Paleo RSL as indicated by the sites described in this study along the coast of Camarones.

## Quaternary and Pliocene sea-level changes at Camarones, central Patagonia, Argentina



**Supplementary Figure 5.9.** Modelled peak GIA at Camarones for the Holocene (Argus et al., 2014; Peltier et al., 2015; Gowan et al., 2021b), MIS 5e (Dyer et al., 2021) and MIS 11 (Raymo and Mitrovica, 2012). The symbols within the Holocene box plot represent the peak as predicted by Gowan et al. (2021b) (circle) and Argus et al. (2014); Peltier et al. (2015) (square). These are the same models shown in Figure 5.9.

**Supplementary Table 5.1.** Results of the PPP-NRCAN processing of the GNSS base station at Camarones

Date	Duration	Latitude	Latitude 95% sigma (m)	Longitude	Longitude 95% sigma (m)	Height Above Ellipsoid (m)	Height Above Ellipsoid 95% sigma (m)
11.04.2022	6h 53min	-44° 48' 2.10081"	0.207	-65° 42' 21.94914"	0.449	25.723	0.439
11.11.2022	5h 11min	-44° 48' 2.10292"	0.243	-65° 42' 21.95060"	0.445	25.884	0.43
12.04.2022	8h 25min	-44° 48' 2.10137"	0.185	-65° 42' 21.95280"	0.322	25.793	0.377
12.11.2019	14h 02min	-44° 48' 2.10228"	0.119	-65° 42' 21.94935"	0.226	25.754	0.232
12.04.2022	13h 10min	-44° 48' 2.10103"	0.131	-65° 42' 21.95229"	0.281	25.792	0.273
<b>Average</b>	N/A	<b>-44.800583809</b>	<b>0.289</b>	<b>-65.706097450</b>	<b>0.335</b>	<b>25.786</b>	<b>0.187</b>

## 6. Paleoenvironmental implications of Late Quaternary bioerosion traces in central Patagonia (southern Atlantic, Argentina)

L. M. Giachetti, S. Richiano, K. Rubio-Sandoval, C.B. Giachetti, D. D. Ryan; D. S. Kaufman, J. Bright, A. Rovere, D. E. Fernández.

Submitted to the Journal of Quaternary Sciences (2024)

### 6.1. Abstract

Bioerosion is a valuable tool for inferring paleoenvironmental and paleoclimatic changes over time and across different regions. However, studies of bioerosion traces are very scarce in the Southern Hemisphere. The Quaternary marine deposits of Patagonia (Argentina) are unique and they are rich in sand, gravel and shells, the main substrates for bioerosion traces. Most of the Quaternary bioerosion studies in Argentina have been done in San Jorge Gulf and very scarce research was made to the north of the Gulf. Regarding the age of these deposits, discrepancies exist among different authors. Therefore, in this work, bioerosion traces on mollusc shells from Quaternary marine deposits at the Bahía Vera-Cabo Raso sites were studied and amino acid racemization analyses were conducted to determine the age of the beach ridges in the study area. The dating results confirm the presence of beach ridge deposits from MIS 9 or MIS 11, MIS 5 and MIS 1. For the first time, 14 ichnotaxa were recorded in the study area. Additionally, distinct variations in the bioerosion pattern across different ages were observed, suggesting environmental changes during the Quaternary. This study reinforces the hypothesis of the association between bioerosion, productivity, and circulation in the Southern Atlantic Ocean.

### 6.2. Introduction

The Atlantic marine coast of Patagonia is characterised by beach ridge deposits, that are parallel to the modern coast. These were created by transgressive and regressive cycles of sea level that affected this area during the Quaternary. The extent and preservation of these Patagonian deposits is unique and has drawn the attention of many researchers (Feruglio, 1950; Rutter et al., 1989; Schellmann and Radtke, 2000, 2010; Rostami et al., 2000; Aguirre et al., 2006; Bini et al., 2013, 2018; Pedoja et al., 2011; Ponce et al., 2011; Ribolini et al., 2011; Richiano et al. 2015,2017; Pappalardo et al., 2019; Gowan et al., 2021). These deposits are characterised by the presence of a rich fauna assemblage of molluscs with a wide diversity of bioerosion traces (e.g., Aguirre et al., 2006; Farinati et al., 2006; Richiano et al., 2012, 2015, 2017, 2021; Charó et al., 2022). The study of bioerosion traces provides palaeoecological information, that can be used as a proxy for environmental conditions when the organism produced the trace (e.g., Bromley and Asgaard, 1993). Therefore, bioerosion is a valuable tool to infer paleoenvironment and paleoclimate changes geographically and through time. Also, according to Edinger (2002), the intensity of bioerosion in similar hosts and facies from different ages can be used to infer changes in marine productivity through time. Most of the studies of bioerosion traces in high latitudes are focused on the North Hemisphere, while in

the South Hemisphere, such studies are very scarce (Wisshak, 2006; Meyer et al., 2021). Therefore, in this study bioerosion on mollusc shells from Pleistocene, Holocene and Modern deposits will be used to provide a comprehensive evaluation of a palaeoenvironmental and paleoclimatic proxy in the understudied Southern Hemisphere.

In Argentina (Figure 6.1A, South America), the analysis of bioerosion traces from marine Quaternary deposits have increased in recent years (e.g., Richiano et al., 2012, 2015; Charó et al., 2018, 2022). Additionally, some authors have studied the bioerosion pattern through time in other regions and concluded that it responds to changes to the biotic parameters (Richiano et al., 2017). Most ichnological studies are concentrated in the San Jorge Gulf (Figure 6.1A, Richiano et al., 2015, 2017, 2021), which is one of the most productive and diverse regions in the Argentine Sea at present (Dans et al., 2021), and little is known about the deposits located north of the Gulf.

The Bahía Vera-Cabo Raso area is located to the north of Bahía Camarones (San Jorge Gulf, Central Patagonia, Argentina, Figure 6.1B-E). Cabo Raso is a natural harbour that was populated until the 20<sup>th</sup> Century, making it easily accessible today. However, this location remains understudied (Busker et al., 2023). Juan Valentin, a German geologist, was the first researcher to provide a geological description of the locality in the 19<sup>th</sup> Century. Unfortunately, his entire study, including the collected material, was lost (Aceñolaza, 2001). A century later, Feruglio (1950) conducted a detailed study of the Argentinean Coast, with a focus on areas from San Antonio Oeste (Río Negro province) to the mouth of the Deseado River (Santa Cruz province), and included the Bahía Vera-Cabo Raso area in his description of the Quaternary marine terraces along the Patagonian coast. The number of studies in Bahía Vera-Cabo Raso area has increased in the last 20 years, revealing that this remarkable area retains well-preserved deposits spanning in age from the Jurassic through the Quaternary (Lema et al., 2001; Aguirre et al., 2006; Schellmann and Radtke, 2010; Ribolini et al., 2011; Pedoja et al., 2011; Richiano et al., 2015; Busker et al., 2023). These studies are mostly related to geological and palaeontological descriptions, while works related to ichnological content continue to be extremely scarce. For instance, in Bahía Vera (Figure 6.1C-D), there are no records of bioerosion or bioturbation trace fossils in the Quaternary marine deposits, and for Cabo Raso (Figure 6.1C and 1E), only two studies have been made, one on continental Miocene deposits (Busker et al., 2023) and the other on Quaternary marine deposits (Richiano et al., 2015). In this latter work, the authors described the presence of bioerosion traces in *Crepidula* Lamarck, identifying one ichnotaxon. However, it is well-known that these Quaternary marine deposits preserve a more diverse fauna association of molluscs (Feruglio, 1950; Aguirre et al., 2006; Ribolini et al., 2011) and the associated bioerosion traces had not been studied until now.

From a geological standpoint, these areas have been well-studied and also have been subjected to radiocarbon (<sup>14</sup>C) dating (Schellmann and Radtke, 2010; Ribolini et al., 2011). Regarding Bahía Vera (Figure 6.1D), Schellmann and Radtke (2010), based on AMS (Accelerator Mass Spectrometry) <sup>14</sup>C dating, concluded that there are three Holocene beach ridges, spanning in age between 3600 and 1200 <sup>14</sup>C a BP (years before present). In Cabo Raso (Figure 6.1E), Ribolini et al. (2011) determined that the first two beach ridges (the two closest to the modern beach) have an age between 4500 ± 20 and 6500 ± 20 a BP, obtained using radiocarbon dating on mollusc shells. However, *Tegula atra* (Lesson) is found in the second (highest) beach ridge and, according to Aguirre et al. (2013), *T. atra* is a Pleistocene

## Paleoenvironmental implications of Late Quaternary bioerosion traces in central Patagonia (southern Atlantic, Argentina)

biostratigraphical marker for Patagonia. Therefore, in this work, amino acid racemization (AAR) dating is used to clarify the differences between the authors for the age of the beach ridges in the Cabo Raso locality (Ribolini et al., 2011; Pedoja et al., 2011) and Bahía Vera. This method provides relative ages indicated by the clustering of D/L values of amino acids. Also, it was used by previous authors to determine shells of MIS 5 age from earlier interglacial in other Quaternary marine deposits from Argentina (Gowan et al., 2021). It is important to know the correct age of the deposits to evaluate the bioerosion pattern across time.

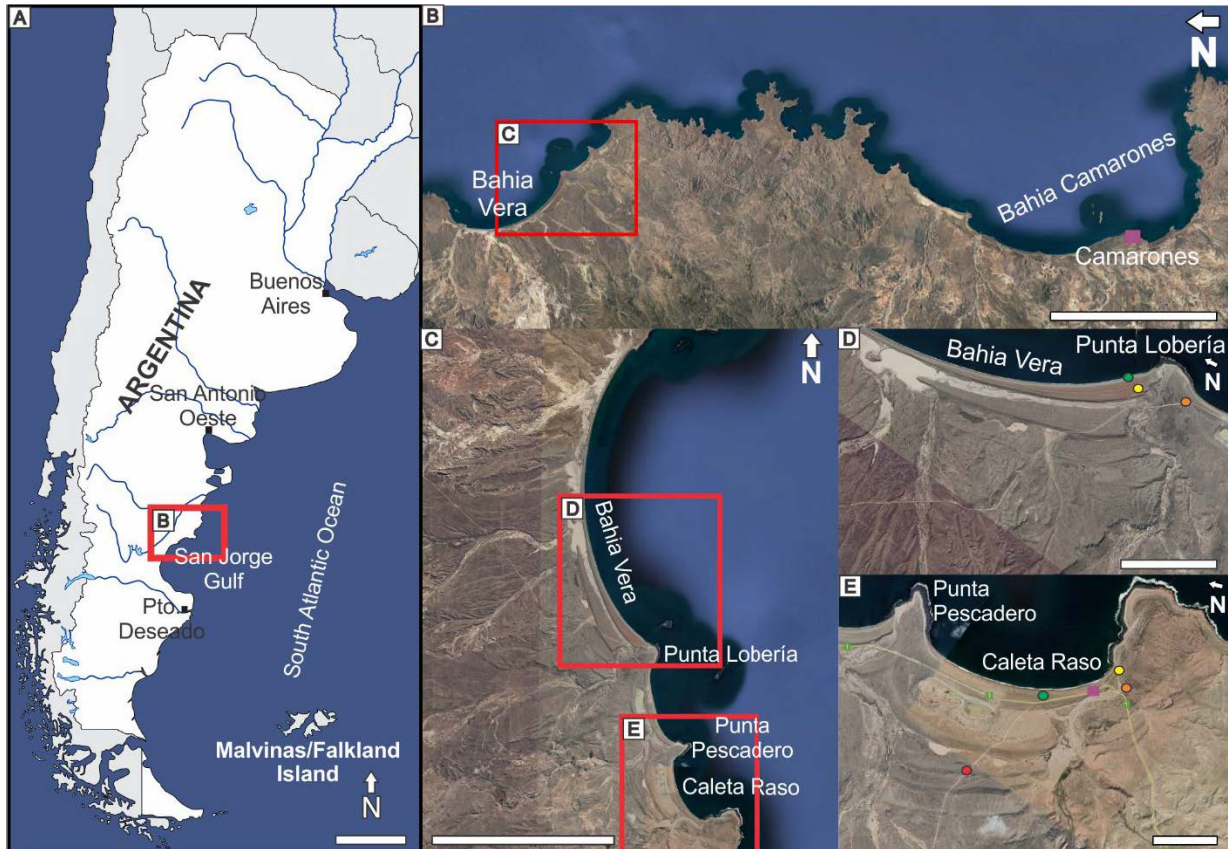


**Figure 6.1.** Location of the study area in Chubut province, Patagonia, Argentina. A. Argentinean map. Red square indicates the geographic position of the study area in Chubut province. Scale bar: 400 km. B. Satellite image of the study area from Bahía Vera to Bahía Camarones (violet square). The red square indicates the geographic position of Bahía Vera-Cabo Raso area. Scale: 20 km. C. Satellite image of Bahía Vera-Cabo Raso area. The red squares indicate the geographical position of the two sites. Scale: 8 km. D. Satellite image of Bahía Vera site. Scale: 2 km. E. Satellite image of Cabo Raso locality (violet square) Scale: 1 km. The circles indicate the geographic position where the samples were collected. Orange circle: Pleistocene (MIS 5e); yellow circle: Holocene (Hol); green circle: Modern (M); red circle: Cabo Raso North Quarry (MIS 9 or 11).

Hence, the aims of this paper are: (1) to characterize the ichnotaxonomic composition recorded in all the diversity of molluscan shells in Bahía Vera and Cabo Raso locality during the Late Quaternary; (2) to compare the bioerosion pattern between those areas; (3) to analyse the potential environmental factors that control the bioerosion pattern during the Late Quaternary in Central Patagonia; and (4) to use the well-proven AAR geochronological method to estimate the age of deposits in the Bahía Vera-Cabo Raso area.

### 6.3. Geological setting

The Bahía Vera-Cabo Raso area (Figure 6.1; reference coordinates: 44°15'4.88" S/ 44°20'30.81" S and 65°13'32.22" W/ 65°18'20.10" W) extends approximately 9 km from north to south and is located on the east coast of the Chubut province (Argentina, Figure 6.1A), approximately 60 km north of Bahía Camarones (Figure 6.1B). Since the description by Feruglio (1950), the geological characterisation of these two places, Bahía Vera and Cabo Raso, has been referred to as one area under the designation "Bahía Vera-Bahía Camarones area" or "Bahía Vera-Cabo Dos Bahías area" (Feruglio, 1950; Aguirre et al., 2006; Pedoja et al., 2011). The generalization of the geological description has posed challenges in segregating information specific to Bahía Vera and Cabo Raso because there are limited works that provide a geological description for each place individually (Schellman and Radtke, 2010; Ribolini et al., 2011).

The marine Quaternary deposits along the Argentinean Coast were divided into five systems based on altitude, associated mollusc fauna and geological age (Feruglio, 1950). Three of these systems belong to the Quaternary: Marine Terrace IV, V (Late Pleistocene), and VI (Holocene). These marine terraces are associated with Marine Isotope Stages (MIS) 11, 9, 7, 5, and 1, reflecting transgressive-regressive cycles from the Pleistocene to the Holocene (Zachos et al., 2001). In his comprehensive work on the geology of Patagonia, Feruglio (1950) divided the study area between Bahía Vera and Cabo Raso into five regions. The first region belongs to Bahía Vera, where the author mentioned the presence of eight vegetation-free ripples parallel to the current coast. The second region, from Bahía Vera to Cabo Raso, was described as having a recent beach ridge covered by vegetation, composed of sand and gravel. Behind this beach ridge, in Punta Lobería (Figure 6.1C-D), there is a marine terrace 15-20 meters above sea level (a.s.l.), composed of sand, gravel and, in some parts, cemented with calcium carbonate. The third region, in Punta Pescadero (Figure 6.1C and 1E), was noted by the author for the presence of mollusc shells, with a diversity similar to the one found in the marine terrace of Bahía Vera. The fourth region, in Caleta Raso (Figure 6.1E), is where Feruglio (1950) described the presence of three beach ridges, from the seaward to the landward: a recent ridge, composed of sand and gravel, 8-11 meters a.s.l., and partially covered by vegetation; an intermediate ridge, separated from the first one by a muddy depression and very similar to the deposits described in Bahía Vera; and a third ridge, 22-24 meters a.s.l., covered by dense vegetation and also separated from the intermediate ridge by a depression. The last region, "*El Faro de Cabo Raso*" (Cabo Raso Lighthouse), is located outside our study area.

In Bahía Vera, these deposits were analysed and described by Schellmann and Radtke (2010). According to them, the area of Bahía Vera has gravel beach ridges that reach a width of 1-4 km and extend over 20 km along the coast. The authors identified four distinctive Pleistocene beach ridge systems with altitudes ranging from 10 to 40 meters a.s.l. and three Holocene beach ridges. From these Holocene ridges, Schellmann and Radtke (2010) conducted AMS <sup>14</sup>C dating on articulated mollusc samples. They described that the oldest beach ridges date back to 3600 <sup>14</sup>C BP and the youngest is from 1200 <sup>14</sup>C BP.

Regarding the Quaternary marine deposits at Cabo Raso, geomorphological, sedimentological and palaeontological studies have been conducted in this location (Aguirre et al., 2006; Pedoja et al., 2011; Ribolini et al., 2011). Pedoja et al. (2011) noted the presence

of four Marine Terraces on Cabo Raso (“TH”, “T1”, “T1’” and “T2”). Based on the altitude of these marine terraces, they concluded that “TH” is from MIS1, “T1” is from MIS5e, and “T2” is from MIS7. However, Ribolini et al. (2011) mentioned that Cabo Raso has six Quaternary beach ridges (Ribolini et al., 2011, Figure 6.1). Using *Aulacomya atra* (Molina) and *Brachidontes purpuratus* (Lamarck) shells from an abandoned quarry in the south of Cabo Raso locality, Ribolini et al. (2011) determined the age of the beach ridges with <sup>14</sup>C dating and concluded that the first and second beach ridges are from the Holocene (6055 ± 20 yr BP, 4500 ± 20 yr BP, respectively). Additionally, this work provided the first complete sedimentological description of the Quaternary deposits from Cabo Raso. According to them, the deposits of these Holocene beach ridges consist of three lithostratigraphic units: “Unit 1” is composed of alternating poorly to moderately sorted sandy and rounded polygenic gravelly layers. It presents horizontal stratification and contains a rich fauna of marine molluscs. Overlying, separated by an erosional contact, is “Unit 2”, which is composed of poorly sorted, matrix-supported, angular, gravelly deposits without fossils. The topmost unit, “Unit 3”, is composed of sorted rounded gravel.

#### 6.4. Paleontological setting

It is well known that the beach ridges from this area present diverse and abundant mollusc shells (Feruglio, 1950; Aguirre et al., 2006, 2019; Ribolini et al., 2011; Richiano et al., 2015). These accumulations of gastropod and bivalve shells are parautochthonous (*sensu* Kidwell, 1986), meaning that the shells were transported a very short distance from their original habitats by the effects of storms (Aguirre et al., 2006; Ribolini et al., 2011). As of now, 22 genera of molluscs have been recorded for the Pleistocene deposits, while 23 genera of molluscs have been recorded for the Holocene. In the modern deposits, 20 genera of molluscs are observed (Aguirre et al., 2006; Ribolini et al., 2011; Aguirre et al., 2019). All the genera of molluscs recorded are benthic euhaline, and most of them live in the intertidal or upper infralittoral zones (Aguirre et al., 2006). These mollusc faunas of all ages are indicative of high-energy conditions and predominantly hard substrates (Aguirre et al., 2006).

Only two previous ichnological studies indicated the presence of trace fossils in the study area (Richiano et al., 2015; Busker et al., 2023) and only one of them analysed bioerosion traces (Richiano et al., 2015). For this area, only the presence of *Finichnus* isp. Taylor et al. (a bioerosion trace produced by cheilostome bryozoans) on *Crepidula* Lamarck shells was mentioned (Richiano et al., 2015). Since then, there have been no other ichnological studies from the Quaternary marine deposits.

#### 6.5. Material and methods

##### 6.5.1. Ichnological analysis

In this study, a total of six bulk samples amounting to a volume of 4000 cm<sup>3</sup>, containing biogenic and sedimentary material from the beach ridges of Cabo Raso and Bahía Vera, were collected: three from the Pleistocene beach ridges (one from Bahía Vera and three from Cabo Raso, Figure 6.2A and 2D) and three from the Holocene beach ridges (two from Bahía Vera

Paleoenvironmental implications of Late Quaternary bioerosion traces in central Patagonia  
(southern Atlantic, Argentina)

and one from Cabo Raso, Figure 6.2B and 6.2E). Following Pedoja et al. (2011), the bulk samples of Cabo Raso belong to the first Pleistocene beach ridge and to the Holocene beach ridge. They were taken from fossiliferous levels in abandoned quarries (Figure 6.3A-D). At Bahía Vera, following Schellmann and Radtke (2010), the bulk samples belong to the first Pleistocene beach ridge and the second Holocene beach ridge. At both Bahía Vera and Cabo Raso, the modern sample material (Figure 6.2C and 2F) was collected within a 1x1 m surface (Figure 6.3E-J). This was repeated three times following a transect from the supratidal to the lower intertidal zone (Figure 6.3E-J). This method allows us to ensure a representative collection of the modern shoreface. Once the material was separated from the sedimentological content through sieves, the shells were washed with water and then, using an ultrasonic cleaner, they were washed with hydrogen peroxide (30% volume). Only macrofauna was taken into account for this study. Later, they were differentiated into taxa. For this study, shells with a spire for gastropods and valves or fragments with preserved dentition for bivalves were recognised as individual shells. Only bioerosion traces produced by macroorganisms were considered and they were identified at the ichnogenic level following recent classification (e.g., Wisshak et al., 2019). Although it is suggested that modern traces should not be formally named after ichnotaxa (Bertling et al., 2006, 2022), in this work, the names were assigned based on the morphological similarity with known ichnotaxa following Dashtgard (2011) and references therein. All these samples are housed in the collection of Paleoinvertebrados e Icnología at the Centro Nacional Patagónico (CCT CONICET-CENPAT), in the Instituto Patagónico de Geología y Paleontología (IPGP, Puerto Madryn, Chubut Province, Argentina).

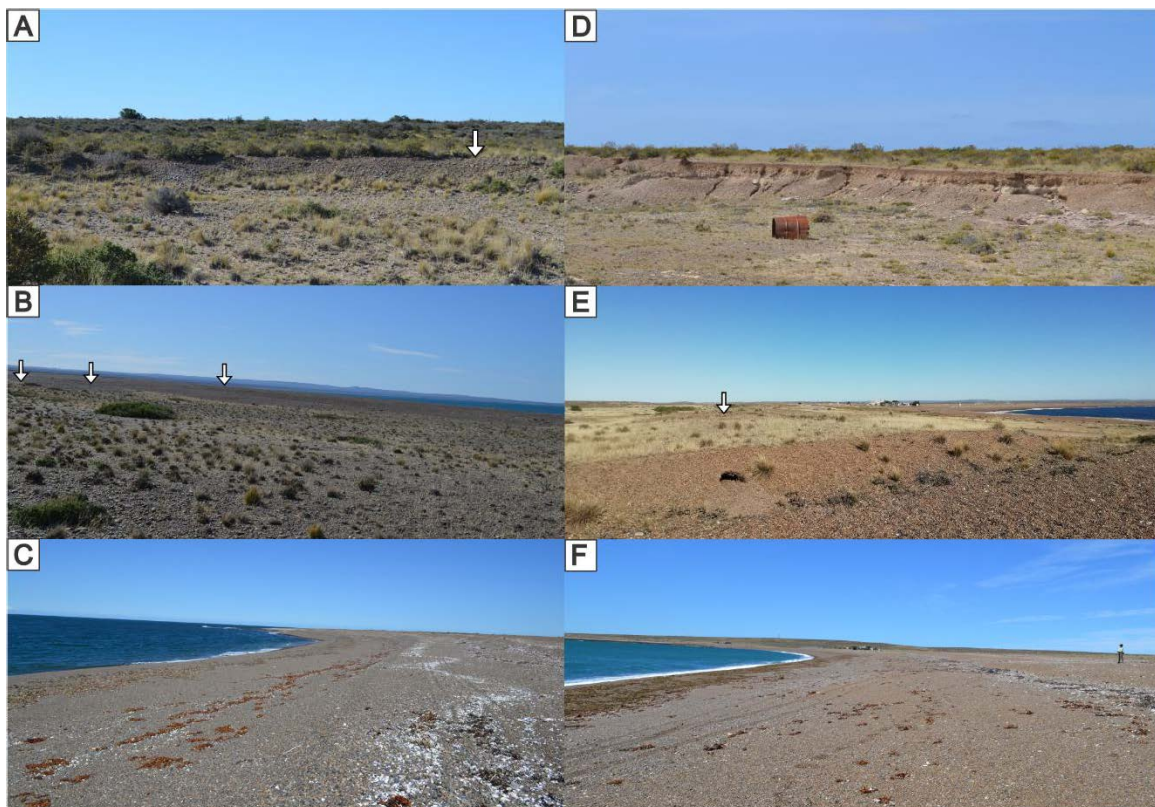


**Figure 6.2.** Panoramic images of the beach ridges deposits in the study area. A. Pleistocene beach ridge deposits from Bahía Vera. B. Holocene beach ridges deposits from Bahía Vera. The black arrow indicates the position of  
Page | 121

## Paleoenvironmental implications of Late Quaternary bioerosion traces in central Patagonia (southern Atlantic, Argentina)

the beach ridges C. Modern coast of Bahía Vera. D. Pleistocene beach ridge deposit in the abandoned quarry from Cabo Raso. E. Holocene beach ridge deposit from Cabo Raso. The black arrow indicates the beach ridge. F. Modern coast of Cabo Raso.

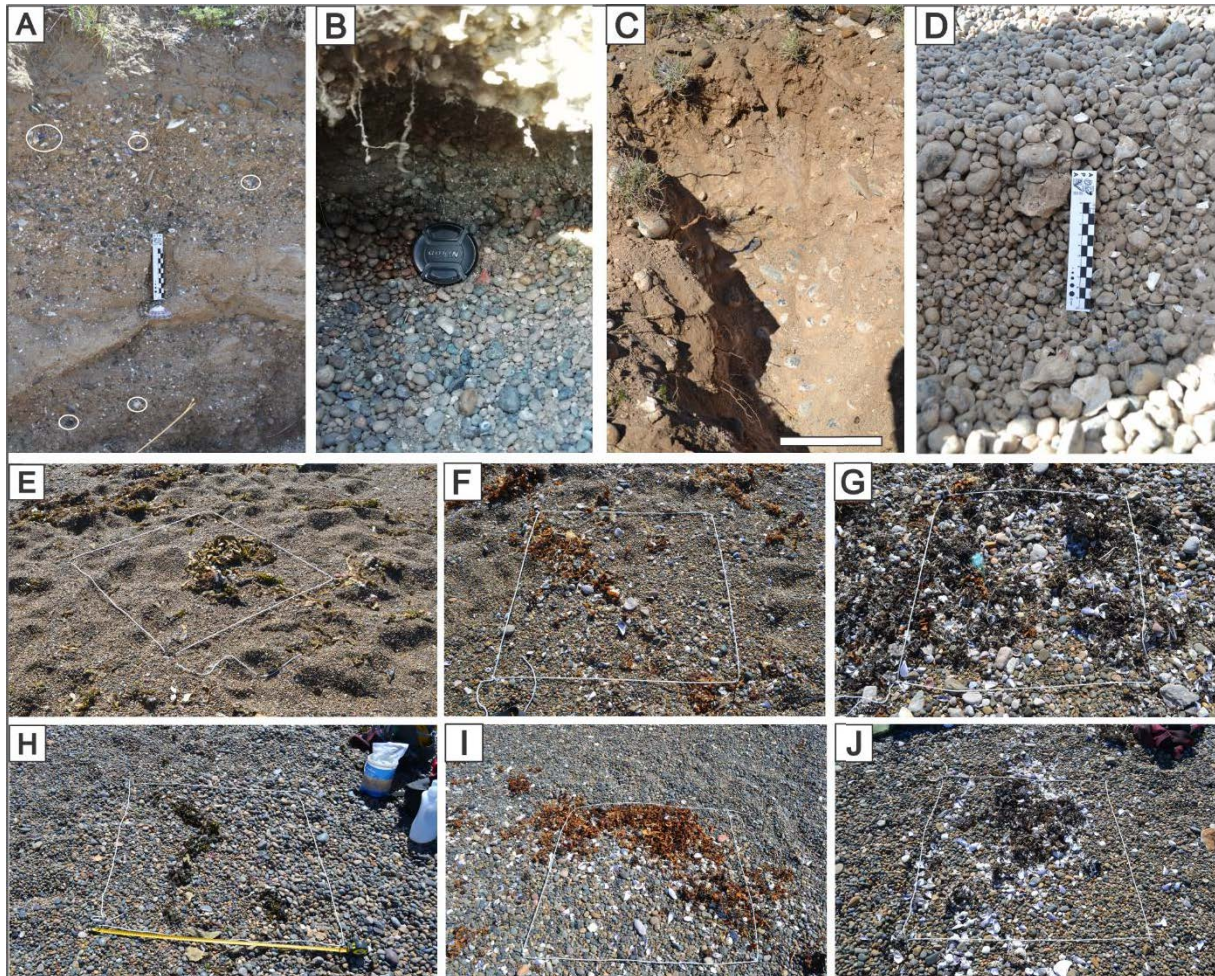


**Figure 6.3.** Images of Quaternary beach ridges deposits from which the mollusc shells were collected. A. Pleistocene beach ridge deposit from Cabo Raso. The white circles indicate the position of *Tegula atra* shells. Scale: 10 cm. B. Holocene beach ridge deposits from Cabo Raso. Lens cover: 33 mm. C. Pleistocene beach ridge deposit from Bahía Vera. Scale bar: 10 cm. D. Holocene beach ridge deposit from Bahía Vera. Scale: 10 cm. E-J. General view of the study section of the modern beach with a detail of the 1x1 m surfaces where the material was collected: E. Lower intertidal zone from Cabo Raso; F. Upper intertidal zone from Cabo Raso; G. Supratidal zone from Cabo Raso; H. Lower intertidal zone from Bahía Vera; I. Upper intertidal zone from Bahía Vera; J. Supratidal zone from Bahía Vera.

### 6.5.1. Amino acid geochronology

Disarticulated valves of *Ameghinomya antiqua* (formerly *Prothotaca antiqua*) were collected from the beach ridge deposits in the Bahía Vera-Cabo Raso area (see Supplementary material Figure 6.1). At the Cabo Raso site (North Quarry), only fragments of shells, tentatively identified as *A. antiqua*, were found. Five shells were chosen from each Pleistocene deposit to date, considering their robust appearance, completeness of valve, abrasion, or dissolution.

The Amino Acid Geochronology Laboratory at Northern Arizona University conducted subsampling of individual valves, sample preparation, and analysis. Shells were subsampled at

the umbo-hinge area and were prepared following the procedures outlined by Kaufman and Manley (1998). The subsamples were analysed using an Agilent 1100 series RP-HPLC (reverse-phase-high-performance liquid chromatography) instrument. Homogenous Pleistocene mollusc powder served as a standard for Interlaboratory comparisons (ILCs; Wehmiller, 2013).

Amino acid racemization (AAR) results underwent data screening to identify and eliminate D/L values that could compromise sample group integrity. Aspartic and glutamic acids D/L values were employed to evaluate amino acid abundance, variance, and relative age. These amino acids were chosen for their high chromatographic resolution and individual characteristics (Goodfriend, 1991). Aspartic acid is abundant in younger fossils, while glutamic acid exhibits stable kinetic behaviour, making it a reliable amino acid for age discrimination in Pleistocene fossils based on racemization extent. Serine was also utilized in data screening, due to its faster decomposition relatively 'high' amounts of serine in Pleistocene samples indicates contamination by modern amino acids (Kosnik and Kaufman, 2008). Using these criteria, all results from Bahía Vera-Cabo Raso area were accepted.

To evaluate the consistency of the chronological attribution, the results were compared with previous AAR data reported on the same shell species in the locality of Bahía Camarones by Rubio-Sandoval et al. (2024), and with previous ESR and U-series dating results from Schellmann and Radtke (2000) and Parappalardo et al. (2015) in the same site.

### 6.5.1. Quantitative and qualitative analysis

In this work, to compare the ichnotaxonomic composition throughout the Quaternary in the area Cabo Raso-Bahía Vera, qualitative and quantitative analyses were conducted. In the qualitative analysis, the material was observed under a binocular stereoscopic microscope (Nikon model C-PS), and the absence/presence of bioerosion traces was recorded and separated according to mollusc taxa and the age of the samples. Following Richiano et al. (2015, 2021), bulk samples from each beach ridge were compared based on the intensity of bioerosion (the number of shells with at least one bioerosion trace divided by the total shells recovered for a particular age). All the material studied was photographed using a digital camera (Nikon D3100) and a digital camera attached to a binocular stereoscopic microscope (Nikon Coolpix S10 VR and Nikon SMZ1000, respectively) at the IPGP-CONICET. A scanning electron microscope (SEM; Zeiss EVO10) from CCT CONICET-CENPAT was also used to measure and photograph relevant details.

Concerning the quantitative analysis, a principal coordinates analysis (PCO) using a Bray Curtis matrix and a cluster analysis of the abundance of ichnotaxa vs sites samples using Ward's method and Euclidean coefficient were performed. The differences among samples were analysed through a non-parametric test, a one-way ANOSIM, for age and sites (Bahía Vera and Cabo Raso) using a Bray-Curtis distance matrix. To analyse the differences in ichnodiversity and richness among ages and localities, a linear model was performed with a normal distribution for Shannon diversity and a generalized linear model with a Poisson distribution for richness (library stats). In both cases, homogeneity of variance was tested through a Levene test. Moreover, in the model with Shannon diversity, normality was tested by a Shapiro-Wilks test; and in the model with richness, dispersion was checked by the analysis

of model residuals. Unfortunately, the Pleistocene deposits in Bahía Vera present a very scarce biogenic content (10 shells in total) and it was not possible to compare with the Pleistocene deposits of Cabo Raso. Therefore, in all the analysis, only the Holocene and Modern ages were taken into account. All the statistical analyses were performed with the software R (R Core Team, 2022), except for the cluster, performed with the paleontological statistics software package program PAST (Hammer et al., 2001).

## 6.6. Results

### 6.6.1. AAR geochronological dating results

To estimate the age of the deposits from the Bahía Vera-Cabo Raso area, we use the AAR technique. To assess the chronological attribution, the results were compared to previous AAR dating on the same shell species (Rubio-Sandoval et al., 2024) and with the available ERS and U-series age (Schellmann and Radtke, 2000; Pappalardo et al., 2015) from Bahía Camarones (60 km south of Bahía Vera-Cabo Raso coastline). Due to the proximity of the sites and the similar mean annual temperature (13 °C in Bahía Camarones and 13 °C in Bahía Vera-Cabo Raso coastal area). The effective diagenetic temperature is expected to be consistent across all sites, and we can dismiss temperature differences as a driver for the distinct grouping. All our analytical findings and dated shells are presented in the Supplementary material and data.

For comparative purposes, Rubio-Sandoval et al. (2024) paired AAR analysis of a disarticulated valve of *A. antiqua* from the modern beach berm of Bahía Camarones locality with radiocarbon, yielding an age of  $698 \pm 137$  cal a BP ( $2\sigma$ ). These results allow for the comparison of Pleistocene D/L values with a more recent fossil.

As shown in Supplementary Figure 6.2, shells sampled from older deposits exhibit much higher D/L ratios of glutamic-aspartic acids than the shells sampled within the Holocene beach ridge. The D/L values of aspartic and glutamic acids form two distinct clusters, indicating at least two different depositional periods. The sites of Bahía Vera (BV, Supplementary Figure 6.2) and Cabo Raso Quarry (CR Quarry, Supplementary Figure 6.2) are clustered within the AAR younger group described in Rubio-Sandoval et al. (2024) comprising the Bahía Camarones sites: WP68, WP70 and RP1. Whereas the older cluster is predominantly formed by shells collected from Cabo Raso North Quarry (CR North Quarry, Supplementary Figure 6.2) and the site RP1/A24. As already noted by Rubio-Sandoval et al. (2024), these groups broadly align with the beach ridge systems dated with ESR and U-series methods reported by earlier authors in the Bahía Camarones area (Schellmann and Radtke, 2000; Pappalardo et al., 2015).

Only two AAR ratios from sites studied in this work (one from Bahía Vera and one from Cabo Raso North Quarry) are split between the groups. However, the geomorphological evidence and former ESR and U-series dating suggest that those single shells were reworked (Supplementary Figure 6.2).

According to the U-series and ESR ages and the interpretations of Rubio-Sandoval et al., (2024), the site of Bahía Vera and Cabo Raso Quarry are clustering within an MIS 5 (possible MIS 5e) group, while Cabo Raso North Quarry belongs to either MIS 9 or MIS 11 (Supplementary Figure 6.2).

## 6.6.2. Ichnological results

For the study area, a total of 778 mollusc shells were analysed, comprising 347 Gastropoda and 431 Bivalvia specimens. From these shells, 15 ichnotaxa were identified (Figure 6.4): *Iramena* isp. Boekschoten, *Maeandropolydora* isp. Voigt, *Oichnus* isp. Bromley, *Podichnus* isp. Bromley and Surlyk, *Finichnus* isp., *Pennatichnus* isp. Mayoral, *Pinaceocladichnus* isp. Mayoral, *Caedichnus* isp. Stafford et al., *Entobia* isp. Bronn, *Caulostrepsis* isp. Clarke, *Stellichnus* isp. Mayoral, *Rogerella* isp. de Saint-Seine, *Radulichnus* isp. Voigt, *Renichnus* isp. Mayoral and *Centrichnus* isp. Bromley and Martinell. However, it is crucial to note that there are differences in bioerosion activity and malacological composition between Cabo Raso and Bahía Vera (Figures 6.5 and 6.6).

Regarding the Cabo Raso North Quarry, only fragments of shells were observed in the bulk samples. These fragments were too small and the proper characters to include in this analysis were not adequate. Therefore, they could not be taken into account in this analysis.

## 6.6.3. Ichnological description

### 6.6.3.1. Bahia Vera

For the first time, a total of 14 ichnogenera were described in this locality, where 57.48% of the 254 mollusc shells recorded are bioeroded. Compared to Cabo Raso, the intensity of bioerosion is lower (Figure 6.5). The most abundant ichnotaxa considering all the samples from this zone are in order of abundance *Iramena* isp., *Renichnus* isp., *Maeandropolydora* isp. and *Finichnus* isp. (Figure 6.6A-C). However, there are differences between the samples over time. For example, *Renichnus* isp. was not documented in the Pleistocene trace fossil association (Figure 6.6A), and the number of ichnotaxa increased in the Holocene samples (Figures 6.6A and 6B, from 4 to 10). Also, the mollusc shells from the Holocene present the highest intensity of bioerosion (74.28%) while those from the Pleistocene show the lowest (40.00%). Regarding the ethological categories, it is very similar to Cabo Raso. Bioerosion traces associated with *Domichnia* class dominated throughout time, and those of *Pascichnia* were only observed in the modern samples. However, at this locality, *Fixichnia* class is higher in all ages reaching a maximum at Pleistocene, when it is equal to *Domichnia*.

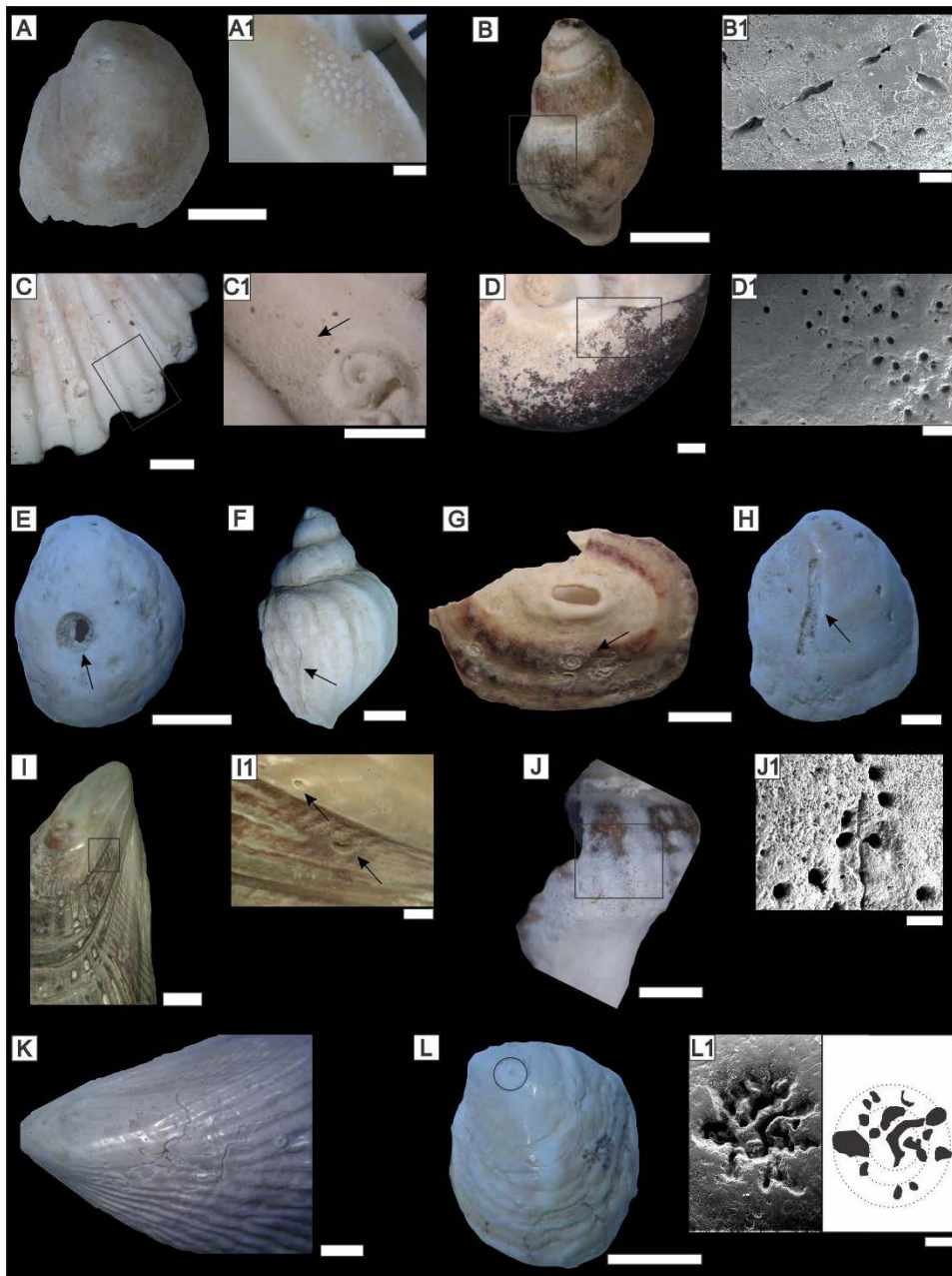


**Figure 6.4.** Examples of the ichnotaxa recorded in the Bahía Vera-Cabo Raso area. A. *Finichnus* isp. in *Crepidula* sp., Holocene from Bahía Vera. Scale bar: 5 mm. A1. Detail of the black square in A. Scale bar: 1 mm; B. *Pinaceocladichnus* isp. in *Buccinanops* sp., Modern from Bahía Vera. Scale bar: 5 mm B1. Detail of the black square in B under SEM. Scale bar: 200  $\mu$ m; C. *Radulichnus* isp. in *Aequipecten tehuelchus*, Modern from Bahía Vera. Scale bar: 5 mm. C1. Detail of the black square in C. Scale bar: 2 mm; D. *Iramena* isp. in *Tegula atra*, Pleistocene from Cabo Raso. Scale bar: 2 mm. D1. Detail of the black square in D under SEM. Scale bar: 400  $\mu$ m; E. *Oichnus* isp. in *Crepidula* sp., Pleistocene from Cabo Raso. Scale bar: 5 mm; F. *Caedichnus* isp. in *Trophon* sp., Holocene from Bahía Vera. Scale bar: 5 mm; G. *Renichnus* isp. in *Fissurella radiosa*, Pleistocene from Cabo Raso. Scale bar: 5 mm; H. *Caulostrepsis* isp. in *Crepidula* sp., Pleistocene from Cabo Raso. Scale bar: 2 mm; I. *Rogerella* isp. in *Aulacomya atra*, Modern from Cabo Raso. Scale bar: 5 mm. I1. Detail of the black square from I. Scale bar: 10 mm; J. *Pennatichnus* isp. in *Trophon* sp., Modern from Bahía Vera. Scale bar: 4 mm. J1. Detail from black square from J under SEM. Scale bar: 200  $\mu$ m. In this sample, it is possible to observe circular borings and circular to drop-shaped boring joined to a fine straight tunnel. The last is *Pennatichnus*, which is dominant in shell; K. *Maeandropolydora* isp., Modern from Cabo Raso. Scale bar: 5 mm; L. *Podichnus* isp. in *Crepidula* sp., Pleistocene from Cabo Raso. Scale bar: 5 mm. L1. Detail of the black square from L under SEM. Scale bar: 30  $\mu$ m.

Paleoenvironmental implications of Late Quaternary bioerosion traces in central Patagonia  
(southern Atlantic, Argentina)

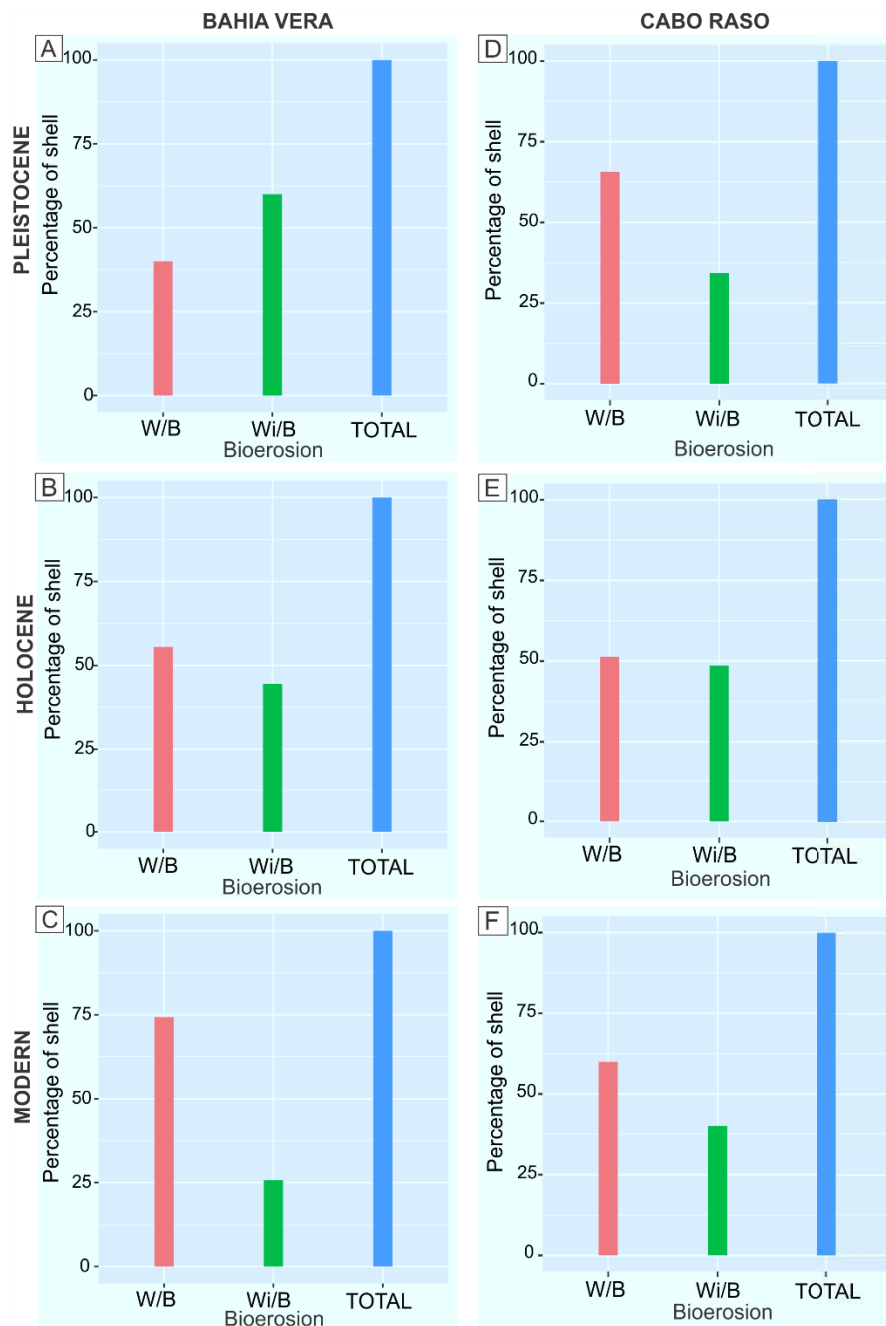


**Figure 6.5. Number of shells versus bioerosion intensity.** Pleistocene, Holocene and Modern samples from Bahía Vera, A-C respectively. Pleistocene, Holocene and Modern samples from Cabo Raso, D-F respectively. Abbreviations: W/B: with bioerosion; Wi/B: without bioerosion; T: total of shells.

### 6.6.3.2. Cabo Raso

In this locality, a total of 14 ichnogenera were recorded in 524 mollusc shells, with 61.96% displaying bioerosion structures. Considering all the mollusc shells from Cabo Raso, the most abundant ichnotaxa were: *Iramena* isp., *Podichnus* isp., *Finichnus* isp., *Maeandropolydora* isp. and *Oichnus* isp. (Figure 6.6D-F). However, *Finichnus* isp. was not recorded in the Holocene bulk samples (Figure 6.6E). This is not the only difference across ages. The highest

Paleoenvironmental implications of Late Quaternary bioerosion traces in central Patagonia  
(southern Atlantic, Argentina)

ichnodiversity was observed in the modern samples (13 ichnotaxa) while the lowest was recorded in the Holocene samples (only 4 ichnotaxa). Considering the intensity of bioerosion, the Pleistocene deposits present higher values (65.71%), while the Holocene present a lower percentage (51.35%). Based on ethological categories, traces belonging to *Domichnia* predominate in all ages. The abundance of traces interpreted as part of the *Fixichnia* class changes over time, being lower in Holocene samples and increasing in modern samples. Finally, traces related to *Pascichnia* class are only present in the modern samples.

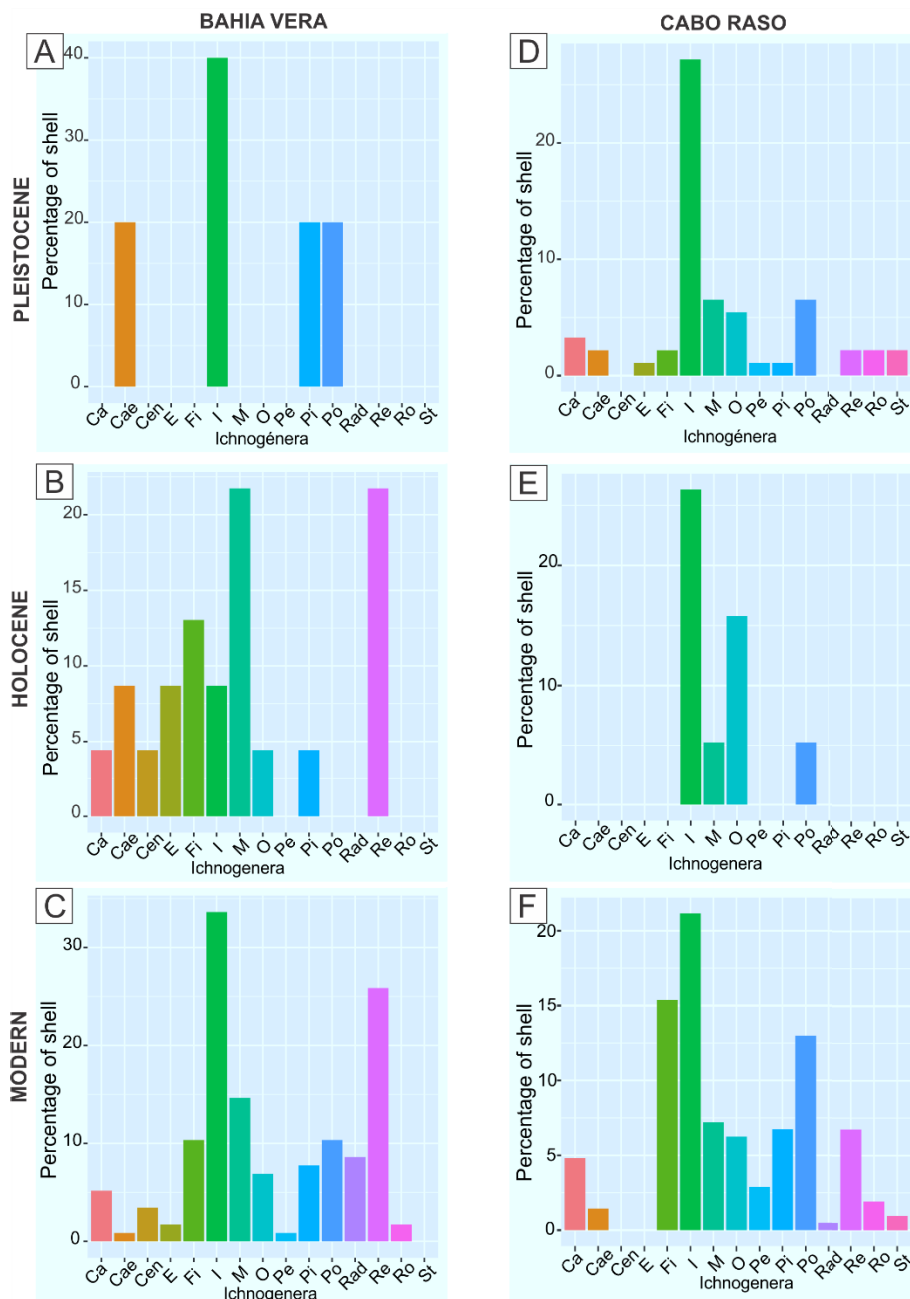


**Figure 6.6.** Number of shells versus ichnotaxa in each age and site. A-C. Pleistocene, Holocene and Modern samples from Bahía Vera, respectively. D-F. Pleistocene, Holocene and Modern samples from Cabo Raso, respectively. Ichnotaxa abbreviations: Ca: *Caulostrepsis*; I: *Iramena*; Fi: *Finichnus*; Pi: *Pinaceocladichnus*; Pe: *Pennatichnus*; Rad: *Radulichnus*; Ro: *Rogerella*; Re: *Renichnus*; O: *Oichnus*; E: *Entobia*; M: *Maendropolydora*; St: *Stellichnus*; Ce: *Centrichnus*; Cae: *Caedichnus*; Po: *Podichnus*.

#### 6.6.4. Malacological results

##### 6.6.4.1. Bahia Vera

A total of 15 genera were identified in all the bulk samples of this zone, with 10 genera belonging to Gastropoda and 5 genera to Bivalvia. The most abundant specimens in the Bahía Vera site included *Nacella deaurata* (Gmelin), *Nacella magellanica* (Gmelin), *Crepidula* sp. Lamark and *Trophon* sp. Montfort for Gastropoda and *Brachidontes* sp., *Aulacomya atra* (Molina), and *Ameghinomya antiqua* (P. P. King) for Bivalvia. Between the samples, the Modern samples exhibited the highest number of mollusc shells and registered the largest number of taxa among all the bulk samples. A total of 11 genera were registered, consisting of 6 genera from Bivalvia and 5 genera from Gastropoda. An important distinction is that, in the Holocene, all the shells identified in this bulk sample belong to Gastropoda. In contrast, in the Pleistocene, only 2 genera of Bivalvia (*Brachidontes* sp. and *Ameghinomya antiqua*) were recorded.

##### 6.6.4.2. Cabo Raso

A total of 17 mollusc genera were identified in the bulk samples from this locality: 11 from Gastropoda and 6 from Bivalvia. Among Gastropoda, *Nacella magellanica* and *Crepidatella dilatata* (Lamark) were the most abundant species across all bulk samples, while *Brachidontes* sp. and *Aulacomya atra* dominated in Bivalvia. The highest taxonomic diversity was observed in the Modern samples, with 16 species in total (4 from Bivalvia and 12 from Gastropoda). *Parvanachis paessleri* (Strebel), *Solariella kempfi* Powell, and *Kellia suborbicularis* (Montagu) were exclusively identified in this sample, each represented by a single specimen. The Holocene bulk sample exhibited the lowest diversity, with 6 species in total (4 from Gastropoda and 2 from Bivalvia).

Other differences were observed among the bulk samples. For example, *Tegula atra*, a modern gastropod from the southeastern Pacific, was only identified in the Pleistocene deposits. The absence of *T. atra* in the Holocene and modern communities in the Atlantic Ocean was studied by Aguirre et al. (2013); they suggested *T. atra* as a Pleistocene biostratigraphical marker for Patagonia. Also, *Scurria ceciliana magellanica* (Strebel), which currently inhabits the intertidal zone (Núñez Cortés and Narosky, 1997), and *Scurria plana* (Philippi) were exclusively identified in the Pleistocene.

#### 6.6.5. Sedimentological description

Beach ridges are narrow, elongated sand, gravel, or shell deposits formed by wave action near high-tide levels on high-tidal beach berm surfaces. They are periodically deposited through shoreline progradation, each representing a certain time interval (Otvos, 2020; Tamura, 2012). As mentioned earlier, according to various authors (Pedoja et al., 2011; Ribolini et al., 2011; Richiano et al., 2017; Schellman and Radtke, 2010), the study area presents parallel beach ridge deposits dating from the Late Quaternary to the present. In both sites, the Pleistocene deposits are very similar (Figures 6.3A and 6.3C). However, there are some differences. The Pleistocene deposits from Cabo Raso (Figure 6.3A) are approximately 90 cm thick and begin

with a sandy matrix-supported medium-grained conglomerate with mollusc shells, followed by a level of fine-grained sandstones to medium-grained conglomerates with occasional mollusc shells. In comparison, the Pleistocene deposits from Bahía Vera (Figure 6.3C) are not as well outcropped as Cabo Raso. This deposit is 30 cm thick and only the unit of sandy matrix-supported conglomerate with scarce mollusc shells is observed.

In the case of Holocene beach ridge deposits in the study area, there are differences between the sites (Figures 6.3B and 6.3D). For Cabo Raso (Figure 6.3B), the exposed Holocene deposits of the beach ridge are characterized by fine to medium-grained sandy-conglomerates with mollusc shells. In contrast, the Bahía Vera beach ridges deposits consist of coarse-grained pebbly deposits without sands and scarce shells (Figure 6.3D).

### 6.6.6. Quantitative analysis description

To analyse the samples from the Quaternary beach ridges from the study area, several quantitative analyses were performed. The ANOSIM test shows that the community did not present differences between ages ( $R = 0.016$ ;  $p = 0.398$ ), or localities ( $R = 0.037$ ;  $p = 0.157$ ). For the ichnodiversity, no differences were observed between ages or locality (LM, Normal distribution,  $p = 0.590$  and  $p = 0.472$ ). Similar results were found for the ichnorichness between ages and locality (GLM, Poisson distribution,  $p = 0.330$  and  $p = 0.373$ , respectively).

The PCO analysis (Figure 6.7), shows that the high richness of ichnogenera is not associated with a particular Class of Mollusca, i.e., any ichnogenera is associated with Bivalvia or Gastropoda samples. Also, according to the PCO, Holocene samples are associated with a lower number of ichnogenera than Modern samples, and could be associated with *Entobia* isp.

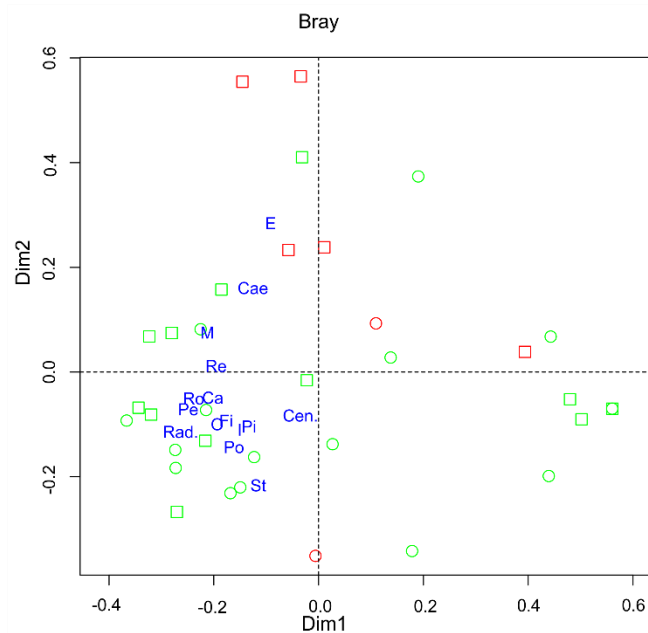


**Figure 6.7.** PCO for ichnogenera (abundance) comparing Holocene and Modern age. Some points might be overlapped. Ichnogenera abbreviations: Ca: *Caulostrepsis*; I: *Iramena*; Fi: *Finichnus*; Pi: *Pinaceocladichnus*; Pe: *Pennatichnus*; Ra: *Radulichnus*; Ro: *Rogerella*; Re: *Renichnus*; O: *Oichnus*; E: *Entobia*; M: *Maeandropolydora*; St: *Stellichnus*; Cen: *Centrichnus*; Cae: *Caedichnus*; Po: *Podichnus*. The green colour indicates modern samples while

## Paleoenvironmental implications of Late Quaternary bioerosion traces in central Patagonia (southern Atlantic, Argentina)

the red colour indicates Holocene samples. The circles indicate bivalve samples while the square indicates gastropod samples.

Finally, the cluster analysis (Figure 6.8) shows information similar to the PCO, but discriminates the samples according to the place of origin (Cabo Raso vs Bahía Vera). The results show a division of two groups: A and B (Figure 6.8). Group A is represented only by modern samples of Bivalvia and Gastropoda from both places and Group B is divided into two sub-groups, B.1 and B.2. Group B.1 is represented only by samples from Bahía Vera from both ages and classes of molluscs while group B.2 is represented mostly by samples from Cabo Raso, mainly Gastropoda and from the two ages. Also, most of the Holocene samples are present in this last sub-group. As samples of both sites are observed in the three groups, it is possible to suggest that the division of these groups is related to the variability of the ichnotaxa. Therefore, a two-way cluster analysis with the same matrix was made to confirm this. The results show that Group A presents a higher variability of ichnotaxa while Group B.1 presents less variability. Group A is represented by modern samples from both places dominated by, in order of abundance, *Iramena* isp., *Finichnus* isp., *Podichnus* isp., *Oichnus* isp., *Renichnus* isp. and *Maeandropolydora* isp.; Group B.1 is represented by samples from both places and both ages are dominated by *Iramena* isp., *Podichnus* isp., *Oichnus* isp. and *Finichnus* isp.; and Group B.2 is represented by samples from Bahía Vera dominated, in order of abundance, by *Iramena* isp., *Maeandropolydora* isp. and *Renichnus* isp.

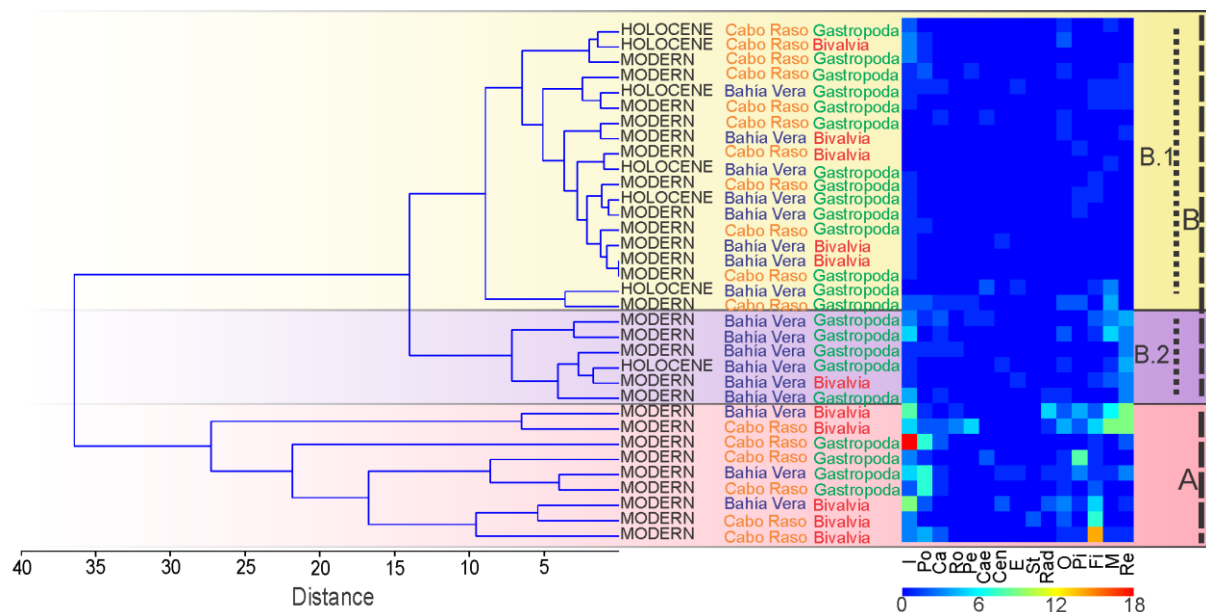


**Figure 6.8.** Cluster Analysis (Ward's method, Euclidean coefficient) based on an abundance matrix of ichnotaxa recorded in gastropod and bivalve shells at Holocene and Modern age from the area of study (Bahía Vera-Cabo Raso). The result shows three groups: A. Group composed by modern samples from both sites and both classes of mollusc. B1. Group composed by modern and Holocene samples from both sites and both classes of mollusc. B2. Group composed by Bahía Vera samples mostly from modern age and both classes of mollusc. Ichnogenera abbreviations: Ca: *Caulostrepsis*; I: *Iramena*; Fi: *Finichnus*; Pi: *Pinaceocladichnus*; Pe: *Pennatichnus*; Rad: *Radulichnus*; Ro: *Rogerella*; Re: *Renichnus*; O: *Oichnus*; E: *Entobia*; M: *Maeandropolydora*; St: *Stellichnus*; Ce: *Centrichnus*; Cae: *Caedichnus*; Po: *Podichnus*.

## 6.7. Discussion

For the first time, 14 ichnogenera were recorded in the study area, increasing the total number of ichnogenera to 15 for the Quaternary deposits in the Bahía Vera-Cabo Raso area. The bioerosion traces recorded were produced by various organisms, including annelids (*Caulostrepsis* isp. and *Maeandropolydora* isp.), brachiopods (*Podichnus* isp.), bryozoans (*Finichnus* isp., *Iramena* isp., *Pennatichnus* isp., *Pinaceocladichnus* isp. and *Stellichnus* isp.), Cirripedia (*Centrichnus* and *Rogerella* isp.), gastropods (*Radulichnus* isp., *Renichnus* isp., *Caedichnus* isp. and *Oichnus* isp.), and sponges (*Entobia* isp.). The bioerosion pattern observed in the Quaternary deposits from the Bahía Vera-Cabo Raso area shows that there is not a great variation between sites (Figures 6.5 and 6.6). This similarity is further supported by the quantitative analysis, as both the PCO analysis (Figure 6.7) and the cluster analysis (Figure 6.8) demonstrate that the sites are not too markedly different. However, some dissimilarities are necessary to address.

### 6.7.1. Geochronological discussion

Concerning the beach ridges deposit from Bahía Vera, as was mentioned earlier, Schellmann and Radtke (2010) described the presence of four distinctive Pleistocene deposits with an elevation between 10 and 40 meters (Schellmann and Radtke, 2010). The authors attempt to date for the first time the beach ridge deposits near the coast using the radiocarbon ( $^{14}\text{C}$ ) technique, giving a Holocene age. Here, the results of the AAR analysis show that the next beach ridge represents a possible MIS 5e age (in Supplementary Figure 6.2) coinciding with previous authors (Schellmann and Radtke, 2010).

At the Cabo Raso site, the AAR analysis indicates that the Cabo Raso North Quarry (red circle in Figure 6.1E) is of MIS 9 or MIS 11 age (in Supplementary Figure 6.2). This result agrees with previous authors who indicate that this deposit is a Pleistocene beach ridge, considering the altitude (Pedoja et al., 2011; Ribolini et al., 2011). Therefore, this work confirms the age of the Cabo Raso North quarry, even if the uncertainties and limitations of the dating techniques make it difficult to disentangle an MIS 11 from a MIS 9 age. Regarding the Cabo Raso Quarry (yellow circle in Figure 6.1E), this deposit was previously dated by Ribolini et al. (2011), which concluded that the deposit presents a Holocene age. Later, Pedoja et al. (2011) concluded that this deposit is from the Pleistocene through a geomorphological methodology. The results obtained with the AAR analysis show that the deposits from the Cabo Raso Quarry present an MIS 5 age, probably an MIS 5e. This is consistent with the presence of *Tegula atra*, a Pleistocene biostratigraphical marker for Patagonia (Aguirre et al., 2013), in the bottom and top of the Cabo Raso Quarry deposit (Figure 6.3A).

Finally, the presence of one reworked shell in the Pleistocene deposits of Bahía Vera and the deposits of Cabo Raso North Quarry might be related to a reworking of the deposits associated with natural or anthropomorphic events. As it is well known, the beach ridges are formed by wave action during transgressive events (Otvos, 2000, 2020) and some authors have suggested that a reoccupation of older deposits during the subsequent high stands allows the reworking of the deposited shells (Rostami et al., 2000; Rubio-Sandoval et al., 2024). Therefore, finding some reworked shells in our deposits is not unexpected. On the other hand, the deposits are related to quarrying activities, which might affect part of the beach ridge

deposits and could explain the presence of reworked shells. However, taking into account the low number of reworked shells in the samples (only one), both events have a low effect on the deposits. Also, as outlined before, the previous geomorphological and chronological evidence of the region (from the Bahía Vera-Cabo Raso area to Bahía Camarones) supports the attribution of the ages in this work (Rostami et al., 2000; Schellmann and Radtke, 2000, 2010; Pappalardo et al., 2015).

### 6.7.2. Sedimentological and malacological discussion

The marine Late Quaternary deposits of the study area represent relict beach ridges parallel to the modern coast. At both localities, Bahía Vera and Cabo Raso, the massive, sandy matrix-supported Pleistocene deposits are interpreted as upper foreshore berms constructed by storm action on the coast (Otvos, 2020). During the Holocene, a similar interpretation can be made for the deposits, but some differences are between the sites. The Bahía Vera deposits consist of clast-supported coarse-grained conglomerates, while Cabo Raso exhibits matrix-supported fine- to medium-grained sandy-conglomerates (Figures 6.3B and 6.3D). This difference in sediment texture could respond to several factors: sediment supply, longshore or wave drift. Of these, sediment supply is probably the less influential, because both sites show small ephemeral streams. On the other hand, the environmental energy conditions related to the coastal shape seem the more influential factor, considering sediment selection, between the two sites. The coastal sectors of Bahía Vera are very different and Caleta Raso (Cabo Raso; Figures 6.1B-E); the former is a small embayment between two peaks, creating a sheltered zone from high-energy waves. In contrast, Bahía Vera is an open coast exposed to Atlantic Ocean waves (Schellman and Radtke, 2010) and, therefore, is more affected by wave action. In the mid-Holocene, occurred a period of maximum warming called the Hypsithermal event (Iriondo, 1998). According to Iriondo (1999), during this event, the Intertropical Convergence zone (ITCZ) shifted 10/11° towards the coast, the South American continental anticyclone disappeared resulting in the Pampean climate moving 500 km southwest into Patagonia and the weakness and surface decrease of the oceanic anticyclones weakened allowing an increase in the energy of marine storms. Similarly, Isla and Espinosa (1995) observed differences in granulometry in Holocene transgression deposits in Buenos Aires province.

The malacofauna associations from these deposits in Bahía Vera and Cabo Raso are very similar and only differ in the Holocene samples. In general, at both sites, *Brachidontes* sp. and *Aulacomya* sp. are the most abundant taxa from Bivalvia and *Nacella magellanica* together with the Calyptraeidae Family for Gastropoda (*Crepidula* sp. and *Crepidatella* sp.). This association is characterised mostly by molluscs from Magellanean and Argentinean Malacological Provinces, which at present live in cold water and in soft and hard substratum (Aguirre et al., 2006). However, in the Holocene deposits from Bahía Vera only gastropod shells were recorded (*Nacella* sp., *Crepidatella dilatata*, *Crepidula* sp. and *Trophon* sp.). Considering that a more energetic beach is interpreted for the Holocene beach ridge deposits from Bahía Vera, this might account for the absence of bivalve shells at this locality during MIS 1. This is consistent with previous authors, which suggested that the Bahía Vera coast was a macro-tidal, high-energy and wave-dominant coast environment during the Holocene (Schellmann and Radtke, 2010).

### 6.7.3. Quaternary bioerosion patterns

The modern bioerosion pattern in both places is dominated by *Iramena* isp., *Finichnus* isp., *Podichnus* isp., *Oichnus* isp., *Renichnus* isp. and *Maeandropolydora* isp. (Figures 6.5C, 6.5F, 6.6C, 6.6F, 6.7 and 6.8). The first three ichnogenera are produced by suspension-feeding organisms, with organic particle capture mechanisms (Mayoral, 1987; Taylor et al., 1999; Bromley and Surlyk, 1973; Richardson, 1981; Hamann and Blanke, 2022). According to Edinger (2002), filter-feeding macroborers tend to grow faster and exhibit greater bioerosion in productive waters. Therefore, it indirectly suggests a higher concentration of organic particles in the water column in the present day. These results agree with oceanographic and biological studies in Patagonia. They align with the biodiversity pattern of modern bryozoans along the Argentine shelf, which is associated with the sea surface temperature (SST) and productivity (Lopez-Gappa, 2000). Previous studies have suggested that the presence of encrustation and boring in the fossil record are useful as an indicator of productivity, as seen with *Renichnus* isp. recorded in our modern samples (Edinger, 2002; Lescinsky et al., 2002). The Patagonian shelf extends from 38°S to 55°S (Matano et al., 2010) and is influenced by the cold Malvinas current, which flows along the Patagonian shelf break and carries cold, fresh and nutrient-rich subantarctic waters (Piola et al., 2010 and references therein). It is well known that the high levels of chlorophyll concentration observed in the Patagonia shelf are associated with the abundant nutrients supplied by the Malvinas current (Figure 6.9; Acha et al., 2004; Romero et al., 2006; Matano et al., 2010; Piola et al., 2010). Also, there is a well-defined Patagonian current generated by the interaction between the Magellan Straits discharge and the Malvinas current to the South of 49°S (Palma et al., 2008; Matano et al., 2010), leading to a localized decrease in the SST correlated with an increase in nutrients (Lopez-Gappa, 2001; Paparazzo et al., 2010).

Paleoenvironmental implications of Late Quaternary bioerosion traces in central Patagonia  
(southern Atlantic, Argentina)

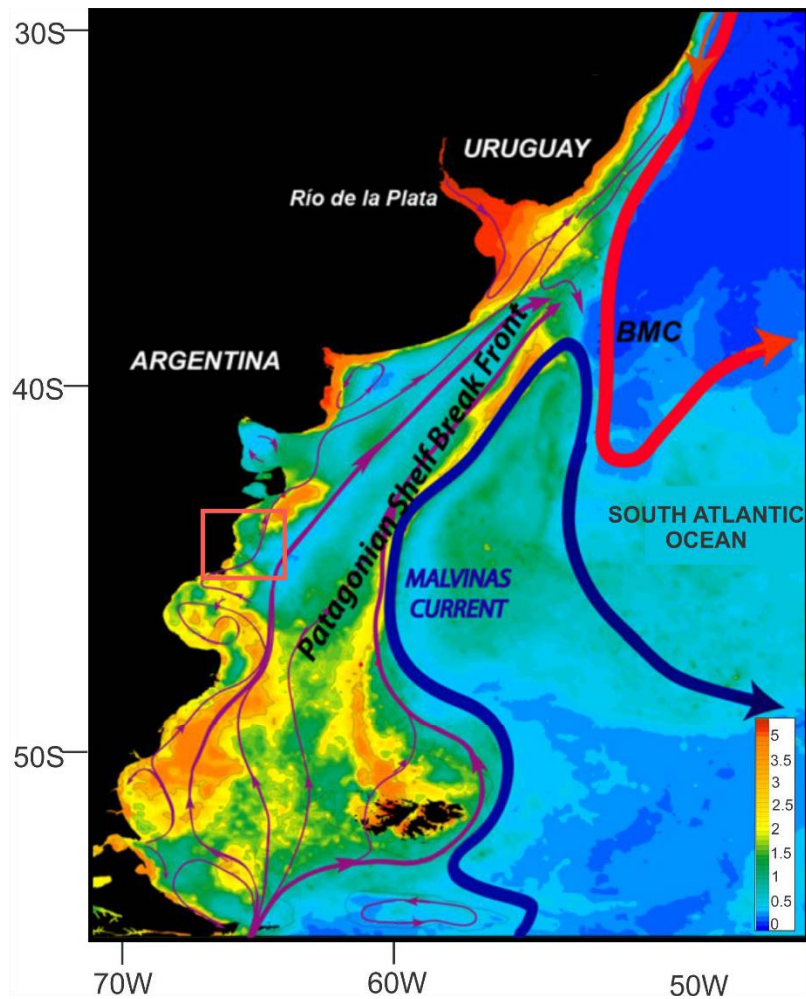


**Figure 6.9.** Schematic maps of South Atlantic Ocean showing the circulation current and the concentration of surface chlorophyll-a (mg m<sup>-3</sup>). The red square indicates the study area (Bahía Vera-Cabo Raso, Chubut province). Abbreviation: BMC: The Brazil-Malvinas Confluences. The image is modified from Franco et al. (2020).

Regarding the bioerosion pattern in the Holocene in the study area Bahía Vera shows a higher intensity of bioerosion (Figures 6.5 and 6.6). The relationship between bioerosion traces and environmental energy has not been extensively studied, but some authors suggest that the higher bioerosion intensity is enhanced by higher water energy in lagoon environments (Abdelhady et al., 2024). As mentioned earlier, Bahía Vera is an open coast affected by wave action. The concentration of gases in the water mass is higher when waves are present and therefore, wave action is considered as a positive factor in oxygenating water bodies (Moutzouris and Daniil, 1995 and references therein). Additionally, wave action leads to a higher suspended sediment concentration (Clark et al., 1982). Therefore, it is plausible that in Bahía Vera, wave action is contributing to a more oxygenated coast with a higher concentration of suspended particles compared to Caleta Raso (Cabo Raso). In figure 6.6B shows that the bioerosion pattern in Bahía Vera presents diversity in the organism producers with the same mechanism of feeding (suspension feeders, Mayoral, 1987; Bromley and D'Alessandro, 1983, 1984; Bromley and Martinell, 1991; Taylor et al., 1999; Taylor et al., 2013; Hamann and Blanke, 2022), bigger than the one observed in the deposits of Cabo Raso (Figure 6.6E). This is alignment with the previously mentioned hypothesis. The active wave action

during the Holocene in Bahía Vera contributes to increased oxygenation and the concentration of particles in the water column.

Moreover, in Figure 6.6, a variation in the abundance of *Pennatichnus* isp. and *Pinnaceocladichnus* isp., trace fossils produced by ctenostome bryozoans (Mayoral, 1988), can be observed across the ages in both places. In recent years, some studies have suggested that the absence of these bioerosion traces, at least in San Jorge Gulf, can serve as a paleoclimatic indicator, potentially indicating warmer waters (Richiano et al., 2017). In the entire study area, these trace fossils are present in the Pleistocene and Modern samples, but they are scarce or absent in the Holocene (Figures 6.6B and 6.6E). Following Richiano et al. (2017), it is possible to suggest that during the Holocene the SST was higher than at present. This agrees with observations from previous studies, which suggest a slightly lower sea-surface temperature and an intensification of the cool Malvinas current after the mid-Holocene climatic optimum (Aguirre et al., 2006, 2013; Schellman and Radtke, 2010; Richiano et al., 2021).

The Pleistocene samples from Cabo Raso are dominated by, in order of abundance, *Iramena* isp., *Maeandropolydora* isp., *Podichnus* isp. and *Oichnus* isp (Figures 6.6D). As described before, the organism producers of these ichnotaxa are bryozoans, annelids, brachiopods and gastropods, respectively (Bromley and Surlyk, 1973; Bromley, 1981; Bromley and D'Alessandro, 1983; Mayoral, 1988; Richardson, 1981; Robinson and Lee, 2018; Wilson, 2007). According to previous studies, bryozoan biodiversity is higher in colder waters with elevated chlorophyll-a concentration (Lopez-Gappa, 2001). Also, the high abundance of *Iramena* isp., *Podichnus* isp. and *Maeandropolydora* isp., with the presence of *Cauloptrepsis* isp., *Finichnus* isp., *Pennatichnus* isp. and *Pinnaceocladichnus* isp. in lower abundances (Figure 6.6D), indicate the presence of filter-feeding organisms (Bromley and Surlyk, 1973; Mayoral, 1988; Robinson and Lee, 2018; Wilson, 2007). Consequently, there is a possibility of a higher concentration of organic particles in the water column. As mentioned before, the Pleistocene deposits in Bahía Vera present a very scarce biogenic content and it is not possible to compare with the Pleistocene deposits of Cabo Raso (Figure 6.5).

The bioerosion pattern observed in the Pleistocene samples for Cabo Raso is very similar to the bioerosion pattern in Modern samples, suggesting comparable environmental conditions for both ages (Figures 6.6D and 6.6F). A comparable outcome was noted in the Quaternary bioerosion pattern from Bahía Camarones (Richiano et al., 2017). The authors concluded that during the Late Pleistocene, there was an active oceanic front similar to the present in the North of San Jorge Gulf reinforcing the idea that bioerosion, productivity and circulation are associated. Therefore, this similarity can suggest that at least Cabo Raso (i.e., Caleta Raso) was affected by an active oceanic front during the Pleistocene such as the present.

#### 6.7.4. Quaternary marine bioerosion pattern along the Patagonian coast

This is not the first instance where the bioerosion-productivity association has been suggested. Previous studies conducted in different countries and localities have reported similar results (Hallock, 1988; Edinger, 2002; Lescinsky et al., 2002; Richiano et al., 2017, 2021). Climate change has profound effects on the ocean environment, leading to alterations in the temperature, acidification, stratification, circulation and oxygenation, among other factors

(Franco et al., 2020 and references therein). In recent years, it has been demonstrated that the mollusc shells (and the associated traces) preserved in the marine Quaternary deposits of Patagonia represent a proxy of paleoenvironmental conditions (Richiano et al., 2015, 2017, 2021). In the case of Patagonia, the bioerosion pattern obtained from the mollusc shells of the Quaternary marine deposits differ between North Patagonia and Central Patagonia. Recent ichnological studies from San Matías Gulf (Río Negro, North Patagonia, Argentina) show that during the Pleistocene the SST was higher than at present (Charó et al., 2017; Giachetti et al., 2022, 2023). However, in Cabo Raso and Bahía Camarones, the Pleistocene and modern bioerosion patterns show that the environment was very similar at present (lower SST with higher nutrient concentration). This difference in the SST between the localities is associated with the changes in the circulation during the Late Quaternary. The southwestern Atlantic shelf is principally influenced by the Brazil- Malvinas currents (Matano et al., 2010) and it is well known that the position of the confluence of these currents changes during the Late Quaternary (e.g., Richiano et al., 2017). This circulation change influences directly on the concentration of nutrients in the water of Patagonia and, therefore, the bioerosion pattern.

Following the ichnological works from San Matías Gulf, during the Pleistocene, North Patagonia presents a warmer water environment than at present because was more influenced by the Brazil warm current (Charó et al., 2021; Giachetti et al., 2022, 2023). However, in this study and following Richiano et al. (2017), the Malvinas current had a higher influence during the Pleistocene in Central and South Patagonia. During the Holocene, the Brazil current was more extensive to the south as a consequence of the Hypsithermal event. This provoked that the influence of the Malvinas current in Central and South Patagonia was lower which is possible to observe in the bioerosion pattern from this age in Bahía Camarones (Richiano et al., 2017). After the mid-Holocene, the Brazil-Malvinas Confluences moved to the north and the influence of the Malvinas currents became stronger in the northern areas and continues at present (Acha et al., 2004; Romero et al., 2006; Matano et al., 2010; Piola et al., 2010). This is possible to observe in the bioerosion pattern at present from the North, Central and South Patagonia (Southern Atlantic Ocean) which shows an increase in the ichnodiversity (Richiano et al., 2017; Charó et al., 2021)

Therefore, this study reinforces the notion that bioerosion traces may offer greater insights than initially anticipated and highlights the importance of sustaining these analyses along coastal areas.

## 6.8. Conclusion

For the first time in marine deposits from the Late Quaternary in the Bahía Vera-Cabo Raso area, 14 ichnotaxa were recorded: *Iramena* isp., *Maeandropolydora* isp., *Caulostrepsis* isp., *Caedichnus* isp., *Podichnus* isp., *Pinaceocladichnus* isp., *Pennatichnus* isp., *Stellichnus* isp., *Radulichnus* isp., *Rogerella* isp., *Centrichnus* isp. and *Entobia* isp. The presence of this ichnotaxa shows that, in addition to the malacofauna previously described by different authors, the marine fauna in the study area during the Late Quaternary included annelids, cheilostome and ctenostome bryozoans, sponges, Cirripedia and brachiopods.

The ARR analysis permits clarifying the age of the Quaternary marine deposits from the entire study area and allows an adequate bioerosion pattern analysis. Hence, in this work,

it was possible to confirm the age of three Pleistocene beach ridge deposits: two from MIS 5 age (Bahía Vera and Cabo Raso Quarry) and one from MIS 9 or MIS 11 (Cabo Raso North Quarry). However, this last deposit only presented small fragments of shell and it was not possible to describe the bioerosion pattern for this age.

The quantitative results presented in this work suggested that the Bahía Vera and Cabo Raso sites can be considered as a single area. However, qualitative analysis shows some differences that might be associated with environmental changes across the Late Quaternary and require further discussion. The beach ridge deposits from the Pleistocene and the modern age from Cabo Raso present a similar bioerosion pattern that indicates similar environmental conditions. This result is consistent with previous analyses in nearby areas (South Patagonia, Bahía Camarones). In this case, the Pleistocene and Modern bioerosion patterns from the area suggest that the active oceanic front, the Patagonia shelf break front, has been present since the Pleistocene.

In the Holocene samples in the entire study area, differences in malacofauna and sedimentology are observed between the sites (Bahía Vera and Cabo Raso). These variations suggest differences in environmental energy, with Bahía Vera exhibiting higher environmental energy than Cabo Raso during the Holocene, associated with the Hypsithermal event. In addition, the bioerosion pattern in Bahía Vera samples is dominated by ichnotaxa produced by suspension feeder organisms suggesting that wave action at this site might increase the oxygenation and the concentration of particles in the water column.

Finally, this study not only reinforces the hypothesis of the association between bioerosion, productivity and circulation in the Southern Atlantic Ocean but also brings new records from bioerosion traces for the South Hemisphere. However, similar studies are necessary in the future to understand the palaeoenvironmental and palaeoclimatic changes across the Quaternary on the Patagonian coast (and in the Southern Atlantic Ocean).

## 6.9. Data availability

All the AAR data described in this paper (license CC-BY4.0) is available at: <https://zenodo.org/records/10828017>

## 6.10. Acknowledgements

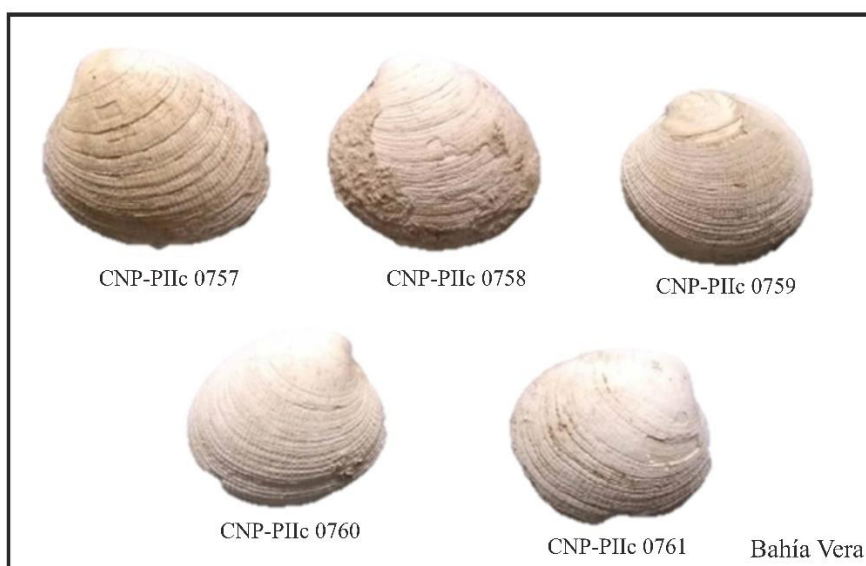
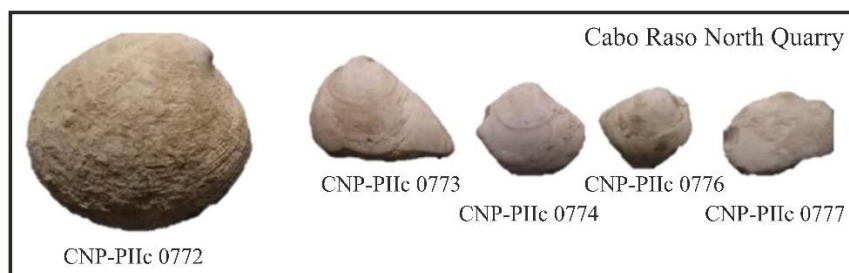
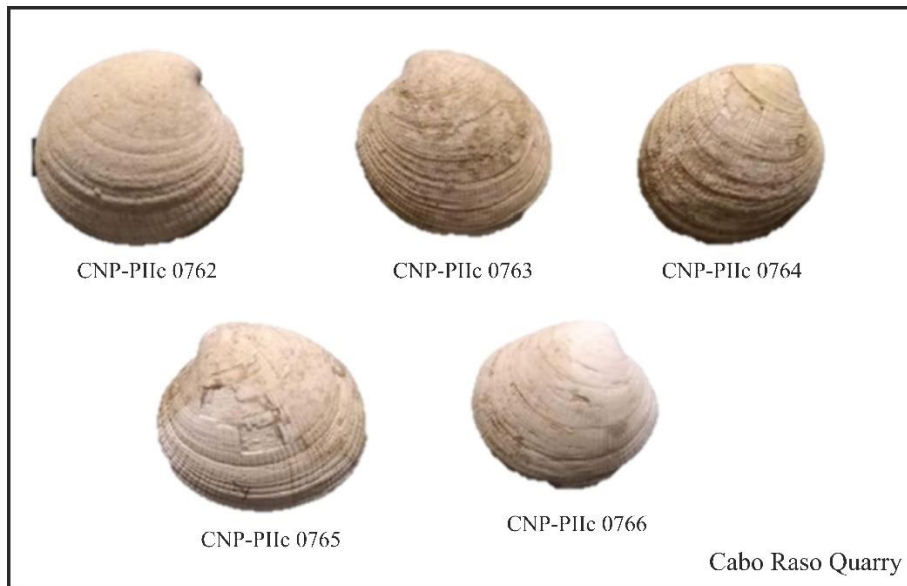
The authors want to thank Dr Felipe Busker and Dr Mariana Viglino (IPGP-CONICET) for their help during the recollection of the samples, Dr. Damián Pérez for his help in the collection of Paleoinvertebrados e Icnología at the Centro Nacional Patagónico and Norberto De Garin for taking the SEM photographs in CCT CONICET CENPAT. This work is part of the first author's Doctoral Thesis at the Universidad de Buenos Aires, Argentina.

This work was supported by grants from Agencia Nacional de Promoción Científica y Tecnológica (PICT 2020A-1763), Universidad Nacional San Juan Bosco (PI 1671) and Proyecto de Unidades Ejecutoras de CONICET PUE-IPGP. LMG was supported by a doctoral fellowship from Consejo Nacional de Investigaciones Científicas y Técnicas (CONICET). The work of KRS,

Paleoenvironmental implications of Late Quaternary bioerosion traces in central Patagonia (southern Atlantic, Argentina)

DDR, and AR is funded by the European Research Council (ERC) under the European Union's Horizon 2020 research and innovation programme (grant agreement no. 802414).

6.11. Supplementary material



Supplementary Figure 6.1. Shells selected for AAR analysis from Bahia Vera-Cabo Raso. The labels below each

## Paleoenvironmental implications of Late Quaternary bioerosion traces in central Patagonia (southern Atlantic, Argentina)

shell describe the unique ID given by the Invertebrate Paleontology and Invertebrate Ichnology Collection (CNP-PIIc; acronyms in Spanish) of the Patagonian Institute of Geology and Palaeontology.

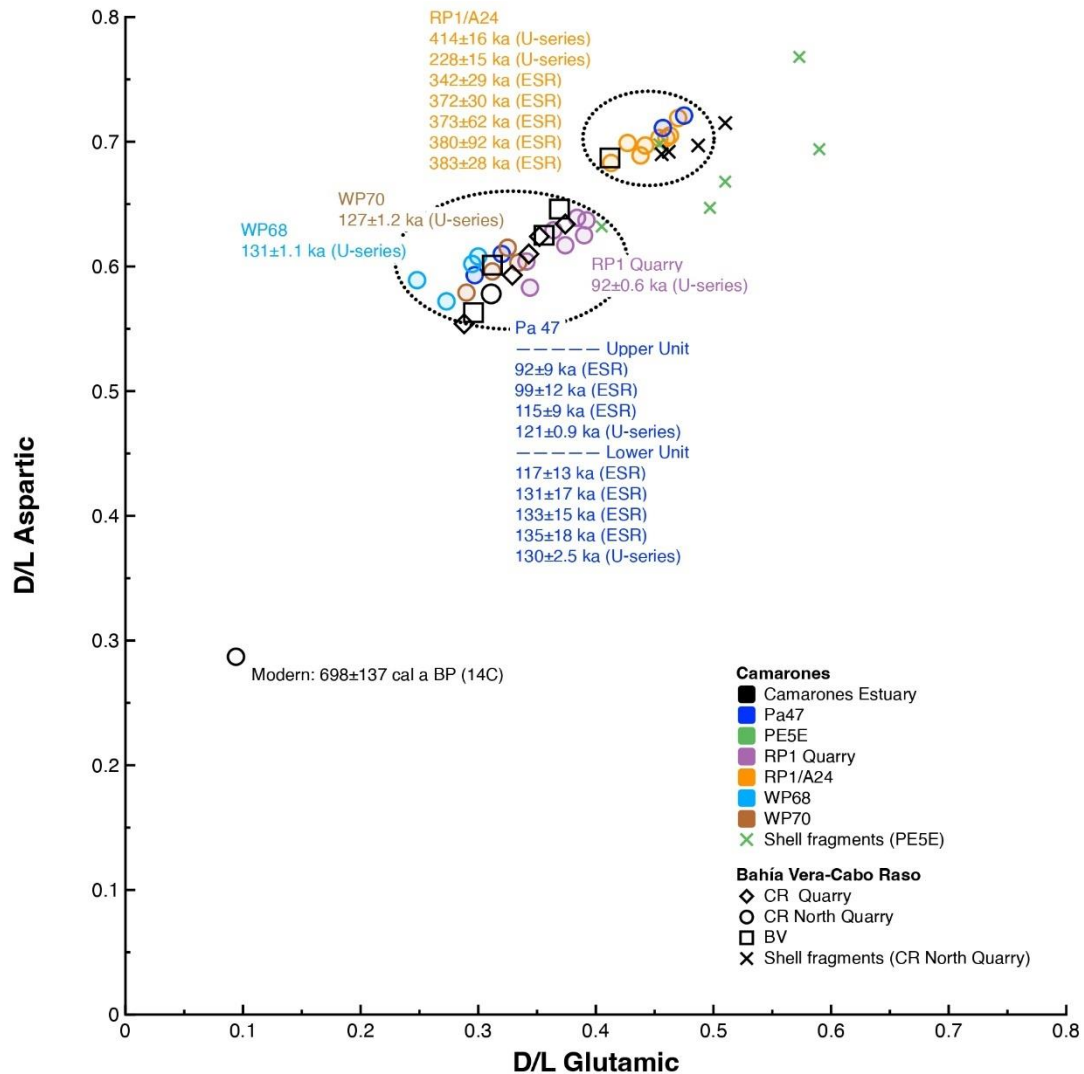


**Figure 6.2.** Results of Amino Acid Racemization (aspartic acid and glutamic acid D/L values) on specimens of *Ameghinomya antiqua* collected from beach ridges in the study area. The unfilled figures correspond to the AAR ratios from the sites described in this study. The filled circles represent the data reported by Rubio-Sandoval et al. (2024) from Bahía Camarones (sites WP68, WP70, RP1 Quarry, RP1/A24). The dotted ellipses identify the two age groups discussed in the main text, and the sounding text reports the results of radiometric dating (ESR and U-Series) on shells from the same beach ridges (age uncertainty assumed as  $2\sigma$  for ESR ages from Schellmann and Radtke, 2000 and  $1\sigma$  as reported by Pappalardo et al., 2015).

## 7. Extended discussion and final remarks

The investigation of paleo-sea levels has a long history, and this has led to the measurement and dating of numerous sites globally. Despite this extensive legacy, there is still limited structured and rigorous analysis of past RSLs, particularly in the southwestern Atlantic (Milne et al., 2005; Angulo et al., 2006; Tomazelli et al., 2006; Schellmann and Radtke, 2010; Pappalardo et al., 2015; Gowan et al., 2021). Through the different chapters of this thesis, we highlight the need for methodologies to improve the study and the report of paleo-sea levels, standardizing the information related to the elevation of the RSL indicators, their indicative meaning, the age attributions, and the analysis of data on post-depositional vertical land movements, following the rigorous protocols outlined in van de Plassche (1986), Hijma et al. (2015), and Shennan (2015). In the introduction, I drafted three research questions that were the core of chapters 3 to 6. In this chapter, I summarize and discuss our findings.

### 7.1 How accurate are Pleistocene and Holocene sea-level data available in the literature for the coasts of the southwestern Atlantic?

In Chapters 3 and 4, we extensively and critically reviewed sea-level published data in a coastal sector from Argentina to Venezuela, including some Caribbean islands. In these studies, reconstructions of past RSL are developed using sea-level indicators, which form in relation to the past position of sea level (Angulo and de Souza, 2014; Rovere et al., 2013, 2015). However, it is outstanding that within the more than 160 papers published in the literature, there is still no standard for reporting the paleo-sea level data and neither for analyzing the RSL indicators. The only study that makes an effort to standardize sea-level data following rigorous protocols in this broad region is the work of Gowan et al. (2021), who standardized data for Last Interglacial sea-level index points published for the Argentinian coastline. Angulo et al. (2006) provide an extensive and valuable review of the Holocene sea-level data of Brazil; however, the previous studies and his review mainly report a paleo-sea level value without a description of the elevation of the sea level indicators, leaving numerous uncertainties associated with these estimates. If any elevation is reported, the description of the method used to calculate it is usually not stated. As described in the previous chapters, the method used to obtain the elevation of an RSL indicator has associated uncertainties that can range from a few centimeters to several meters, so it is crucial to know them (Shennan, 2015; Casella et al., 2022).

It was not until recent years that research employed high-accuracy elevation measurements, and these elevations were even referred to vertical datums. For example, the work of Tomazelli et al. (2006) and Pappalardo et al. (2015) for Pleistocene sea-level reconstructions in Brazil and Argentina, respectively, and the works of Castro et al. (2014), Bini et al. (2018), Angulo et al. (2022a), Angulo et al. (2022b), and Richiano et al. (2022) for the Holocene sea-level reconstructions from Brazil to Argentina. Applying these methodologies to further research will help improve the quality of a significant amount of sea level data, which would allow the refinement of the GIA models and, in turn, improve the estimations of future sea level rise (Milne and Mitrovica, 2008; Horton et al., 2018).

Once the elevation and its associated error are determined, it is important to provide each measured RSL indicator with an estimation of its indicative meaning. The indicative meaning includes the indicative range (IR), which outlines the potential vertical occurrence of the indicator, and the reference water level (RWL), which indicates the distance between the midpoint of the IR and the mean sea level (Lorscheid and Rovere, 2019). However, despite its relevance, the description of the indicative meaning in the paleo-sea level studies of the southwestern Atlantic is limited, and in some cases, its definition for specific indicators is still under debate; for example, the indicative meaning of beach ridges (Pappalardo et al., 2015). Beach ridges form above sea level, between the ordinary berm and the storm wave swash height (Rovere et al., 2016); therefore, paleo tidal range changes may affect the indicative meaning of these indicators. In Chapters 4 and 5, we propose to use satellite-derived wave measurements and wave runup models to calculate the indicative meaning of beach ridges. This method appears to reduce the vertical uncertainties as it relies on local wave and beach topography data (Rubio-Sandoval et al., 2024). Furthermore, in our research comprising Chapters 3 and 4, we propose definitions of the indicative meaning of two fixed biological indicators such as *Ophiomorpha* burrows and vermetids. These indicators are the foundation of the paleo-sea level reconstructions of the Pleistocene and Holocene in Brazil (Barbosa et al., 1986; Tomazelli and Dillenburg, 2007; Angulo et al., 2022c). Considering these definitions in future studies would provide more accurate and standardized paleo RSL estimates.

Finally, the quality of the chronology attribution of the deposits also needs further work. We can summarize that the few sites that have good chronological control within the Last interglacial sea-level reconstructions are the Caribbean islands Bonaire and Curaçao, Brazil, and Argentina (Tomazelli et al., 2006; Felis et al., 2015; Lorscheid et al., 2017; Pappalardo et al., 2015), as there are still many uncertainties surrounding the chronological assignments in the coastal sector from the French Guiana to Venezuela. So far, in these sites, the paleo-sea level reconstructions rely on an age estimation through geomorphological analysis of the deposit sequences or minimum radiocarbon ages (Brinkman and Pons, 1968; Audemard, 1996; Iriondo, 2013). On the other hand, while the use of radiocarbon can improve the chronological quality of Holocene sea-level estimates, places like Argentina represent a challenge because there is not much data to allow the correction of the marine reservoir effect, resulting in unmeasurable age uncertainties (Reimer and Reimer, 2001; Schellmann and Radtke, 2010).

Based on previous evidence, the data quality in the southwestern Atlantic region is generally low except for areas that have been recently re-surveyed, among these Camarones, Río de la Plata, and the eastern coastal sector of Brazil (Tomazelli et al., 2006; Pappalardo et al., 2015; Rovere et al., 2020; Angulo et al., 2022a,b; Richiano et al., 2022). Therefore, this area holds the potential to advance the accuracy of future paleo-sea level reconstructions.

## 7.2 What are the Holocene patterns and rates of RSL changes? Does this data help better constrain the departures from eustasy caused by glacial isostatic adjustment in MIS 5e?

As outlined in Chapter 4, after our standardization of the data, we can conclude that the observed and predicted RSL changes document a rapidly rising rate of sea level with a mean value of 0.80 mm/yr between ~8000 and ~5000 years cal BP, this rise corresponds to the mid-Holocene transgression. RSL rose to about 2 to ~4 m above the present level during this highstand, followed by a subsequent fall to its current position (Angulo et al., 2006; Schellmann and Radtke, 2010; Bracco et al., 2011; Martínez and Rojas, 2013).

Generally, the reconstructed RSL trends are as follows: the northeast coastal sector of Brazil describes a highstand (ca. 5 m a.s.l.) between 8000 to 7000 years cal BP followed by an RSL steep fall towards the present (1.16 mm/yr) (Martin et al., 2003; Angulo et al., 2006; Angulo et al. 2022a). The southeast coastal sector of Brazil suggests a mid-Holocene rising sea level between ~8000 to ~5000 years cal BP at an average rate of 0.96 mm/yr. The RSL reaches its maximum value of ~3 m a.s.l. around 5000 years cal BP. After this highstand, the RSL follows a steady and slow decay (0.26 mm/yr) until its present position (Martin et al., 1985; Suguio et al. 1985; Angulo et al., 2006). From Río de la Plata delta to Tierra del Fuego, the mid-Holocene highstand occurred early in time (from ~8500 to ~6500 years cal BP) and, as expected, is followed by an RSL decay towards the late Holocene. However, the elevation of the highstand and the amplitude of the subsequent sea-level fall differ between all the coastlines, implying a significant non-eustatic component of the RSL (Rostami et al., 2000; Milne et al., 2005; Schellmann and Radtke, 2010; Bracco et al., 2014; Björck et al., 2021).

Despite the prior projections, we emphasize that before generating a unique solution of Holocene RSLs per each coastal sector, it is necessary to address the hiatuses in the geomorphological and chronostratigraphic datasets. Therefore, in its current state, the Holocene sea level data cannot be used to constrain the RSL estimations during the Last Interglacial.

## 7.3 What are the highest possible age and elevation accuracies that can be obtained for MIS 11 and MIS 5e sea-level reconstructions in a coastal site of the southwestern Atlantic?

In Chapters 5 and 6 of this dissertation, we explore the use of new methodologies to address some of the uncertainties identified in the previous chapters. As several authors highlight, Argentina's coastlines are a suitable location for the study of interglacial sea levels since they contain well-preserved geological records of past sea levels from the Pliocene to the Holocene (Schellmann and Radtke, 2010; Pappalardo et al., 2015; Rovere et al., 2020; Gowan et al., 2021). Specifically, the town of Camarones within Patagonian Argentina stands out for its well-preserved beach ridges from the current coastline up to 2 km inland (Pappalardo et al., 2015; Rovere et al., 2020). At this site, we tested the use of GNSS equipment to survey the elevations of the deposits, and we also evaluated the use of AAR to improve their chronological attribution. In Chapter 6, we also tested this dating methodology in the coastal region of Bahia

Vera- Cabo Raso, about 60km north of Camarones, yielding consistent results that support the use of this chronological method to determine the relative age of the deposits.

Our results identified four deposits associated with the Holocene, MIS 5e, MIS 9 or 11, and early Pliocene interglacial periods. Elevations and further paleo RSL calculations had uncertainties of  $1\sigma$  and sea level errors of around 2 m. Therefore, we can conclude that the use of accurate topographic methods to determine the elevation of geological sea-level records leads to more precise estimations of paleo-sea levels. The paleo RSLs (i.e., uncorrected for post-depositional vertical land motions) associated with the four interglacials are  $6\pm 1.5$  m (Holocene),  $8.7\pm 2.1$  m (MIS 5e),  $14.5\pm 1.5$  m (MIS 9 or 11); and  $36.2\pm 2.7$  m (Early Pliocene); in general, these values show smaller estimates than those reported by previous authors where, for example, suggests paleo-sea levels of 8 to 10 m for the Holocene or 10 to 20 m for MIS 5 (Codignotto, 1983; Rostami et al., 2000; Pappalardo et al., 2015). As pointed out in the chapter, once the GIA and DT models are corrected, the global mean sea levels (sea level values corrected for post-depositional effects) can be calculated precisely.

Regarding the chronological attribution, it can be concluded that the use of AAR allows the assessment of the deposit's ages in conjunction with other methodologies (e.g., U/Series and ESR). However, further refinement in all these methods is required to clarify certain uncertainties, for example, to clarify whether an MIS 9 or MIS 11 age is appropriate for the third beach ridge system in the region. To this end, a calibration of the amino acid kinetics in modern shells of *Ameghinomya antiqua* could clarify the chronological queries and allow the calculation of precise ages rather than a relative estimation (Miller et al., 2013).

## 8. Outcome and research horizons

The compilation of our research fills the existing gap of standardized sea-level data for the Atlantic coasts, uniting a post-last glacial maximum (LGM) pole-to-pole transect (Figure 8.1.A); this transect finds a counterpart also on sea-level index points (the past position of sea level in space and time) dating to the Last Interglacial (MIS 5, Figure 8.1.B). Both transects have the potential to assess future projections of sea levels in a warmer world once the remaining uncertainties are solved.

Our broad dataset faces the same data quality issues highlighted by previous authors: a lack of high-precision elevation benchmarked to a tidal datum, a clear description of the indicative meaning of sea-level index points, and, in some areas, a lack of local Delta-R correction to improve radiocarbon dating calibration. Here, we surmise that the only way to solve these issues is with more fieldwork collecting data considering the standard protocols of sea level research.

Despite data quality and uncertainties, sea-level indicators preserved along the southwestern Atlantic describe a trend of a Last Interglacial sea level from 6 to 20 m above sea level (a.s.l.) and a mid-Holocene sea-level highstand of 2 to 4 m a.s.l. with a subsequent fall to its present position. This highstand occurs later in the Holocene and decreases in magnitude, moving towards the North, following the GIA patterns across the large latitudinal gradient covered in this thesis.

By using more accurate methodologies to evaluate the elevation of the geological indicators, their ages, and the precise definition of their indicative meanings, we can improve the prediction of paleo-sea levels during the interglacial periods from the Holocene to the Pliocene. Moreover, with future corrections of the isostatic models, calculations of global mean sea levels will be possible.

Finally, the analysis of bioerosion patterns provides insights into Late Quaternary environmental changes, which can further improve our understanding of past sea-level changes. In our specific case, the bioerosion trace analysis identifies similar environmental conditions between the Pleistocene interglacials and the Holocene, suggesting the possibility of refining our estimates of older paleo-sea levels with the Holocene estimates.

To conclude, our research identifies the southwestern Atlantic as a pivotal region for understanding Earth's climatic and environmental patterns. This knowledge is crucial for unraveling the intricate history of past sea levels, and therefore refining any future sea level rise predictions.

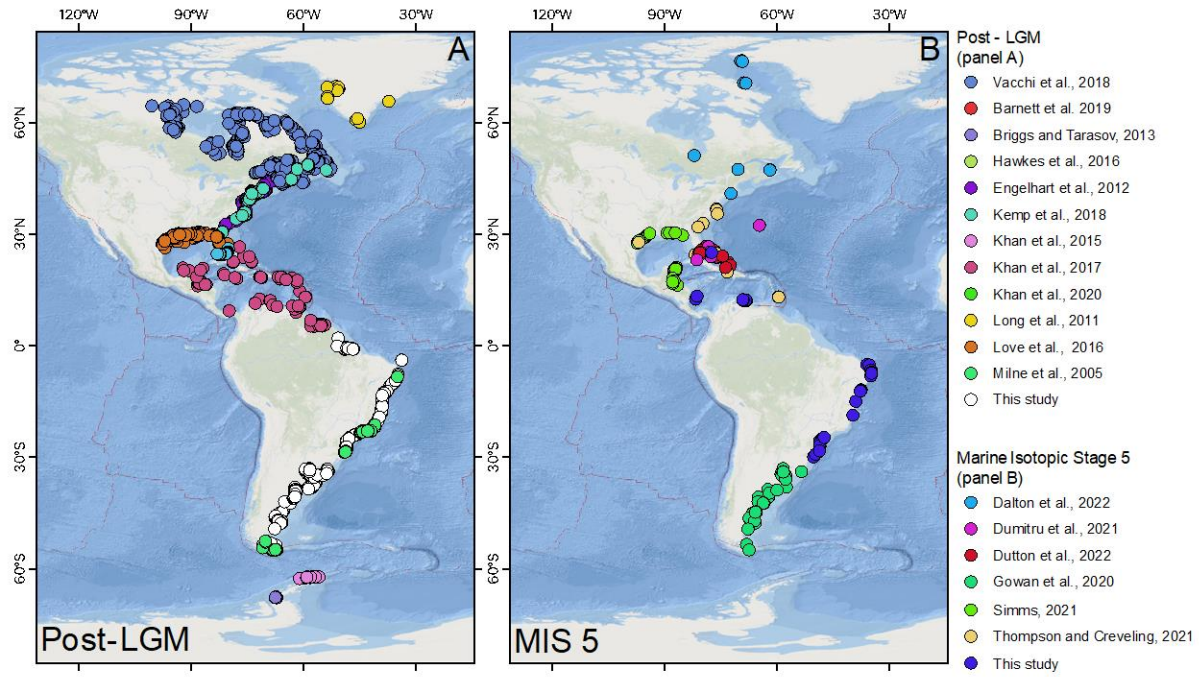


**Figure 8.1.** A) Post-deglacial (12 ka to present) and B) Marine Isotopic Stage 5 (120 to 80 ka) sea-level index points along the Atlantic coasts.

## 9. References

### 9.1. Chapter 1

- Adebisi, N., Balogun, A. L., Min, T. H., Tella, A. 2021. Advances in estimating Sea Level Rise: A review of tide gauge, satellite altimetry, and spatial data science approaches. *Ocean & Coastal Management*, 208, 105632.
- Angulo, R. J., de Souza, M. C. 2014. Conceptual review of Quaternary coastal paleo-sea level indicators from Brazilian coast. *Quaternary and Environmental Geosciences*, 05(2), 1–32.
- Angulo, R.J., de Souza, M.C., da Camara Rosa, M.L.C., Caron, F., Barboza, E.G., Costa, M.B.S.F., Macedo, E., Vital, H., Gomes, M.P., Garcia, K.B.L., 2022. Paleo-sea levels, Late-Holocene evolution, and a new interpretation of the boulders at the Rocas Atoll, southwestern Equatorial Atlantic. *Mar Geol* 447. <https://doi.org/10.1016/j.margeo.2022.106780>
- Angulo, R., Lessa, G., Souza, M. 2006. A critical review of mid- to late-Holocene sea-level fluctuations on the eastern Brazilian coastline. *Quaternary Science Reviews*, 25(5–6), 486–506. <https://doi.org/10.1016/j.quascirev.2005.03.008>
- Audemard, F. A. 1996. Late Quaternary marine deposits of the Paraguana peninsula, state of Falcon, northwestern Venezuela: preliminary geological observations and neotectonic implications, *Quaternary Int.*, 31, 5–11.
- Austermann, J., Mitrovica, J. X., Huybers, P., and Rovere, A. 2017. Detection of a dynamic topography signal in last interglacial sea-level records. *Science Advances*, 3(7):e1700457.
- Baril, A., Garrett, E., Milne, G. A., Gehrels, W. R., Kelley, J. T. 2023. Postglacial relative sea-level changes in the Gulf of Maine, USA: Database compilation, assessment and modelling. *Quaternary Science Reviews*, 306, 108027.
- Barreto, A.M.F., Bezerra, F.H.R., Suguio, K., Tatumi, S.H., Yee, M., Paiva, R.P., Munita, C.S., 2002. Late Pleistocene marine terrace deposits in northeastern Brazil: sea-level change and tectonic implications. *Paleogeography, Paleoclimatology, Paleoecology* 179, 57–69.
- Berger, B., Crucifix, M., Hodell, D. A., Mangili, C., McManus, J. F., Otto-Bliesner, B., Pol, K., Raynaud, D., Skinner, L. C., Tzedakis, P. C., Wolff, E. W., Yin, Q. Z., Abe-Ouchi, A., Barbante, C., Brovkin, V., Cacho, I., Capron, E., Ferretti, P., Ganopolski, A., Vazquez Riveiros, N. 2016. Interglacials of the last 800,000 years. In *Reviews of Geophysics* (Vol. 54, Issue 1, pp. 162–219). Blackwell Publishing Ltd. <https://doi.org/10.1002/2015RG000482>
- Bezerra, F.H.R., Vita-Finzi, C., 2000. How active is a passive margin? Paleoseismicity in northeastern Brazil. *Geology* 591–595.
- Bini, M., Isola, I., Zanchetta, G., Pappalardo, M., Ribolini, A., Ragaini, L., Baroni, C., Boretto, G., Fuck, E., Morigi, C., Salvatore, M.C., Bassi, D., Marzaioli, F., Terrasi, F., 2018. Mid-Holocene relative sea-level changes along Atlantic Patagonia: New data from Camarones, Chubut, Argentina. *Holocene* 28, 56–64. <https://doi.org/10.1177/0959683617714596>

- Bini, M., Isola, I., Zanchetta, G., Pappalardo, M., Ribolini, A., Ragaini, L., Baroni, C., Boretto, G., Fuck, E., Morigi, C., Salvatore, M.C., Bassi, D., Marzaioli, F., Terrasi, F., 2018. Mid-Holocene relative sea-level changes along Atlantic Patagonia: New data from Camarones, Chubut, Argentina. *Holocene* 28, 56–64. <https://doi.org/10.1177/0959683617714596>
- Björck, S., Lambeck, K., Möller, P., Waldmann, N., Bennike, O., Jiang, H., Li, D., Sandgren, P., Nielsen, A. B., Porter, C. T. 2021. Relative sea level changes and glacio-isostatic modelling in the Beagle Channel, Tierra del Fuego, Chile: Glacial and tectonic implications. *Quaternary Science Reviews*, 251. <https://doi.org/10.1016/j.quascirev.2020.106657>
- Castro, J.W.A., Suguio, K., Seoane, J.C.S., Da Cunha, A.M., Dias, F.F. 2014. Sea-level fluctuations and coastal evolution in the state of Rio de Janeiro, southeastern Brazil. *An Acad Bras Cienc* 86, 671–683. <https://doi.org/10.1590/0001-3765201420140007>
- Chen, F., Friedman, S., Gertler, C. G., Looney, J., O’Connell, N., Sierks, K., Mitrovica, J. X. 2014. Refining Estimates of Polar Ice Volumes during the MIS11 Interglacial Using Sea Level Records from South Africa. *Journal of Climate*, 27(23), 8740–8746. <https://doi.org/10.1175/JCLI-D-14-00282.1>
- Cipollini, P., Calafat, F. M., Jevrejeva, S., Melet, A., Prandi, P. 2017. Monitoring Sea Level in the Coastal Zone with Satellite Altimetry and Tide Gauges. In *Surveys in Geophysics* (Vol. 38, Issue 1, pp. 33–57). Springer Netherlands. <https://doi.org/10.1007/s10712-016-9392-0>
- Clark, P. U., He, F., Golledge, N. R., Mitrovica, J. X., Dutton, A., Hoffman, J. S., Dendy, S., 2020. Oceanic forcing of penultimate deglacial and last interglacial sea-level rise. *Nature*, 577(7792), 660–664. <https://doi.org/10.1038/s41586-020-1931-7>
- Codignotto, J. O., Marcomini, S. C., and Santillana, S. N. 1988. Terrazas marinas entre Puerto Deseado y Bahía Bustamante, Santa Cruz, Chubut, *Revista de la Asociación Geológica Argentina*, 43, 43–50.
- Danielo, A. 1976. Formes et dépôts littoraux de la côte septentrionale du Venezuela. *Annales de Géographie*, 85(467), 68–97. <https://doi.org/10.3406/geo.1976.17409>
- Dyer, B., Austermann, J., D’Andrea, W. J., Creel, R. C., Sandstrom, M. R., Cashman, M., Rovere, A., Raymo, M. E. 2021. Sea-level trends across The Bahamas constrain peak last interglacial ice melt. *Proceedings of the National Academy of Sciences*, 118(33), e2026839118.
- Dumitru, O. A., Dyer, B., Austermann, J., Sandstrom, M. R., Goldstein, S. L., D’Andrea, W. J., Cashman, M., Creel, R., Bolge, L., Raymo, M. E. 2023. Last interglacial global mean sea level from high-precision U-series ages of Bahamian fossil coral reefs. *Quaternary Science Reviews*, 318, 108287. <https://doi.org/10.1016/j.quascirev.2023.108287>
- Engelhart SE, Horton BP. 2012. Holocene sea level database for the Atlantic coast of the United States. *Quaternary Science Reviews* 54: 12–25
- Fox-Kemper, B., Hewitt, H., Xiao, C., Aðalgeirsdóttir, G., Drijfhout, S., Edwards, T., Golledge, N., Hemer, M., Kopp, R., Krinner, G., Mix, A., Notz, D., Nowicki, S., Nurhati, I., Ruiz, L.,

- Sallée, J.-B., Slangen, A., Yu, Y. 2023. Ocean, Cryosphere and Sea Level Change. In *Climate Change 2021 – The Physical Science Basis* (pp. 1211–1362). Cambridge University Press. <https://doi.org/10.1017/9781009157896.011>
- Gowan, E. J. 2023. Paleo sea-level indicators and proxies from Greenland in the GAPSLIP database and comparison with modelled sea level from the PaleoMIST ice-sheet reconstruction. *GEUS Bulletin*, 53.
- Hartt, C. F. 1870. *Geology and physical geography of Brazil*. Fields, Osgood & Co.
- Hearty, P. J., Kindler, P., Cheng, H., Edwards, R. L. 1999. A +20 m middle Pleistocene sea-level highstand (Bermuda and the Bahamas) due to partial collapse of Antarctic ice. *Geology*, 27(4), 375. [https://doi.org/10.1130/0091-7613\(1999\)027<0375:AMMPSL>2.3.CO;2](https://doi.org/10.1130/0091-7613(1999)027<0375:AMMPSL>2.3.CO;2)
- Hijma, M. P., Engelhart, S. E., Törnqvist, T. E., Horton, B. P., Hu, P., Hill, D. F. 2015. A protocol for a geological sea-level database. In *Handbook of Sea-Level Research* (pp. 536–553). Wiley. <https://doi.org/10.1002/9781118452547.ch34>
- Holgate, S. J., Matthews, A., Woodworth, P. L., Rickards, L. J., Tamisiea, M. E., Bradshaw, E., Foden, P. R., Gordon, K. M., Jevrejeva, S., Pugh, J. 2012. New Data Systems and Products at the Permanent Service for Mean Sea Level. *Journal of Coastal Research*, 29(3), 493. <https://doi.org/10.2112/JCOASTRES-D-12-00175.1>
- Hollyday, A., Austermann, J., Lloyd, A., Hoggard, M., Richards, F., and Rovere, A. 2023. A Revised Estimate of Early Pliocene Global Mean Sea Level Using Geodynamic Models of the Patagonian Slab Window. *Geochemistry, Geophysics, Geosystems*, 24(2): e2022GC010648.
- Horton, B. P., Engelhart, S. E., Hill, D. F., Kemp, A. C., Nikitina, D., Miller, K. G., Peltier, W. R. 2013. Influence of tidal-range change and sediment compaction on Holocene relative sea-level change in New Jersey, USA. *Journal of Quaternary Science*, 28(4), 403-411.
- Horton, B. P., Kopp, R. E., Garner, A. J., Hay, C. C., Khan, N. S., Roy, K., Shaw, T. A. 2018. Mapping Sea-Level Change in Time, Space, and Probability. *The Annual Review of Environment and Resources*, 43, 418–521.
- Isla, F.I., Angulo, R.J., 2016. Tectonic Processes along the South America Coastline Derived from Quaternary Marine Terraces. *J Coast Res* 32, 840–852. <https://doi.org/10.2112/JCOASTRES-D-14-00178.1>
- Khan, N.S., Ashe, E., Horton, B.P., Dutton, A., Kopp, R.E., Brocard, G., Engelhart, S.E., Hill, D.F., Peltier, W.R., Vane, C.H., Scatena, F.N., 2017. Drivers of Holocene sea-level change in the Caribbean. *Quat Sci Rev*. <https://doi.org/10.1016/j.quascirev.2016.08.032>
- Khan, N. S., Ashe, E., Shaw, T. A., Vacchi, M., Walker, J., Peltier, W. R., Kopp, R. E., Horton, B. P. 2015. Holocene Relative Sea-Level Changes from Near-, Intermediate-, and Far-Field Locations. *Curr Clim Change Rep*, 1, 247–262.

- Khan, N. S., Horton, B. P., Engelhart, S., Rovere, A., Vacchi, M., Ashe, E. L., Törnqvist, T. E., Dutton, A., Hijma, M. P., Shennan, I. 2019. Inception of a global atlas of sea levels since the Last Glacial Maximum. *Quaternary Science Reviews*, 220, 359–371. <https://doi.org/10.1016/j.quascirev.2019.07.016>
- Martínez, S., Rojas, A., 2013. Relative sea level during the Holocene in Uruguay. *Palaeogeogr Palaeoclimatol Palaeoecol* 374, 123–131. <https://doi.org/10.1016/j.palaeo.2013.01.010>
- Milne, G. A., Mitrovica, J. X. 2008. Searching for eustasy in deglacial sea-level histories. *Quaternary Science Reviews*, 27(25-26), 2292-2302.
- Milne, G.A., Long, A.J., Bassett, S.E., 2005. Modelling Holocene relative sea-level observations from the Caribbean and South America. *Quat Sci Rev* 24, 1183–1202. <https://doi.org/10.1016/j.quascirev.2004.10.005>
- Pappalardo, M., Aguirre, M., Bini, M., Consoloni, I., Fucks, E., Hellstrom, J., Isola, I., Ribolini, A., Zanchetta, G. 2015. Coastal landscape evolution and sea-level change: A case study from Central Patagonia (Argentina). In *Zeitschrift fur Geomorphologie* (Vol. 59, Issue 2, pp. 145–172). Schweizerbart Science Publishers. <https://doi.org/10.1127/0372-8854/2014/0142>
- Peltier, W.R., Argus, D.F., Drummond, R., 2015. Space geodesy constrains ice age terminal deglaciation: The global ICE-6G\_C (VM5a) model. *Journal of Geophysical Research: Solid Earth* 120, 450-487
- Raymo, M. E., Mitrovica, J. X. 2012. Collapse of polar ice sheets during the stage 11 interglacial. *Nature*, 483(7390), 453–456. <https://doi.org/10.1038/nature10891>
- Raymo, M. E., Mitrovica, J. X., O’Leary, M. J., DeConto, R. M., Hearty, P. J. 2011. Departures from eustasy in Pliocene sea-level records. *Nature Geoscience*, 4(5), 328–332. <https://doi.org/10.1038/ngeo1118>
- Reimer, P.J., Reimer, R.W., 2001. A marine reservoir correction database and On-line interface.
- Richiano, S., Varela, A. N., D’Elia, L., Bilmes, A., Gómez-Dacal, A., Sial, A. N., Aguirre, M.L., Mari, F., Scivetti, N. 2022. Beach ridge evolution during the Holocene Climatic Optimum at Río de la Plata estuary, Argentina: Former answers for future questions? *Quaternary International*, 638, 56-69.
- Roberts, D. L., Karkanias, P., Jacobs, Z., Marean, C. W., Roberts, R. G. 2012. Melting ice sheets 400,000 yr ago raised sea level by 13 m: Past analogue for future trends. *Earth and Planetary Science Letters*, 357–358, 226–237. <https://doi.org/10.1016/j.epsl.2012.09.006>
- Rostami, K., Peltier, W.R., Mangini, A., 2000. Quaternary marine terraces, sea-level changes and uplift history of Patagonia, Argentina: comparisons with predictions of the ICE-4G (VM2) model of the global process of glacial isostatic adjustment. *Quat Sci Rev* 19, 1496–1525.

- Rovere, A., Pappalardo, M., Richiano, S., Aguirre, M., Sandstrom, M. R., Hearty, P. J., Austermann, J., Castellanos, I., Raymo, M. E. 2020. Higher than present global mean sea level recorded by an Early Pliocene intertidal unit in Patagonia (Argentina). *Communications Earth & Environment*, 1(1), 68.
- Rovere, A., Raymo, M. E., Vacchi, M., Lorscheid, T., Stocchi, P., Gómez-Pujol, L., Harris, D. L., Casella, E., O'Leary, M. J., Hearty, P. J. 2016b. The analysis of Last Interglacial (MIS 5e) relative sea-level indicators: Reconstructing sea-level in a warmer world. *Earth-Science Reviews*, 159, 404–427. <https://doi.org/10.1016/j.earscirev.2016.06.006>
- Rovere, A., Ryan, D. D., Vacchi, M., Dutton, A., Simms, A. R., Murray-Wallace, C. V. 2023. The World Atlas of Last Interglacial Shorelines (version 1.0). *Earth System Science Data*, 15(1), 1–23. <https://doi.org/10.5194/essd-15-1-2023>
- Rovere, A., Stocchi, P., Vacchi, M. 2016a. Eustatic and Relative Sea Level Changes. In *Current Climate Change Reports* (Vol. 2, Issue 4, pp. 221–231). Springer. <https://doi.org/10.1007/s40641-016-0045-7>
- Rutter, N., Radtke, U., and Schnack, E. J., 1990. Comparison of ESR and amino acid data in correlating and dating Quaternary shorelines along the Patagonian coast, Argentina, *Journal of Coastal Research*, pp. 391–411.
- Schellmann, G., Radtke, U. 2010. Timing and magnitude of Holocene sea-level changes along the middle and south Patagonian Atlantic coast derived from beach ridge systems, littoral terraces and valley-mouth terraces. In *Earth-Science Reviews* (Vol. 103, Issues 1–2, pp. 1–30). <https://doi.org/10.1016/j.earscirev.2010.06.003>
- Schellmann, G., Beerten, K., Radtke, U., 2008. Electron spin resonance (ESR) dating of Quaternary materials. E & G (Eiszeitalter u. Gegenwart). *Quaternary Science Journal* 57, 150–178.
- Shennan, I. 2015. Handbook of sea-level research. In I. Shennan, A. J. Long, & B. P. Horton (Eds.), *Handbook of Sea-Level Research* (pp. 3–25). Wiley. <https://doi.org/10.1002/9781118452547.ch2>
- Siddall, M., Chappell, J., Potter, E.-K. 2007. *Eustatic sea level during past interglacials* (pp. 75–92). [https://doi.org/10.1016/S1571-0866\(07\)80032-7](https://doi.org/10.1016/S1571-0866(07)80032-7)
- Simms, A. R.: Last interglacial sea levels within the Gulf of Mexico and northwestern Caribbean Sea, *Earth Syst. Sci. Data*, 13, 1419–1439, <https://doi.org/10.5194/essd-13-1419-2021>, 2021.
- Suguo, K., Bezerra, F. H. R., and Barreto, A. M. F. 2011. Luminescence dated Late Pleistocene wave-built terraces in northeastern Brazil, *An. Acad. Bras. Ciênc.*, 83, 907–920.
- Tomazelli, L. J., Dillenburg, S. R., J.A. Villwock. 2006. Geological Evolution of Rio Grande do Sul Coastal Plain, Southern Brazil. *Journal of Coastal Research*, 1, 257–278.

- Vacchi, M., Engelhart, S. E., Nikitina, D., Ashe, E. L., Peltier, W. R., Roy, K., Kopp, R.; Horton, B. P. (2018). Postglacial relative sea-level histories along the eastern Canadian coastline. *Quaternary Science Reviews*, 201, 124-146.
- van Andel, T. H., Laborel, J. 1964. Recent High Relative Sea Level Stand near Recife, Brazil. *Science*, 145(3632), 580–581. <https://doi.org/10.1126/science.145.3632.580>
- van de Plassche, O. 1986. *Sea-Level Research: A Manual for the Collection and Evaluation of Data* (O. van de Plassche, Ed.). Geo Books.
- Van Daele, M., van Welden, A., Moernaut, J., Beck, C., Audemard, F., Sanchez, J., Jouanne, F., Carrillo, E., Malavé, G., Lemus, A., De Batist, M. 2011. Reconstruction of Late-Quaternary sea-and lake-level changes in a tectonically active marginal basin using seismic stratigraphy: The Gulf of Cariaco, NE Venezuela. *Marine Geology*, 279(1-4), 37-51
- Wilcox, P. S., Honiat, C., Trüssel, M., Edwards, R. L., Spötl, C. 2020. Exceptional warmth and climate instability occurred in the European Alps during the Last Interglacial period. *Communications Earth & Environment*, 1(1), 57. <https://doi.org/10.1038/s43247-020-00063-w>
- Wong, T. E., de Kramer, R., de Boer, P. L., Langereis, C., Sew-A-Tjon, J. 2009. The influence of sea-level changes on tropical coastal lowlands; the Pleistocene Coropina Formation, Suriname. *Sedimentary Geology*, 216(3–4), 125–137.
- Woodroffe, S. A., Barlow, N. L. 2015. Reference water level and tidal datum. *Handbook of Sea-Level Research*, 171-180.

## 9.2. Chapter 2

- Ashe, E. L., Cahill, N., Hay, C., Khan, N. S., Kemp, A., Engelhart, S. E., Benjamin, P.H, Parnell, A.C., Kopp, R. E., 2019. Statistical modeling of rates and trends in Holocene relative sea level. *Quaternary Science Reviews*, 204, 58-77.
- Carrere, L., Lyard, F., Cancet, M., Guillot, A., Picot, N., 2016. Fes2014, a new tidal model–validation results and perspectives for improvements, presentation to esa living planet conference.
- de Boer, B., Stocchi, P., and van de Wal, R. S.W.2014. A fully coupled 3- D ice-sheet–sea-level model: algorithm and applications, *Geosci. Model Dev.*, 7, 2141–2156, <https://doi.org/10.5194/gmd-7-2141-2014>.
- Gowan, E.J., Zhang, X., Khosravi, S., Rovere, A., Stocchi, P., Hughes, A.L.C., Gyllencreutz, R., Mangerud, J., Svendsen, J., Lohmann, G., 2021b. A new global ice sheet reconstruction for the past 80 000 years. *Nature Communications* 12, 1199.
- Hajdas, I., Ascough, P., Garnett, M. H., Fallon, S. J., Pearson, C. L., Quarta, G., Spalding, K.L., Yamaguchi, H., Yoneda, M. 2021. Radiocarbon dating. *Nature Reviews Methods Primers*, 1(1), 62.

- Heaton, T.J., Köhler, P., Butzin, M., Bard, E., Reimer, R.W., Austin, W.E.N., Bronk Ramsey, C., Grootes, P.M., Hughen, K.A., Kromer, B., Reimer, P.J., Adkins, J., Burke, A., Cook, M.S., Olsen, J., Skinner, L.C., 2020. Marine20 - The Marine Radiocarbon Age Calibration Curve (0-55,000 cal BP). *Radiocarbon* 62, 779–820. <https://doi.org/10.1017/RDC.2020.68>
- Hellstrom, J., & Pickering, R. 2015. Recent advances and future prospects of the U–Th and U–Pb chronometers applicable to archaeology. *Journal of Archaeological Science*, 56, 32–40.
- Hogg, A. G., Heaton, T. J., Hua, Q., Palmer, J. G., Turney, C. S., Southon, J., Bayliss, A., Blackwell, P.G., Boswijk, G., Ramsey, C.B., Pearson, C., Petchey, F., Reimer, P., Reimer, R., Wacker, L. (2020). SHCal20 Southern Hemisphere calibration, 0–55,000 years cal BP. *Radiocarbon*, 62(4), 759–778.
- Hollyday, A., Austermann, J., Lloyd, A., Hoggard, M., Richards, F., and Rovere, A. 2023. A Revised Estimate of Early Pliocene Global Mean Sea Level Using Geodynamic Models of the Patagonian Slab Window. *Geochemistry, Geophysics, Geosystems*, 24(2):e2022GC010648.
- Hu, P. 2010. Developing a Quality-controlled Postglacial Sea-level Database for Coastal Louisiana to Assess Conflicting Hypotheses of Gulf Coast Sea-level Change (MSc Thesis). Tulane University, New Orleans.
- Kaufman, D. S. and Manley, W. F. (1998). A new procedure for determining dl amino acid ratios in fossils using reverse phase liquid chromatography. *Quaternary Science Reviews*, 17(11):987–1000.
- Khan, N. S., Ashe, E., Moyer, R. P., Kemp, A. C., Engelhart, S. E., Brain, M. J., Toth, L.T., Chappel, A. Christie, M., Kopp, R.E, Horton, B. P., 2022. Relative sea-level change in South Florida during the past~ 5000 years. *Global and Planetary Change*, 216, 103902.
- Kvenvolden, K. A. 1975. Advances in the geochemistry of amino acids. *Annual Review of Earth and Planetary Sciences*, 3(1), 183–212.
- Leaman, C., Beuzen, T., Goldstein E. B., 2020. Chisleaman/py-wave-runup: v0.1.10
- Lyard, F. H., Allain, D. J., Cancet, M., Carrère, L., Picot N., 2021. Fes2014 global ocean tide atlas: design and performance. *Ocean Science* 17(3), 615–649.
- Peltier, W. R. 2004. Global glacial isostasy and the surface of the ice-age Earth: the ICE-5G (VM2) model and GRACE, *Annu. Rev. Earth Planet. Sc.*, 32, 111–149.
- Peltier, W.R., Argus, D.F., Drummond, R., 2015. Space geodesy constrains ice age terminal deglaciation: The global ICE-6G\_C (VM5a) model. *Journal of Geophysical Research: Solid Earth* 120, 450–487.
- Pradhan, A. S., Lee, J. I., & Kim, J. L. 2008. Recent developments of optically stimulated luminescence materials and techniques for radiation dosimetry and clinical applications. *Journal of medical physics/Association of Medical Physicists of India*, 33(3), 85.

- Radtke, Ulrich; Grün, Rainer; Schwarcz, Henry P. 1988. Electron spin resonance dating of the Pleistocene coral reef tracts of Barbado". *Quaternary Research*. 29 (3): 197–215. Bibcode:1988QuRes..29..197R
- Reimer, P.J., Austin, W.E.N., Bard, E., Bayliss, A., Blackwell, P.G., Bronk Ramsey, C., Butzin, M., Cheng, H., Edwards, R.L., Friedrich, M., Grootes, P.M., Guilderson, T.P., Hajdas, I., Heaton, T.J., Hogg, A.G., Hughen, K.A., Kromer, B., Manning, S.W., Muscheler, R., Palmer, J.G., Pearson, C., Van Der Plicht, J., Reimer, R.W., Richards, D.A., Scott, E.M., Southon, J.R., Turney, C.S.M., Wacker, L., Adolphi, F., Büntgen, U., Capano, M., Fahrni, S.M., Fogtmann-Schulz, A., Friedrich, R., Köhler, P., Kudsk, S., Miyake, F., Olsen, J., Reinig, F., Sakamoto, M., Sookdeo, A., Talamo, S., 2020. The IntCal20 Northern Hemisphere Radiocarbon Age Calibration Curve (0-55 cal kBP). *Radiocarbon* 62, 725–757. <https://doi.org/10.1017/RDC.2020.41>
- Reimer, P.J., Reimer, R.W., 2001. A marine reservoir correction database and On-line interface.
- Sasabe, J., & Suzuki, M. 2018. Emerging role of d-amino acid metabolism in the innate defense. *Frontiers in microbiology*, 9, 933.
- Shennan, I., 2015. Handbook of sea-level research: Framing research questions, in: *Handbook of Sea-Level Research*. Wiley Blackwell, pp. 3–25.
- Smith, C., Salles, T., Concejo, A. V., 2020. pyReefmodel/RADWave: RADWave: Python code for ocean surface wave analysis by satellite radar altimeter.
- Spada, G. and Stocchi, P. 2007. SELEN: A Fortran 90 program for solving the “sea-level equation”, *Comput. Geosci.*, 33, 538–562.
- Stuiver, M., Polach, H.A., 1977. Discussion Reporting of 14 C Data. *Radiocarbon* 19, 355–363. <https://doi.org/10.1017/s0033822200003672>
- Vos, K., Harley, M. D., Splinter, K. D., Walker, A., Turner, I. L., 2020. Beach slopes from satellite-derived shorelines. *Geophysical Research Letters* 47(14), e2020GL088365. e2020GL088365 2020GL088365.
- Vos, K., Splinter, K. D., Harley, M. D., Simmons, J. A., Turner, I. L., 2019. Coastsat: A google earth engine-enabled python toolkit to extract shorelines from publicly available satellite imagery. *Environmental Modelling Software* 122, 104528.

### 9.3. Chapter 3

- Alexander, C. S. 1961. The marine terraces of Aruba, Bonaire, and Curaçao, Netherlands Antilles, *Ann. Assoc. Am. Geogr.*, 51, 102–123.
- Almeida, F. D. 1955. *Geologia e petrologia do Arquipelago de Fernando de Noronha: [Brazil]* Div. Geologia e Mineralogia do Depto. Nac. Prod. Mineral. Mon. XIII, 181 pp., Brazil.

- Angulo, R. J., Pessenda, L. C. R., and de Souza, M. C. 2002. O significado das datações ao  $^{14}\text{C}$  na reconstrução de paleoníveis marinhos e na evolução das barreiras quaternárias do litoral paranaense, *Revista Brasileira de Geociências*, 32, 95–106.
- Angulo, R. J., Lessa, G. C., and de Souza, M. C. 2006. A critical review of mid-to late-Holocene sea-level fluctuations on the eastern Brazilian coastline, *Quaternary Sci. Rev.*, 25, 486–506.
- Angulo, R. J., de Souza, M. C., Fernandes, L. A., and Disaró, S. T. 2013. Quaternary sea-level changes and aeolianites in the Fernando de Noronha archipelago, northeastern Brazil, *Quaternary Int.*, 305, 15–30.
- Antonioli, F., Presti, V. L., Rovere, A., Ferranti, L., Anzidei, M., Furlani, S., Mastronuzzi, G., Orru, P., Scicchitano, G., Sannino, G., Spampinato, C., Pagliarulo, R., Deiana, G., de Sabata, E., Sansò, P., Vacchi, M., and Vecchio, A. 2015. Tidal notches in Mediterranean Sea: a comprehensive analysis, *Quaternary Sci. Rev.*, 119, 66–84.
- Audemard, F. A. 1996a. Late Quaternary marine deposits of the Paraguana peninsula, state of Falcon, northwestern Venezuela: preliminary geological observations and neotectonic implications, *Quaternary Int.*, 31, 5–11.
- Audemard, F. A. 1996b. Field-trip guidebook to “The late Quaternary marine deposits of the Paraguaná peninsula and Coro surroundings”, in: 5th Annual CLIP Meeting, July 1996, Punta Cardon, Venezuela.
- Austermann, J., Mitrovica, J. X., Huybers, P., and Rovere, A. 2017. Detection of a dynamic topography signal in last interglacial sea-level records, *Sci. Adv.*, 3, e1700457, <https://doi.org/10.1126/sciadv.1700457>.
- Baker, R. F. and Watkins, M. 1991. Guidance notes for the determination of mean high water mark for land title surveys, Professional Development Committee of the New Zealand Institute of Surveyor, New Zealand.
- Barbosa, L. M., Bittencourt, A. C. S. P., Dominguez, J. M. L., and Martin, L. 1986. The Quaternary coastal deposits of the State of Alagoas: influence of the relative sea-level changes, *Quat. S. Am. A.*, 4, 269–290.
- Barlow, N. L., McClymont, E. L., Whitehouse, P. L., Stokes, C. R., Jamieson, S. S., Woodroffe, S. A., Bentley, M. J., Callard, S. L., Cofaigh, C. Ó., Evans, D. J. A., Horrocks, J. R., Lloyd, J. M., Long, A. J., Margold, M., Roberts, D. H., and Sanchez-Montes, M. L. 2018. Lack of evidence for a substantial sea-level fluctuation within the Last Interglacial, *Nat. Geosci.*, 11, 627–634.
- Barreto, A. M. F., Bezerra, F. H. R., Suguio, K., Tatum, S. H., Yee, M., Paiva, R. P., and Munita, C. S. 2002. Late Pleistocene marine terrace deposits in northeastern Brazil: sea-level change and tectonic implications, *Palaeogeogr. Palaeoclimatol.*, 179, 57–69.

- Bauch, T., Reijmer, J. J. G., McNeill, D. F., and Schäfer, P. 2011. Development of a Pliocene mixed-carbonate siliciclastic reef (Limon, Costa Rica), *Sediment. Geol.*, 239, 37–47.
- Bee, B. 1999. Rapid Quaternary uplift of marine terraces: Cabo Blanco to Montezuma area, Península de Nicoya, Costa Rica, *Geol. Soc. Am. Bull.*, 89, 981–999.
- Bergoeing, J. P. 2006. El Cuaternario en Costa Rica. Proposición cronológica, *Rev. Reflexiones*, 85, 207–226.
- Bergoeing, J. P. 2008. La transgresión Flandense, *Revista Geográfica*, 144, 229–239.
- Bermudez, P. J. 1969. Cuaternario y reciente en Venezuela, *Mem. Soc. Cienc. Nat. La Salle*, 24, 43–59.
- Bermudez, P. J. and Farias, J. 1975. Contribucion al estudio del Pleistocene marine de Venezuela, *Mem. Soc. Venez. Cienc. Nat. La Salle*, 35, 69–118.
- Bernat, M., Martin, L., Bittencourt, A. C. S. P., and Vilas Boas, G. 1983. <sup>10</sup>-U dates of a coral formation from the last interglacial age on the Brazilian coast. Use of <sup>229</sup>Th as a tracer, *Comptes Rendus des Seances de l'Academie des Sciences. Serie 2*, 296, 197–200.
- Bezerra, F. H., Ferreira, J. M., and Sousa, M. O. 2006. Review of seismicity and Neogene tectonics in northeastern Brazil, *Revista de la Asociación Geológica Argentina*, 61, 525–535.
- Bezerra, I. S. A. A., Nogueira, A. C. R., Guimarães, J. T. F., and Truckenbrodt, W. 2015. Late Pleistocene sea-level changes recorded in tidal and fluvial deposits from Itaubal Formation, onshore portion of the Foz do Amazonas Basin, Brazil, *Braz. J. Geol.*, 45, 63–78.
- Bittencourt, A. C. S. P., Martin, L., Vilas Boas, G., and Flexor, J. M. 1979. Quaternary marine formations of the coast of the State of Bahia (Brazil), IGCP, São Paulo.
- Bittencourt, A. C. S. P., Martin, L., Dominguez, J. M. L., and Ferreira, Y. D. A. 1983. Evolução paleogeográfica quaternária da costa do Estado de Sergipe e da costa sul do Estado de Alagoas, *Revista Brasileira de Geociências*, 13, 93–97.
- Boyé, M. and Cruys, H. 1961. New data on the coast sedimentary formations in French Guiana, Geological Survey Department, Guyana.
- Branco, J. C., Ângulo, R. J., de Souza, M. C., Disaró, S. T., Pupo, D. V., Scheel-Ybert, R., Gonçalves, T., and Pessenda, L. C. R. 2010. Fósseis e idade de um setor da barreira pleistocênica paranaense, *Revista de Gestão Costeira Integrada*, 20, 5–25, <https://doi.org/10.5894/rgci-n197>.
- Brinkman, R. and Pons, L. J. 1968. A pedo-geomorphological classification and map of the Holocene sediments in the coastal plain of the three Guianas, Stichting voor Bodemkartering Wageningen, Soil Survey Institute, Wageningen, the Netherlands.

- Brocas, W. M., Felis, T., Obert, J. C., Gierz, P., Lohmann, G., Scholz, D., Kölling, M., and Scheffers, S. R. 2016. Last interglacial temperature seasonality reconstructed from tropical Atlantic corals, *Earth Planet. Sc. Lett.*, 449, 418–429.
- Buchmann, F. S. C. and Tomazelli, L. J. 2003. Relict nearshore shoals of Rio Grande do Sul, southern Brazil: Origin and effects on nearby modern beaches, *J. Coastal Res.*, 35, 318–322.
- Bürgli, H. 1961. Contribución a la estratigrafía y litogénesis de la Isla de San Andrés, *Boletín Geológico*, 7, 5–25.
- Cavada-Blanco, F., Croquer, A., Villamizar, A., Arocha, D., Agudo, E., Villamizar, E., González, G., Boadas, H., Naveda, J., Rodríguez, J., Pellegrini, N., and Sánchez, R. 2016. A Survival Blueprint for the Pillar coral, *Dendrogyra cylindrus*. Compilation from the Workshop “Strategic planning for the conservation and management of the Caribbean threatened species: *Dendrogyra cylindrus*, *Acropora palmata* and *A. cervicornis* and their habitat at Archipelago Los Roques National Park, South Caribbean”, 24–28 November 2015, Universidad Simon Bolivar, Caracas, Venezuela.
- Choubert, B. 1965. French Guiana, *Geol. Soc. Am. Mem.*, 65, 63–75.
- Chutcharavan, P. M. and Dutton, A. 2021. A global compilation of U-series-dated fossil coral sea-level indicators for the Last Interglacial period (Marine Isotope Stage 5e), *Earth Syst. Sci. Data*, 13, 3155–3178, <https://doi.org/10.5194/essd-13-3155-2021>.
- Danielo, A. 1976. Formes et dépôts littoraux de la côte septentrionale du Vénézuéla, *JSTOR, Annales de Géographie*, 467, 68–97.
- Davidson, D. 2010. Recent Uplift of the Burica Peninsula, Panama and Costa Rica, Recorded by Marine Terraces, e Geosciences Department, Stanford, California.
- de Boer, B., Stocchi, P., and van de Wal, R. S. W. 2014. A fully coupled 3-D ice-sheet–sea-level model: algorithm and applications, *Geosci. Model Dev.*, 7, 2141–2156, <https://doi.org/10.5194/gmd-7-2141-2014>.
- de Oliveira Soares, M., da Cruz Lotufo, T. M., Vieira, L. M., Salani, S., Hajdu, E., Matthews-Cascon, H., Leão, Z. M. A. N., and Kikuchi, P. 2017. Brazilian Marine Animal Forests: A New World to Discover in the Southwestern Atlantic, in: *Marine Animal Forests*, Springer International Publishing, Cham., 73–110.
- Dillenburg, S. R., Barboza, E. G., Tomazelli, L. J., Ayup-Zouain, R. N., Hesp, P. A., and Clerot, L. C. P. 2009. The Holocene Coastal Barriers of Rio Grande do Sul, in: *Geology and Geomorphology of Holocene Coastal Barriers of Brazil*, 53–91, Springer, Berlin, Heidelberg.
- Dominguez, J. M. L., Bittencourt, A. C. S. P., Leão, Z. M. A. N., and de Azevedo, A. E. G. 1990. Geologia do Quaternário costeiro do estado de Pernambuco, *Revista Brasileira de Geociências*, 20, 208–215.

- Felis, T., Giry, C., Scholz, D., Lohmann, G., Pfeiffer, M., Pätzold, J., Kölling, M., and Scheffers, S. R. 2015. Tropical Atlantic temperature seasonality at the end of the last interglacial, *Nat. Commun.*, 6, 6159, <https://doi.org/10.1038/ncomms7159>.
- Frey, R. W., Howard, J. D., and Pryor, W. A. 1978. Ophiomorpha: its morphologic, taxonomic, and environmental significance, *Palaeogeogr. Palaeoclimatol.*, 23, 199–229.
- Geister, J. 1972. Nota sobre la edad de las calizas coralinas del Pleistoceno marino en las Islas de San Andres y Providencia (Mar Caribe occidental, Colombia), *Mitt. Inst. Colombo-Alemán Invest. Cient.*, 6, 135–140.
- Geister, J. 1986. Recent coral reefs and geology history of providencia island (western caribbean sea, colombia), *Geología Colombiana*, 15, 115–134.
- Geister, J. 1992. Modern reef development and Cenozoic evolution of an oceanic island/reef complex: Isla de Providencia (Western Caribbean Sea, Colombia), *Facies*, 27, 1, <https://doi.org/10.1007/BF02536804>.
- Giannini, P. C. F., Sawakuchi, A. O., Martinho, C. T., and Tatum, S. H. 2007. Eolian depositional episodes controlled by Late Quaternary relative sea-level changes on the Imbituba–Laguna coast (southern Brazil), *Mar. Geol.*, 237, 143–168.
- Gowan, E. J., Rovere, A., Ryan, D. D., Richiano, S., Montes, A., Pappalardo, M., and Aguirre, M. L. 2021. Last interglacial (MIS 5e) sea-level proxies in southeastern South America, *Earth Syst. Sci. Data*, 13, 171–197, <https://doi.org/10.5194/essd-13-171-2021>.
- Hamelin, B., Bard, E., Zindler, A., and Fairbanks, R. G. 1991. mass spectrometry of corals: How accurate is the UTh age of the last interglacial period?, *Earth Planet. Sc. Lett.*, 106, 169–180.
- Hartt, C. F. and Agassiz, L. 1870. *Scientific Results of a Journey in Brazil by Louis Agassiz and His Travelling Companions: Geology and Physical Geography of Brazil*, Fields, Osgood., London.
- Hearty, P. J., Hollin, J. T., Neumann, A. C., O'Leary, M. J., and McCulloch, M. 2007. Global sea-level fluctuations during the Last Interglaciacion (MIS 5e), *Quaternary Sci. Rev.*, 26, 2090–2112.
- Herweijer, J. P. and Focke, J. W. 1978. Late Pleistocene depositional and denudational history of Aruba, Bonaire and Curaçao (Netherlands Antilles), *Geol. en Mijnb.*, 57, 177–187.
- Hippolyte, J.-C. and Mann, P. 2011. Neogene–Quaternary tectonic evolution of the Leeward Antilles islands (Aruba, Bonaire, Curaçao) from fault kinematic analysis, *Mar. Petrol. Geol.*, 28, 259–277.
- Horn Filho, N. O. and Simó, D. H. 2008. The upper pleistocene of São Francisco do Sul Island coastal plain: geomorphologic, sedimentologic and evolutive aspects, *Braz. J. Oceanogr.*, 56, 179–187.

- Horn Filho, N. O. and Vieira, C. V. 2017. Mapa geoevolutivo da planície costeira da Ilha de São Francisco do Sul, SC, Brasil.
- Horn Filho, N. O., Schmidt, A. D., Benedet, C., Neves, J., Pimenta, L. H. F., Paquette, M., Alencar, R., Silva, W. B., Villela, E., Genovez, R., and Santos, C. G. 2014. Estudo geológico dos depósitos clásticos quaternários superficiais da planície costeira de Santa Catarina, Brasil, *GRAVEL*, 12, 41–107.
- Horn Filho, N. O., Lima, A. de S., Pereira, A., Covello, C., Porto Filho, E., Sanchez, G. M., Goés, I. M. de A., Matos, I. da S., Silva, M., and Souza, R. R. 2017. Roteiro geológico na planície costeira de Santa Catarina, Brasil, Florianópolis, Edições do Bosque.
- Iriondo, M. 2013. El cuaternario de las Guayanas, Museo Provincial de Ciencias Naturales Florentino Ameghino, Santa Fe, Argentina.
- Isla, F. I. and Angulo, R. J. 2016. Tectonic processes along the South America coastline derived from Quaternary marine terraces, *J. Coastal Res.*, 32, 840–852.
- Kennedy, D. M., Tannock, K. L., Crozier, M. J., and Rieser, U. 2007. Boulders of MIS 5 age deposited by a tsunami on the coast of Otago, New Zealand, *Sediment. Geol.*, 200, 222–231.
- Khan, N. S., Ashe, E., Horton, B. P., Dutton, A., Kopp, R. E., Brocard, G., Engelhart, S. E., Hill, D. F., Peltier, W. R., Vane, C. H., and Scatena, F. N. 2017. Drivers of Holocene sea-level change in the Caribbean, *Quaternary Sci. Rev.*, 155, 13–36.
- Khan, N. S., Horton, B. P., Engelhart, S., Rovere, A., Vacchi, M., Ashe, E. L., Törnqvist, T. E., Dutton, A., Hijma, M., and Shennan, I. 2019. Inception of a global atlas of sea levels since the Last Glacial Maximum, *Quaternary Sci. Rev.*, 220, 359–371.
- Kim, K. H. and Lee, D. J. 1999. Distribution and depositional environments of coralline lithofacies in uplifted Pleistocene coral reefs of Bonaire, Netherlands Antilles, *Journal of the Paleontological Society of Korea*, 15, 115–133.
- Laborel, J. 1970. Madreporaires et hydrocoralliaires récifaux des cotes Bresiliennes. Systematique, ecologie. repartition verticale et géographique, *Results Scientifique du Campagne de Calypso*, 9, 171–229.
- Lighty, R. G., Macintyre, I. G., and Stuckenrath, R. 1982. *Acropora palmata* reef framework: a reliable indicator of sea level in the western Atlantic for the past 10,000 years, *Coral reefs*, 1, 125–130.
- Lorscheid, T. and Rovere, A. 2019. The indicative meaning calculator—quantification of paleo sea-level relationships by using global wave and tide datasets, *Open Geospatial Data, Software and Standards*, 4, 10, <https://doi.org/10.1186/s40965-019-0069-8>.
- Lorscheid, T., Felis, T., Stocchi, P., Obert, J. C., Scholz, D., and Rovere, A. 2017. Tides in the Last Interglacial: insights from notch geometry and palaeo tidal models in Bonaire,

- Netherland Antilles, *Sci. Rep.-UK*, 7, 16241, <https://doi.org/10.1038/s41598-017-16285-6>.
- Martin, L. and Suguio, K. 1976. Etude Preliminaire du Quaternaire Marin: Comparaison du Litoral de São Paulo et de Salvador de Bahia (BRESIL), *Inst. Geoci., Cidade Univ. C.P. 20899, Sao Paulo, Brazil*.
- Martin, L., Bittencourt, A. C. S. P., and Boas, G. da S. V. 1982. Primeira ocorrência de corais pleistocênicos da costa brasileira: datação do máximo da penúltima transgressão, *Ciências da Terra*, 3, 16–17.
- Martin, L., Dominguez, J. M. L., and Suguío, K. 1986. Consequence of relative sea-level changes during the Quaternary on sandy coastal sedimentation: examples from Brazil, in: *International symposium on sea-level changes and quaternary shorelines*, 119–135, CRC Press, USA.
- Martin, L., Suguio, K., and Flexor, J.-M. 1988. Hauts niveaux marins Pleistocenes du littoral bresilien, *Palaeogeogr. Palaeoclimatol.*, 68, 231–239.
- Martin, L., Flexor, J.-M., and Suguio, K. 1998. Pleistocene wave-built terraces of Northern Rio de Janeiro State, Brazil.
- Martins, D. C., Cancelli, R. R., Lopes, R. P., Hanler, P., Testa, E. H., and Barboza, E. G. 2018. Ocorrência de *Ophiomorpha nodosa* em sedimentos pleistocênicos da Planície Costeira da Pinheira, Santa Catarina, Brasil, *Rev. Bras. Paleontolog.*, 21, 79–86.
- Mauz, B., Vacchi, M., Green, A., Hoffmann, G., and Cooper, A. 2015. Beachrock: a tool for reconstructing relative sea level in the far-field, *Mar. Geol.*, 362, 1–16.
- Meyer, D., Bries, J., Greenstein, B., and Debrot, A. 2003. Preservation of in situ reef framework in regions of low hurricane frequency: Pleistocene of Curaçao and Bonaire, southern Caribbean, *Lethaia*, 36, 273–285.
- Muhs, D. R., Pandolfi, J. M., Simmons, K. R., and Schumann, R. R. 2012. Sea-level history of past interglacial periods from uranium-series dating of corals, Curaçao, Leeward Antilles islands, *Quaternary Res.*, 78, 157–169.
- Obert, J. C., Scholz, D., Felis, T., Brocas, W. M., Jochum, K. P., and Andreae, M. O. 2016. dating of Last Interglacial brain corals from Bonaire (southern Caribbean) using bulk and theca wall material, *Geochim. Cosmochim. Acta.*, 178, 20–40.
- O'Leary, M. J., Hearty, P. J., Thompson, W. G., Raymo, M. E., Mitrovica, J. X., and Webster, J. M. 2013. Ice sheet collapse following a prolonged period of stable sea level during the last interglacial, *Nat. Geosci.*, 6, 796–800.
- Pandolfi, J. M. and Jackson, J. B. C. 2001. Community structure of Pleistocene coral reefs of Curaçao, Netherlands Antilles, *Ecol. Monogr.*, 71, 49–67.

- Pavlis, N. K., Holmes, S. A., Kenyon, S. C., and Factor, J. K. 2012. The development and evaluation of the Earth Gravitational Model 2008 (EGM2008), *J. Geophys. Res.-Sol. Ea.*, 117, B04406, <https://doi.org/10.1029/2011JB008916>.
- Peltier, W. R. 2004. Global glacial isostasy and the surface of the ice-age Earth: the ICE-5G (VM2) model and GRACE, *Annu. Rev. Earth Planet. Sc.*, 32, 111–149.
- Pico, T. 2020. Towards assessing the influence of sediment loading on Last Interglacial sea level, *Geophys. J. Int.*, 220, 384–392.
- Pirazzoli, P. A. 2005. Marine terraces, *Encyclopedia of Coastal Science*, Springer Netherlands, Dordrecht, 632–633.
- Polyak, V. J., Onac, B. P., Fornós, J. J., Hay, C., Asmerom, Y., Dorale, J. A., Ginés, J., Tuccimei, P., and Ginés, A. 2018. A highly resolved record of relative sea level in the western Mediterranean Sea during the last interglacial period, *Nat. Geosci.*, 11, 860–864.
- Porta, J. and de Porta, N. S. 1960. El cuaternario marino de la isla de Tierrabomba (Bolívar), *Boletín de Geología*, 4, 19–44.
- Porta, J., Barrera, R., and Julià, R. 2008. Raised marsh deposits near Cartagena de Indias, Colombia: evidence of eustatic and climatic instability during the late Holocene, *Boletín de Geología*, 30, 21–28.
- Poupeau, G., Soliani, J. R. E., Rivera, A., Loss, E., and Vasconcellos, M. 1988. Datação por termoluminescência de alguns depósitos arenosos costeiros do último ciclo climático, no nordeste do Rio Grande do Sul, *Pesquisas em Geociências*, 21, 25–47.
- Rees-Jones, J., Rink, W. J., Norris, R. J., and Litchfield, N. J. 2000. Optical luminescence dating of uplifted marine terraces along the Akatore Fault near Dunedin, South Island, New Zealand, *New Zeal. J. Geol. Geop.*, 43, 419–424.
- Rey, O. 1996. Estratigrafía de la península de Paraguaná, Venezuela, *Rev. Fac. Ing.*, 11, 35–45.
- Rossetti, D. F., Bezerra, F. H. R., Góes, A. M., Valeriano, M. M., Andrades-Filho, C. O., Mittani, J. C. R., Tatum, S. H., and Brito-Neves, B. B. 2011. Late Quaternary sedimentation in the Paraíba Basin, Northeastern Brazil: landform, sea level and tectonics in Eastern South America passive margin, *Palaeogeogr. Palaeoclimatol.*, 300, 191–204.
- Rovere, A., Raymo, M. E., Vacchi, M., Lorscheid, T., Stocchi, P., Gomez-Pujol, L., Harris, D. L., Casella, E., O'Leary, M. J., and Hearty, P. J. 2016. The analysis of Last Interglacial (MIS 5e) relative sea-level indicators: Reconstructing sea-level in a warmer world, *Earth-Sci. Rev.*, 159, 404–427.
- Rovere, A., Ryan, D., Murray-Wallace, C., Simms, A., Vacchi, M., Dutton, A., Lorscheid, T., Chutcharavan, P., Brill, D., Bartz, M., Jankowski, N., Mueller, D., Cohen, K., and Gowan, E. 2020. Descriptions of database fields for the World Atlas of Last Interglacial Shorelines (WALIS), Zenodo [data set], <https://doi.org/10.5281/zenodo.3961544>.

- Rubio-Sandoval, K., Rovere, A., Cerrone, C., Stocchi, P., Lorscheid, T., Felis, T., Petersen, A. K., and Ryan, D. D. 2021. Last Interglacial sea-level proxies in the Western Atlantic and Southwestern Caribbean, from Brazil to Honduras (Version 1.02), Zenodo, <https://doi.org/10.5281/zenodo.5516444>.
- Schellmann, G., Radtke, U., Scheffers, A., Whelan, F., and Kelletat, D. 2004. ESR dating of coral reef terraces on Curaçao (Netherlands Antilles) with estimates of younger Pleistocene sea level elevations, *J. Coastal Res.*, 20, 947–957.
- Schubert, C. and Szabo, B. J. 1987. Uranium-series ages of pleistocene marine deposits on the islands of Curaçao and La Blanquilla, Caribbean Sea, *Geol. Mijnbouw*, 57, 325–332.
- Segal, B. and Castro, C. B. 2000. Slope preferences of reef corals (Cnidaria, Scleractinia) in the Abrolhos Archipelago, Brazil, *Bolm Mus. Nac., ns Zool.*, 418, 1–10.
- Shennan, I. 1982. Interpretation of Flandrian sea-level data from the Fenland, England, *P. Geol. Assoc.*, 93, 53–63.
- Shennan, I. 1986. Flandrian sea-level changes in the Fenland. I: The geographical setting and evidence of relative sea-level changes, *J. Quaternary Sci.*, 1, 119–153.
- Shennan, I. 1989. Holocene crustal movements and sea-level changes in Great Britain, *J. Quaternary Sci.*, 4, 77–89.
- Shennan, I., Tooley, M. J., Davis, M. J., and Haggart, B. A. 1989. Analysis and interpretation of Holocene sea-level data, *Nature*, 302, 404–406.
- Simms, A. R. 2021. Last interglacial sea levels within the Gulf of Mexico and northwestern Caribbean Sea, *Earth Syst. Sci. Data*, 13, 1419–1439, <https://doi.org/10.5194/essd-13-1419-2021>.
- Smith, D. A. and Small, H. J. 1999. The CARIB97 high-resolution geoid height model for the Caribbean Sea, *J. Geodesy*, 73, 1–9, <https://doi.org/10.1007/s001900050212>.
- Spada, G. and Stocchi, P. 2007. SELEN: A Fortran 90 program for solving the “sea-level equation”, *Comput. Geosci.*, 33, 538–562.
- Styron, R. and Pagani, M. 2020. The GEM global active faults database, *Earthq. Spectra*, 36, 160–180.
- Suguio, K. and Martin, L. 1995. Brazilian Coastline Quaternary Foriviations – The States of São Paulo and Bahia Litoral Zone Evolutive Schemes, *An. Acad. Bras. Ciênc.*, 48, 325–334.
- Suguio, K. and Petri, S. 1973. Stratigraphy of the Iguapé-Cananéia lagoonal region sedimentary deposits, São Paulo State, Brazil: part I: field observations and grain size analysis, *Boletim IG*, 4, 01–20.
- Suguio, K., Barreto, A. M. F., Bezerra, F. H. R., and de Oliveira, P. E. 2005. Síntese sobre prováveis níveis relativos do mar acima do atual no pleistoceno do Brasil.

- Suguio, K., Martin, L., and Dominguez, J. M. L. 1982. Evolução da planície costeira do Rio Doce (ES) durante o quaternário: Influência das flutuações do nível do mar.
- Suguio, K., Tatumi, S. H., Kowata, E. A., Munita, C. S., and Paiva, R. P. 2003. Upper Pleistocene deposits of the Comprida Island (São Paulo State) dated by thermoluminescence method, *An. Acad. Bras. Ciênc.*, 75, 91–96.
- Suguio, K., Bezerra, F. H. R., and Barreto, A. M. F. 2011. Luminescence dated Late Pleistocene wave-built terraces in northeastern Brazil, *An. Acad. Bras. Ciênc.*, 83, 907–920.
- Tomazelli, L. J. and Dillenburg, S. R. 2007. Sedimentary facies and stratigraphy of a last interglacial coastal barrier in south Brazil, *Mar. Geol.*, 244, 33–45.
- Tomazelli, L. J., Dillenburg, S. R., and Villwock, J. A. 2006. Geological evolution of Rio Grande do Sul coastal plain, southern Brazil, *J. Coastal Res.*, 1, 275–278.
- Villwock, J. A. 1984. Geology of the Coastal Province of Rio Grande do Sul, Southern Brazil. A Synthesis, *Pesquisas em Geociências*, 16, 5–49.
- Watanabe, S., Ortega, N. R. S., Ayta, W. E. F., Coaquira, J. A. H., Cortezao, S. U., and Arenas, J. S. A. 1997. TL dating of sands from Ilha de Cananeia, *Radiat. Meas.*, 27, 373–376.
- Wong, T. 1992. Quaternary Stratigraphy of Suriname, in: *Evolution des littoraux de Guyane et de la zone caraïbe méridionale pendant le quaternaire*, ORSTOM, Paris.
- Wong, T. E., de Kramer, R., de Boer, P. L., Langereis, C., and Sew-A-Tjon, J. 2009. The influence of sea-level changes on tropical coastal lowlands; the Pleistocene Coropina Formation, Suriname, *Sediment. Geol.*, 216, 125–137.
- Zecchin, M., Ronald, N., and Cesare, R. 2004. Raised Pleistocene marine terraces of the Crotona peninsula (Calabria, southern Italy): facies analysis and organization of their deposits, *Sediment. Geol.*, 172, 165–185.

#### 9.4. Chapter 4

- Aguirre, M.L., 1993. Palaeobiogeography of the Holocene molluscan fauna from Northeastern Buenos Aires Province, Argentina: its relation to coastal evolution and sea level changes. *Palaeogeogr Palaeoclimatol Palaeoecol* 102, 1–26.
- Albero, M.C., Angiolini, F.E., 1983. Ingeis Radiocarbon Laboratory Dates. *Radiocarbon* 831–842.
- Amato, S., Busso, A.S., 2009. Estratigrafía Cuaternaria del subsuelo de la cuenca inferior del Río Paraná, *Revista de la Asociación Geológica Argentina*.
- Angulo, R.J., 1992. Ambientes de sedimentação planície costeira com cordões litorâneos no estado do Paraná. *Boletim Paranaense de Geociências* 40, 69–114.

- Angulo, R.J., 1989. Fossil vermetidae between latitudes 25° 34' S and 27° 09' S state of Paraná and state of Santa Catarina- Brazil. International symposium on global changes in South America during the Quaternary: Past- Present- Future 263–268.
- Angulo, R.J., Camargo Lessa, G., 1997. The Brazilian sea-level curves: a critical review with emphasis on the curves from the Paranaguá and Cananéia regions, Marine Geology.
- Angulo, R. J., de Souza, M. C., 2014. Conceptual review of Quaternary coastal paleo-sea level indicators from Brazilian coast. Quaternary and Environmental Geosciences, 5(2), 01–32.
- Angulo, R.J., de Souza, M.C., da Camara Rosa, M.L.C., Barboza, E.G., Lessa, G.C., Pessenda, L.C.R., Ferreira Junior, A.L., 2022b. Mid- to Late Holocene sea level changes at Abrolhos Archipelago and Bank, southwestern Atlantic, Brazil. Mar Geol 450. <https://doi.org/10.1016/j.margeo.2022.106841>
- Angulo, R.J., de Souza, M.C., da Camara Rosa, M.L.C., Caron, F., Barboza, E.G., Costa, M.B.S.F., Macedo, E., Vital, H., Gomes, M.P., Garcia, K.B.L., 2022a. Paleo-sea levels, Late-Holocene evolution, and a new interpretation of the boulders at the Rocas Atoll, southwestern Equatorial Atlantic. Mar Geol 447. <https://doi.org/10.1016/j.margeo.2022.106780>
- Angulo, R. J., de Souza, M. C., Giannini, P. C. F., Dillenburg, S. R., Barboza, E. G., da Camara Rosa, M. L. C., Hesp, P.A., Pessenda, L. C. R., 2022c. Late-Holocene sea levels from vermetids and barnacles at Ponta do Papagaio, 27° 50' S latitude and a comparison with other sectors of southern Brazil. Quaternary Science Reviews, 286, 107536.
- Angulo, R.J., Giannini, P.C.F., De Souza, M.C., Lessa, G.C., 2016. Holocene paleo-sea level changes along the coast of Rio de Janeiro, southern Brazil: Comment on Castro et al. (2014). An Acad Bras Cienc 88, 2105–2111. <https://doi.org/10.1590/0001-3765201620140641>
- Angulo, R.J., Giannini, P.C.F., Souza, M.C., Lessa, G.C., 2018. Reply to Castro et al. 2018 on “Holocene paleo-sea level changes along the coast of Rio de Janeiro, southern Brazil”. An Acad Bras Cienc 90, 1377–1380. <https://doi.org/10.1590/0001-3765201820180376>
- Angulo, R.J., Giannini, P.C.F., Suguio, K., Pessenda, L.C.R., Braziliense, B., 1999. Relative sea-level changes in the last 5500 years in southern Brazil Laguna-Imbituba region, Santa Catarina State based on vermetid 14 C ages, Marine Geology.
- Angulo, R.J., Lessa, G.C., de Souza, M. c, 2006. A critical review of mid-to late-Holocene sea-level fluctuations on the eastern Brazilian coastline. Quat Sci Rev 25, 486–506.
- Argus, D.F., Peltier, W.R., Drummond, R., Moore, A.W., 2014. The Antarctica component of postglacial rebound model ICE-6G\_C (VM5a) based upon GPS positioning, exposure age dating of ice thicknesses, and relative sea level histories. Geophys. J. Int., 198(1), 537–563,
- Angulo, R.J., Pessenda, L., Souza, M.C., 2002. O significado das datações ao 14C na reconstrução de paleoníveis marinhos e na evolução das barreiras Quaternárias do litoral paranaense. Revista Brasileira de Geociências 32, 95–106.

- Ashe, E. L., Cahill, N., Hay, C., Khan, N. S., Kemp, A., Engelhart, S. E., Benjamin, P.H, Parnell, A.C., Kopp, R. E., 2019. Statistical modeling of rates and trends in Holocene relative sea level. *Quaternary Science Reviews*, 204, 58-77.
- Backeuser E., 1918. A faixa litorânea do Brasil Meridional. *Ontem e hoje*. Typ. Besnard Frères, Rio de Janeiro. 207p.
- Barbosa, L.M., Bittencourt, A.C.D.A., Dominguez, J.M., Martin, L., 1986. The Quaternary coastal deposits of the State of Alagoas: influence of the relative sea-level changes, in: *Quaternary of South America and Antarctic Peninsula*. pp. 269–290.
- Baril, A., Garrett, E., Milne, G. A., Gehrels, W. R., Kelley, J. T. 2023. Postglacial relative sea-level changes in the Gulf of Maine, USA: Database compilation, assessment and modelling. *Quaternary Science Reviews*, 306, 108027.
- Barreto, A.M.F., Bezerra, F.H.R., Suguio, K., Tatumi, S.H., Yee, M., Paiva, R.P., Munita, C.S., 2002. Late Pleistocene marine terrace deposits in northeastern Brazil: sea-level change and tectonic implications. *Paleogeography, Paleoclimatology, Paleoecology* 179, 57–69.
- Behling, H., Cohen, M.C.L., Lara, R.J., 2004. Late Holocene mangrove dynamics of Marajó Island in Amazonia, northern Brazil. *Veg Hist Archaeobot* 13, 73–80. <https://doi.org/10.1007/s00334-004-0031-1>
- Behling, H., Cohen, M.C.L., Lara, R.J., 2001. Studies on Holocene mangrove ecosystem dynamics of the Bragança Peninsula in north-eastern Pará, Brazil. *Palaeogeography, Palaeoclimatology, Palaeoecology* 167, 225–242.
- Bernal, J.P., Beramedí, L.E., Lugo-Ibarra, K.C., Walter, L., 2010. Revisión a algunos geocronómetros radiométricos aplicables al Cuaternario. *Boletín de la Sociedad Geológica Mexicana* 62, 305–323.
- Bezerra, F.H.R., Vita-Finzi, C., 2000. How active is a passive margin? Paleoseismicity in northeastern Brazil. *Geology* 591–595.
- Bini, M., Isola, I., Zanchetta, G., Pappalardo, M., Ribolini, A., Ragaini, L., Baroni, C., Boretto, G., Fuck, E., Morigi, C., Salvatore, M.C., Bassi, D., Marzaioli, F., Terrasi, F., 2018. Mid-Holocene relative sea-level changes along Atlantic Patagonia: New data from Camarones, Chubut, Argentina. *Holocene* 28, 56–64. <https://doi.org/10.1177/0959683617714596>
- Bird, P. (2003). An updated digital model of plate boundaries. *Geochemistry, Geophysics, Geosystems*, 4(3).
- Bittencourt, A.D.S., Martin, L., Vilas Boas, G.D.S., Flexor, J.M., 1978. Quaternary marine formations of the coast of the state of Bahia (Brazil), in: *Proceedings of 1978 International Symposium on Coastal Evolution in the Quaternary*, 232–253.
- Björck, S., Lambeck, K., Möller, P., Waldmann, N., Bennike, O., Jiang, H., Li, D., Sandgren, P., Nielsen, A.B. and Porter, C.T., 2021. Relative sea level changes and glacio-isostatic

- modelling in the Beagle Channel, Tierra del Fuego, Chile: Glacial and tectonic implications. *Quaternary Science Reviews*, 251, 106-657.
- Bracco, R., 1991 Dataciones <sup>14</sup>C en Sitios con Elevación. *Rev. Antropología*, año 1, /: 11-17.
- Bracco, R., 2000. Aproximación al registro arqueológico del sitio La Esmeralda (“conchero”) desde su dimensión temporal. *Anales de Arqueología y Etnología* 54–55.
- Bracco, R., García-Rodríguez, F., Inda, H., del Puerto, L., Castiñeira, c, Penario, D., 2011. Niveles relativos del mar durante el Pleistoceno final-Holoceno en la costa de Uruguay, in: *El Holoceno En La Zona Costera de Uruguay*. pp. 65–92.
- Bracco, R., Inda, H., del Puerto, L., Capdepont, I., Panario, D., Castiñeira, C., García-Rodríguez, F., 2014. A reply to “Relative sea level during the Holocene in Uruguay.” *Palaeogeogr Palaeoclimatol Palaeoecol*.
- Bracco, R., Ures, M.C., 1998. Las variaciones del nivel del mar y el desarrollo de las culturas prehistóricas del Uruguay. *Revista do Museu de Arqueologia e Etnologia*, (8), 109-115.
- Branner J.C, 1889. The geology of Fernando de Noronha. *American Journal of Science*. 37:145-161.
- Branner J.C., 1890. The aeolian sandstones of Fernando de Noronha. *American Journal of Science*. 39:247-257.
- Branner J.C., 1902. Geology of northeast coast of Brazil. *Bulletin of the Geological Society of America*, 13:41-98.
- Branner J.C., 1904. The stone reef of Brazil, their geological and geographical relations, with a chapter on the coral reefs. *Bulletin of the Museum of Comparative Zoology at Harvard College* v. 44, *Geological Series* v. 7. Cambridge, Massachuset, U.S.A. 285p. 99
- Bujalesky, 2007. Coastal geomorphology and evolution of Tierra del Fuego (Southern Argentina).
- Carrere, L., Lyard, F., Cancet, M., Guillot, A., Picot, N., 2016. Fes2014, a new tidal model–validation results and perspectives for improvements, presentation to esa living planet conference.
- Castro, A., Wagner, J., Sicoli, S., Fernandes, D., Cabral, C., Meneguci da Cunha, A., Malta, J., Miguel, L., Areia de Oliveira, C., Spotorno de Oliveira, P., Tapajós de Souza Tamega, F., 2021. Relative sea-level curve during the Holocene in Rio de Janeiro, Southeastern Brazil: A review of the indicators - RSL, altimetric and geochronological data. *J South Am Earth Sci* 112. <https://doi.org/10.1016/j.jsames.2021.103619>
- Castro, J.W.A., Seoane, J.C.S., Cunha, A.M., Malta, J. V., Oliveira, C.A., VAZ, S.R., Suguio, K., 2018. Comments to Angulo et al. 2016 on “Sea-level fluctuations and coastal evolution in the state of Rio de Janeiro, southeastern - Brazil” by Castro et al. 2014. *An Acad Bras Cienc* 90, 1369–1375. <https://doi.org/10.1590/0001-3765201820171010>

- Castro, J.W.A., Suguio, K., Seoane, J.C.S., Da Cunha, A.M., Dias, F.F., 2014. Sea-level fluctuations and coastal evolution in the state of Rio de Janeiro, southeastern Brazil. *An Acad Bras Cienc* 86, 671–683. <https://doi.org/10.1590/0001-3765201420140007>
- Cavallotto, J.L., 2002. Evolución holocena de la llanura costera del margen sur del Río de la Plata. *Rev. Asoc. Geol. Argent* 57, 376–388.
- Cavallotto, J.L., 1995. Evolución geomorfológica de la llanura costera ubicada en el margen sur del Río de la Plata. Universidad Nacional de La Plata.
- Cavallotto, J.L., Violante, R.A., Colombo, F., 2005. Evolución y cambios ambientales de la llanura costera de la cabecera del río de la Plata.
- Cavallotto, J.L., Violante, R.A., Parker, G., 2004. Sea-level fluctuations during the last 8600 years in the de la Plata river (Argentina). *Quaternary International* 114, 155–165. [https://doi.org/10.1016/S1040-6182\(03\)00050-8](https://doi.org/10.1016/S1040-6182(03)00050-8)
- Codignotto, J.O., Kokot, R.R., Marcomini, S.C., 1992. Neotectonism and Sea-Level Changes in the Coastal Zone of Argentina, Source: *Journal of Coastal Research*.
- Cohen, M.C.L., Behling, H., Lara, R.J., 2005. Amazonian mangrove dynamics during the last millennium: The relative sea-level and the Little Ice Age. *Rev Palaeobot Palynol* 136, 93–108. <https://doi.org/10.1016/j.revpalbo.2005.05.002>
- Cohen, M.C.L., Pessenda, L.C.R., Behling, H., de Fátima Rossetti, D., França, M.C., Guimarães, J.T.F., Friaes, Y., Smith, C.B., 2012. Holocene palaeoenvironmental history of the Amazonian mangrove belt. *Quat Sci Rev* 55, 50–58. <https://doi.org/10.1016/j.quascirev.2012.08.019>
- Colado, U., Figini, A., Fidalgo, F., Fucks, E., 1995. Los depósitos marinos del Cenozoico Superior aflorantes en la zona comprendida entre Punta Indio y el río Samborombón, provincia de Buenos Aires.
- Cortezzi, C.R., 1977. Datación de las formaciones marinas en el Cuaternario en las proximidades de la Plata-Magdalena, Providencia de Buenos Aires. *Anales del Laboratorio de Ensayo de Materiales e Investigaciones Tecnológicas* 75–93.
- Cortezzi, C.R., Pavlicelic, R.E., Pitori, C.A., Parodi, A.V., 1992. Variaciones del nivel del mar en el Holoceno en los alrededores de La Plata y Berisso. *Actas. IV Reunión Argentina de Sedimentología, La Plata* 2, 131–138.
- de Boer, B., Stocchi, P., Van De Wal, R. 2014. A fully coupled 3-D ice-sheet-sea-level model: algorithm and applications. *Geoscientific Model Development* 7, 2141–2156.
- de Boer, B., Stocchi, P., Whitehouse, P.L., van de Wal, R.S. 2017. Current state and future perspectives on coupled ice-sheet – sea-level modelling. *Quaternary Science Reviews* 169, 13–28.
- Delibrias, C., Laborel, J., 1971. Recent variations of the sea level along the Brazilian Coast. *Quaternaria* 45–49.

- Dominguez, J.M.L., Bittencourt, A.C.S.P., Leão, Z.M.A.N., Azevedo, A.E.G., 1990. Geologia do Quaternário costeiro do estado de Pernambuco. *Revista Brasileira de Geociências* 20.
- Düsterhus, A., Rovere, A., Carlson, A.E., Horton, B.P., Klemann, V., Tarasov, L., Barlow, N.L.M., Bradwell, T., Clark, J., Dutton, A., Roland Gehrels, W., Hibbert, F.D., Hijma, M.P., Khan, N., Kopp, R.E., Sivan, D., Törnqvist, T.E., 2016. Palaeo-sea-level and palaeo-ice-sheet databases: Problems, strategies, and perspectives. *Climate of the Past* 12, 911–921. <https://doi.org/10.5194/cp-12-911-2016>
- Engelhart, S.E., Horton, B.P., 2012. Holocene sea level database for the Atlantic coast of the United States. *Quat. Sci. Rev.* 54, 12e25. <https://doi.org/10.1016/j.quascirev.2011.09.013>.
- Fasano, J., Ilsa, F., Schnack, E., 1983. Un análisis comparativo sobre la evolución de ambientes litorales durante el Pleistoceno tardío-Holoceno: Laguna Mar Chiquita (Buenos Aires) - Caleta Valdes (Chubut). In Simposio "Oscilaciones del nivel del mar durante el ultimo hemicycle deglacial en la Argentina". CONICET, CAPICG, IGCP 61, 27–47.
- Figini, A., 1992. Edades <sup>14</sup>C de sedimentos marinos holocénicos de la provincia de Buenos Aires. *Actas de las Terceras Jornadas Geológicas Bonaerenses* 1, 147–151.
- Flexor, J.M., Martin, L., 1979. Sur l'utilisation des gres coquilliers de la region de Salvador (Bresil) dans la reconstruction des lignes de rivages Holocenes. *Proceedings of the "1978 International symposium on coastal evolution in the Quaternary"* 343–355.
- Fontes, N.A., Moraes, C.A., Cohen, M.C.L., Alves, I.C.C., França, M.C., Pessenda, L.C.R., Francisquini, M.I., Bendassolli, J.A., Macario, K., Mayle, F., 2017. The impacts of the middle holocene high Sea-Level stand and climatic changes on mangroves of the jucuruÇu river, southern Bahia-Northeastern Brazil. *Radiocarbon* 59, 215–230. <https://doi.org/10.1017/RDC.2017.6>
- Fucks, E., De Francesco, F.O., 2003. Ingresiones marinas al norte de la ciudad de Buenos Aires. Su Ordenamiento Estratigráfico. *Actas 2º Congreso Argentino de Cuaternario y Geomorfología* 101-103.
- Gherardi, D.F.M., Bosence, D.W.J., 2005. Late Holocene reef growth and relative sea-level changes in Atol das Rocas, equatorial South Atlantic. *Coral Reefs* 24, 264–272. <https://doi.org/10.1007/s00338-005-0475-5>
- González, M.A., Ravizza, G., 1987. Sedimentos estuáricos del Pleistoceno tardío y Holoceno en la isla Martín García, río de la Plata. *Revista Asociación Geológica Argentina* 42, 231–243.
- Gordillo, S., Coronato, A.M.J., Rabassa, J.O., 1993. Late Quaternary evolution of a Subantarctic Paleofjord, Tierra del fuego, *Science Reviews*.
- Gowan., 2023. Comparison of the PaleoMIST 1.0 ice sheet margins, ice sheet and paleo-topography reconstruction with paleo sea level indicators (2.0). Zenodo. <https://doi.org/10.5281/zenodo.7923553>

- Gowan, E.J., Rovere, A., Ryan, D.D., Richiano, S., Montes, A., Pappalardo, M., Aguirre, M.L., 2021a. Last interglacial (MIS 5e) sea-level proxies in southeastern South America. *Earth Syst Sci Data* 13, 171–197. <https://doi.org/10.5194/essd-13-171-2021>.
- Gowan, S. M., Ryves, D. B., Anderson, N. J. 2003. Holocene records of effective precipitation in West Greenland. *The Holocene*, 13(2), 239-249.
- Gowan, E.J., Zhang, X., Khosravi, S., Rovere, A., Stocchi, P., Hughes, A.L.C., Gyllencreutz, R., Mangerud, J., Svendsen, J., Lohmann, G., 2021b. A new global ice sheet reconstruction for the past 80 000 years. *Nature Communications* 12, 1199.
- Guida, N., González, M.A., 1984. Evidencias paleoestuáricas en el sudeste de Entre Ríos, su evolución con niveles marinos relativamente elevados del Pleistoceno Superior y Holoceno.
- Guimarães, J.T.F., Cohen, M.C.L., Pessenda, L.C.R., França, M.C., Smith, C.B., Nogueira, A.C.R., 2012. Mid- and late-Holocene sedimentary process and palaeovegetation changes near the mouth of the Amazon River. *Holocene* 22, 359–370. <https://doi.org/10.1177/0959683611423693>
- Hall, G.F., Hill, D.F., Horton, B.P., Engelhart, S.E., Peltier, W.R., 2013. A high-resolution study of tides in the Delaware Bay: Past conditions and future scenarios. *Geophys Res Lett* 40, 338–342. <https://doi.org/10.1029/2012GL054675>
- Hart C. F., 1870. *Geology and physical geography of Brazil*. Fields, Osgood & Co., Boston, 620p.
- Heaton, T.J., Köhler, P., Butzin, M., Bard, E., Reimer, R.W., Austin, W.E.N., Bronk Ramsey, C., Grootes, P.M., Hughen, K.A., Kromer, B., Reimer, P.J., Adkins, J., Burke, A., Cook, M.S., Olsen, J., Skinner, L.C., 2020. Marine20 - The Marine Radiocarbon Age Calibration Curve (0–55,000 cal BP). *Radiocarbon* 62, 779–820. <https://doi.org/10.1017/RDC.2020.68>
- Hijma, M.P., Engelhart, S.E., Törnqvist, T.E., Horton, B.P., Hu, P., Hill, D.F., 2015. A protocol for a geological sea-level database, in: *Handbook of Sea-Level Research*. Wiley Blackwell, pp. 536–553. <https://doi.org/10.1002/9781118452547.ch34>
- Hill, D.F., Griffiths, S.D., Peltier, W.R., Horton, B.P., Törnqvist, T.E., 2011. High-resolution numerical modeling of tides in the western Atlantic, Gulf of Mexico, and Caribbean Sea during the Holocene. *J Geophys Res Oceans* 116. <https://doi.org/10.1029/2010JC006896>
- Hogg, A. G., Heaton, T. J., Hua, Q., Palmer, J. G., Turney, C. S., Southon, J., Bayliss, A., Blackwell, P.G., Boswijk, G., Ramsey, C.B., Pearson, C., Petchey, F., Reimer, P., Reimer, R., Wacker, L. (2020). SHCal20 Southern Hemisphere calibration, 0–55,000 years cal BP. *Radiocarbon*, 62(4), 759-778.
- Horton, B.P., Engelhart, S.E., Hill, D.F., Kemp, A.C., Nikitina, D., Miller, K.G., Peltier, W.R., 2013. Influence of tidal-range change and sediment compaction on Holocene relative sea-level change in New Jersey, USA. *J Quat Sci* 28, 403–411. <https://doi.org/10.1002/jqs.2634>

- Horton, B.P., Kopp, R.E., Garner, A.J., Hay, C.C., Khan, N.S., Roy, K., Shaw, T.A., 2018. Annual Review of Environment and Resources Mapping Sea-Level Change in Time, Space, and Probability. <https://doi.org/10.1146/annurev-environ>
- Hu, P., 2010. Developing a Quality-controlled Postglacial Sea-level Database for Coastal Louisiana to Assess Conflicting Hypotheses of Gulf Coast Sea-level Change (MSc Thesis). Tulane University, New Orleans.
- Isla, F.I., Angulo, R.J., 2016. Tectonic Processes along the South America Coastline Derived from Quaternary Marine Terraces. *J Coast Res* 32, 840–852. <https://doi.org/10.2112/JCOASTRES-D-14-00178.1>
- Isla, F.I., Bujalesky, G.G., 2008. Coastal Geology and Morphology of Patagonia and the Fuegian Archipelago. *Developments in Quaternary Science*. [https://doi.org/10.1016/S1571-0866\(07\)10010-5](https://doi.org/10.1016/S1571-0866(07)10010-5)
- Khan, N.S., Ashe, E., Horton, B.P., Dutton, A., Kopp, R.E., Brocard, G., Engelhart, S.E., Hill, D.F., Peltier, W.R., Vane, C.H., Scatena, F.N., 2017. Drivers of Holocene sea-level change in the Caribbean. *Quat Sci Rev*. <https://doi.org/10.1016/j.quascirev.2016.08.032>
- Khan, N. S., Ashe, E., Moyer, R. P., Kemp, A. C., Engelhart, S. E., Brain, M. J., Toth, L.T., Chappel, A. Christie, M., Kopp, R.E, Horton, B. P., 2022. Relative sea-level change in South Florida during the past~ 5000 years. *Global and Planetary Change*, 216, 103902.
- Khan, N.S., Ashe, E., Shaw, T.A., Vacchi, M., Walker, J., Peltier, W.R., Kopp, R.E., Horton, B.P., 2015. Holocene Relative Sea-Level Changes from Near-, Intermediate-, and Far-Field Locations. *Curr Clim Change Rep* 1, 247–262. <https://doi.org/10.1007/s40641-015-0029-z>
- Khan, N.S., Horton, B.P., Engelhart, S., Rovere, A., Vacchi, M., Ashe, E.L., Törnqvist, T.E., Dutton, A., Hijma, M.P., Shennan, I., 2019. Inception of a global atlas of sea levels since the Last Glacial Maximum. *Quat Sci Rev* 220, 359–371. <https://doi.org/10.1016/j.quascirev.2019.07.016>
- Kikuchi, R., Leao, Z., 1997. Rocas (Southwestern Equatorial Atlantic, Brazil): An atoll built primarily by coralline algae. *Proc 8th Int Coral Reef Sym* 1, 731–736.
- Laborel, J., 1969. Les peuplements de Madréporaires des côtes tropicales du Brésil. *Annales de l'Université d'Abidjan* 2.
- Laborel, J. 1986. Vermetid gastropods as sea-level indicators. *In Sea-level research: a manual for the collection and evaluation of data* (pp. 281-310). Dordrecht: Springer Netherlands.
- Leaman, C., Beuzen, T., Goldstein E. B., 2020. Chrisleaman/py-wave-runup: v0.1.10
- Lorscheid, T., Rovere, A., 2019. The indicative meaning calculator – quantification of paleo sea-level relationships by using global wave and tide datasets. *Open Geospatial Data, Software and Standards* 4. <https://doi.org/10.1186/s40965-019-0069-8>
- Lyard, F. H., Allain, D. J., Cancet, M., Carrère, L., Picot N., 2021. Fes2014 global ocean tide atlas: design and performance. *Ocean Science* 17(3), 615–649.

- Macario, K. D., Alves, E. Q., Oliveira, F. M., Scheel-Ybert, R., Dias, F. F., & Lima, G. M., 2023. The variable nature of the coastal  $^{14}\text{C}$  marine reservoir effect: A temporal perspective for Rio de Janeiro. *Quaternary Science Advances*, 11, 100086.
- Martínez, S.A., Rojas, A., Verde, M., Piñeiro, G., 2006. Molluscan assemblages from the marine Holocene of Uruguay: Composition, geochronology, and paleoenvironmental signals. *Palaeontology and Palaeoenvironments of continental invertebrates from Argentina View project Origin and evolution of the NW Pacific Cenozoic sand dollar fauna View project*.
- Martínez, S., Rojas, A., 2013. Relative sea level during the Holocene in Uruguay. *Palaeogeogr Palaeoclimatol Palaeoecol* 374, 123–131. <https://doi.org/10.1016/j.palaeo.2013.01.010>
- Martin, L., Bittencourt, A. C. S. P., Dominguez, J. M. L., Flexor, J. M., Suguio, K. 1998 Oscillations or not oscillations, that is the question: Comment on Angulo, RJ and Lessa, GC “The Brazilian sea-level curves: a critical review with emphasis on the curves from the Paranaguá and Cananeia regions [Mar. Geol. 140,141–166]. *Marine Geology*, 150, 179-187.
- Martin, L., Bittencourt, A.C.S.P., Vilas Boas, G.S., 1982. Primeira ocorrência de corais pleistocênicos na costa brasileira- Datação do máximo da Penúltima Transgressão.
- Martin, L., Dominguez, J. M., Bittencourt, A. C. 2003. Fluctuating Holocene sea levels in eastern and southeastern Brazil: evidence from multiple fossil and geometric indicators. *Journal of Coastal Research*, 101-124.
- Martin, L.K., Suguio, J.M., Flexor, J., Dominguez, M.L., Bittencourt, A.C.S.P., 1996. Quaternary sea-level history along the central Part of the Brazilian Coast. Variations in coastal dynamics and their consequences on coastal plain construction. *An.Acad.bras.Ci.* 68, 303–354.
- Martin, L., Suguio, K., Flexor, J.M., Bittencourt, A.C.S.P., Vilas-Boas, G.S., 1979. Le quaternaire marin bresilien (littoral pauliste, sud fluminense et bahianais). *Serie Geologie* 11, 95–124.
- Martin, L., Suguio, K., 1989. Excursion route along the Brazilian coast between Santos (state of São Paulo) and Campos (state of Rio de Janeiro). *International Symposium on Global Changes in South America during the Quaternary 2*.
- Martin, L., Suguio, K., 1978. Excursion route along the coastline between the town of Cananéia (state of São Paulo) and Guaratiba outlet (state Rio de Janeiro), in: *International Symposium on Coastal Evolution* . pp. 1–98.
- Martin, L., Suguio, K., 1975. Étude préliminaire du Quaternaire Marin: comparaison du littoral de Sao-Paulo et de Salvador de Bahia (Brésil). *Cah.O.R.S.T.O.M.* 8, 33–47.
- Martin, L., Suguio, K., Dominguez, J.M.L., Flexor, J.M., 1997. *Geologia do Quaternário Costeiro do Litoral Norte do Rio de Janeiro e do Espírito Santo*. Belo Horizonte: CPRM Serviço Geológico do Brasil.
- Martin, L., Flexor, J. M., Blitzkow, D., Suguio, K. 1985. Geoid change indications along the Brazilian coast during the last 7.000 years. In *Proceedings*

- Mauz, B., Vacchi, M., Green, A., Hoffmann, G., Cooper, A., 2015. Beachrock: A tool for reconstructing relative sea level in the far-field. *Mar Geol* 362, 1–16. <https://doi.org/10.1016/j.margeo.2015.01.009>
- McHutchon, A., Rasmussen, C.E., 2011. Gaussian Process Training with Input Noise. In: Shawe-Taylor, J., Zemel, R.S., Bartlett, P.L., Pereira, F., Weinberger, K.Q. (Eds.), *Advances in Neural Information Processing Systems 24*. Curran Associates, Inc., pp. 1341–1349.
- Milne, G. A., Mitrovica, J. X. 2008. Searching for eustasy in deglacial sea-level histories. *Quaternary Science Reviews*, 27(25-26), 2292-2302.
- Milne, G.A., Long, A.J., Bassett, S.E., 2005. Modelling Holocene relative sea-level observations from the Caribbean and South America. *Quat Sci Rev* 24, 1183–1202. <https://doi.org/10.1016/j.quascirev.2004.10.005>
- Peltier, W.R., Argus, D.F., Drummond, R., 2015. Space geodesy constrains ice age terminal deglaciation: The global ICE-6G\_C (VM5a) model. *Journal of Geophysical Research: Solid Earth* 120, 450-487.
- Porter, S.C., Stuiver, M., Heusser, C.J., 1984. Holocene Sea-Level Changes along the Strait of Magellan and Beagle Channel, Southernmost South America, *Quaternary Research*.
- Prieto, A.R., Mourelle, D., Peltier, W.R., Drummond, R., Vilanova, I., Ricci, L., 2017. Relative sea-level changes during the Holocene in the Río de la Plata, Argentina and Uruguay: A review. *Quaternary International* 442, 35–49. <https://doi.org/10.1016/j.quaint.2016.02.044>
- Rabassa, J., Coronato, A., Bujalesky, G., nica Salemme, M.H., Roig, C., Meglioli, A., Heusser, C., Gordillo, S., Roig, F., Borrromei, A., Quattrocchio, M., 2000. Quaternary of Tierra del Fuego, Southernmost South America: an updated review.
- Rasmussen, C., Williams, C., 2006. *Gaussian Processes for Machine Learning*. MIT Press, Cambridge, MA.
- Reimer, P.J., Austin, W.E.N., Bard, E., Bayliss, A., Blackwell, P.G., Bronk Ramsey, C., Butzin, M., Cheng, H., Edwards, R.L., Friedrich, M., Grootes, P.M., Guilderson, T.P., Hajdas, I., Heaton, T.J., Hogg, A.G., Hughen, K.A., Kromer, B., Manning, S.W., Muscheler, R., Palmer, J.G., Pearson, C., Van Der Plicht, J., Reimer, R.W., Richards, D.A., Scott, E.M., Southon, J.R., Turney, C.S.M., Wacker, L., Adolphi, F., Büntgen, U., Capano, M., Fahrni, S.M., Fogtmann-Schulz, A., Friedrich, R., Köhler, P., Kudsk, S., Miyake, F., Olsen, J., Reinig, F., Sakamoto, M., Sookdeo, A., Talamo, S., 2020. The IntCal20 Northern Hemisphere Radiocarbon Age Calibration Curve (0-55 cal kBP). *Radiocarbon* 62, 725–757. <https://doi.org/10.1017/RDC.2020.41>
- Reimer, P.J., Reimer, R.W., 2001. A marine reservoir correction database and On-line interface.

- Ribeiro, S. R., Valadao, R. C., Gomes, M. O. S., Bittencourt, J. S., Alves, R. A., 2023. Paleocological indicators of the highstand sea level on the Amazonian supralittoral until the last two millennia. *Journal of South American Earth Sciences*, 104422.
- Ribolini, A., Aguirre, M., Baneschi, I., Consoloni, I., Fucks, E., Isola, I., Mazzarini, F., Pappalardo, M., Zanchetta, G., Bini, M., 2011. Holocene beach ridges and coastal evolution in the Cabo Raso bay (Atlantic Patagonian Coast, Argentina). *J Coast Res* 27, 973–983. <https://doi.org/10.2112/JCOASTRES-D-10-00139.1>
- Richiano, S., Varela, A. N., D'Elia, L., Bilmes, A., Gómez-Dacal, A., Sial, A. N., Aguirre, M.L., Mari, F., Scivetti, N. 2022. Beach ridge evolution during the Holocene Climatic Optimum at Río de la Plata estuary, Argentina: Former answers for future questions? *Quaternary International*, 638, 56-69.
- Rostami, K., Peltier, W.R., Mangini, A., 2000. Quaternary marine terraces, sea-level changes and uplift history of Patagonia, Argentina: comparisons with predictions of the ICE-4G (VM2) model of the global process of glacial isostatic adjustment. *Quat Sci Rev* 19, 1496–1525.
- Rovere, A., Antonioli, F., Bianchi, C. N. 2015. Fixed biological indicators. *Handbook of Sea-Level Research*, 268-280.
- Rovere, A., Raymo, M.E., Vacchi, M., Lorscheid, T., Stocchi, P., Gómez-Pujol, L., Harris, D.L., Casella, E., O'Leary, M.J., Hearty, P.J., 2016. The analysis of Last Interglacial (MIS 5e) relative sea-level indicators: Reconstructing sea-level in a warmer world. *Earth Sci Rev.* <https://doi.org/10.1016/j.earscirev.2016.06.006>
- Rovere, A., Ryan, D.D., Vacchi, M., Dutton, A., Simms, A.R., Murray-Wallace, C. V., 2023. The World Atlas of Last Interglacial Shorelines (version 1.0). *Earth Syst Sci Data* 15, 1–23. <https://doi.org/10.5194/essd-15-1-2023>
- Rubio-Sandoval, K., Rovere, A., Cerrone, C., Stocchi, P., Lorscheid, T., Felis, T., Petersen, A.K., Ryan, D.D., 2021. A review of last interglacial sea-level proxies in the western Atlantic and southwestern Caribbean, from Brazil to Honduras. *Earth Syst Sci Data* 13, 4819–4845. <https://doi.org/10.5194/essd-13-4819-2021>
- Rubio-Sandoval, K., Ryan, D. D., Richiano, S., Giachetti, L. M., Hollyday, A., Bright, J., Gowan, E., Pappalardo, M., Austermann, J., Kaufman, D., Rovere, A. 2024. Quaternary and Pliocene sea-level changes at Camarones, central Patagonia, Argentina. *Preprint*
- Rutter, N., Radtke, U., and Schnack, E. J., 1990. Comparison of ESR and amino acid data in correlating and dating Quaternary shorelines along the Patagonian coast, Argentina, *Journal of Coastal Research*, pp. 391–411.
- Ryan, W. B. F., Carbotte, S. M., Coplan, J. O., O'Hara, S., Melkonian, A., Arko, R., Weissel, R. A., Ferrini, V., Goodwillie, A., Nitsche, F., Bonczkowski, J., and Zemsky, R. 2009. Global Multi-Resolution Topography synthesis. *Geochemistry, Geophysics, Geosystems*, 10(3).

- Schellmann, G., 2007. Bamberger geographische schriften herausgegeben von Heft 22 Teil I: Holozäne Meeresspiegelschwankungen-ESR-Datierungen aragonitischer Muschelschalen-Paläotsunamis. Institut für Geographie an der Universität Bamberg, Bamberg.
- Schellmann, G., Beerten, K., Radtke, U., 2008. Electron spin resonance (ESR) dating of Quaternary materials. *E & G (Eiszeitalter u. Gegenwart)*. *Quaternary Science Journal* 57, 150–178.
- Schellmann, G., Radtke, U., 2010. Timing and magnitude of Holocene sea-level changes along the middle and south Patagonian Atlantic coast derived from beach ridge systems, littoral terraces and valley-mouth terraces. *Earth Sci Rev* 103, 1–30. <https://doi.org/10.1016/j.earscirev.2010.06.003>
- Schellmann, G., Radtke, U., 2007. Zur ESR-Datierung holozäner sowie jung- bis mittelpleistozäner Muschelschalen—aktuelle Möglichkeiten und Grenzen. *Bamberger Geographische Schriften* 22, 113–152.
- Schellmann, G., Radtke, U., 2003. Coastal Terraces and Holocene Sea-Level Changes along the Patagonian Atlantic Coast, Source: *Journal of Coastal Research*.
- Schellmann, G., Radtke, U., 2000. ESR dating stratigraphically well-constrained marine terraces along the Patagonian Atlantic coast (Argentina).
- Shennan, I., 2015. Handbook of sea-level research: Framing research questions, in: *Handbook of Sea-Level Research*. Wiley Blackwell, pp. 3–25. <https://doi.org/10.1002/9781118452547.ch2>
- Shennan, I., Bradley, S.L., Edwards, R., 2018. Relative sea-level changes and crustal movements in Britain and Ireland since the Last Glacial Maximum. *Quat Sci Rev* 188, 143–159. <https://doi.org/10.1016/j.quascirev.2018.03.031>
- Shennan, I., Tooley, M.J., Davis, M.J., Andrew Haggart, B., 1993. Analysis and interpretation of Holocene sea-level data. *Nature* 302.
- Smith, C., Salles, T., Concejo, A. V., 2020. pyReefmodel/RADWave: RADWave: Python code for ocean surface wave analysis by satellite radar altimeter.
- Souza, M.C., Angulo, R.J., Pessenda, L.C.R., 2001. Evolução geológica e paleogeográfica da planície costeira de Itapoá, litoral norte de Santa Catarina. *Revista Brasileira de Geociências* 31, 223–230.
- Spada, G., Stocchi, P., 2007. SELEN: A Fortran 90 program for solving the "sea-level equation". *Computers & Geosciences* 33, 538–562.
- Spotorno, P., Tâmega, F. T., Bemvenuti, C. E. 2012. An overview of the recent vermetids (Gastropoda: Vermetidae) from Brazil. *Strombus*, 19(1/2), 1.
- Stuiver, M., Polach, H.A., 1977. Discussion Reporting of 14 C Data. *Radiocarbon* 19, 355–363. <https://doi.org/10.1017/s0033822200003672>

- Suguio, K., Flexor, J.M., Nacional, O., 1980. Le Quaternaire marin brésilien (Littoral pauliste, sud fluminense et bahianais).
- Suguio, K., Martin, L., 1978. Formações quaternarias marinhas do litoral paulista e sul fluminense = quaternary marine formations of the state of Sao Paulo and Southern Rio de Janeiro.
- Suguio, K., Martin, L., Bittencourt, A. C., Dominguez, J. M., Flexor, J. M., de Azevedo, A. E. 1985. Flutuações do nível relativo do mar durante o Quaternário Superior ao longo do litoral brasileiro e suas implicações na sedimentação costeira. *Revista Brasileira de Geociências*, 15(4), 273-86.
- Sulzbach, R., Klemann, V., Knorr, G., Dobsław, H., Dümpelmann, H., Lohmann, G., Thomas, M., 2023. Evolution of Global Ocean Tide Levels Since the Last Glacial Maximum. *Paleoceanogr Paleoclimatol* 38. <https://doi.org/10.1029/2022PA004556>
- Styron, R. 2019. GEMScienceTools/gem-global-active-faults: First release of 2019.
- Tamura, T., 2012. Beach ridges and prograded beach deposits as palaeoenvironment records. *Earth Sci Rev.* <https://doi.org/10.1016/j.earscirev.2012.06.004>
- Tan, F., Khan, N. S., Li, T., Meltzner, A. J., Majewski, J., Chan, N., Chutcharavan, P., Cahill, N., Vacchi, M., Peng, D., Horton, B. P. 2023. Holocene relative sea-level histories of far-field islands in the mid-Pacific. *Quaternary Science Reviews*, 107995.
- Thompson, S. B., Creveling, J. R., 2021. A global database of marine isotope substage 5a and 5c marine terraces and paleoshoreline indicators. *Earth System Science Data*, 13(7), 3467-3490.
- Toniolo, T., Giannini, P. C. F., Angulo, R. J., de Souza, M. C., Pessenda, L. C. R., Spotorno-Oliveira, P., 2020. Sea-level fall and coastal water cooling during the Late Holocene in Southeastern Brazil based on vermetid bioconstructions. *Marine Geology*, 428, 106281.
- Törnqvist, T.E., Rosenheim, B.E., Hu, P., Fernandez, A.B., 2015. Radiocarbon dating and calibration, in: *Handbook of Sea-Level Research*. Wiley Blackwell, pp. 347–360. <https://doi.org/10.1002/9781118452547.ch23>
- US Geological Survey, E. H. P. (2017). Advanced National Seismic System (ANSS) comprehensive catalog of earthquake events and products: Various.
- Vacchi, M., Engelhart, S.E., Nikitina, D., Ashe, E.L., Peltier, W.R., Roy, K., Kopp, R.E., Horton, B.P., 2018a. Postglacial relative sea-level histories along the eastern Canadian coastline. *Quat. Sci. Rev.* 201, 124e146. <https://doi.org/10.1016/j.quascirev.2018.09.043>.
- van Andel, T.H., Laborel, J., 1964. Recent high relative sea level stand near Recife, Brazil. *Science* (1979) 145, 580–581. <https://doi.org/10.1126/science.145.3632.580>
- van de Plassche, O., 1986. *Sea-level research: a manual for the collection and evaluation of data*. Geo Books, Norwich.

- Vos, K., Harley, M. D., Splinter, K. D., Walker, A., Turner, I. L., 2020. Beach slopes from satellite-derived shorelines. *Geophysical Research Letters* 47(14), e2020GL088365. e2020GL088365 2020GL088365.
- Vos, K., Splinter, K. D., Harley, M. D., Simmons, J. A., Turner, I. L., 2019. Coastsat: A google earth engine-enabled python toolkit to extract shorelines from publicly available satellite imagery. *Environmental Modelling Software* 122, 104528.
- Zanchetta, G., Bini, M., Isola, I., Pappalardo, M., Ribolini, A., Consoloni, I., Boretto, G., Fucks, E., Ragaini, L., Terrasi, F., 2014. Middle- to late-Holocene relative sea-level changes at Puerto Deseado (Patagonia, Argentina). *Holocene* 24, 307–317. <https://doi.org/10.1177/0959683613518589>
- Zanchetta, G., Consoloni, I., Isola, I., Pappalardo, M., Ribolini, A., Aguirre, M., Fucks, E., Baneschi, I., Bini, M., Ragaini, L., Terrasi, F., Boretto, G., 2012. New insights on the Holocene marine transgression in the Bahía Camarones (Chubut, Argentina). *Italian Journal of Geosciences* 131, 19–31. <https://doi.org/10.3301/IJG.2011.20>

## 9.5. Chapter 5

- Aguirre, M. L., Richiano, S., Donato, M., and Farinati, E. A. 2013. Tegula atra (Lesson, 1830)(Mollusca, Gas- tropoda) in the marine Quaternary of Patagonia (Argentina, SW Atlantic): Biostratigraphical tool and palaeoclimate- palaeoceanographical signal. *Quaternary International*, 305:163–187.
- Argus, D. F., Peltier, W., Drummond, R., and Moore, A. W. 2014. The Antarctica component of postglacial rebound model ICE-6G\_C (VM5a) based on GPS positioning, exposure age dating of ice thicknesses, and relative sea level histories. *Geophysical Journal International*, 198(1):537– 563.
- Austermann, J., Mitrovica, J. X., Huybers, P., and Rovere, A. 2017. Detection of a dynamic topography signal in last interglacial sea-level records. *Science Advances*, 3(7):e1700457.
- Bayarsky, A. and Codignotto, J. O. 1982. Pleistoceno- Holoceno marino en Puerto Lobos, Chubut. *Revista de la Asociación Geológica Argentina*, 37(1):91–99.
- Beuzen, T., Goldstein, E. B., and Splinter, K. D. 2019. Ensemble models from machine learning: an example of wave runup and coastal dune erosion. *Natural Hazards and Earth System Sciences*, 19(10):2295–2309.
- Bini, M., Isola, I., Zanchetta, G., Pappalardo, M., Ribolini, A., Ragaini, L., Baroni, C., Boretto, G., Fucks, E., Morigi, C., et al. 2018. Mid-holocene relative sea-level changes along atlantic Patagonia: new data from Camarones, Chubut, Argentina. *The Holocene*, 28(1):56–64.
- Bird, P. 2003. An updated digital model of plate boundaries. *Geochemistry, Geophysics, Geosystems*, 4(3).
- Björck, S., Lambeck, K., Möller, P., Waldmann, N., Bennike, O., Jiang, H., Li, D., Sandgren, P.,

- Nielsen, A. B., and Porter, C. T. 2021. Relative sea level changes and glacio-isostatic modeling in the Beagle Channel, Tierra del Fuego, Chile: Glacial and tectonic implications. *Quaternary Science Reviews*, 251:106657.
- Bowen, D. 2010. Sea level ~ 400 000 years ago (MIS 11): analogue for present and future sea-level? *Climate of the Past*, 6(1):19–29.
- Braun, J. 2010. The many surface expressions of mantle dynamics. *Nature Geoscience*, 3(12):825–833.
- Carrere, L., Lyard, F., Cancet, M., Guillot, A., and Picot, N. 2016. FES2014, a new tidal model—Validation results and perspectives for improvements, presentation to ESA Living Planet Conference.
- Chen, F., Friedman, S., Gertler, C. G., Looney, J., O’Connell, N., Sierks, K., and Mitrovica, J. X. 2014. Refining Estimates of Polar Ice Volumes during the MIS11 Interglacial Using Sea Level Records from South Africa. *Journal of Climate*, 27(23):8740 – 8746.
- Clark, P. U., He, F., Golledge, N. R., Mitrovica, J. X., Dutton, A., Hoffman, J. S., and Dendy, S. 2020. Oceanic forcing of penultimate deglacial and last interglacial sea-level rise. *Nature*, 577(7792):660–664.
- Codignotto, J. 1983. Depósitos elevados y/o de acreción Pleistoceno-Holoceno en la costa Fueguino-Patagónica. In *Simposio Oscilaciones del nivel del mar durante el último hemicycleo deglacial en la Argentina*, pages 12–26.
- Codignotto, J. O., Kokot, R. R., and Marcomini, S. C. 1992. Neotectonism and sea-level changes in the coastal zone of Argentina. *Journal of coastal research*, pages 125–133.
- Creel, R. C., Austermann, J., Kopp, R., Khan, N. S., Albrecht, T., and Kingslake, J. 2023. Global mean sea level higher than present during the Holocene.
- Creveling, J. R., Mitrovica, J. X., Clark, P. U., Waelbroeck, C., and Pico, T. 2017. Predicted bounds on peak global mean sea level during marine isotope stages 5a and 5c. *Quaternary Science Reviews*, 163:193–208.
- Darwin, C. 1851. *Geological observations on coral reefs, volcanic islands, and on South America: Being the geology of the voyage of the Beagle, under the command of Captain Fitzroy, RN, during the years 1832 to 1836*. Smith, Elder & Company.
- DeConto, R. M., Pollard, D., Alley, R. B., Velicogna, I., Gasson, E., Gomez, N., Sadai, S., Condrón, A., Gilford, D. M., Ashe, E. L., et al. 2021. The Paris Climate Agreement and future sea-level rise from Antarctica. *Nature*, 593(7857):83–89.
- Del Río, C. J., Griffin, M., McArthur, J. M., Martínez, S., and Thirlwall, M. F. 2013. Evidence for early Pliocene and late Miocene transgressions in southern Patagonia (Argentina): <sup>87</sup>Sr/<sup>86</sup>Sr ages of the pectinid “*Chlamys*” actinodes (Sowerby). *Journal of South American Earth Sciences*, 47:220–229.

- Dumitru, O. A., Austermann, J., Polyak, V. J., Fornós, J. J., Asmerom, Y., Ginés, J., Ginés, A., and Onac, B. P. 2019. Constraints on global mean sea level during Pliocene warmth. *Nature*, 574(7777):233–236.
- Dumitru, O. A., Dyer, B., Austermann, J., Sandstrom, M. R., Goldstein, S. L., D’Andrea, W. J., Cashman, M., Creel, R., Bolge, L., and Raymo, M. E. 2023. Last interglacial global mean sea level from high-precision U-series ages of Bahamian fossil coral reefs. *Quaternary Science Reviews*, 318:108287.
- Dutton, A., Carlson, A. E., Long, A. J., Milne, G. A., Clark, P. U., DeConto, R., Horton, B. P., Rahmstorf, S., and Raymo, M. E. 2015. Sea-level rise due to polar ice-sheet mass loss during past warm periods. *science*, 349(6244):aaa4019.
- Duval, M., Arnold, L. J., and Rixhon, G. 2020. Electron spin resonance (ESR) dating in Quaternary studies: evolution, recent advances and applications. *Quaternary International*, 556:1–10.
- Dyer, B., Austermann, J., D’Andrea, W. J., Creel, R. C., Sandstrom, M. R., Cashman, M., Rovere, A., and Raymo, M. E. 2021. Sea-level trends across The Bahamas constrain peak last interglacial ice melt. *Proceedings of the National Academy of Sciences*, 118(33):e2026839118.
- Fedorov, A. V., Brierley, C., Lawrence, K. T., Liu, Z., Dekens, P., and Ravelo, A. 2013. Patterns and mechanisms of early Pliocene warmth. *Nature*, 496(7443):43–49.
- Feruglio, E. 1949. Descripción geológica de la Patagonia. (No Title). Fox-Kemper, B., Hewitt, H., Xiao, C., Aðalgeirsdóttir, G., Dri- jfhout, S., Edwards, T., Golledge, N., Hemer, M., Kopp, R., Krinner, G., Mix, A., Notz, D., Nowicki, S., Nurhati, I., Ruiz, L., Sallée, J.-B., Slangen, A., and Yu, Y. (2021). Ocean, Cryosphere and Sea Level Change. In Masson-Delmotte, V., Zhai, P., Pirani, A., Connors, S. L., Péan, C., Berger, S., Caud, N., Chen, Y., Goldfarb, L., Gomis, M. I., Huang, M., Leitzell, K., Lonnoy, E., Matthews, J. B. R., Maycock, T. K., Water- field, T., Yelekçi, O., Yu, R., and Zhou, B., editors, *Climate Change 2021: The Physical Science Basis. Contribution of Working Group I to the Sixth Assessment Report of the In- tergovernmental Panel on Climate Change*, book section 9. Cambridge University Press, Cambridge, UK and New York, NY, USA. GEBCO Bathymetric Compilation Group 2023 (2023). The GEBCO\_2023 Grid - a continuous terrain model of the global oceans and land.
- Gilford, D. M., Ashe, E. L., DeConto, R. M., Kopp, R. E., Pollard, D., and Rovere, A. 2020. Could the last interglacial constrain projections of future Antarctic ice mass loss and sea-level rise? *Journal of Geophysical Research: Earth Surface*, 125(10):e2019JF005418.
- Goodfriend, G. A. 1991. Patterns of racemization and epimerization of amino acids in land snail shells over the course of the Holocene. *Geochimica et Cosmochimica Acta*, 55(1):293– 302.
- Gowan, E. J., Rovere, A., Ryan, D. D., Richiano, S., Montes, A., Pappalardo, M., and Aguirre, M. L. 2021a. Last interglacial (MIS 5e) sea-level proxies in southeastern South America. *Earth System Science Data*, 13(1):171–197.
- Gowan, E. J., Zhang, X., Khosravi, S., Rovere, A., Stocchi, P., Hughes, A. L., Gyllencreutz, R., Mangerud, J., Svendsen, J.-I., and Lohmann, G. 2021b. A new global ice sheet reconstruction

- for the past 80,000 years. *Nature communications*, 12(1):1199.
- Grant, G., Naish, T., Dunbar, G., Stocchi, P., Kominz, M., Kamp, P. J., Tapia, C., McKay, R., Levy, R., and Patterson, M. 2019. The amplitude and origin of sea-level variability during the Pliocene epoch. *Nature*, 574(7777):237–241.
- Hay, C., Mitrovica, J. X., Gomez, N., Creveling, J. R., Auster- mann, J., and E. Kopp, R. 2014. The sea-level fingerprints of ice-sheet collapse during interglacial periods. *Quaternary Science Reviews*, 87:60–69.
- Hearty, P. J., Kindler, P., Cheng, H., and Edwards, R. 1999. A+ 20 m middle Pleistocene sea-level highstand (Bermuda and the Bahamas) due to partial collapse of Antarctic ice. *Geology*, 27(4):375–378.
- Heaton, T. J., Köhler, P., Butzin, M., Bard, E., Reimer, R. W., Austin, W. E. N., Bronk Ramsey, C., Grootes, P. M., Hughen, K. A., Kromer, B., and et al. 2020. Marine20—The Marine Radiocarbon Age Calibration Curve (0–55,000 cal BP). *Radiocarbon*, 62(4):779–820.
- Hillaire-Marcel, C., Gariépy, C., Ghaleb, B., Goy, J.-L., Zazo, C., and Cuerda Barcelo, J. 1996. U-series measurements in tyrrhenian deposits from mallorca — Further evidence for two last-interglacial high sea levels in the Balearic Islands. *Quaternary Science Reviews*, 15(1):53–62.
- Hollyday, A., Austermann, J., Lloyd, A., Hoggard, M., Richards, F., and Rovere, A. 2023. A Revised Estimate of Early Pliocene Global Mean Sea Level Using Geodynamic Models of the Patagonian Slab Window. *Geochemistry, Geophysics, Geosystems*, 24(2):e2022GC010648.
- Holman, R. 1986. Extreme value statistics for wave run-up on a natural beach. *Coastal Engineering*, 9(6):527–544.
- IMOS. 2023. IMOS - SRS Surface Waves Sub-Facility - altimeter wave/wind. Technical report, Australia’s Integrated Marine Observing System (IMOS).
- Jedoui, Y., Reyss, J.-L., Kallel, N., Montacer, M., Ismail, H. B., and Davaud, E. 2003. U-series evidence for two high Last Interglacial sea levels in southeastern Tunisia. *Quaternary Science Reviews*, 22(2):343–351.
- Kaufman, D. S. and Manley, W. F. 1998. A new procedure for determining dl amino acid ratios in fossils using reverse phase liquid chromatography. *Quaternary Science Reviews*, 17(11):987–1000.
- Khan, N. S., Hibbert, F., and Rovere, A. 2019a. sea-level databases. *Past Global Changes Magazine*, 27:10–11.
- Khan, N. S., Horton, B. P., Engelhart, S., Rovere, A., Vacchi, M., Ashe, E. L., Törnqvist, T. E., Dutton, A., Hijma, M. P., and Shennan, I. 2019b. Inception of a global atlas of sea levels since the Last Glacial Maximum. *Quaternary Science Reviews*, 220:359–371.
- Kosnik, M. A. and Kaufman, D. S. 2008. Identifying outliers and assessing the accuracy of amino

- acid racemization measurements for geochronology: II. Data screening. *Quaternary Geochronology*, 3(4):328–341.
- Labonne, M. and Hillaire-Marcel, C. 2000. Geochemical gradients within modern and fossil shells of *Concholepas concholepas* from northern Chile: an insight into U–Th systematics and diagenetic/authigenic isotopic imprints in mollusk shells. *Geochimica et Cosmochimica Acta*, 64(9):1523–1534.
- Lamothe, M. 2016. Luminescence dating of interglacial coastal depositional systems: Recent developments and future avenues of research. *Quaternary Science Reviews*, 146:1–27.
- Leaman, C., Beuzen, T., and Goldstein, E. B. 2020. *chrisleaman/py-wave-runup*: v0.1.10.
- Lorscheid, T. and Rovere, A. 2019. The indicative meaning calculator—quantification of paleo sea-level relationships by using global wave and tide datasets. *Open Geospatial Data, Software and Standards*, 4:1–8.
- Lyard, F. H., Allain, D. J., Cancet, M., Carrère, L., and Picot, N. 2021. FES2014 global ocean tide atlas: design and performance. *Ocean Science*, 17(3):615–649.
- Marra, F., Florindo, F., Gaeta, M., and Jicha, B. 2023.  $^{40}\text{Ar}/^{39}\text{Ar}$  age constraints on MIS 5.5 and MIS 5.3 paleo-sea levels: Implications for global sea levels and ice-volume estimates. *Paleoceanography and Paleoclimatology*, page e2023PA004679.
- Milne, G. A., Long, A. J., and Bassett, S. E. 2005. Modeling Holocene relative sea-level observations from the Caribbean and South America. *Quaternary Science Reviews*, 24(10–11):1183–1202.
- Mitrovica, J. and Milne, G. 2002. On the origin of late Holocene sea-level highstands within equatorial ocean basins. *Quaternary Science Reviews*, 21(20):2179–2190.
- Mitrovica, J. X., Milne, G. A., and Davis, J. L. 2001. Glacial isostatic adjustment on a rotating earth. *Geophysical Journal International*, 147(3):562–578.
- Muhs, D. R., Simmons, K. R., Schumann, R. R., Groves, L. T., Mitrovica, J. X., and Laurel, D. 2012. Sea-level history during the Last Interglacial complex on San Nicolas Island, California: implications for glacial isostatic adjustment processes, paleozoogeography and tectonics. *Quaternary Science Reviews*, 37:1–25.
- Murray-Wallace, C. V. 2002. Pleistocene coastal stratigraphy, sea-level highstands and neotectonism of the southern Australian passive continental margin—a review. *Journal of Quaternary Science*, 17(5–6):469–489.
- Naish, T., Powell, R., Levy, R., Wilson, G., Scherer, R., Talarico, F., Krissek, L., Niessen, F., Pompilio, M., Wilson, T., et al. 2009. Obliquity-paced Pliocene West Antarctic ice sheet oscillations. *Nature*, 458(7236):322–328.
- Nielsen, P. 2009. Coastal and estuarine processes, volume 29. World Scientific Publishing Company.

- Olson, S. L. and Hearty, P. J. 2009. A sustained +21 m sea-level highstand during MIS 11 (400 ka): direct fossil and sedimentary evidence from Bermuda. *Quaternary Science Reviews*, 28(3-4):271–285.
- Pappalardo, M., Aguirre, M. L., Bini, M., Consoloni, I., Fucks, E. E., Hellstrom, J., Isola, I., Ribolini, A., and Zanchetta, G. 2015. Coastal landscape evolution and sea-level change: a case study from Central Patagonia (Argentina).
- Pappalardo, M., Baroni, C., Bini, M., Isola, I., Ribolini, A., Salvatore, M. C., and Zanchetta, G. 2019. Challenges in relative sea-level change assessment highlighted through a case study: The central coast of Atlantic Patagonia. *Global and Planetary Change*, 182:103008.
- Passarella, M., Goldstein, E. B., De Muro, S., and Coco, G. 2018. The use of genetic programming to develop a predictor of swash excursion on sandy beaches. *Natural Hazards and Earth System Sciences*, 18(2):599–611.
- Pedoja, K., Regard, V., Husson, L., Martinod, J., Guillaume, B., Fucks, E., Iglesias, M., and Weill, P. 2011. Uplift of Quaternary shorelines in eastern Patagonia: Darwin revisited. *Geomorphology*, 127(3-4):121–142.
- Peltier, W. R. 2002. Global glacial isostatic adjustment: palaeogeodetic and space-geodetic tests of the ICE-4G (VM2) model. *Journal of Quaternary Science*, 17(5-6):491–510.
- Peltier, W. R., Argus, D., and Drummond, R. 2015. Space geodesy constrains ice age terminal deglaciation: The global ICE-6G\_C (VM5a) model. *Journal of Geophysical Research: Solid Earth*, 120(1):450–487.
- Piñón, D., Zhang, K., Wu, S., and Cimbaro, S. 2018. A new Argentinean gravimetric geoid model: GEOIDEAR. In *International Symposium on Earth and Environmental Sciences for Future Generations: Proceedings of the IAG General Assembly, Prague, Czech Republic, June 22–July 2, 2015*, pages 53–62. Springer.
- Polyak, V. J., Onac, B. P., Fornós, J. J., Hay, C., Asmerom, Y., Dorale, J. A., Ginés, J., Tuccimei, P., and Ginés, A. 2018. A highly resolved record of relative sea level in the western Mediterranean Sea during the last interglacial period. *Nature geoscience*, 11(11):860–864.
- Raymo, M. E. and Mitrovica, J. X. 2012. Collapse of polar ice sheets during the stage 11 interglacial. *Nature*, 483(7390):453–456.
- Raymo, M. E., Mitrovica, J. X., O’Leary, M. J., DeConto, R. M., and Hearty, P. J. 2011. Departures from eustasy in Pliocene sea-level records. *Nature Geoscience*, 4(5):328–332.
- Reimer, P. J. and Reimer, R. W. 2001. A Marine Reservoir Correction Database and On-Line Interface. *Radiocarbon*, 43(2A):461–463.
- Ribolini, A., Aguirre, M., Baneschi, I., Consoloni, I., Fucks, E., Isola, I., Mazzarini, F., Pappalardo, M., Zanchetta, G., and Bini, M. 2011. Holocene beach ridges and coastal evolution in the Cabo Raso bay (Atlantic Patagonian coast, Argentina). *Journal of Coastal Research*,

- 27(5):973–983.
- Roberts, D. L., Karkanas, P., Jacobs, Z., Mearan, C. W., and Roberts, R. G. 2012. Melting ice sheets 400,000 yr ago raised sea level by 13 m: Past analogue for future trends. *Earth and Planetary Science Letters*, 357:226–237.
- Rojas, A. and Martínez, S. 2016. Marine Isotope Stage 3 (MIS 3) Versus Marine Isotope Stage 5 (MIS 5) Fossiliferous Marine Deposits from Uruguay. In *Marine Isotope Stage 3 in Southern South America*, 60 KA BP–30 KA BP, pages 249–278. Springer.
- Rostami, K., Peltier, W., and Mangini, A. 2000. Quaternary marine terraces, sea-level changes and uplift history of Patagonia, Argentina: comparisons with predictions of the ICE-4G (VM2) model of the global process of glacial isostatic adjustment. *Quaternary Science Reviews*, 19(14-15):1495–1525.
- Rovere, A. 2021. GPS-Utilities ver. 1.0.
- Rovere, A., Pappalardo, M., Richiano, S., Aguirre, M., Sandstrom, M. R., Hearty, P. J., Austermann, J., Castellanos, I., and Raymo, M. E. 2020. Higher than present global mean sea level recorded by an Early Pliocene intertidal unit in Patagonia (Argentina). *Communications Earth & Environment*, 1(1):68.
- Rovere, A., Rubio Sandoval, K. Z., Ryan, D. D., Richiano, S., Giachetti, L. M., Bright, J., Gowan, E., PAPPALARDO, M., and Kaufman, D. 2023a. Supplementary Information and data for: "Quaternary and Pliocene sea-level changes at Camarones, central Patagonia, Argentina".
- Rovere, A., Ryan, D. D., Vacchi, M., Dutton, A., Simms, A. R., and Murray-Wallace, C. V. 2023b. The World Atlas of Last Interglacial Shorelines (version 1.0). *Earth System Science Data*, 15(1):1–23.
- Rovere, A., Stocchi, P., and Vacchi, M. 2016. Eustatic and relative sea level changes. *Current Climate Change Reports*, 2:221–231.
- Rubio-Sandoval, K., Rovere, A., Cerrone, C., Stocchi, P., Lorscheid, T., Felis, T., Petersen, A.-K., and Ryan, D. D. 2021. A review of last interglacial sea-level proxies in the western Atlantic and southwestern Caribbean, from Brazil to Honduras. *Earth System Science Data*, 13(10):4819–4845.
- Ruggiero, P., Komar, P. D., McDougal, W. G., Marra, J. J., and Beach, R. A. 2001. Wave runup, extreme water levels and the erosion of properties backing beaches. *Journal of coastal research*, pages 407–419.
- Rutter, N., Schnack, E. J., del Rio, J., Fasano, J. L., Isla, F. I., and Radtke, U. 1989. Correlation and dating of Quaternary littoral zones along the Patagonian coast, Argentina. *Quaternary Science Reviews*, 8(3):213–234.
- Ryan, W. B. F., Carbotte, S. M., Coplan, J. O., O'Hara, S., Melkonian, A., Arko, R., Weissel, R. A., Ferrini, V., Goodwillie, A., Nitsche, F., Bonczkowski, J., and Zemsky, R. 2009. Global Multi-Resolution Topography Synthesis. *Geochemistry, Geophysics, Geosystems*, 10(3).

- Schellmann, G. 1998. Jungkänozoische Landschaftsgeschichte Patagoniens (Argentinien): andine Vorlandvergletscherungen, Talentwicklung und marine Terrassen. 1. Auflage, Essen: Klartext, 1998.
- Schellmann, G., Beerten, K., and Radtke, U. 2008. Electron spin resonance (ESR) dating of Quaternary materials. *E&G Quaternary Science Journal*, 57(1/2):150–178.
- Schellmann, G. and Radtke, U. 2000. ESR dating stratigraphically well-constrained marine terraces along the Patagonian Atlantic coast (Argentina). *Quaternary International*, 68:261–273.
- Schellmann, G. and Radtke, U. 2003. Coastal terraces and Holocene sea-level changes along the Patagonian Atlantic coast. *Journal of Coastal Research*, pages 983–996.
- Schellmann, G. and Radtke, U. 2007. Neue Befunde zur Verbreitung und chronostratigraphischen Gliederung holozäner Küstenterrassen an der mittel- und südpatagonischen Atlantikküste (Argentinien)–Zeugnisse holozäner Meeresspiegelveränderungen. *Bamberger Geographische Schriften*, 22:1–91.
- Schellmann, G. and Radtke, U. 2010. Timing and magnitude of Holocene sea-level changes along the middle and south Patagonian Atlantic coast derived from beach ridge systems, littoral terraces and valley-mouth terraces. *Earth-Science Reviews*, 103(1-2):1–30.
- Schwarcz, H. P. 1994. Current challenges to ESR dating. *Quaternary Science Reviews*, 13(5):601–605.
- Scussolini, P., Dullaart, J., Muis, S., Rovere, A., Bakker, P., Coumou, D., Renssen, H., Ward, P. J., and Aerts, J. C. J. H. 2023. Modeled storm surge changes in a warmer world: the last interglacial. *Climate of the Past*, 19(1):141–157.
- Senechal, N., Coco, G., Bryan, K. R., and Holman, R. A. 2011. Wave runoff during extreme storm conditions. *Journal of Geophysical Research: Oceans*, 116(C7).
- Shennan, I. 2015. Handbook of sea-level research: framing research questions. *Handbook of sea-level research*, pages 3–25.
- Siddall, M., Chappell, J., and Potter, E.-K. 2007. 7. Eustatic sea level during past interglacials. In *Developments in Quaternary Sciences*, volume 7, pages 75–92. Elsevier.
- Simms, A. R., Rouby, H., and Lambeck, K. 2016. Marine terraces and rates of vertical tectonic motion: The importance of glacio-isostatic adjustment along the Pacific coast of central North America. *Bulletin*, 128(1-2):81–93.
- Smith, C., Salles, T., and Concejo, A. V. 2020. pyReef- model/RADWave: RADWave: Python code for ocean surface wave analysis by satellite radar altimeter.
- Solgaard, A. M., Reeh, N., Japsen, P., and Nielsen, T. 2011. Snapshots of the Greenland ice sheet configuration in the Pliocene to early Pleistocene. *Journal of Glaciology*, 57(205):871–880.

- Spratt, R. M. and Lisiecki, L. E. 2016. A Late Pleistocene sea level stack. *Climate of the Past*, 12(4):1079–1092.
- Stockdon, H. F., Holman, R. A., Howd, P. A., and Sallenger, A. H. 2006. Empirical parameterization of setup, swash, and runup. *Coastal Engineering*, 53(7):573–588.
- Styron, R. 2019. GEMScienceTools/gem-global-active-faults: First release of 2019.
- Tawil-Morsink, K., Austermann, J., Dyer, B., Dumitru, O. A., Precht, W. F., Cashman, M., Goldstein, S. L., and Raymo, M. E. 2022. Probabilistic investigation of global mean sea level during MIS 5a based on observations from Cave Hill, Barbados. *Quaternary Science Reviews*, 295:107783.
- Thompson, S. B. and Creveling, J. R. 2021. A global database of marine isotope substage 5a and 5c marine terraces and paleo-shoreline indicators. *Earth System Science Data*, 13(7):3467–3490.
- Tzedakis, P. C., Hodell, D. A., Nehrbass-Ahles, C., Mitsui, T., and Wolff, E. W. 2022. Marine Isotope Stage 11c: An unusual interglacial. *Quaternary Science Reviews*, 284:107493.
- US Geological Survey, E. H. P. 2017. Advanced National Seismic System (ANSS) comprehensive catalog of earthquake events and products: Various.
- Van de Plassche, O. 2013. *Sea-level Research: a Manual for the Collection and Evaluation of Data*. Springer.
- van de Wal, R. S., Nicholls, R. J., Behar, D., McInnes, K., Stamer, D., Lowe, J. A., Church, J. A., DeConto, R., Fettweis, X., Goelzer, H., et al. 2022. A High-End Estimate of Sea Level Rise for Practitioners. *Earth's future*, 10(11):e2022EF002751.
- Vos, K., Harley, M. D., Splinter, K. D., Walker, A., and Turner, I. L. 2020. Beach Slopes From Satellite-Derived Shorelines. *Geophysical Research Letters*, 47(14):e2020GL088365.
- Vos, K., Splinter, K. D., Harley, M. D., Simmons, J. A., and Turner, I. L. 2019. CoastSat: A Google Earth Engine-enabled Python toolkit to extract shorelines from publicly available satellite imagery. *Environmental Modelling & Software*, 122:104528.
- Vousdoukas, M. I., Wziatek, D., and Almeida, L. P. 2012. Coastal vulnerability assessment based on video wave runup observations at a mesotidal, steep-sloped beach. *Ocean Dynamics*, 62:123–137.
- Wehmler, J. F. 1982. A review of amino acid racemization studies in Quaternary mollusks: Stratigraphic and chronologic applications in coastal and interglacial sites, Pacific and Atlantic coasts, United States, United Kingdom, Baffin Island, and tropical islands. *Quaternary Science Reviews*, 1(2):83–120.
- Wehmler, J. F. 2013a. Interlaboratory comparison of amino acid enantiomeric ratios in Pleistocene fossils. *Quaternary Geochronology*, 16:173–182.
- Wehmler, J. F. 2013b. United States Quaternary coastal sequences and molluscan

- racemization geochronology – What have they meant for each other over the past 45 years? *Quaternary Geochronology*, 16:3–20.
- Wehmiller, J. F. and Miller, G. H. 2000. Aminostratigraphic Dating Methods in Quaternary Geology, pages 187–222. American Geophysical Union (AGU).
- Yousefi, M., Milne, G., Li, S., Wang, K., and Bartholet, A. 2020. Constraining Interseismic Deformation of the Cascadia Subduction Zone: New Insights From Estimates of Vertical Land Motion Over Different Timescales. *Journal of Geophysical Research: Solid Earth*, 125(3):e2019JB018248.
- Zanchetta, G., Consoloni, I., Isola, I., Pappalardo, M., Ribolini, A., Aguirre, M., Fucks, E., Baneschi, I., Bini, M., Ragaini, L., et al. 2012. New insights on the Holocene marine transgression in the Bahía Camarones (Chubut, Argentina). *Italian Journal of Geosciences*, 131(1):19–31.
- ## 9.6. Chapter 6
- Abdelhady, A. A., Hassan, H. F., Balboul, B. A. A., et al. 2024. “Taphonomic damage of molluscan shells in the Nile Delta under natural and anthropogenic sources of environmental variability” *Journal of African Earth Sciences*, 210, 105159. DOI: <https://doi.org/10.1016/j.jafrearsci.2023.105159>
- Aceñolaza, F. G. 2011. “Juan Valentín: un geólogo que supo resumir la geología argentina” *Revista de la Asociación Geológica Argentina*, 68(3), pp. 315–321.
- Aguirre, M. L., Richiano, S. and Sirch, Y. N. 2006. “Palaeoenvironments and palaeoclimates of the Quaternary molluscan faunas from the coastal area of Bahía Vera–Camarones (Chubut, Patagonia)”. *Palaeogeography, Palaeoclimatology, Palaeoecology*, 229(4), pp. 251–286.
- Aguirre, M.L., Richiano, S., Donato, M., et al. 2013. “*Tegula atra* (Lesson, 1830) (Mollusca, Gastropoda) in the marine Quaternary of Patagonia (Argentina, SW Atlantic): biostratigraphical tool and paleoclimate-palaeoceanographical signal”, *Quaternary International*, 305, pp.163–187.
- Bertling, M., Braddy, S. J., Bromley, R. G., et al. 2006. “Names for trace fossils: a uniform approach”, *Lethaia*, 39, pp. 265–286. DOI: <https://doi.org/10.1080/00241160600787890>
- Bertling, M., Buatois, L.A., Knaust, D., et al. 2022. “Names for trace fossils 2.0: theory and practice in ichnotaxonomy” *Lethaia Review*, 55(3), pp. 1-19. DOI: <https://doi.org/10.18261/let.55.3.3>
- Bini, M., Consoloni, I., Isola, I., et al. 2013. “Markers of palaeo sea-level in rocky coasts of Patagonia (Argentina)” *Rendiconti online della Società Geologica Italiana*, 28, pp. 24–27.
- Bini, M., Isola, I., Zanchetta, G., et al. 2018. “Mid–Holocene relative sea-level changes along

- Atlantic Patagonia: New data from Camarones, Chubut, Argentina” *The Holocene*, 28(1), pp. 56–64. DOI: <https://doi.org/10.1177/0959683617714596>
- Bromley, R. G. and Asgaard, U. 1993. “Two bioerosion ichnofacies produced by early and late burial associated with sea-level change.” *Geologische Rundschau*, 82, 276–280. DOI: <https://doi.org/10.1007/BF00191833>
- Bromley, R. G. and Surlyk, F. 1973. “Borings produced by brachiopod pedicles, fossil and Recent.” *Lethaia*, 6, pp. 349–365.
- Bromley, R.G. and D’Alessandro, A. 1983. “Bioerosion in the Pleistocene of southern Italy: ichnogenera *Caulostrepsis* and *Maeandropolydora*.” *Rivista Italiana Di Paleontologia e Stratigrafia*, 89, pp. 283–309.
- Bromley, R. G. and Martinell, J. 1991. “*Centrichnus*, new ichnogenus for centrally patterned attachment scars on skeletal substrates.” *Bulletin of the Geological Society of Denmark*, 38, pp. 243–252. DOI: <https://doi.org/10.37570/bgsd-1990-38-21>.
- Busker, F., Giachetti, L. M. and Martínez, G. M. 2023. “Un pueblo olvidado y su resurgimiento: primeros registros fósiles del Cenozoico de Cabo Raso (Chubut, Argentina) y sus implicancias paleobioestratigráficas.” *Publicación Electrónica de la Asociación Paleontológica Argentina*, 23 (2), pp.146–163.
- Charó, M. P., Charó, G.D., Aceñolaza, G., et al. 2022. “Bioerosion on Late Pleistocene marine mollusks: a paleoclimatological and paleoecological comparison of MIS 7 and MIS 5e with modern beaches (Río Negro, Argentina)” *Acta Geologica Sinica*, 96 (4), pp. 1181–1198. DOI: <https://doi.org/10.1111/1755-6724.14692>
- Clark, T. L., Lesht, B., Young, R. A. et al. 1982. “Sediment resuspension by surface-wave action: an examination of possible mechanisms”, *Marine Geology*, 49, pp. 43–59.
- Núñez Cortés, C. and Narosky, T. 1997. “Cien caracoles argentinos”, in *Albastros* (Ed.), Buenos Aires, pp. 158.
- Dans, S., Cefarelli, A., Galván, D., et al. 2021. “El Golfo San Jorge como área prioritaria de investigación, manejo y conservación en el marco de la iniciativa Pampa Azul” *Ciencia e Investigación*, 71 (2), pp. 21-43.
- Dashtgard, S., 2011. “Linking invertebrate burrow distributions (neoichnology) to physicochemical stresses on a sandy tidal flat: implications for the rock record” *Sedimentology*, 58, pp. 1303–1325. DOI: <https://doi.org/10.1111/j.1365-3091.2010.01210.x>
- Edinger, E. N. 2002. “Bioerosion”, in: Briggs, D.E.G., Crowther, P.R. (Eds.), *Palaeobiology II*, Blackwell Publishing, Oxford. pp. 273-277.
- Farinati, E. A., Spagnuolo, J. O. and Aliotta, S. 2006. “Bioerosión en micromoluscos holocenos del estuario de Bahía Blanca, Argentina” *Ameghiniana*, 43 (1), pp. 45–50.

- Feruglio, E. 1950. "Descripción geológica de la Patagonia" División General de Yacimientos Petrolíferos Fiscales, 3, pp. 74–196.
- Franco, B. C., Defeo, O., Piola, A. R., et al. 2020. "Climate change impacts on the atmospheric circulation, ocean, and fisheries in the southwest South Atlantic Ocean: A review" *Climatic Change*, 162, pp. 2359–2377. DOI: <https://doi.org/10.1007/s10584-020-02783-6>.
- Giachetti, L. M., Richiano, S., Fernández, D.E. et al. 2022. "Aspectos icnológicos de los depósitos cuaternarios marinos (MIS 7?, 5, 1) en Puerto Lobos (Chubut, Argentina) y su interpretación paleoambiental: Resultados preliminares", VIII Congreso Argentino de Cuaternario y Geomorfología. San Juan, September 2022. Asociación Argentina de Cuaternario y Geomorfología, pp. 187.
- Giachetti, L. M., Richiano, S. And Fernández, D.E. 2023. "Bioerosion pattern as a paleotool to environmental interpretation: a case of study of Cabo Raso (Patagonia, Argentina)" XVIII Reunión Argentina de Sedimentología and IX Congreso Latinoamericano de Sedimentología. Buenos Aires, September 2023. Asociación Argentina de Sedimentología, pp. 369.
- Goodfriend, G. A. 1991. "Patterns of racemization and epimerization of amino acids in land snail shells over the course of the Holocene" *Geochimica et Cosmochimica Acta*, 55(1), pp. 293–302.
- Gowan, E. J., Rovere, A., Ryan, D. D., et al. 2021. "Last interglacial (MIS 5e) sea-level proxies in southeastern South America" *Earth System Science Data* 13, pp. 171–197. DOI: <https://doi.org/10.5194/essd-13-171-2021>
- Hamann, L. and Blanke, A. 2022. "Suspension feeders: diversity, principles of particle separation and biomimetic potential" *Journal of The Royal Society Interface*, 19, 20210741. DOI: <https://doi.org/10.1098/rsif.2021.0741>
- Hammer, Ø., Harper, D. A. T. and Ryan, P. D. 2001. "PAST: paleontological statistics software package for education and data analysis." *Palaeontological Electronica*, 4 (1), 9 pp. DOI: [http://palaeoelectronica.org/2001\\_1/past/issue1\\_01.htm](http://palaeoelectronica.org/2001_1/past/issue1_01.htm)
- Iriondo, M. H. 1999. "Last Glacial Maximum and Hypsithermal in the Southern Hemisphere" *Quaternary International*, 62, pp. 11–19.
- Iriondo, M. H. 1998. "Paleoclimas del Hemisferio Sur. Primeros Resultados (Conferencia para la IV Reunión de Cuaternario Ibérico)" *Cuaternario y Geomorfología*. 12 (1–2), pp. 95–104.
- Isla, F. and Espinoza, M., 1995. "Coastal environmental changes associated with Holocene sea-level fluctuation: SEW Buenos Aires. Argentina" *Quaternary International*, 26, pp. 55–60.
- Kaufman, D. S. and Manley, W. F. 1998. "A new procedure for determining dl amino acid ratios in fossils using reverse phase liquid chromatography" *Quaternary Science Reviews*, 17(11), pp. 987–1000.
- Kidwell, S. M., Fürsich, F., Aigner, T. 1986. "Conceptual framework for the analysis and

- classification of fossil concentrations” *Palaios*, 1, pp. 228–238.
- Kosnik, M. A. and Kaufman, D. S. 2008. “Identifying outliers and assessing the accuracy of amino acid racemization measurements for geochronology: II. Data screening”. *Quaternary Geochronology*, 3(4), pp. 328–341.
- Lema, H. et al. 2001. Hoja geológica 4566–II y IV: Camarones, Provincia del Chubut. Boletín 261. Buenos Aires: Instituto de Geología y Recursos Minerales, Servicio Geológico Minero Argentino.
- Lescinsky, H. L, Edinger, E. and Risk, M. J. 2002. “Mollusc shell encrustation and bioerosion rates in a modern Epeiric Sea: taphonomy experiments in the Java Sea, Indonesia.” *Palaios*, 17, pp. 171–191. DOI: [https://doi.org/10.1669/0883-1351\(2002\)017<0171:MSEABR>2.0.CO;2](https://doi.org/10.1669/0883-1351(2002)017<0171:MSEABR>2.0.CO;2)
- López Gappa, J. 2000. “Species richness of marine Bryozoa in the continental shelf and slope off Argentina (south–west Atlantic)” *Diversity and Distributions*, 6, pp. 15–27. DOI: <https://doi.org/10.1046/j.1472-4642.2000.00067.x>
- Matano, R. P., Palma, E. D., and Piola, A. R. 2010. “The influence of the Brazil and Malvinas Currents on the Southwestern Atlantic Shelf circulation” *Ocean Sciences*, 6, pp. 983–995.
- Mayoral, E. 1988. “*Pennatichnus* nov. icnogen.; *Pinaceocladichnus* nov. icnogen. e *Iramena*. Huellas de bioerosión debidas a Bryozoa perforantes (Ctenostomata, Plioceno Inferior) en la cuenca del Bajo Guadalquivir.” *Revista Española de Paleontología*, 3, pp. 13–22. DOI: <https://doi.org/10.7203/sjp.25139>.
- Meyer, N., Wisshak, M. and Freiwald, A. 2021. “Bioerosion ichnodiversity in barnacles from the Ross Sea, Antarctica”. *Polar Biology*, 44, pp. 667–668. DOI: <https://doi.org/10.1007/s00300-021-02825-4>.
- Moutzouris, C. I. and Daniil, E. I. 1995. “Water oxygenation in the vicinity of coastal structures due to wave breaking”, in Edge, B.L. (ed.), *Coastal Engineering 1994*. New York: American Society of Civil Engineers, pp. 3167–3177. DOI: <https://doi.org/10.1061/9780784400890.229>
- Palma, E. D., R. P. Matano, and Piola, A. R. 2008. “A numerical study of the Southwestern Atlantic Shelf circulation: Stratified Ocean response to local and offshore forcing” *Journal of Geophysical Research*, 113, C11010, DOI: <https://doi.org/10.1029/2007JC004720>.
- Paparazzo, F., Bianucci, L., Schloss, I., et al. 2010. “Crossfrontal distribution of inorganic nutrients and chlorophyll-a on the Patagonian Continental Shelf of Argentina during summer and fall” *Revista de Biología Marina y Oceanografía*, 45, pp. 107–119.
- Pappalardo, M., Aguirre, M., Bini, et al. 2015. “Coastal landscape evolution and sea-level change: a case study from Central Patagonia (Argentina)” *Zeitschrift Für Geomorphologie*, 59, pp. 145–172. DOI: <https://doi.org/10.1127/0372-8854/2014/0142>
- Pappalardo, M., Baroni, C., Bini, M., et al. 2019. “Challenges in relative sea–level change

- assessment highlighted through a case study” *Global and Planetary Change*, 182, 103008. DOI: <https://doi.org/10.1016/j.gloplacha.2019.103008>.
- Pedoja, K., Regard, V., Husson, L., et al. 2011. “Uplift of Quaternary shorelines in eastern Patagonia: Darwin revisited.” *Geomorphology*, 127, pp. 121–142. DOI: <https://doi.org/10.1016/j.geomorph.2010.08.003>
- Piola, A.R., Martínez Avellaneda, N., Guerrero, R. A., et al. 2010. “Malvinas-slope water intrusions on the northern Patagonia continental shelf” *Ocean Science*, 6, pp. 345–359. DOI: <https://doi.org/10.5194/os-6-345-2010>
- Ponce, J., Rabassa, J., Coronato, A., et al. 2011. “Palaeogeographical evolution of the Atlantic coast of Pampa and Patagonia from the last glacial maximum to the Middle Holocene” *Biological Journal of the Linnean Society*, 103, pp. 363–379. DOI: <https://doi.org/10.1111/j.1095-8312.2011.01653.x>
- R Core Team., 2022. R: A language and environment for statistical computing. R Foundation for Statistical Computing, Vienna, Austria. URL: <https://www.R-project.org/>.
- Ribolini, A., Aguirre, M., Baneschi, I., et al. 2011. “Holocene beach ridges and coastal evolution in the Cabo Raso Bay (Atlantic Patagonian coast, Argentina)” *Journal of Coastal Research*, 27, pp. 973–983. DOI: <https://doi.org/10.2112/JCOASTRES-D-10-00139.1>
- Richardson, J. R. 1981. “Brachiopods and pedicles”. *Paleobiology*, 7(1), pp. 87–95. DOI: <https://doi.org/10.1017/S0094837300003808>
- Richiano, S., Aguirre, M., Farinati, E., et al. 2015. “Bioerosion structures in *Crepidula* (Mollusca, Gastropoda) as indicators of latitudinal palaeoenvironmental changes: example from the marine Quaternary of Argentina” *Palaeogeography, Palaeoclimatology, Palaeoecology*. 439, pp. 63–78. DOI: <https://doi.org/10.1016/j.palaeo.2015.05.003>
- Richiano, S., Aguirre, M., Castellanos, I., et al. 2017. “Do coastal fronts influence bioerosion pattern along Patagonia? Late Quaternary ichnological tools from Golfo San Jorge” *Journal of Marine System*, 176, pp. 38–53. DOI: <https://doi.org/10.1016/j.jmarsys.2017.07.010>
- Richiano, S., Aguirre, M. L. and Giachetti, L. 2021. “Bioerosion on marine Quaternary gastropods from the southern Golfo San Jorge, Patagonia, Argentina: What do they tell US?” *Journal of South American Earth Science*, 107, pp. 103106. <https://doi.org/10.1016/j.jsames.2020.103106>
- Rostami, K., Peltier, W. R. and Mangini, A. 2000. “Quaternary marine terraces, sea-level changes and uplift history of Patagonia, Argentina: comparisons with predictions of the ICE-4G (VM2) model of the global process of glacial isostatic adjustment” *Quaternary Science Reviews*, 19, pp. 1495–1525. DOI: [https://doi.org/10.1016/S0277-3791\(00\)00075-5](https://doi.org/10.1016/S0277-3791(00)00075-5)
- Robinson, J. H. and Lee, D. E. 2008. “Brachiopod pedicle traces: recognition of three separate type of trace and redefinition of *Podichnus centrifugalis* Bromley and Surlyk, 1973” *Fossils*

- and Strata, 54, pp. 219–225.
- Rutter, N., Schnack, E., Del Río, J., et al. 1989. “Correlation and dating of Quaternary littoral zones along the Patagonian coast, Argentina” *Quaternary Science Reviews*, 8, pp. 213–234. DOI: [https://doi.org/10.1016/0277-3791\(89\)90038-3](https://doi.org/10.1016/0277-3791(89)90038-3)
- Rubio-Sandoval, K., Ryan, D.D., Richiano, S. et al. 2024. “Quaternary and Pliocene sea-level changes at Camarones, central Patagonia, Argentina” Preprint, <https://doi.org/10.31223/X5X11H>
- Schellmann, G. and Radtke, U. 2000. “ESR dating of stratigraphically well–constrained marine terraces along the Patagonian Atlantic coast (Argentina)” *Quaternary International*, 68–71, pp. 261–273. DOI: [https://doi.org/10.1016/S1040-6182\(00\)00049-542](https://doi.org/10.1016/S1040-6182(00)00049-542)
- Schellmann, G. and Radtke, U. 2010. “Timing and magnitude of Holocene sea–level changes along the middle and south Patagonian Atlantic coast derived from beach ridge systems, littoral terraces and valley–mouth terraces” *Earth Science Review*, 103, 1–30. DOI: <https://doi.org/10.1016/j.earscirev.2010.06.003>
- Taylor, P.D., Wilson, M.A. and Bromley, R.G. 1999. “A new ichnogenus for etchings made by cheilostome bryozoans into calcareous substrates” *Palaeontology*, 42, pp. 595–604. DOI: <https://doi.org/10.1111/1475-4983.00087>
- Taylor, P.D., Wilson, M.A. and Bromley, R.G. 2013. “Finichnus, a new name for the ichnogenus Leptichnus Taylor, Wilson and Bromley 1999, preoccupied by Leptichnus Simroth, 1896 (Mollusca, Gastropoda)” *Palaeontology*, 56, pp. 456. DOI: <https://doi.org/10.1111/pala.12000>
- Wehmiller, J. F. 2013. “Interlaboratory comparison of amino acid enantiomeric ratios in Pleistocene fossils” *Quaternary Geochronology*, 16, pp. 173–182.
- Wisshak, M. 2006. “High-Latitude Bioerosion: The Kosterfjord Experiment”, in Bhattacharji, S et al. (Eds.), *Lecture notes in Earth Sciences*. Berlin, pp. 202. DOI: <https://doi.org/10.1007/978-3-540-36849-6>
- Wisshak, M., Knaust, D. and Bertling, M. 2019. “Bioerosion ichnotaxa: review and annotated list” *Facies*, 65, 24, pp. 1–39. DOI: <https://doi.org/10.1007/s10347-019-0561-8>.
- Wilson, M.A. 2007. “Macroborings and the Evolution of Marine Bioerosion”, in Miller, W. (Ed.), *Trace Fossils: Concepts, Problems, Prospect*, Elsevier. Amsterdam, pp 356–367. DOI: <https://doi.org/10.1016/B978-044452949-7/50146-7>
- Zachos, J., Pagani, M., Sloan, L., et al. 2001. “Trends, rhythms, and aberrations in global climate 65 Ma to Present” *Science*, 292, pp. 686–693. DOI: <https://doi.org/10.1126/science.105941>

## 9.7. Chapter 7

- Angulo, R. J., de Souza, M. C. 2014. Conceptual review of Quaternary coastal paleo-sea level indicators from Brazilian coast. *Quaternary and Environmental Geosciences*, 05(2), 1–32.
- Angulo, R., Lessa, G., Souza, M. 2006. A critical review of mid- to late-Holocene sea-level fluctuations on the eastern Brazilian coastline. *Quaternary Science Reviews*, 25(5–6), 486–506. <https://doi.org/10.1016/j.quascirev.2005.03.008>
- Angulo, R.J., de Souza, M.C., da Camara Rosa, M.L.C., Barboza, E.G., Lessa, G.C., Pessenda, L.C.R., Ferreira Junior, A.L., 2022b. Mid- to Late Holocene sealevel changes at Abrolhos Archipelago and Bank, southwestern Atlantic, Brazil. *Mar Geol* 450. <https://doi.org/10.1016/j.margeo.2022.106841>
- Angulo, R.J., de Souza, M.C., da Camara Rosa, M.L.C., Caron, F., Barboza, E.G., Costa, M.B.S.F., Macedo, E., Vital, H., Gomes, M.P., Garcia, K.B.L., 2022a. Paleo-sea levels, Late-Holocene evolution, and a new interpretation of the boulders at the Rocas Atoll, southwestern Equatorial Atlantic. *Mar Geol* 447. <https://doi.org/10.1016/j.margeo.2022.106780>
- Angulo, R. J., de Souza, M. C., Giannini, P. C. F., Dillenburg, S. R., Barboza, E. G., da Camara Rosa, M. L. C., Hesp, P.A. Pessenda, L. C. R. 2022c. Late-Holocene sea levels from vermetids and barnacles at Ponta do Papagaio, 27 50' S latitude and a comparison with other sectors of southern Brazil. *Quaternary Science Reviews*, 286, 107536.
- Audemard, F. A. 1996. Field-trip guidebook to “The late Quaternary marine deposits of the Paraguana peninsula and Coro surroundings”, in: 5th Annual CLIP Meeting, July 1996, Punta Cardon, Venezuela.
- Barbosa, L. M., Bittencourt, A. C. S. P., Dominguez, J. M. L., Martin, L. 1986. The Quaternary coastal deposits of the State of Alagoas: influence of the relative sea-level changes, *Quat. S. Am. A.*, 4, 269–290.
- Barnett, R. L., Bernatchez, P., Garneau, M., Brain, M. J., Charman, D. J., Stephenson, D. B., Haley, S., Sanderson, N., 2019. Late Holocene sea-level changes in eastern Québec and potential drivers. *Quaternary Science Reviews*, 203, 151-169.
- Bini, M., Isola, I., Zanchetta, G., Pappalardo, M., Ribolini, A., Ragaini, L., Baroni, C., Boretto, G., Fuck, E., Morigi, C., Salvatore, M.C., Bassi, D., Marzaioli, F., Terrasi, F., 2018. Mid-Holocene relative sea-level changes along Atlantic Patagonia: New data from Camarones, Chubut, Argentina. *Holocene* 28, 56–64. <https://doi.org/10.1177/0959683617714596>
- Björck, S., Lambeck, K., Möller, P., Waldmann, N., Bennike, O., Jiang, H., Li, D., Sandgren, P., Nielsen, A.B. and Porter, C.T., 2021. Relative sea level changes and glacio-isostatic modelling in the Beagle Channel, Tierra del Fuego, Chile: Glacial and tectonic implications. *Quaternary Science Reviews*, 251, 106-657.
- Bracco, R., García-Rodríguez, F., Inda, H., del Puerto, L., Castiñeira, c, Penario, D., 2011. Niveles relativos del mar durante el Pleistoceno final-Holoceno en la costa de Uruguay, in: *El Holoceno En La Zona Costera de Uruguay*. pp. 65–92.

- Bracco, R., Inda, H., del Puerto, L., Capdepon, I., Panario, D., Castiñeira, C., García-Rodríguez, F., 2014. A reply to “Relative sea level during the Holocene in Uruguay.” *Palaeogeogr Palaeoclimatol Palaeoecol*.
- Briggs, R.D., Tarasov, L., 2013. How to evaluate model-derived deglaciation chronologies: a case study using Antarctica. *Quat. Sci. Rev.* 63, 109e127. <https://doi.org/10.1016/j.quascirev.2012.11.021>.
- Brinkman, R., Pons, L. J. 1968. A pedo-geomorphological classification and map of the Holocene sediments in the coastal plain of the three Guianas, Stichting voor Bodemkartering Wageningen, Soil Survey Institute, Wageningen, the Netherlands.
- Casella, E., Lewin, P., Ghilardi, M., Rovere, A., Bejarano, S. 2022. Assessing the relative accuracy of coral heights reconstructed from drones and structure from motion photogrammetry on coral reefs. *Coral Reefs*, 41(4), 869–875. <https://doi.org/10.1007/s00338-022-02244-9>
- Castro, J.W.A., Suguio, K., Seoane, J.C.S., Da Cunha, A.M., Dias, F.F., 2014. Sea-level fluctuations and coastal evolution in the state of Rio de Janeiro, southeastern Brazil. *An Acad Bras Cienc* 86, 671–683. <https://doi.org/10.1590/0001-3765201420140007>
- Codignotto, J. O. 1983. Depósitos elevados y/o de acreción Pleistoceno-Holoceno en la costa Fueguino-Patagónica, in: Simposio Oscilaciones del nivel del mar durante el último hemicyclo deglacial en la Argentina, 6–7 April 1983, Mar del Plata, Argentina, 12–26.
- Dalton, A. S., Gowan, E. J., Mangerud, J., Möller, P., Lunkka, J. P., Astakhov, V., 2022. Last interglacial (MIS 5e) sea level proxies in the glaciated Northern Hemisphere. *Earth System Science Data*.
- Dumitru, O. A., Polyak, V. J., Asmerom, Y., Onac, B. P., 2021. Last interglacial sea-level history from speleothems: a global standardized database. *Earth System Science Data*, 13(5), 2077-2094.
- Dutton, A., Villa, A., Chutcharavan, P. M., 2022. Compilation of Last Interglacial (Marine Isotope Stage 5e) sea-level indicators in the Bahamas, Turks and Caicos, and the east coast of Florida, USA. *Earth System Science Data*, 14(5), 2385-2399.
- Felis, T., Giry, C., Scholz, D., Lohmann, G., Pfeiffer, M., Pätzold, J., Kölling, M., Scheffers, S. R. 2015. Tropical Atlantic temperature seasonality at the end of the last interglacial, *Nat. Commun.*, 6, 6159, <https://doi.org/10.1038/ncomms7159>.
- Gowan, E. J., Rovere, A., Ryan, D. D., Richiano, S., Montes, A., Pappalardo, M., Aguirre, M. L. 2021. Last interglacial (MIS 5e) sea-level proxies in southeastern South America. *Earth System Science Data*, 13(1), 171–197. <https://doi.org/10.5194/essd-13-171-2021>
- Hijma, M. P., Engelhart, S. E., Törnqvist, T. E., Horton, B. P., Hu, P., Hill, D. F. 2015. A protocol for a geological sea-level database. In *Handbook of Sea-Level Research* (pp. 536–553). Wiley. <https://doi.org/10.1002/9781118452547.ch34>

- Hawkes, A.D., Kemp, A.C., Donnelly, J.P., Horton, B.P., Peltier, W.R., Cahill, N., Hill, D.F., Ashe, E., Alexander, C.R., 2016. Relative sea-level change in northeastern Florida (USA) during the last ~ 8.0 ka. *Quat. Sci. Rev.* 142 (2016), 90e101.
- Horton, B. P., Kopp, R. E., Garner, A. J., Hay, C. C., Khan, N. S., Roy, K., Shaw, T. A. 2018. Mapping Sea-Level Change in Time, Space, and Probability. *The Annual Review of Environment and Resources*, 43, 418–521.
- Iriondo, M. 2013. El cuaternario de las Guayanas, Museo Provincial de Ciencias Naturales Florentino Ameghino, Santa Fe, Argentina.
- Kemp, A.C., Wright, A.J., Edwards, R.J., Barnett, R.L., Brain, M.J., Kopp, R.E., Cahill, N., Horton, B.P., Charman, D.J., Hawkes, A.D., Hill, T.D., van de Plassche, O., 2018. Relative sea-level change in Newfoundland, Canada during the past ~3000 years. *Quat. Sci. Rev.* 201, 89e110. <https://doi.org/10.1016/j.quascirev.2018.10.012>.
- Khan, N.S., Ashe, E., Horton, B.P., Dutton, A., Kopp, R.E., Brocard, G., Engelhart, S.E., Hill, D.F., Peltier, W.R., Vane, C.H., Scatena, F.N., 2017. Drivers of Holocene sea-level change in the Caribbean. *Quat Sci Rev.* <https://doi.org/10.1016/j.quascirev.2016.08.032>
- Khan, N.S., Ashe, E., Shaw, T.A., Vacchi, M., Walker, J., Peltier, W.R., Kopp, R.E., Horton, B.P., 2015. Holocene Relative Sea-Level Changes from Near-, Intermediate-, and Far-Field Locations. *Curr Clim Change Rep* 1, 247–262.
- Khan, N.S., Horton, B.P., Engelhart, S., Rovere, A., Vacchi, M., Ashe, E.L., Törnqvist, T.E., Dutton, A., Hijma, M.P., Shennan, I., 2019. Inception of a global atlas of sea levels since the Last Glacial Maximum. *Quat Sci Rev* 220, 359–371. <https://doi.org/10.1016/j.quascirev.2019.07.016>
- Long, A.J., Woodroffe, S.A., Roberts, D.H., Dawson, S., 2011. Isolation basins, sea-level changes and the Holocene history of the Greenland Ice Sheet. *Quat. Sci. Rev.* 30, 3748e3768. <https://doi.org/10.1016/j.quascirev.2011.10.013>.
- Lorscheid, T., Felis, T., Stocchi, P., Obert, J. C., Scholz, D., Rovere, A. 2017. Tides in the Last Interglacial: insights from notch geometry and palaeo tidal models in Bonaire, Netherland Antilles, *Sci. Rep.-UK*, 7, 16241, <https://doi.org/10.1038/s41598-017-16285-6>, 2017.
- Lorscheid, T., Rovere, A. 2019. The indicative meaning calculator – quantification of paleo sea-level relationships by using global wave and tide datasets. *Open Geospatial Data, Software and Standards*, 4(1), 10. <https://doi.org/10.1186/s40965-019-0069-8>
- Love, R., Milne, G.A., Tarasov, L., Engelhart, S.E., Hijma, M.P., Latychev, K., Horton, B.P., Törnqvist, T.E., 2016. The contribution of glacial isostatic adjustment to projections of sea-level change along the Atlantic and Gulf coasts of North America. *Earths Future* 4, 440e464. <https://doi.org/10.1002/2016EF000363>.
- Martin, L., Flexor, J. M., Blitzkow, D., Suguio, K. 1985. Geoid change indications along the Brazilian coast during the last 7.000 years. In *Proceedings*

- Martínez, S., Rojas, A., 2013. Relative sea level during the Holocene in Uruguay. *Palaeogeogr Palaeoclimatol Palaeoecol* 374, 123–131. <https://doi.org/10.1016/j.palaeo.2013.01.010>
- Miller, G. H., Kaufman, D. S., & Clarke, S. J. (2013). AMINO ACID DATING. *Encyclopedia of Quaternary Science: Second Edition*, 37–48. <https://doi.org/10.1016/B978-0-444-53643-3.00054-6>
- Milne, G. A., Long, A. J., Bassett, S. E. 2005. Modelling Holocene relative sea-level observations from the Caribbean and South America. *Quaternary Science Reviews*, 24(10–11), 1183–1202. <https://doi.org/10.1016/j.quascirev.2004.10.005>
- Milne, G. A., Mitrovica, J. X. 2008. Searching for eustasy in deglacial sea-level histories. *Quaternary Science Reviews*, 27(25–26), 2292–2302. <https://doi.org/10.1016/j.quascirev.2008.08.018>
- Pappalardo, M., Aguirre, M., Bini, M., Consoloni, I., Fucks, E., Hellstrom, J., Isola, I., Ribolini, A., Zanchetta, G. 2015. Coastal landscape evolution and sea-level change: A case study from Central Patagonia (Argentina). In *Zeitschrift fur Geomorphologie* (Vol. 59, Issue 2, pp. 145–172). Schweizerbart Science Publishers. <https://doi.org/10.1127/0372-8854/2014/0142>
- Reimer, P.J., Reimer, R.W., 2001. A marine reservoir correction database and On-line interface.
- Richiano, S., Varela, A. N., D'Elia, L., Bilmes, A., Gómez-Dacal, A., Sial, A. N., Aguirre, M.L., Mari, F., Scivetti, N. 2022. Beach ridge evolution during the Holocene Climatic Optimum at Río de la Plata estuary, Argentina: Former answers for future questions? *Quaternary International*, 638, 56-69.
- Rostami, K., Peltier, W.R., Mangini, A., 2000. Quaternary marine terraces, sea-level changes and uplift history of Patagonia, Argentina: comparisons with predictions of the ICE-4G (VM2) model of the global process of glacial isostatic adjustment. *Quat Sci Rev* 19, 1496–1525.
- Rovere, A., Antonioli, F., Bianchi, C. N. 2015. Fixed biological indicators. In I. Shennan, A. J. Long, and B. P. Horton (Eds.), *Handbook of Sea-Level Research* (pp. 268–280).
- Rovere, A., Pappalardo, M., O'Leary, M. 2013. Geomorphological Indicators. In A. E. Scott and Cary J. M. (Eds.), *Encyclopedia of Quaternary Science: Second Edition* (Second Edition, pp. 377–384). Elsevier Inc. <https://doi.org/10.1016/B978-0-444-53643-3.00133-3>
- Rovere, A., Pappalardo, M., Richiano, S., Aguirre, M., Sandstrom, M. R., Hearty, P. J., Austermann, J., Castellanos, I., Raymo, M. E. (2020). Higher than present global mean sea level recorded by an Early Pliocene intertidal unit in Patagonia (Argentina). *Communications Earth & Environment*, 1(1):68.
- Rovere, A., Raymo, M.E., Vacchi, M., Lorscheid, T., Stocchi, P., Gómez-Pujol, L., Harris, D.L., Casella, E., O'Leary, M.J., Hearty, P.J., 2016. The analysis of Last Interglacial (MIS 5e) relative sea-level indicators: Reconstructing sea-level in a warmer world. *Earth Sci Rev*.

- <https://doi.org/10.1016/j.earscirev.2016.06.006>
- Rubio-Sandoval, K., Ryan, D. D., Richiano, S., Giachetti, L. M., Hollyday, A., Bright, J., Gowan, E., Pappalardo, M., Austermann, J., Kaufman, D., Rovere, A. 2024. Quaternary and Pliocene sea-level changes at Camarones, central Patagonia, Argentina. Preprint
- Schellmann, G., Radtke, U. 2010. Timing and magnitude of Holocene sea-level changes along the middle and south Patagonian Atlantic coast derived from beach ridge systems, littoral terraces and valley-mouth terraces. In *Earth-Science Reviews* (Vol. 103, Issues 1–2, pp. 1–30). <https://doi.org/10.1016/j.earscirev.2010.06.003>
- Shennan, I. 2015. Handbook of sea-level research. In I. Shennan, A. J. Long, and B. P. Horton (Eds.), *Handbook of Sea-Level Research* (pp. 3–25). Wiley. <https://doi.org/10.1002/9781118452547.ch2>
- Simms, A. R., 2021. Last interglacial sea levels within the Gulf of Mexico and northwestern Caribbean Sea. *Earth System Science Data*, 13(3), 1419-1439.
- Suguío, K., Martin, L., Bittencourt, A. C., Dominguez, J. M., Flexor, J. M., de Azevedo, A. E. 1985. Flutuações do nível relativo do mar durante o Quaternário Superior ao longo do litoral brasileiro e suas implicações na sedimentação costeira. *Revista Brasileira de Geociências*, 15(4), 273-86.
- Tomazelli, L. J., Dillenburg, S. R. 2007. Sedimentary facies and stratigraphy of a last interglacial coastal barrier in south Brazil, *Mar. Geol.*, 244, 33–45.
- Tomazelli, L. J., Dillenburg, S. R., J.A. Villwock. 2006. Geological Evolution of Rio Grande do Sul Coastal Plain, Southern Brazil. *Journal of Coastal Research*, 1, 257–278.
- Thompson, S. B., Creveling, J. R., 2021. A global database of marine isotope substage 5a and 5c marine terraces and paleoshoreline indicators. *Earth System Science Data*, 13(7), 3467-3490.
- Vacchi, M., Engelhart, S.E., Nikitina, D., Ashe, E.L., Peltier, W.R., Roy, K., Kopp, R.E., Horton, B.P., 2018. Postglacial relative sea-level histories along the eastern Canadian coastline. *Quat. Sci. Rev.* 201, 124e146. <https://doi.org/10.1016/j.quascirev.2018.09.043>.
- van de Plassche, O. 1986. *Sea-Level Research: A Manual for the Collection and Evaluation of Data* (O. van de Plassche, Ed.). Geo Books .

## 10. Appendix

During this PhD project, I had the privilege to repeatedly present my work at several conferences and participate in workshops with international colleagues.

### 10.1. GSA Connects, 2020, Online

#### A review of Last Interglacial Sea-Level Indicators in the Southern Western Atlantic: State-of-the-art and future perspectives

Karla Rubio-Sandoval, Deirdre Ryan, Matteo Vacchi, Sebastian Richiano, Alessio Rovere

Interglacials are generally characterized by warmer temperatures and smaller-than-present ice sheets. In particular, the Last Interglacial (LIG, ~128-116 ka) is often regarded as a process-analog for a future climate. During this period, global average temperatures were 2°C higher than pre-industrial time, and the global mean sea level was higher. Estimates of LIG sea-levels in the Southern Western Atlantic coasts (from Brazil northwards to Colombia) range approximately from 2 to 12 m above the present level; however, there are large uncertainties associated with these values. We use the World Atlas of Last Interglacial Shorelines (WALIS) database to standardize and evaluate the quality of the sea-level record and its uncertainties. Using WALIS, we reviewed published data for the countries of Brazil, French Guiana, Surinam, Guyana, Venezuela, Colombia, as well as the islands Bonaire, Curaçao and Aruba, documenting and standardizing both geological and chronological information. While not all the reviewed papers fulfilled the database standards (e.g. missing or unclear information), the review allowed us to estimate the current state-of-the-art. Sea-level indicators are well preserved in the Southern Western Atlantic providing an almost continuous record between the states. Despite this and the relative sea-level indicators variety, there are main gaps related to the accuracy of elevation measurements and the reliability of chronology; uncertainties that hinder our ability to precisely estimate effects causing departures from eustasy. Improve our knowledge of sea-level changes during the LIG is a key to assessing the future of the coastlines under warmer climatic conditions.

### 10.2. Bremen PhD Days, 2020, Online

#### State-of-the-art and future perspectives of Last Interglacial sea-level in the Western Atlantic: a profile from Brazil to Honduras

Karla Rubio-Sandoval, Deirdre Ryan, Matteo Vacchi, Sebastian Richiano, Alessio Rovere

Interglacials are generally characterized by warmer temperatures and smaller-than-present ice sheets. In particular, the Last Interglacial (LIG, ~128-116 ka) is often regarded as a process-analog for a future climate. During this period, global average temperatures were 2°C higher than pre-industrial time, and the global mean sea level was higher. Estimates of LIG sea-levels in the Southern Western Atlantic coasts (from Brazil northwards to Honduras) range approximately from 2 to 12 m above the present level; however, there are large uncertainties

associated with these values. We use the World Atlas of Last Interglacial Shorelines (WALIS) database to standardize and evaluate the quality of the sea-level record and its uncertainties. Using WALIS, we reviewed published data for the countries of Brazil, French Guiana, Surinam, Guyana, Venezuela, Colombia, Panama, Costa Rica, Nicaragua, Honduras, as well as the islands Bonaire, Curaçao and Aruba, documenting and standardizing both geological and chronological information. While not all the reviewed papers fulfilled the database standards (e.g. missing or unclear information), the review allowed us to estimate the current state-of-the-art. Sea-level indicators are well preserved in the Southern Western Atlantic providing an almost continuous record between the states. Despite this and the relative sea-level indicators variety, there are main gaps related to the accuracy of elevation measurements and the reliability of chronology; uncertainties that hinder our ability to precisely estimate effects causing departures from eustasy. Improve our knowledge of sea-level changes during the LIG is a key to assess the future of the coastlines under warmer climatic conditions.

### 10.3. PALSEA meeting, 2021, Online

#### A standardized database of Last interglacial (MIS 5e) sea-level indicators in the Western Atlantic and Southwestern Caribbean, from Brazil to Honduras

Karla Rubio-Sandoval, Alessio Rovere, Ciro Cerrone, Paolo Stocchi, Thomas Lorscheid, Thomas Felis, Ann-Kathrin Petersen, Deirdre D. Ryan

Interglacials are generally characterized by warmer temperatures and smaller-than-present ice sheets. In particular, the Last Interglacial (LIG, ~128-116 ka) is often regarded as a process-analog for a future climate. During this period, global average temperatures were 2°C higher than pre-industrial time, and the global mean sea level was higher. Estimates of LIG sea-levels in the Western Atlantic and Southwestern Caribbean coasts (from Brazil northwards to Honduras) range approximately from 2 to 12 m above the present level; however, there are large uncertainties associated with these values. We use the World Atlas of Last Interglacial Shorelines (WALIS) database to standardize and evaluate the quality of the sea-level record and its uncertainties. Using WALIS, we reviewed published data for the countries of Brazil, French Guiana, Surinam, Guyana, Venezuela, Colombia, Panama, Costa Rica, Nicaragua, Honduras as well as the islands Bonaire, Curaçao and Aruba. Our review produced 55 standardized datapoints, each assigned to one or more age constraints. Sea-level indicators are well preserved along the Brazilian coasts, providing an almost continuous north-to-south transect, despite this and the variety of relative sea-level indicators (i.e. beach deposits, coral reef terraces, marine terraces, Ophiomorpha burrows, and tidal notches) our data compilation highlights several concerns related to age control and the accuracy of elevation measurements. We identify that the coasts of Northern Brazil, French Guiana, Suriname, Guyana, and Venezuela would benefit from a renewed study of Pleistocene sea-level indicators, as it was not possible to identify sea-level datapoints for the last interglacial coastal outcrops along the coasts of these countries. Future research must also be directed at improving the chronological control at several locations, and several sites would benefit from re-measurement of sea-level indicators using more accurate elevation measurement

techniques. Improve our knowledge of sea-level changes during the LIG is a key to assess the future of the coastlines under warmer climatic conditions.

#### 10.4. Reunión Argentina de Sedimentología, 2021, Online

##### Niveles del mar durante el Último Interglacial (MIS 5e) en el Atlántico Occidental: Un Perfil de Brasil a Honduras

Karla Rubio-Sandoval, Alessio Rovere, Ciro Cerrone, Paolo Stocchi, Thomas Lorscheid, Thomas Felis, Ann-Kathrin Petersen, Deirdre D. Ryan

Durante el Cuaternario se alternaron periodos glaciares e interglaciares debido a cambios en la órbita terrestre. Los interglaciares se caracterizan generalmente por presentar temperaturas más cálidas y una disminución de la extensión de la capa de hielo. En particular, el Último Interglacial (MIS 5e, ~128-116 ka) se considera a menudo como un análogo para las proyecciones climáticas futuras. Durante este periodo, las temperaturas medias mundiales fueron 2°C más altas que en la época preindustrial, y el nivel medio del mar fue más alto. Las estimaciones del nivel del mar del MIS 5e en las costas del Atlántico occidental (desde Brasil hasta Honduras) oscilan aproximadamente entre 2 y 12 m por encima del nivel actual; sin embargo, existen grandes incertidumbres asociadas a estos valores. Utilizamos la base de datos del Atlas Mundial de las Líneas de Costa del Último Interglacial (WALIS, por sus siglas en inglés) para estandarizar y evaluar la calidad del registro del nivel del mar y sus incertidumbres. Utilizando WALIS, revisamos los datos publicados para los países de Brasil, Guayana Francesa, Surinam, Guyana, Venezuela, Colombia, Panamá, Costa Rica, Nicaragua, Honduras, así como las islas Bonaire, Curaçao y Aruba. Nuestra revisión produjo 55 datos del nivel del mar estandarizados, cada uno asignado a uno o más datos de edad. Los indicadores del nivel del mar están bien conservados a lo largo de las costas brasileñas, proporcionando un transecto casi continuo de norte a sur. A pesar de esto, y de la variedad de indicadores relativos del nivel del mar (p.ej. depósitos de playa, terrazas de arrecifes de coral, terrazas marinas y madrigueras de *Ophiomorpha*), nuestra compilación de datos pone de manifiesto varias incertidumbres relacionadas con el control de la edad y la precisión de las mediciones de elevación. Identificamos que las costas del norte de Brasil, la Guayana Francesa, Surinam, Guayana y Venezuela se beneficiarían de un estudio renovado de los indicadores del nivel del mar del MIS 5, ya que no fue posible identificar puntos de referencia del nivel del mar para los afloramientos costeros de este periodo. Las investigaciones futuras también deben dirigirse a mejorar el control cronológico en varios lugares, y a evaluar el efecto de la tectónica en la zona, ya que, con excepción de las islas del Caribe, existe una controversia sobre el efecto que puede tener en el resto de la región. Por último, varios lugares se beneficiarían de una nueva medición de los indicadores del nivel del mar utilizando técnicas más precisas. Mejorar nuestro conocimiento de los cambios en el nivel del mar durante el Último Interglacial es clave para evaluar el futuro de las costas en condiciones climáticas más cálidas.

## 10.5. PALSEA meeting, 2022, Singapore

### Holocene sea-level change in the southwestern Atlantic: A standardized database

Karla Rubio-Sandoval, Timothy A. Shaw, Ben Horton, Nicole S. Khan, Augusto Luiz Ferreira-Júnior, Rodolfo J. Angulo, Maíra Oneda Dal Pai, Guilherme C. Lessa, Maria Cristina de Souza, Matteo Vacchi, Deirdre D. Ryan, Sebastian Richiano, Evan J. Gowan, Abdullah S. Kahn, Alessio Rovere

Relative sea-level (RSL) studies along the southwestern Atlantic coasts confirm the presence of several Holocene sea-level index points in the facies of beach ridges, marine terraces, beach, lagoon and estuarine deposits, fixed biological indicators. Here, we present a standardized database of Holocene sea-level index points for this region, compiled using the HOLSEA template. We reviewed published data for the countries of Argentina, Uruguay, and Brazil. Our preliminary review produced 800 standardized datapoints and more than 1000 re-calibrated radiocarbon dates, providing an almost continuous south-to-north transect of sea-level data along the southwestern Atlantic. Our data compilation highlights that several sites show a mid-Holocene maximum transgression, with RSL rising 2-4m above its present level, with a subsequent fall to its modern position. This trend seems to be predominantly driven by glacio-isostatic processes. However, we also highlight that elevation measurements, sea-level interpretations, as well as the chronological control at several locations may be improved by future research.

## 10.6. EGU General Assembly, 2023, Online

### Argentinean raised beaches: evidence of a millenary sea-level history

Karla Rubio-Sandoval, Deirdre D. Ryan, Sebastian Richiano, Luciana M. Giachetti, Andrew Hollyday, Jordon Bright, Evan J. Gowan, Marta Pappalardo, Jacqueline Austermann, Darrell S. Kaufman, Alessio Rovere

In about 20 km of the coast near the town of Camarones (Central Patagonia, Argentina), sea level has left its imprint over four interglacials from the Holocene to the Pliocene. These were generally preserved as beach ridges deposited by storm waves above modern sea level. Based on a morphological and chronostratigraphic approach, we recognized four beach ridge systems from the present-day coastline up to 2 km inland and associated them with four interglacial periods (Holocene, MIS 5 e, MIS 9 or MIS 11, and Early Pliocene). Using high-precision GNSS, we measured the elevation of these raised beaches; we calculated their indicative meaning with satellite-derived wave measurements and wave runup models to finally calculate their paleo-relative sea levels. The uncorrected for post-depositional vertical land motions paleo-relative sea levels values associated with the four interglacials (with  $1\sigma$  uncertainties) are  $6\pm 1.5$  m (Holocene),  $8.7\pm 2.1$  m (MIS 5),  $14.5\pm 1.5$  m (MIS 9 or 11), and  $36.2\pm 2.7$  m (Pliocene). We compare these results with Glacial Isostatic Adjustment and Dynamic Topography predictions in the study area; however, our results highlight that there is a need to refine these models to allow the calculation of the global mean sea level of each interglacial period. This research outlines the millenary relative sea level history of the Camarones coastline and can help constrain projections of sea level rise in a warmer world.

## 10.7. Bremen PhD Days, 2023, Bremen

### A millennial history of sea level changes in the southwestern Atlantic

Karla Rubio-Sandoval, Timothy A. Shaw, Ben Horton, Nicole S. Khan, Augusto Luiz Ferreira-Júnior, Rodolfo J. Angulo, Guilherme C. Lessa, Maria Cristina de Souza, Matteo Vacchi, Deirdre D. Ryan, Sebastian Richiano, Evan J. Gowan, Ciro Cerrone, Paolo Stocchi, Thomas Lorscheid, Thomas Felis, Ann-Kathrin Petersen, Alessio Rovere

Warmer temperatures and smaller-than-present ice sheets generally characterize interglacials. Determining the rates and geographic variability of relative sea-level (RSL) change during these periods provides insights into the future of the coastlines under warmer climatic conditions. Since the early 1940s, RSL studies along the southwestern Atlantic Coasts confirm the presence of several Last Interglacial (LIG, ~128-116 ka) and Holocene (HOL, 11 ka – to present) sea-level indicators. We use WALIS and HOLSEA templates to standardize and evaluate the quality and uncertainties of these published sea-level records. Our preliminary review produced more than 1000 standardized data points (55 LIG and 1177 HOL); more than 300 inconclusive data were rejected after being examined by quality control. Our data indicate that during the LIG, the paleo sea-level values range from ~5.6 to 20 m above sea level (a.s.l.) in the continental sector and from ~2 to 10 m a.s.l. in the Caribbean islands. Regarding the Holocene data, several sites show a mid-Holocene maximum transgression, with RSL rising 2-4 m above its present level, with a subsequent fall to its current position. This trend seems to be predominantly driven by glacial-isostatic adjustment processes. From our review, we identify that the coasts of Brazil, French Guiana, Suriname, Guyana, and Venezuela would benefit from a renewed study of Quaternary sea-level indicators. We also highlight that elevation measurements, sea-level interpretations, as well as chronological control at several locations may be improved by future research.

## 10.8. MARUM Excellent Cluster Annual Retreat, 2023, Bremen

### The Southwest Atlantic and its coastal memory: Reconstructing ancient sea levels along the Argentinean coasts

Karla Rubio-Sandoval, Timothy A. Shaw, Ben Horton, Nicole S. Khan, Matteo Vacchi, Deirdre D. Ryan, Sebastian Richiano, Luciana Giachetti, Evan J. Gowan, Abdullah S. Kahn, Alessio Rovere

Relative sea-level (RSL) studies along the southwestern Atlantic coasts confirm the presence of several Holocene sea-level index points in the facies of beach ridges, marine terraces, beach, lagoon and estuarine deposits, fixed biological indicators. Here, we present a standardized database of Holocene sea-level index points for this region, compiled using the HOLSEA template. We reviewed published data for the countries of Argentina, Uruguay, and Brazil. Our preliminary review produced 800 standardized datapoints and more than 1000 re-calibrated radiocarbon dates, providing an almost continuous south-to-north transect of sea-level data along the southwestern Atlantic. Our data compilation highlights that several sites show a mid-Holocene maximum transgression, with RSL rising 2-4m above its present level, with a subsequent fall to its modern position. This trend seems to be predominantly driven by

glacio-isostatic processes. However, we also highlight that elevation measurements, sea-level interpretations, as well as the chronological control at several locations may be improved by future research.

## 10.9. Sea Level Rise Conference, 2023, Venice

### Holocene sea-level trends in the southwestern Atlantic: A story behind the data

Karla Rubio-Sandoval, Timothy A. Shaw, Ben Horton, Nicole S. Khan, Augusto Luiz Ferreira-Júnior, Rodolfo J. Angulo, Maíra Oneda Dal Pai, Guilherme C. Lessa, Maria Cristina de Souza, Matteo Vacchi, Deirdre D. Ryan, Sebastian Richiano, Evan J. Gowan, Abdullah S. Kahn, Alessio Rovere

Determine the rates and geographic variability of Relative sea-level (RSL) change during the Holocene provides insights about the future of the coastlines under warmer climatic conditions. Since the early 1940s, RSL studies along the southwestern Atlantic Coasts confirm the presence of several Holocene sea-level indicators. We use the HOLSEA template to standardize and evaluate the quality and uncertainties of these published sea-level records from the countries of Argentina, Uruguay, and Brazil. Our preliminary review produced 553 standardized datapoints (261 index points and 292 limiting data), and around 117 inconclusive data were considered as rejected after being examined by quality control. Our data indicates that several sites show a mid-Holocene maximum transgression, with RSL rising 2-4m above its present level, with a subsequent fall to its modern position. This trend seems to be predominantly driven by glacio-isostatic adjustment processes. We also highlight that elevation measurements, sea-level interpretations, as well as the chronological control at several locations may be improved by future research.

## 11. Epilogue

As we conclude our study on sea level changes, it becomes evident that our understanding of this phenomenon is still evolving. While our detailed analysis of paleoclimate data and historical reconstructions has elucidated the complexities of past sea level changes, our work as researchers remains unfinished. As we navigate the challenges of the 21st century, urgent issues related to climate change and sea level rise demand our attention.

Research and monitoring are imperative to deepen our understanding of the causes and consequences of these changes, and to develop effective strategies for adaptation and mitigation. Moreover, it is crucial to emphasize the significance of international collaborations and collective actions to face global warming, protect our coastlines, and support vulnerable communities.

Only through a global and multidisciplinary approach we can effectively address these challenges and implement the necessary actions to create a sustainable and resilient future for generations to come.

### Epilogue Spanish version

A medida que concluimos nuestro estudio sobre los cambios del nivel del mar, es evidente que nuestra comprensión de este fenómeno sigue evolucionando. Aunque nuestro análisis detallado de los datos paleoclimáticos y de las reconstrucciones históricas ha dilucidado las complejidades de los cambios del nivel del mar en el pasado, nuestra labor como investigadores sigue incompleta. Mientras nos enfrentamos a los retos del siglo XXI, las cuestiones urgentes relacionadas con el cambio climático y el incremento del nivel del mar exigen nuestra atención.

La investigación y el monitoreo continuos son imperativos para profundizar nuestra comprensión de las causas y consecuencias de estos cambios, así como para desarrollar estrategias efectivas de adaptación y mitigación. Además, es crucial subrayar la importancia de las colaboraciones internacionales y las acciones colectivas para combatir el calentamiento global, proteger nuestras costas y apoyar a las comunidades vulnerables.

Sólo mediante un enfoque global y multidisciplinario podremos afrontar eficazmente estos retos y aplicar las medidas necesarias para crear un futuro sostenible y resiliente para las generaciones venideras.